海外出張報告書

サーマルストライピング／ストラティフィケーションに関する日米専門家会議

（付　　録）

日本側発表資料

1983年2月

動力炉・核燃料開発事業団
大洗工学センター

動力炉・核燃料開発事業団（Power Reactor and Nuclear Fuel Development Corporation）

JAPANESE PRESENTATIONS

DOE/PNC SPECIALIST MEETING ON REACTOR THERMAL-HYDRAULIC PERFORMANCE

U.S. DEPARTMENT OF ENERGY | JAPAN-POWER REACTOR AND NUCLEAR FUEL DEVELOPMENT CORPORATION

OCTOBER 1982
SUNNYVALE, CA

TABLE OF CONTENTS

PNC TN960 83-01

MONJU THERMAL STRIPING DESIGN CONCEPT

OCTOBER, 1982

PNC / MONJU PROJECT

MONJU THERMAL STRIPING DESIGN CONCEPT

ABSTRACT

MONJU components will be operated in dynamic sodium environments in the high-temperature range of 400°c to 530°c for a design life of 30 years.

Therefore, the thermal and hydraulic properties test program have been conducted to predict the heat transfer and fluid flow environment on reactor components to eliminate unnecessary conservatisms in analysis procedres. The parameters that have been developed, based on test datas, include thermal striping at normal operation.

This session deals with MONJU thermal striping design concept.

1. General

In the design of Monju plant, particular attention has been given to safety and to achieving reliable operation. Monju components will be operated in dynamic sodium environments in the high-temperature range of 400°C to 530°C for a design life of 30 years shown in Fig. 1. Therefore, various thermal and hydraulic test programs have been initiated and are supplying valuable data that will be used as confirmatory information and to make design condition. Those programs also will provide the data essential to elimination of unnecessary conservatism in analysis procedures. Thermal and hydraulic properties test programs have been conducted to predict the heat transfer and fluid flow environment on reactor components. The parameters that have been developed, based on test data, includes thermal striping at normal operation.

As shown in Fig. 2, the reactor vessel is supported at its upper end of the concrete ledge which surrounds the vessel, and its thermal expansion is free downward. It is about 17,800 mm high and constructed of 304 stainless steel. It has inside diameters of about 7,800 mm at the upper part (which surrounds the shielding part of the closure head) and about 7,100 mm at the lower part, with a wall thickness of about 50 mm.

Primary sodium coolant enters the reactor vessel through three 24-inch nozzles located 120° apart in the lower plenum of the reactor vessel, and is discharged from the vessel through three 32-inch nozzles which are also located 120° apart in the upper plenum. The reactor vessel has also an outlet nozzle of the overflow system at its upper part.

The horizontal movement of the reactor vessel in the event of earthquake is prevented by the structure provided on the bottom of the reactor vessel pit and it works through the guard vessel. The reactor internal structures consist of the upper internal structure and the lower internal structures. The upper internal structure (UIS) is a cylindrical plug with an outer diameter of about 1,800 mm at its lower part and with a total height of about 13,400 mm, and its lower end is 50 mm above the top of fuel subassemblies. UIS comprises 19-CRDM guide pipes, thermocouples and flow-meters for measuring temperature and flow rate at the outlet of each fuel subassembly.

The sodium level in the reactor vessel during normal reactor operation is about 6,000 mm above the top of the fuel subassemblies (in another words, about 500 mm below the lower surface of the closure head) and the all lower internal structures are submerged in sodium. The free surface of sodium is covered by argon gas and the level is kept constant by the over-flow system.

Figure 3 shows the core configuration. The core consists of 198 core fuel subassemblies. It is surrounded by axial and radial blankets. The radial blanket consists of 172 blanket fuel subassemblies and its equivalent thickness is 30.6 cm. The core contains 19 control rod guide tubes through which 13 regulating and safety rods and 6 back up safety rods are inserted for reactor power control and shutdonw.

Coolant flow rate through the reactor is 15.36 x 10^6 kg/hr. The flow distribution in the core is controlled by fixed orifices at the bottom of the fuel subassembly. The flow fraction is 79.7%, 10.3%, 10.0% to the core, radial blanket and bypass, respectively.

2. Overview

The outlet plenum design must be evaluated for the transient and steady state operations for the MONJU plant. During steady state conditions, temperature fluctuations arising from the temperature difference among the subassemblies must be mainly evaluated. Flow and power variation between individual subassemblies, particularly at the core fuel/control rod, lead to significant temperature difference between the streams of sodium emerging from adjacent subassemblies. These streams of sodium at differing temperature persist for a substantial distance down-stream and, since the flow is unsteady, any structure immersed in this flow is subjected to fluctuating sodium temperatures. This phenomenon, known as thermal striping, caused the surface temperature of the structure to fluctuate, leading to high-cyclic thermal fatigue, and possible surface crack formation and propagation.

A comprehensive experimental program has been conducted in Japan to address the problem of Monju outlet plenum mixing during steady state conditions. Test was performed with different test rigs mainly using water as the test fluid and in future additional

test using sodium has been planned to be conducted.

3. Design Methodology

From the thermal-hydraulic design for core subassemblies, there presume to be fairly large temperature difference between the coolant from the adjacent subassemblies. So thermal striping must be taken into account for the design of the upper core structure which is positioned just above the fuel and blanket subassemblies and is under the severe thermal condition. Design method for thermal striping which make assure of structural reliability is as followed.

Fig. 4 shows how to evaluate thermal striping for the upper core structure (UCS). At the first, outlet coolant temperature at the fuel subassemblies and the control rod are individually given from the result of core design analysis as shown in Table 1. Maximum temperature of 610°C is settled from the analysis data at the outlet of core fuel subassembly in zone I in consideration of safety margin in engineering. Minimum temperature of 430°C is settled at the outlet of backup safety rod. The temperature difference between adjacent subassemblies which differ from each field of the core has been evaluated conservatively as the maximum temperature difference ($\Delta T' = 180°C$). The thermal striping condition is evaluated as the temperature and its fluctuation amplitude and frequency which are given from the thermal striping tests data.

The coolant temperature is considered to change the fluctuation amplitude and frequency as going up to the upper plenum from the subassemblies through the upper core structure. Table 2 shows the design conditions for thermal striping at various points of the upper plenum structure which is shown in Fig. 5. As the results of test, relatively large amplitude were observed at the lower part of the upper core structure. The fluctuations which are the result of wave motion and turbulent eddies at the interface have a amplitude of nearly 80% of the overall fuel $\Delta T'$ and have a dominant frequency of about $1 \sim 5$ Hz.

For the evaluation of thermal striping at the upper core structure, the temperature amplitude, ΔT is calculated by the temperature fluctuation factor, α which is given by the results of the water test and the water-sodium convertion factor, β which shall be given by comparing sodium test data with water one and overall fuel temperature difference, $\Delta T'$, as follows:

$$\Delta T = \alpha \times \beta \times \Delta T'$$

The high thermal conductivity of sodium tends to make gentle the temperature gradient. The magnitude and frequency of thermal fluctuation are found to be less severe in sodium than in water. Since it is evident that using water data as a basis for the thermal design of components located near the hot-cold interface will lead to a extremely conservative design, water-sodium convertion factor, β must be confirmed experimentary to make the

more rational design condition. As the results of the simple jet flow tests, the β value of approximately 80% is estimated now.

4. Design Accomodation

The temperature measurements obtained from the water test have provided the thermal boundary conditions required for calculating thermal stresses in Monju outlet plenum components. Thermal condition of the lower part of the upper core structure seems to be severe because of direct impingement of sodium flow from the core subassemblies. So, for the reduction of thermal stress, the use of protective INCONEL 718 for liners and other portions of the upper core structure has been considered. Temperature fluctuation amplitude at another portion of the reactor internal structures were observed to be so small that no problem has been identified which jeopardizes the structural integrity.

These striping evaluations are based on the core exit temperature analysis and test data which obtained from the tests by feature model and 1/3 sector model of reactor upper plenum using water.

Fig. 6 provides a schematic diagram showing the relationships that have been established in this study between plenums having different type of test rig and opeating fluid. Tests have been performed with water and sodium using three types of test rig in order to decide the design conditions of thermal striping around

upper core structure during steady state conditions.

By using simple test rig which was not so perfectly simulated by the Monju feature but selected as the simplist feature model to be required, the fundamental experiment was conducted to investigate the difference between sodium and water thermal properties. To utilize the experimental data for design, feature flow test and 1/3 sector flow test for the upper core structure was conducted to be simulated by the upper plenum geometry and steady state condition.

As the result of these tests data application, Monju upper core structure design condition have been fixed except for water-sodium convertion factor, β which shall be given by comparing feature flow test data with multi-jet flow test data.

Detailed discussion of these thermal striping tests shall be given in session A-2.

High temperature property tests for upper core structure material INCONEL 718 have been conducted to gain the structural intensity data for design which include the low and high fatigue data.

TABLE.1

Core Subassemblies Design Outlet Temperature

THERMAL CONDITION IN NORMAL OPERATION		TEMPERATURE(°C)
FUEL	HOT CHANNEL	610
	AVERAGE	550
CONTROL ROD	REGULATING ROD	440
	BACKUP SAFETY ROD	430

TABLE. 2 Thermal Striping Condition

PRELIMINARY

POINT	AMPLITUDE	FREQUENCY (Hz)	EVALUATION TEMPERATURE (°C)
LOWER PART OF FLOW STRAIGHTENER	0.7 ΔT′	5	610
INSTRUMENT WELL	0.1 ΔT′	3	610
FINGER	0.2 ΔT′	3	550
THERMAL BUFFER	0.2 ΔT′	3	580
FLOW STRAIGHTENER SUPPORT PLATE	0.3 ΔT′	5	580
CRD GRIPPER	0.6 ΔT′	3	550

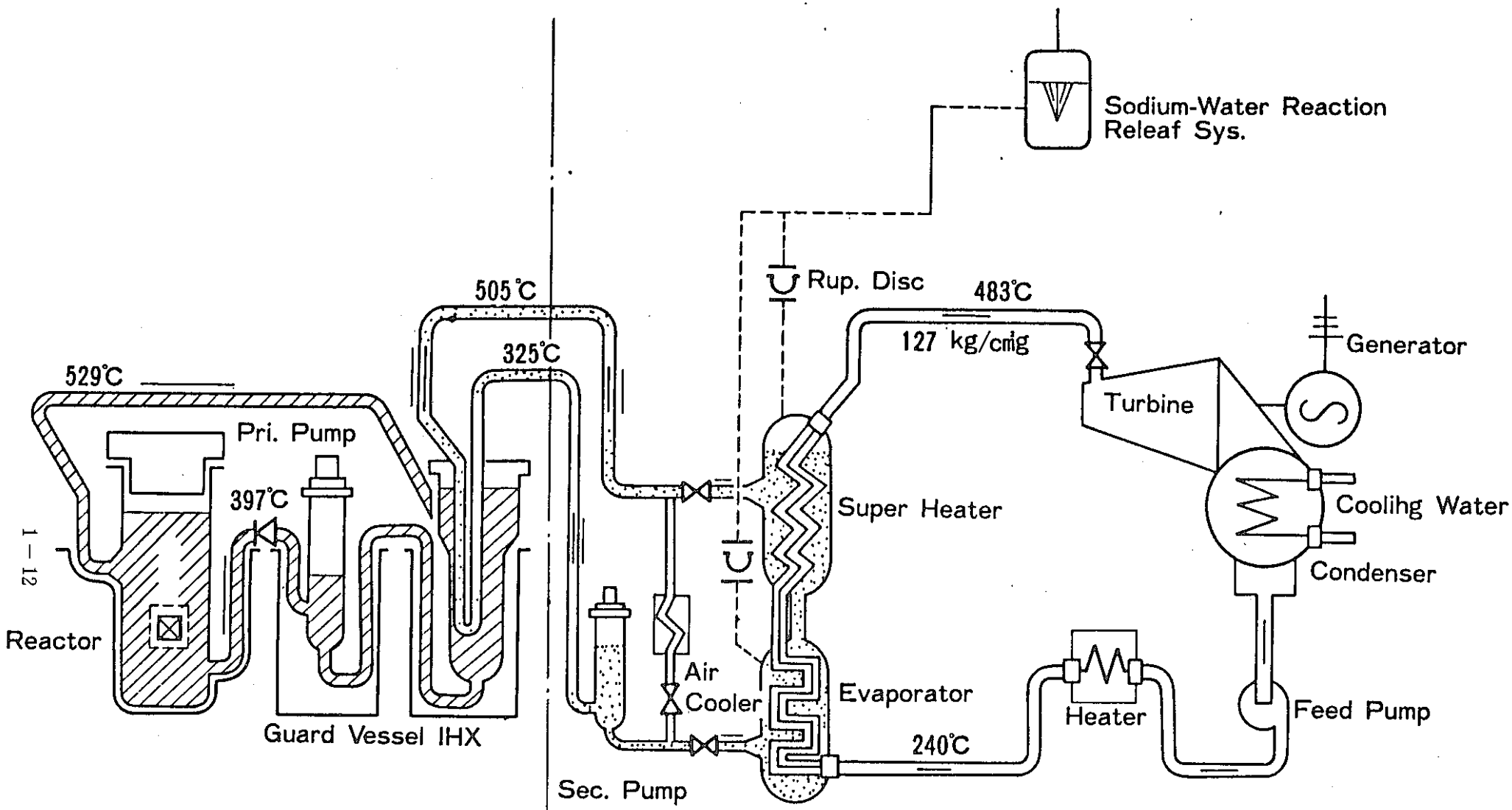

FIG.1 **Main System of MONJU**

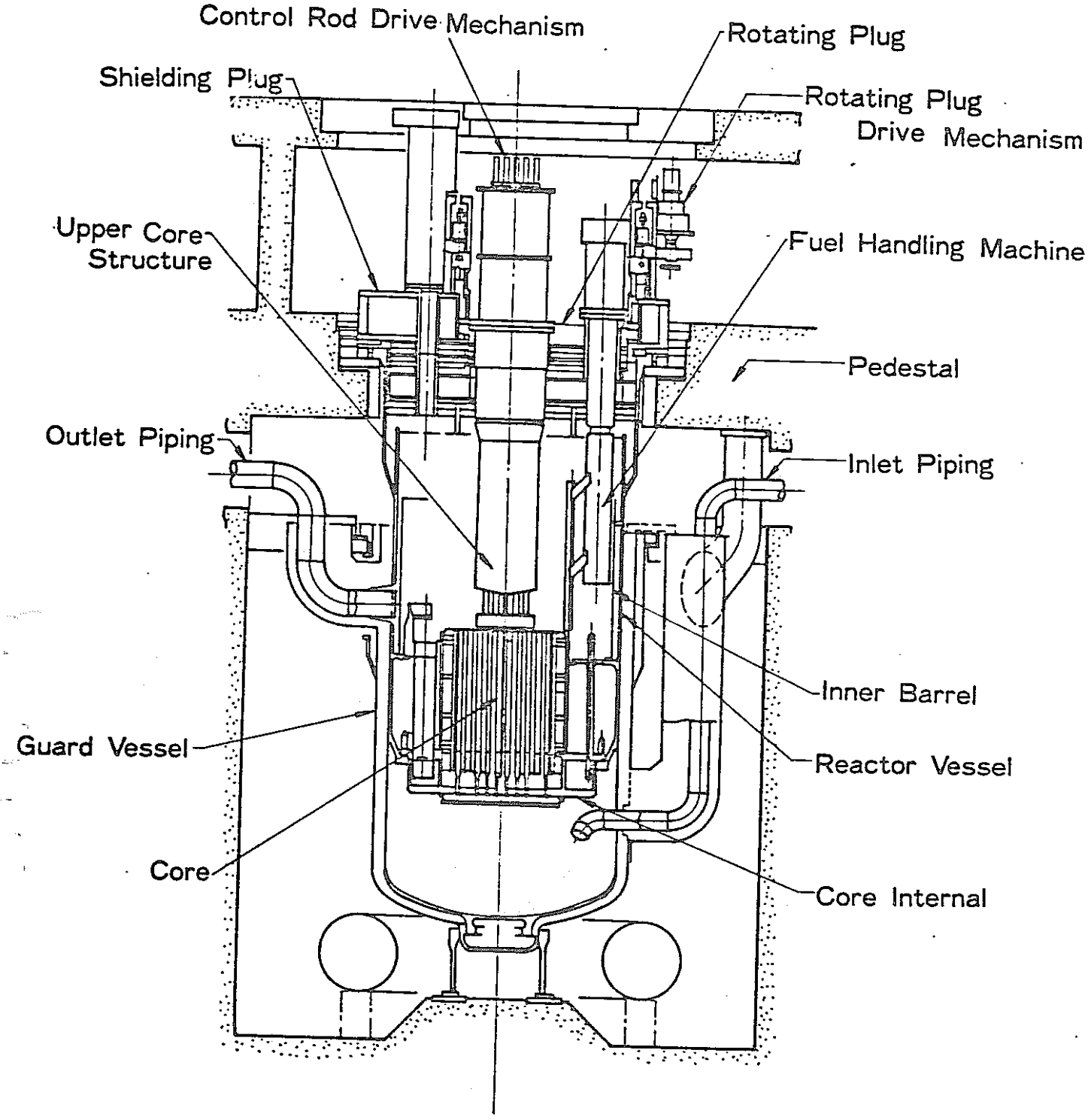

FIG.2 "MONJU" Reactor System

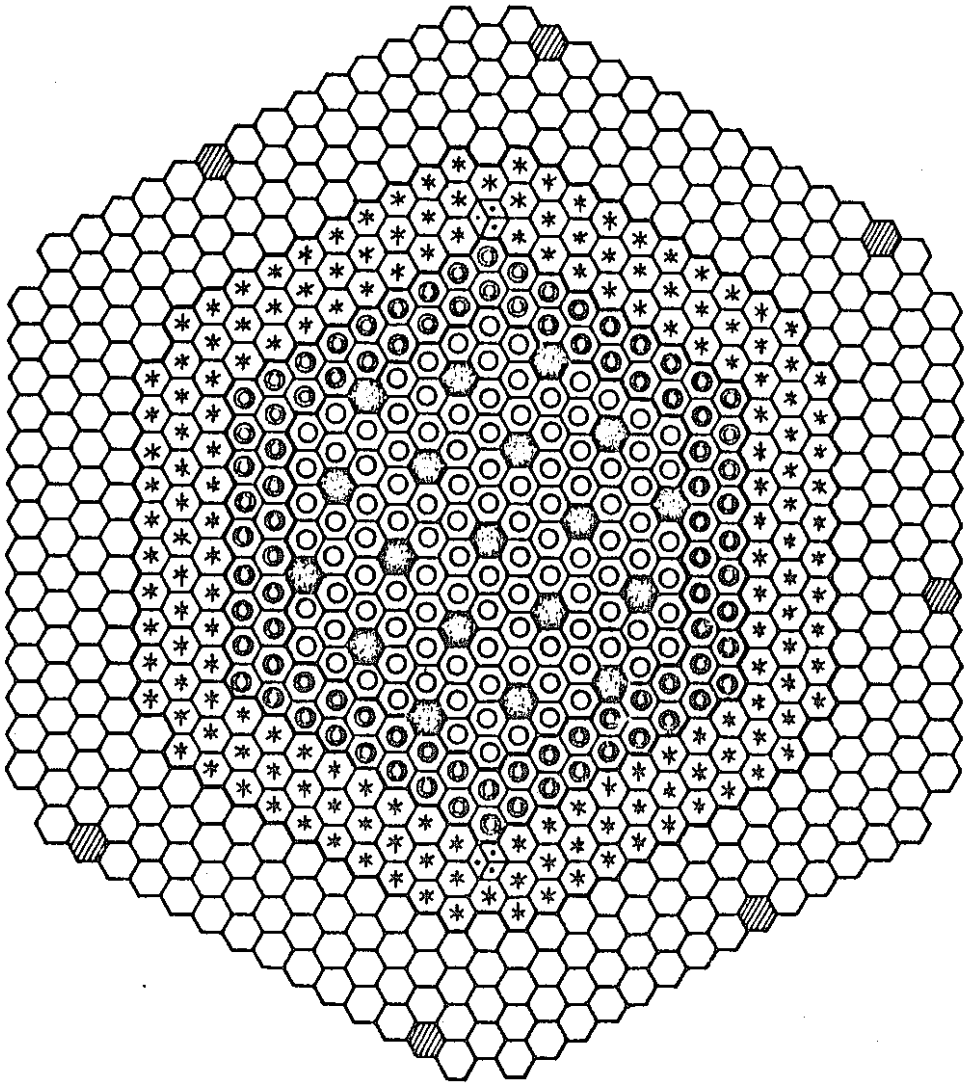

core elements		marks	quantities
core fuel—S/A	zone I		108
	zone II		90
radial blanket fuel S/A			172
control rod			19
neutron surce			2
neutron shielding			316
surveillance S/A			8

FIG.3 **Core Configuration**

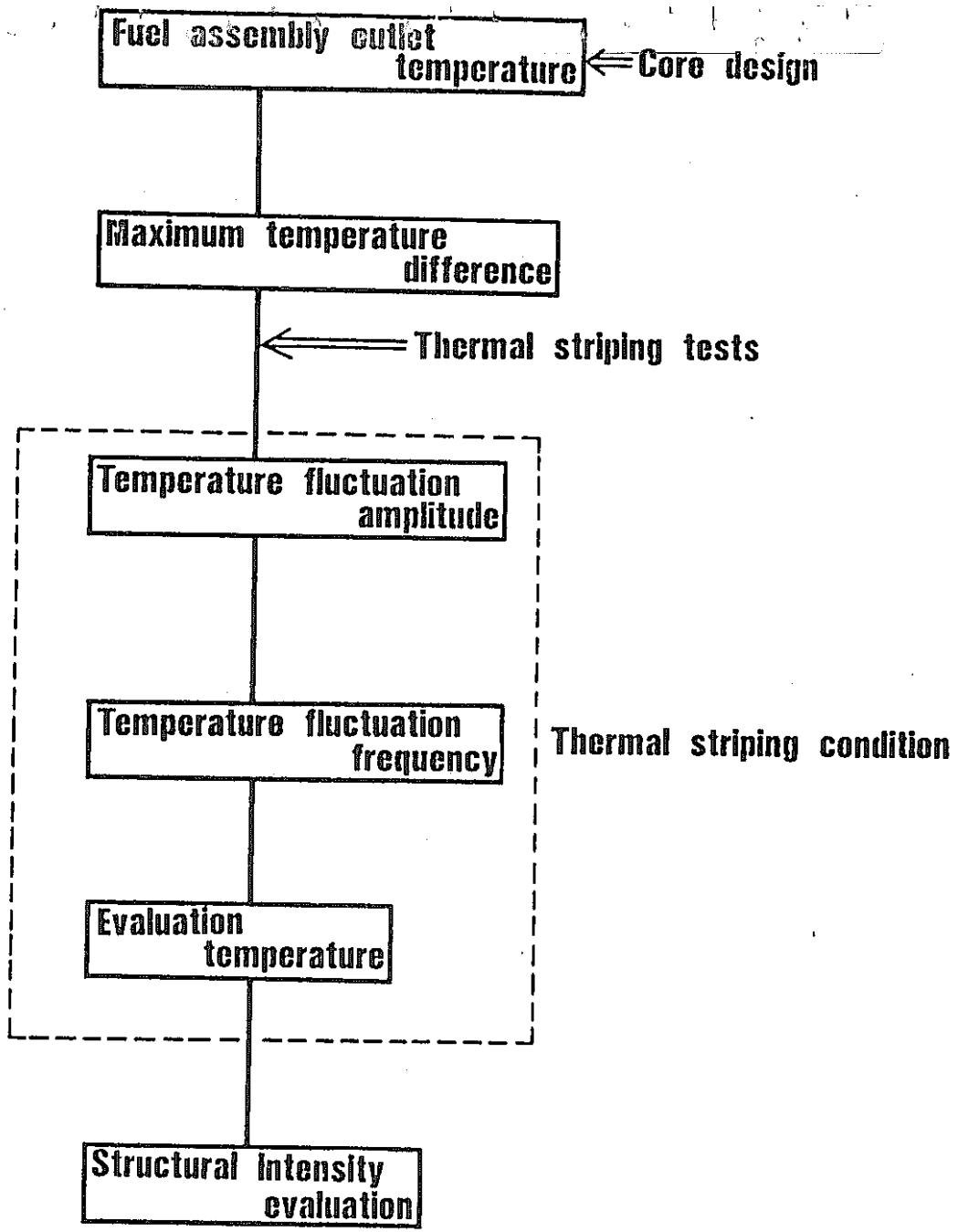

FIG.4 DESIGN SEQUENCE FOR THERMAL STRIPING

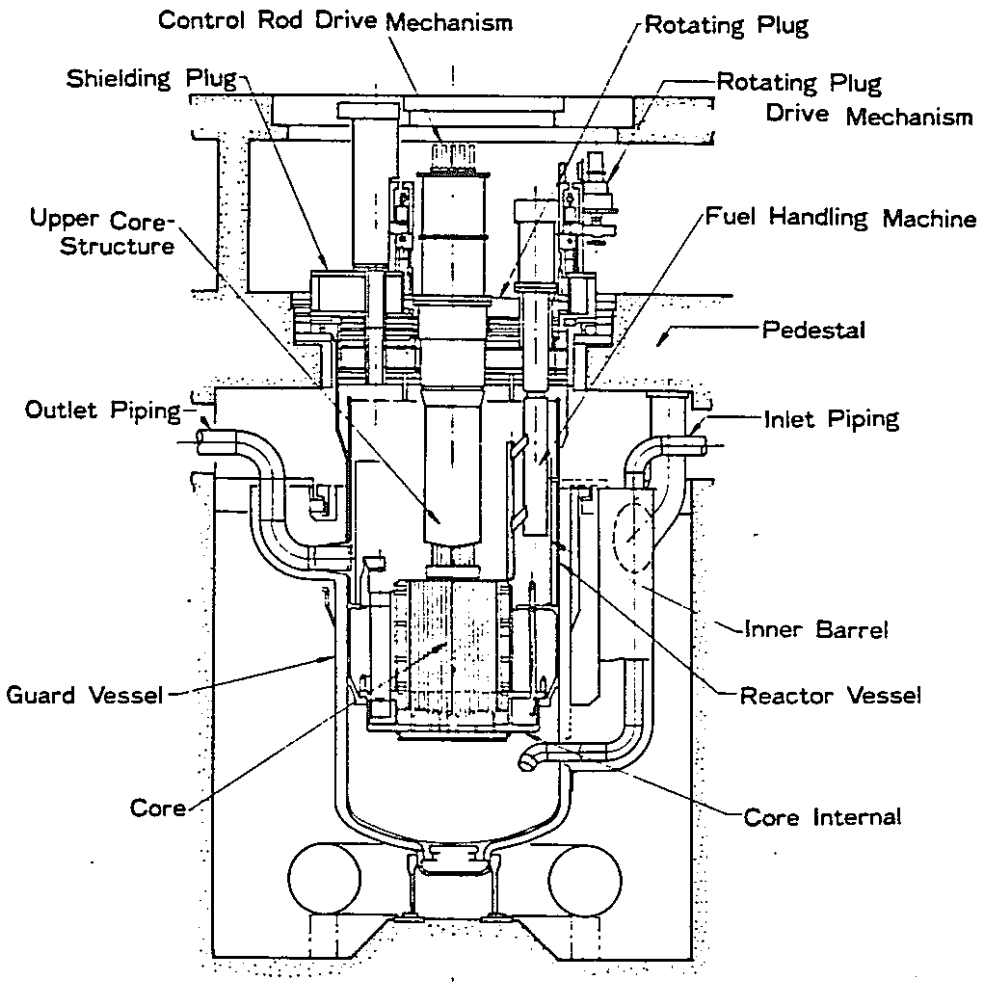

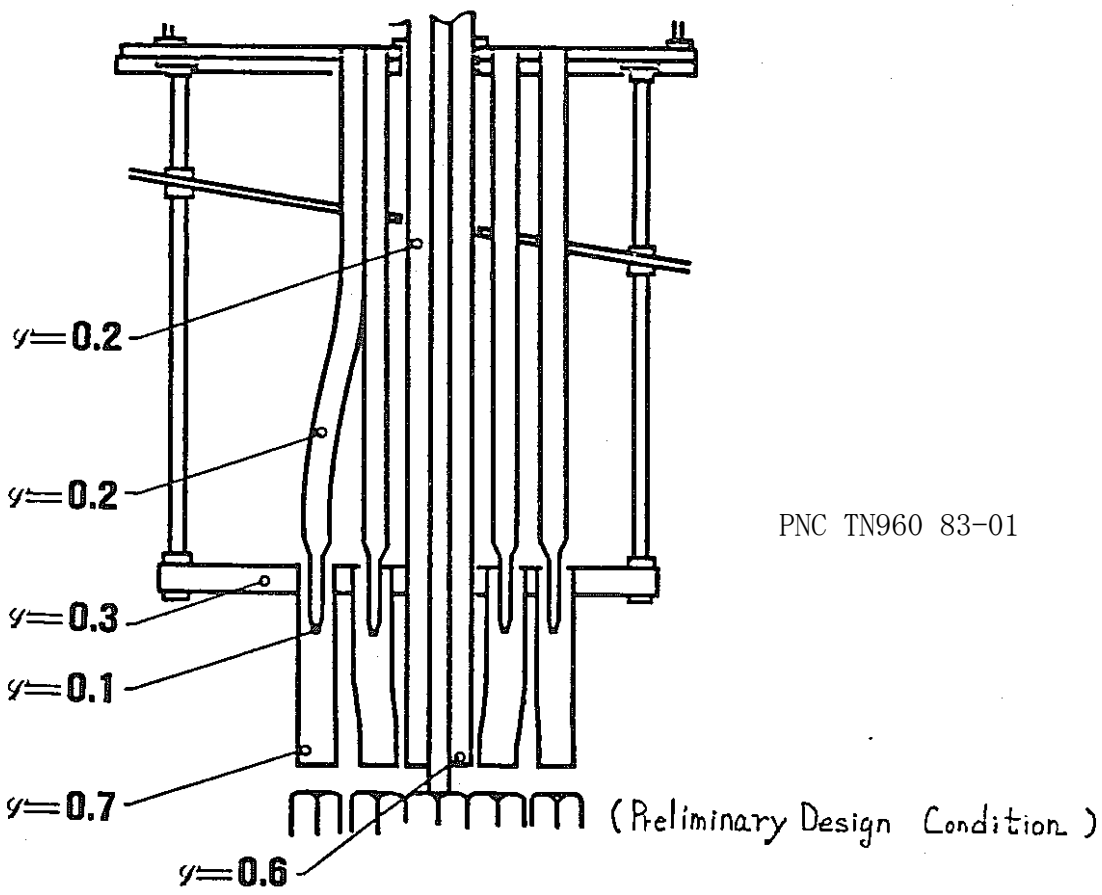

PNC TN960 83-01

FIG.5

TEMPERATURE FLUCTUATION AMPLITUDE

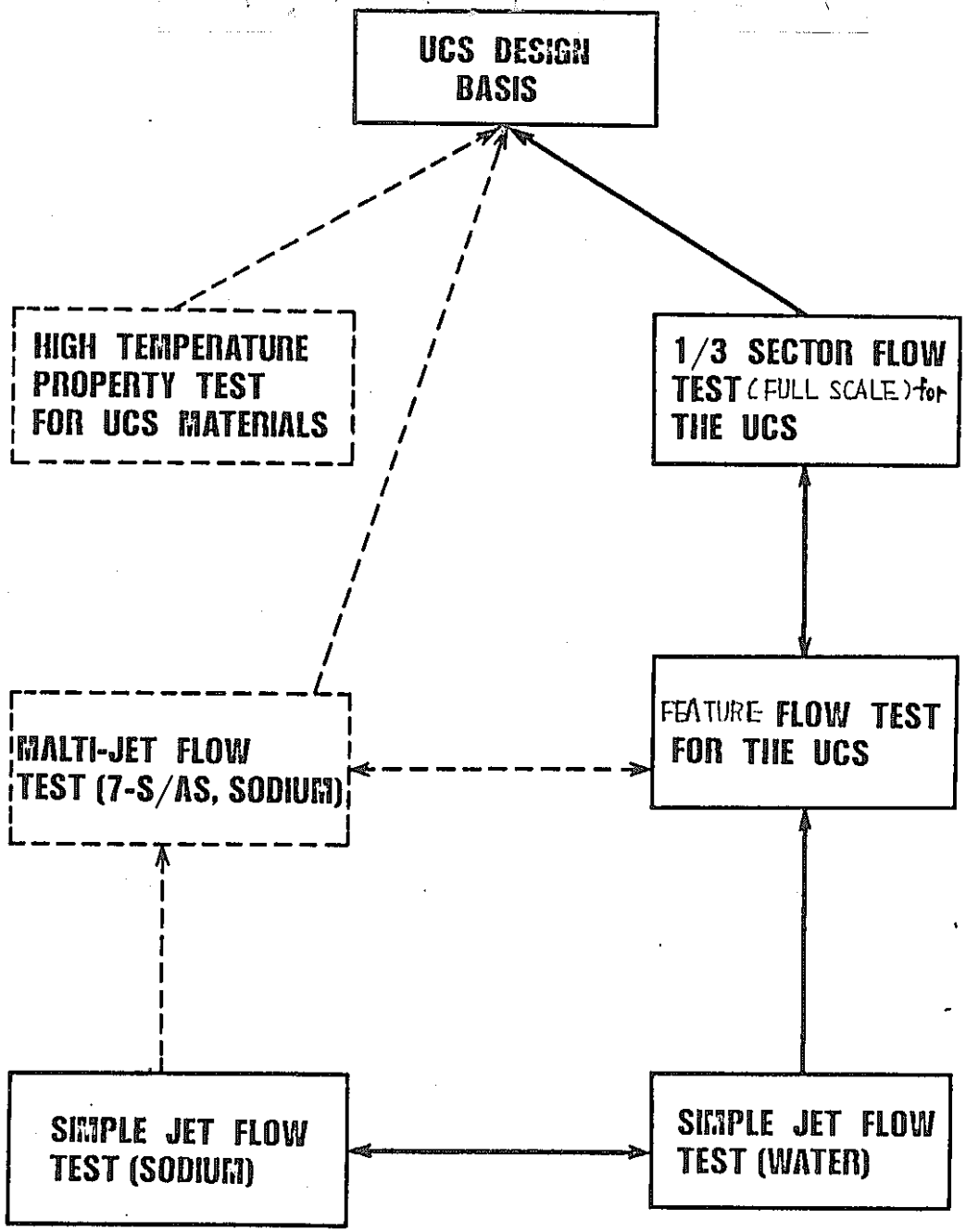

FIG. 6 THERMAL STRIPING TESTS AND DESIGN APPLICATION

EVALUATION OF WATER SIMULATION TEST RESULTS

ABSTRACT

Experimental investigations of Monju upper plenum temperature fluctuations during steady state conditions were conducted. The following test rigs were used in order to determine the design conditions of thermal striping around Upper Core Structure (UCS).

(1) Full scale feature model of UCS flow test rig using water

(2) Full scale 1/3 sector model of Monju upper plenum flow test rig using water

(3) Simple test rig with jet flow using water and sodium

Experimental results:

(1) The peak to peak thermal fluctuation is about 80% of the fuel/control rod ΔT, and is in the frequency range of 3-5 Hz at the lower part.

PNC TN960 83-01

(2) There are no significant differences between water tests and sodium tests in frequency, but the peak to peak amplitude in sodium tests is about 80% of that in water tests.

OBJECTIVES

(1) To clarify thermal striping phenomena around UCS of Monju by using water test facilities (full scale feature model of UCS and full scale 1/3 sector model).

(2) To compare thermal striping phenomena between water and sodium flow tests by using simple test rig with jet flow.

Table A2 - 1 Test Conditions

Test Rigs	Scale	Fluid	Temperature	Flow Rate	
				Fuel Assembly	Control Rod Assembly
Feature Model of UCS Flow Test Rig	Full Scale	Water	Hot 54-63°C Cold 10-30°C	1.4 m³/min	0.78 m³/min
1/3 Sector Model of the Monju Upper Plenum Flow Test Rig	Full Scale	Water	Hot 54-63°C Cold 10-30°C	1.4 m³/min	0.78 m³/min
Simple Test Rig with Jet Flow	Inner Flow: 21.4mm dia. Outer Flow: 34.0mm I.D. 41.2mm O.D.	Water	Hot 84-90°C (Inner Flow) Cold 40-46°C (Outer Flow)	Inner Flow: 1.0 m/s 0.5 m/s 0.2 m/s Outer Flow: 1.0 m/s 0.5 m/s 0.2 m/s	
		Sodium	Hot 296-325°C (Inner Flow) Cold 265-285°C (Outer Flow)		

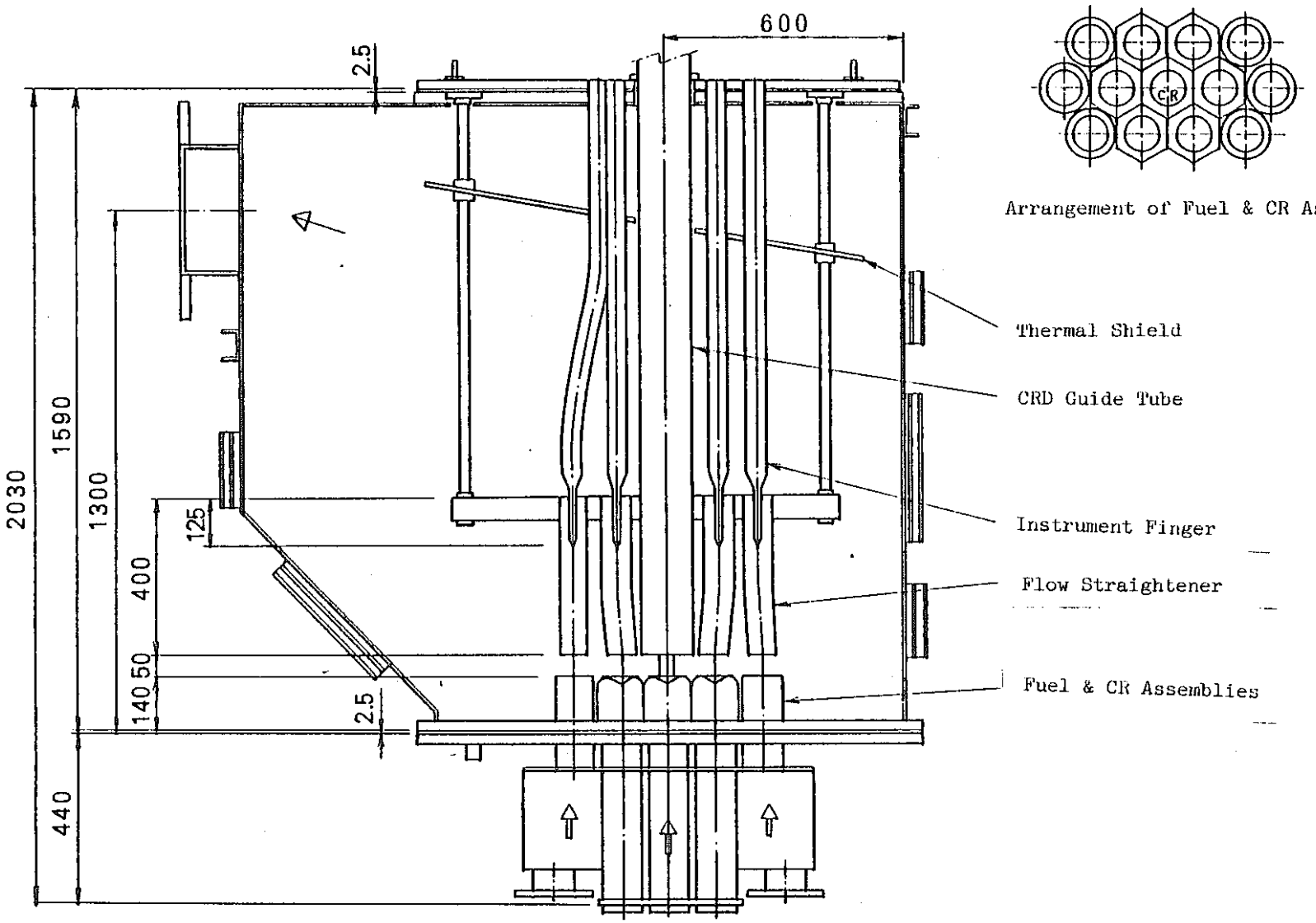

Arrangement of Fuel & CR Assemblies

Fig. A2 - 1 Full Scale Feature Model of UCS Flow Test Rig

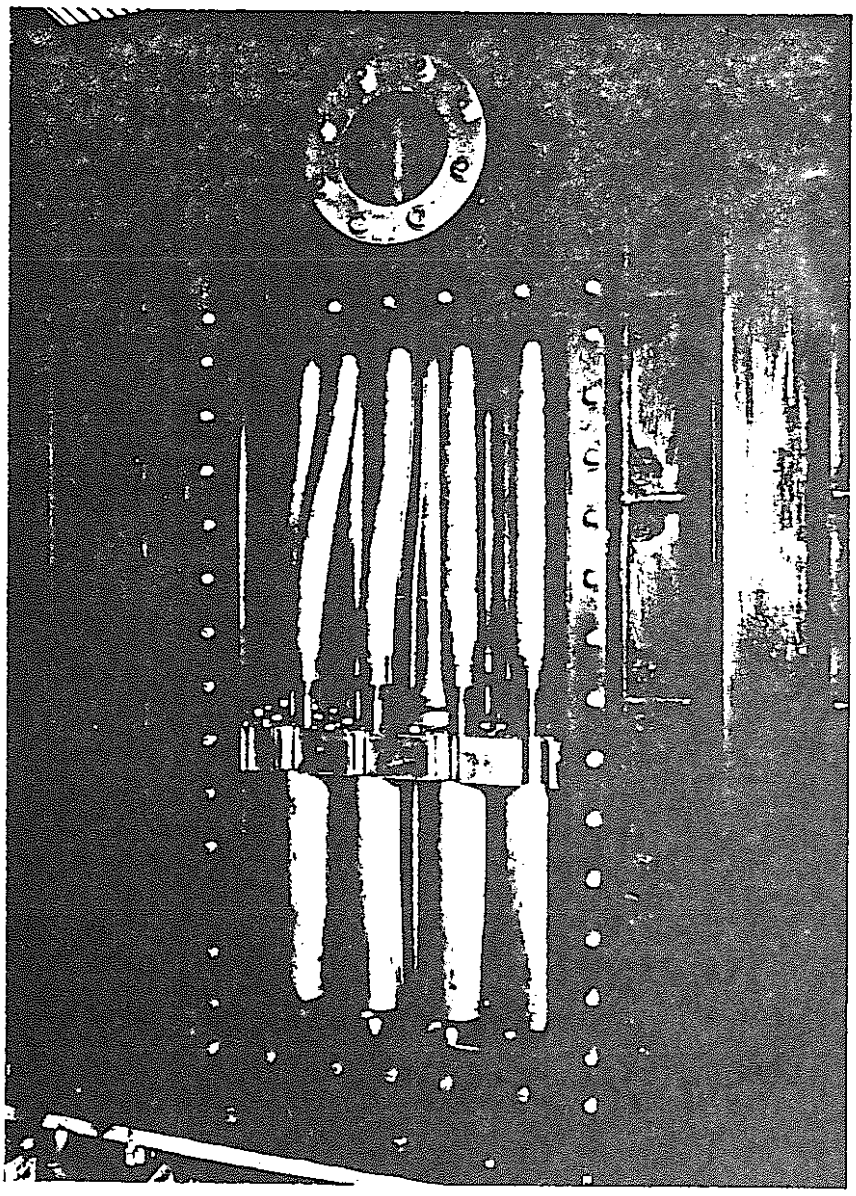

Fig. A2-2 Full Scale Feature Model of UCS Flow Test Rig Using Water

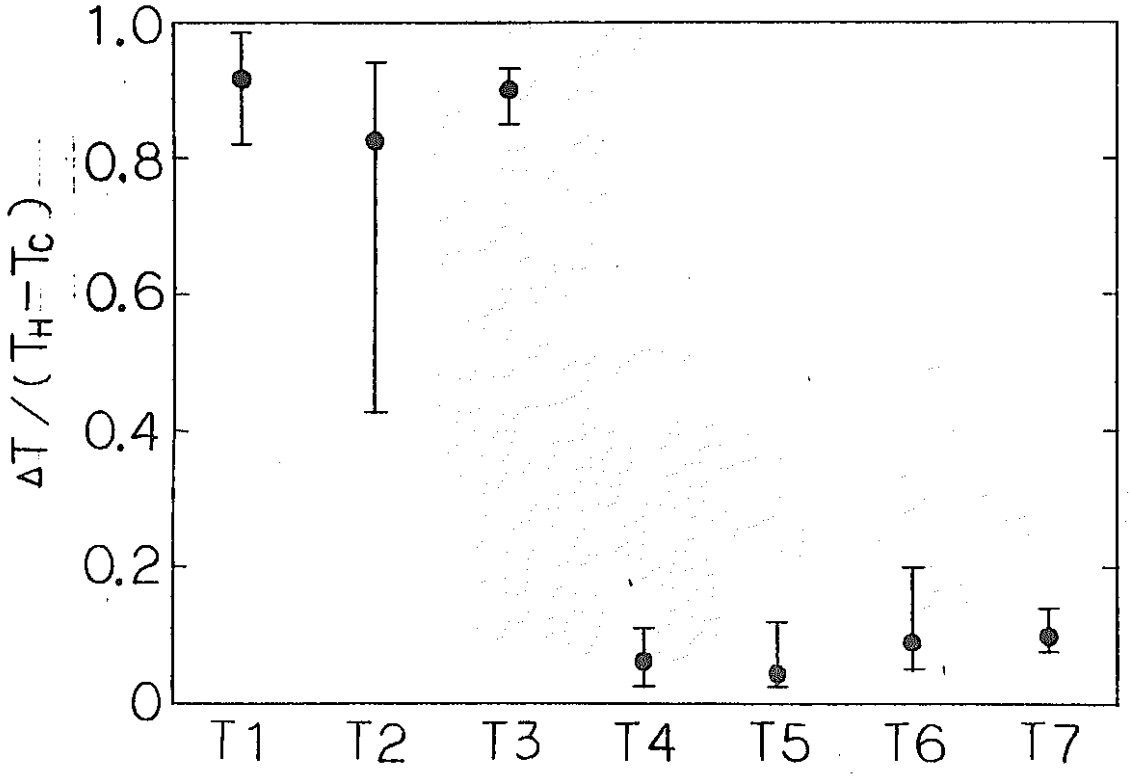

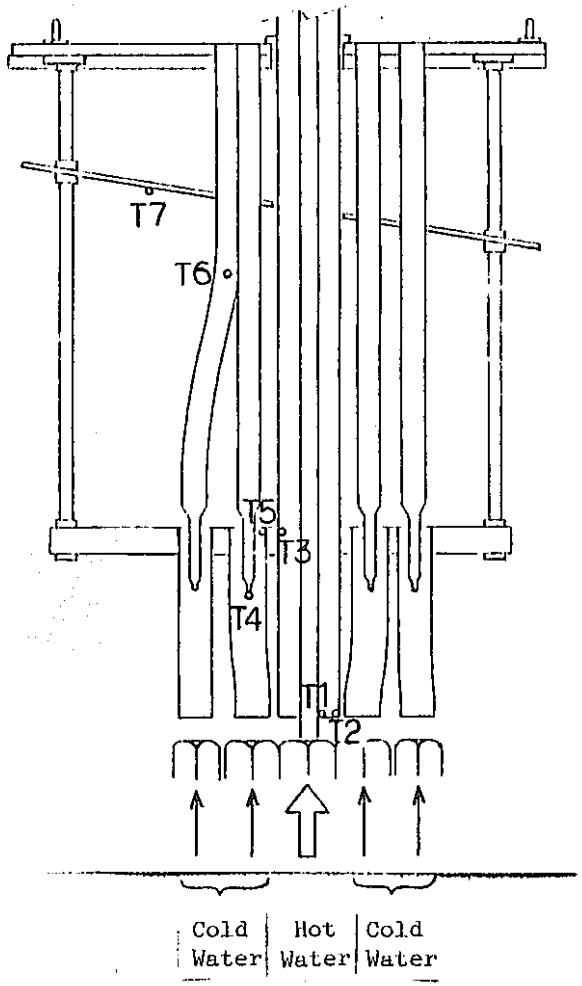

Fig. A2-3 Thermal Striping in the Feature Model of UCS Using Water

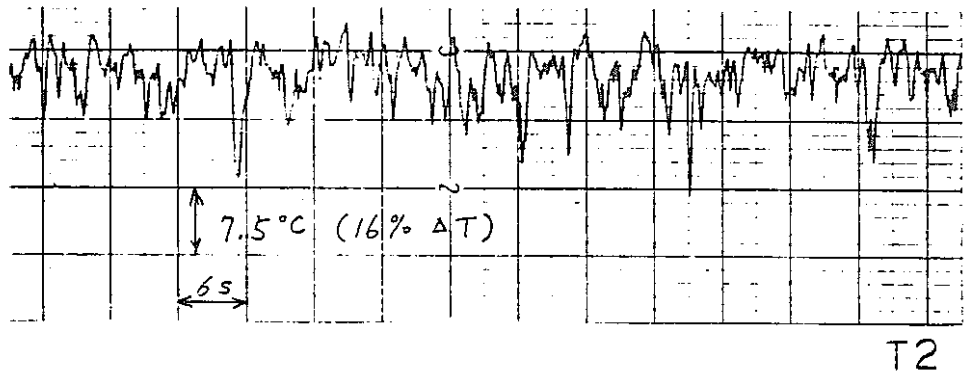

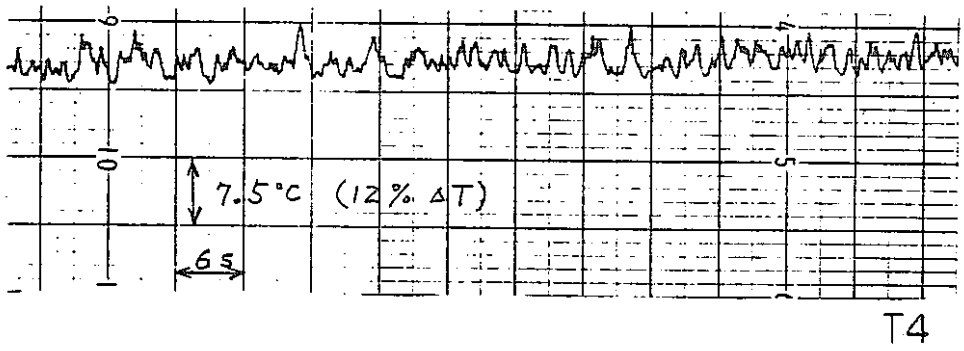

Fig. A2 - 4 Steady State Temperature-Time Plots in Full Scale Feature Model of UCS Using Water

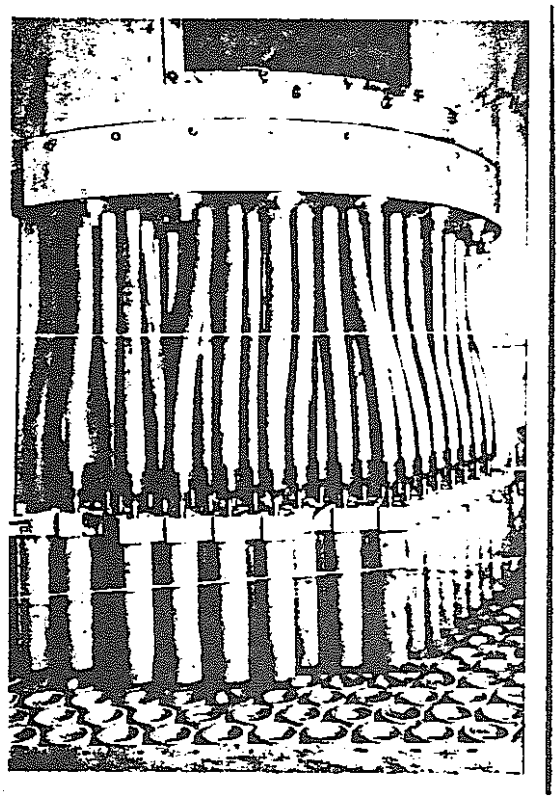

Fig. A2-5 Lower Part of UCS 1/3 Sector Mockup

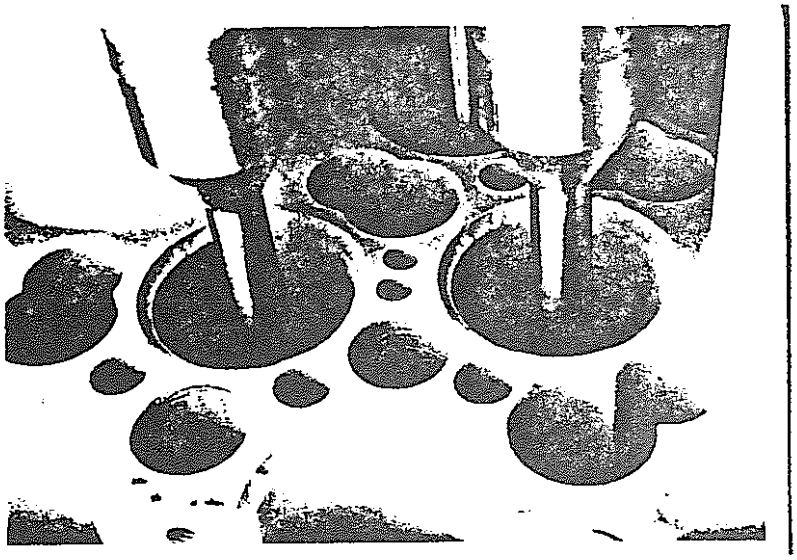

Fig. A2-6 Flow Straightener Support Plate of UCS 1/3 Sector Mockup

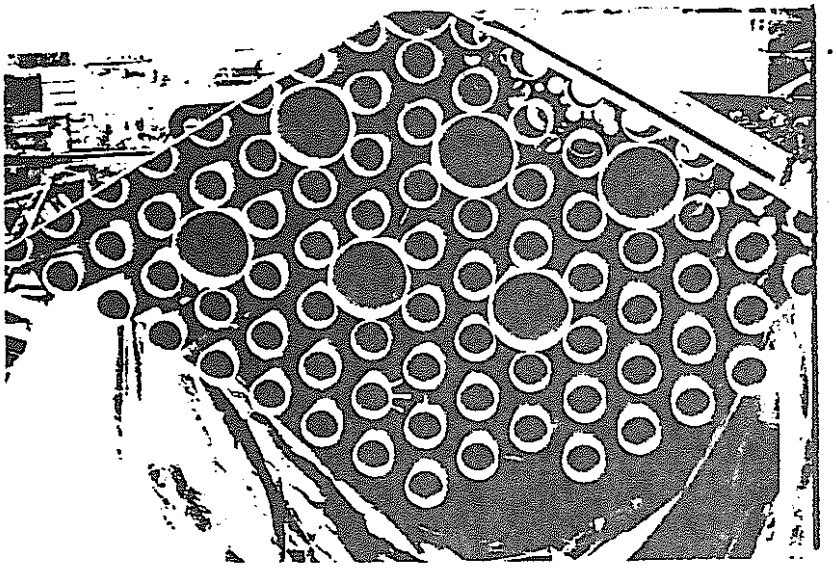

Fig. A2-7 Lower End View of UCS 1/3 Sector Mockup

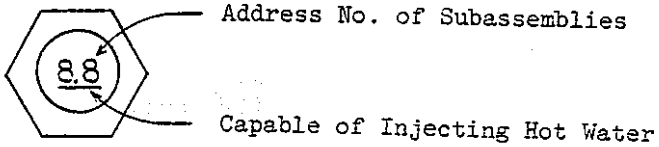

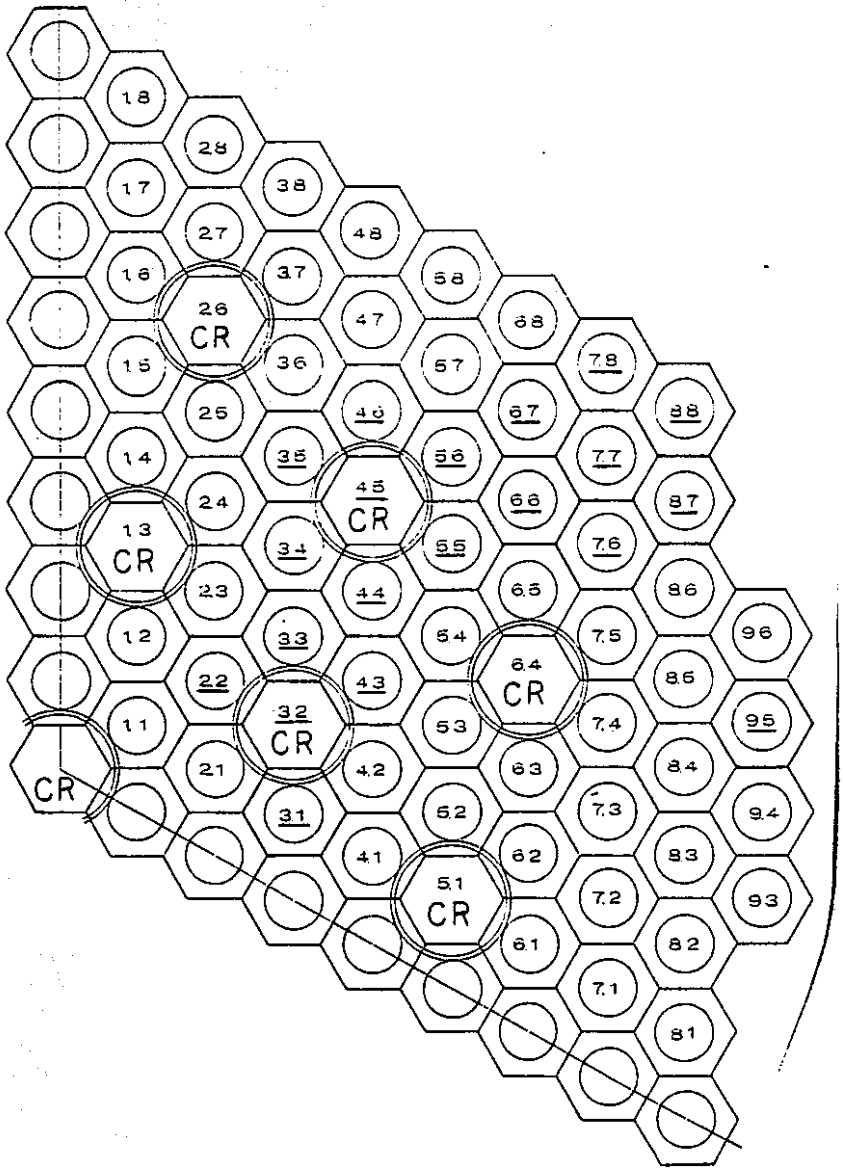

Fig. A2-8 Address Definition of Subassemblies

Table A2-2 Standard Deviation of Temperature Re se around UCS

SUBASSEMBLY FROM WHERE HOT WATER INJECTED	(4,5)		(3,3)	(3,4)	(5,6)	(4,4)	(3,5)	(6,6)	)	(7,7)	σmax
TEST No.	1	2	3	4	5	6	7	8		10	
T 1	2.6	3.0	0.4	1.2	0.7	13.3	0.7	0.3	0.6	0.4	13.3
T 2	1.0	0.8	1.2	9.1	6.2	6.0	0.5	0.9	0.8	0.4	9.1
T 3	0.3	0.3	2.6	6.3	0.4	7.1	0.3	0.3	0.3	0.4	7.1
T 4	1.6	2.0	0.5	0.9	4.9	1.2	4.6	0.4	3.4	0.4	4.9

PNC TN960 83-01

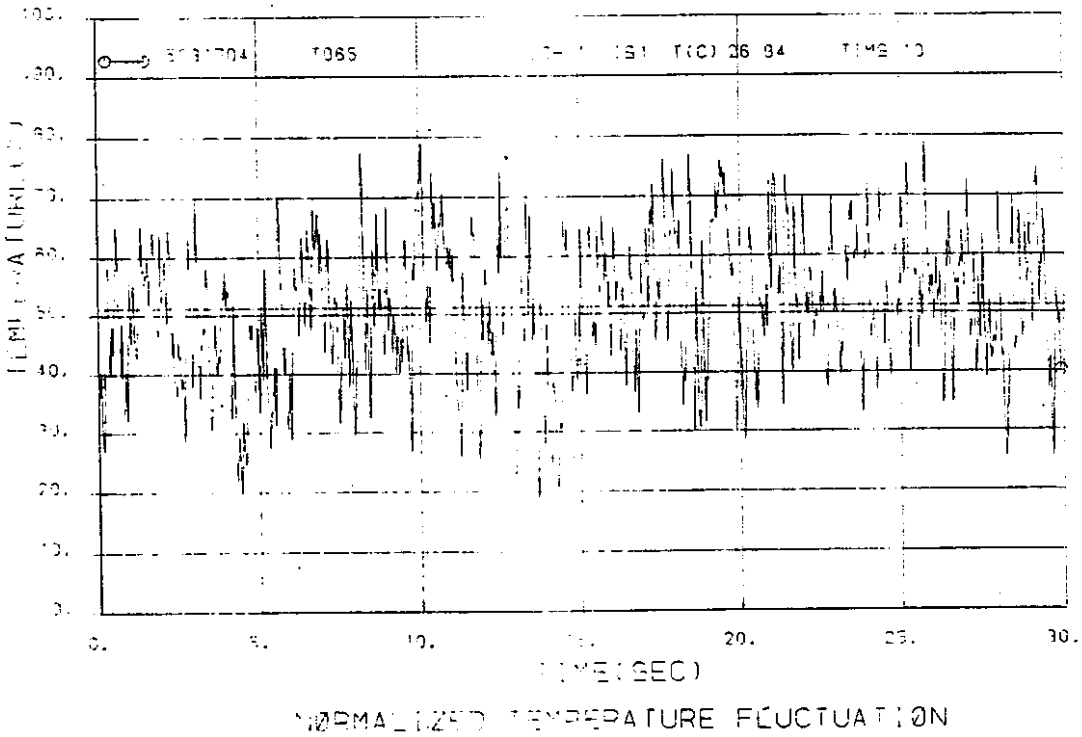

Fig. A2-9 Steady State Temperature-Time Plots in Full Scale 1/3 Sector Model Using Water (T1)

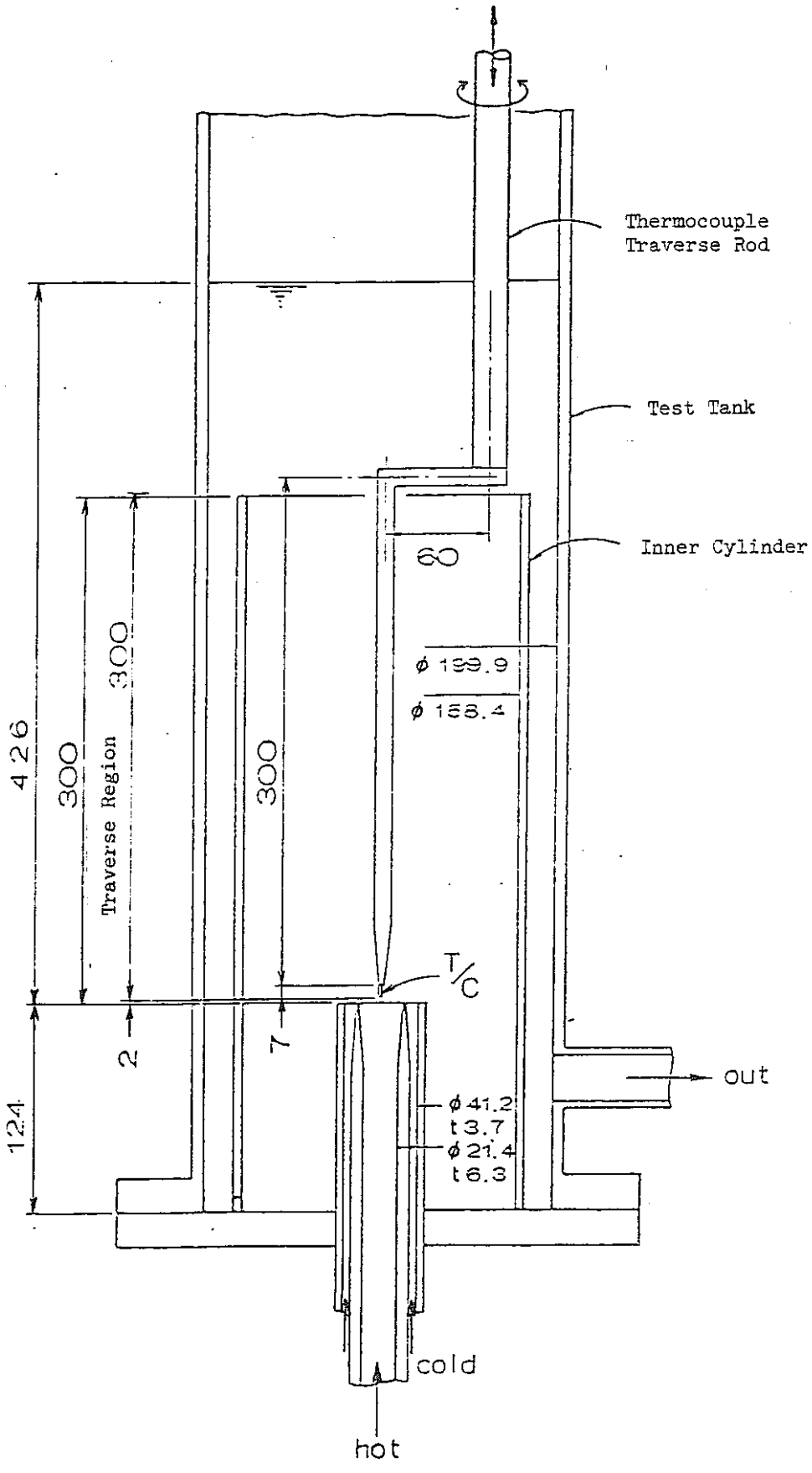

Fig A2-10 Simple Test Rig with Jet Flow Using Water and Sodium

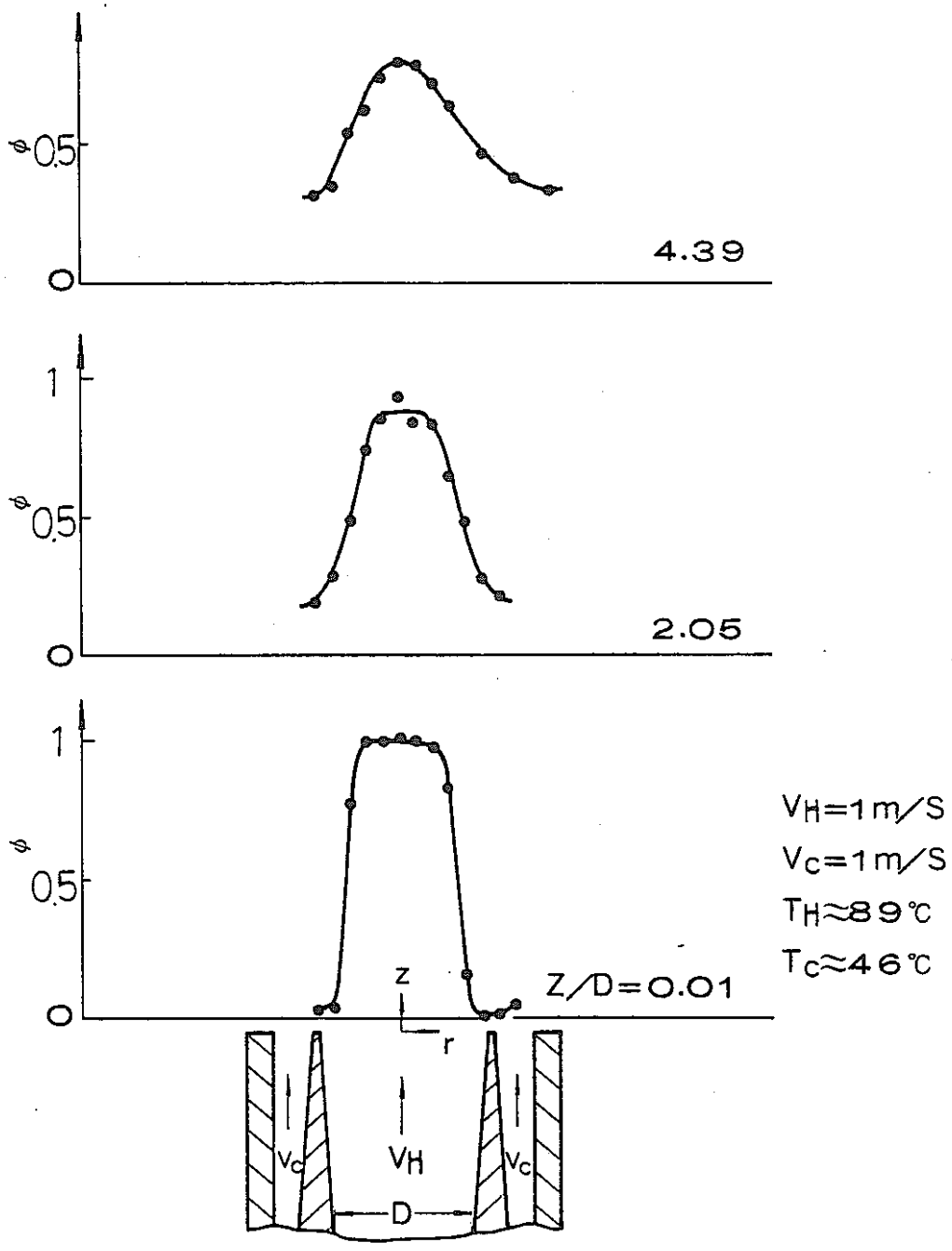

Fig. A2-11 Temperature Profile in Simple Test Rig with Jet Flow Using Water

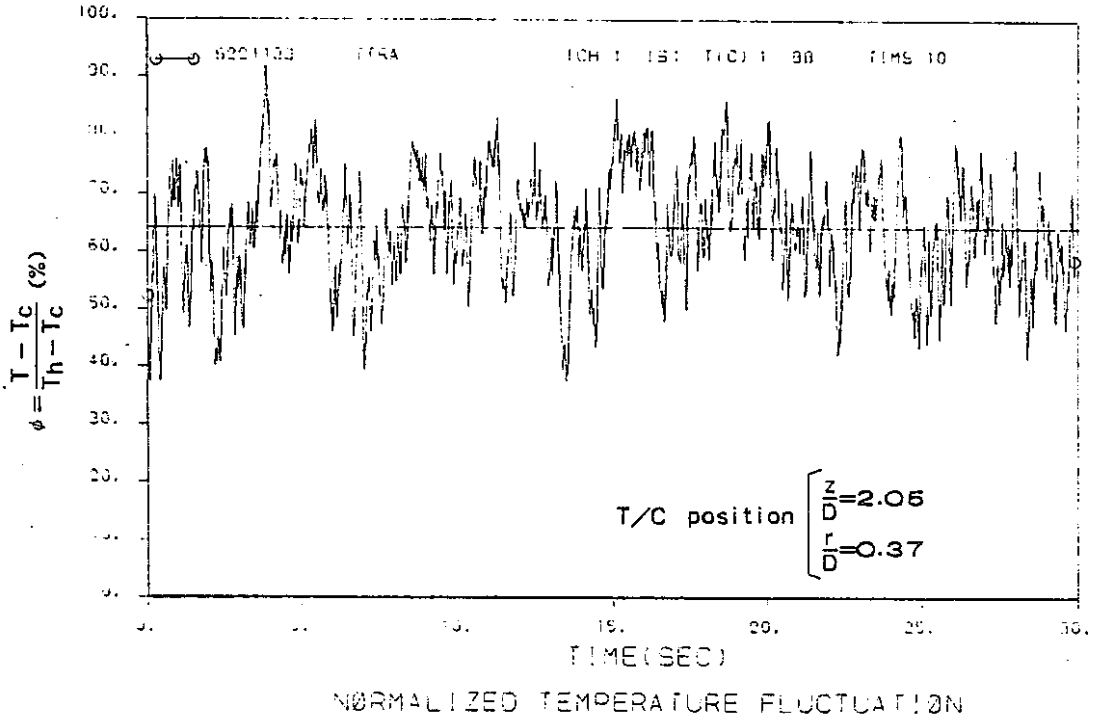

WATER (VH=1m/S, Vc=1m/S, TH=89℃, Tc=46℃)

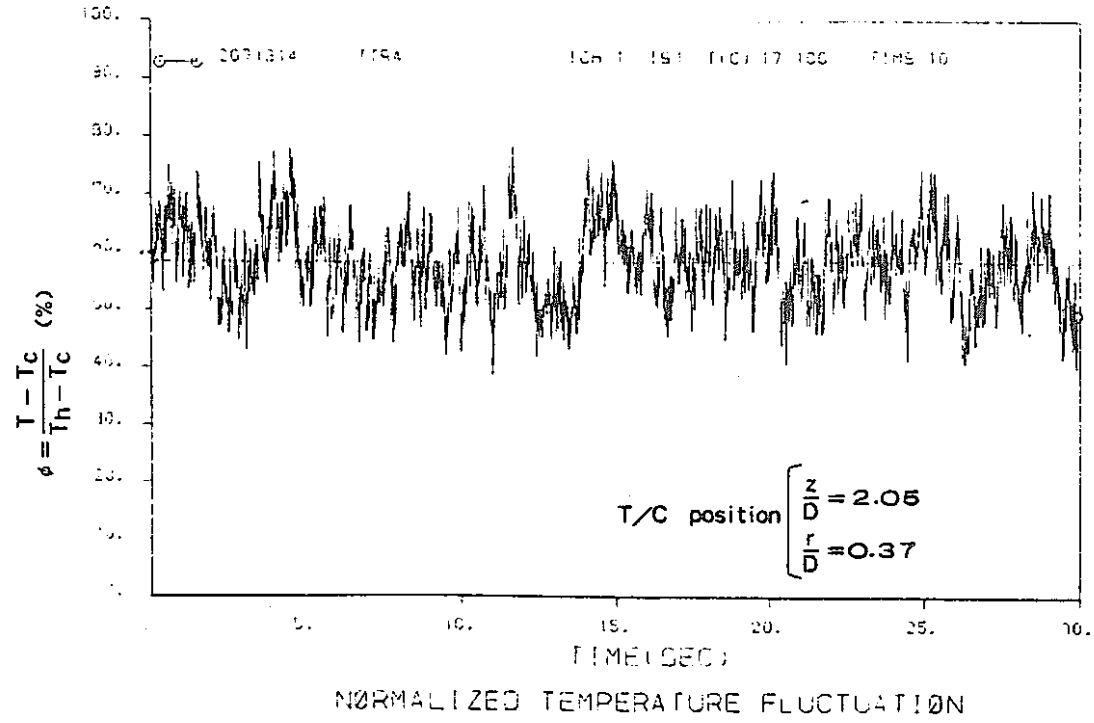

Sodium (VH=1m/S, Vc=1m/S, TH=314℃, Tc=286℃)

Fig. A2-12 Steady State Temperature-Time Plots in Simple Test Rig with Jet Flow

CONCLUSION

(1) The peak to peak thermal fluctuation is about 80% of the fuel/control rod ΔT, and is in the frequency range of 3-5 Hz at the lower part of the flow straightener.

(2) Good agreement is obtained between the feature model of UCS and 1/3 sector model tests.

(3) There are no significant differences betwwen water and sodium flow tests by using simple test rig with jet flow. These results are consistent with those of mixing tee tests.

A-3 HIGH-CYCLE THERMAL FATIGUE ANALYSIS

ABSTRACT

High frequency sodium temperature fluctuations in the LMFBR reactor upper plenum above the core region may result in high cycle fatigue damage in the components before the expected reactor service life. This problem, known as thermal striping, is one of the concerns in the MONJU design, and the application of a cladding having a high cycle fatigue strength, such as INCONEL 718, is being considered to protect the surface of the components.

In this report, a thermal stress due to temperature fluctuation was analyzed using a flat plate model with a cladding. The analyzed results were put in the form of a stress chart to calculate a peak stress and a secondary stress for SUS 316 and INCONEL 718. This enables one to make a quick evaluation of the expected fatigue life of such materials.

A 3

HIGH CYCLE THERMAL FATIGUE ANALYSIS

THERMAL STRESS INDUCED IN THE FLAT PLATE DUE TO FLUID TEMPERATURE FLUCTUATION

Analytical Model for Stress Calculation

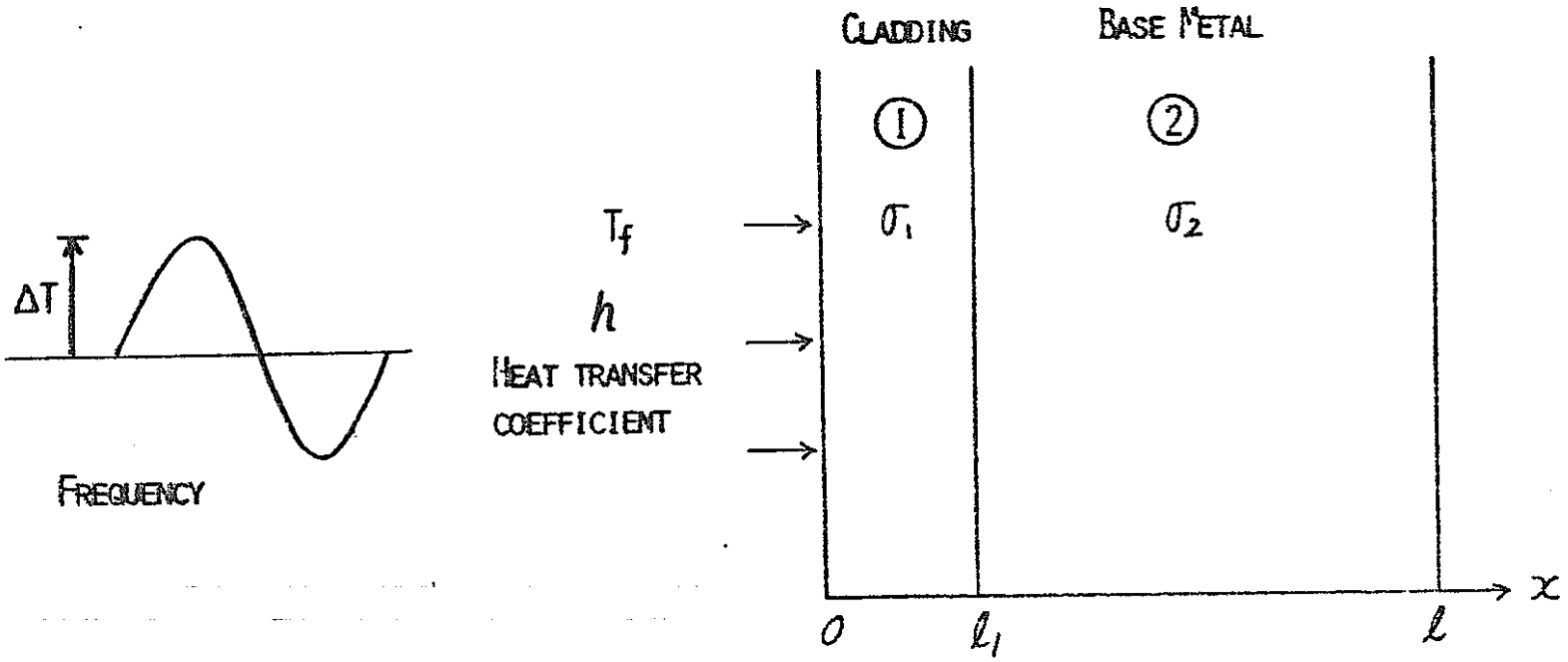

Fig. A3-1 Stress Calculation Model

ANALYTICAL MODEL FOR TEMPERATURE CALCULATION IN THE PLATE

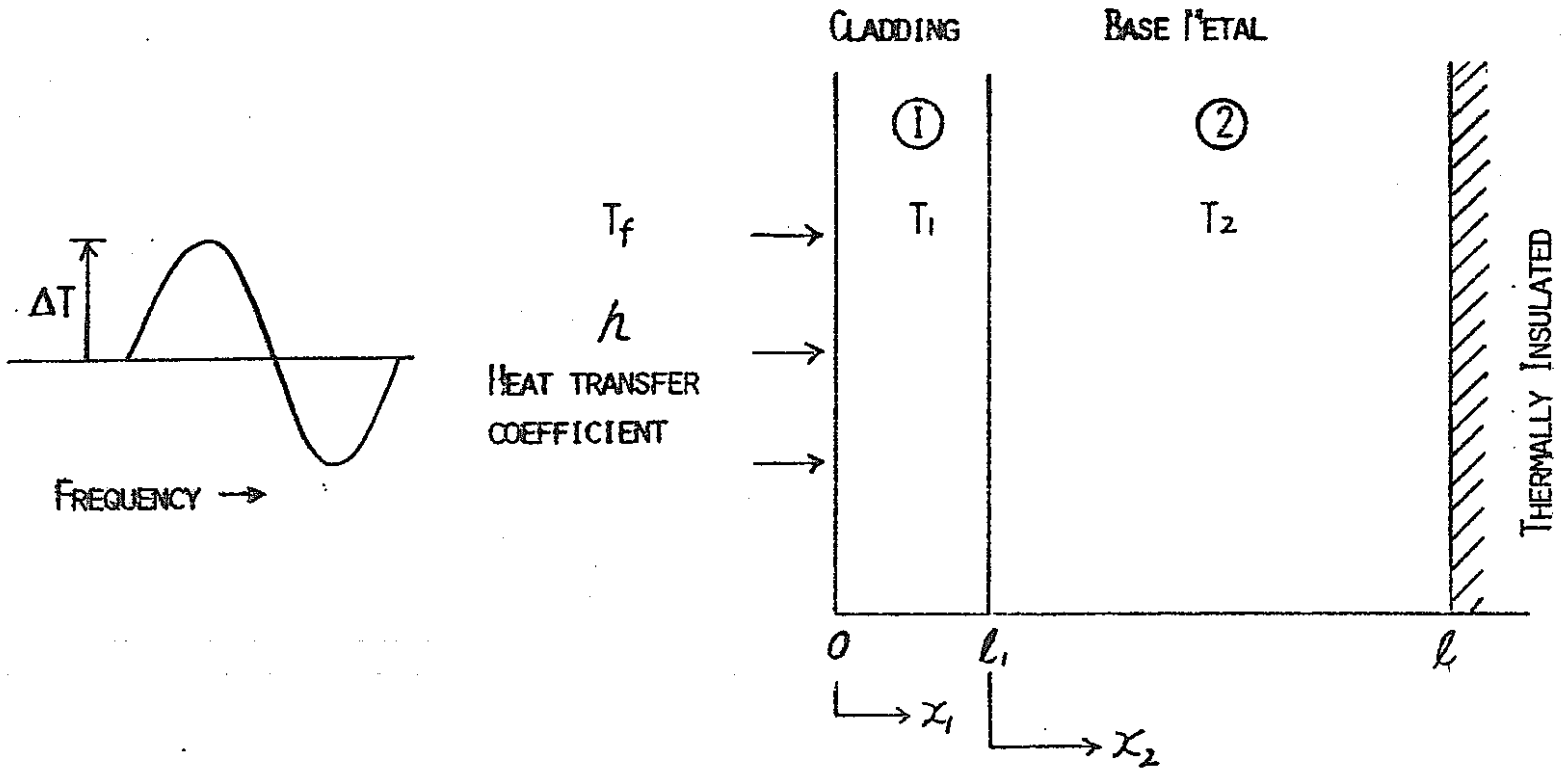

FIG. A3-2 TEMPERATURE CALCULATION MODEL

GOVERNING EQUATIONS FOR STRESS CALCULATION:

$$\varepsilon_1 = \frac{1-\nu_1}{E_1}\sigma_1 + \beta_1 T_1 \qquad 0 \le x \le \ell_1$$

$$\varepsilon_2 = \frac{1-\nu_2}{E_2}\sigma_2 + \beta_2 T_2 \qquad \ell_1 \le x \le \ell$$

WHERE E : YOUNG'S MODULUS

ν : POISSON'S PATIO

β : LINERAR EXPANSION COEFFICIENT

STRESS SOLUTION:

$$\sigma_1 = \frac{E_1}{1-\nu_1}\left\{\frac{1-\nu_2}{E_2(\ell-\ell_1)} S_2 + \frac{\beta_2}{\ell-\ell_1}\int_{\ell_1}^{\ell} T_2\, dx_2 - \beta_1 T_1\right\}$$

$$\sigma_2 = \frac{E_2}{1-\nu_2}\left\{\frac{1-\nu_2}{E_2(\ell-\ell_1)} S_2 + \frac{\beta_2}{\ell-\ell_1}\int_{\ell_1}^{\ell} T_2\, dx_2 - \beta_2 T_2\right\}$$

WHERE

$$S_1 = \int_0^{\ell_1} \sigma_1\, dx$$

$$S_2 = \int_{\ell_1}^{\ell} \sigma_2\, dx$$

GOVERNING EQUATIONS FOR TEMPERATURE CALCULATION:

$$\frac{\partial T_1}{\partial t} = a_1 \frac{\partial^2 T_1}{\partial x_1^2} \qquad 0 \le x_1 \le \ell_1$$

$$\frac{\partial T_2}{\partial t} = a_2 \frac{\partial^2 T_2}{\partial x_2^2} \qquad 0 \le x_2 \le \ell_2$$

B.C. (1) $h(T_f - T_1) = -k_1 \left.\frac{\partial T_1}{\partial x_1}\right|_{x_1=0}$ (3) $k_1 \left.\frac{\partial T_1}{\partial x_1}\right|_{x_1=\ell_1} = k_2 \left.\frac{\partial T_2}{\partial x_2}\right|_{x_2=0}$

(2) $T_1(x=\ell_1) = T_2(x_2=0)$ (4) $k_2 \left.\frac{\partial T_2}{\partial x_2}\right|_{x_2=\ell_2} = 0$

TEMPERATURE SOLUTION:

$$T_1 = \frac{B_i\left[\eta_2 e^{-2\sqrt{\frac{s}{a_1}}\ell_1 + \sqrt{\frac{s}{a_2}}x_1} - \eta_1 e^{-\sqrt{\frac{s}{a_1}}x_1}\right]}{\eta_2 e^{-\sqrt{\frac{s}{a_1}}\ell_1}\left(-\sqrt{\frac{s}{a_1}}\ell_1 + B_i\right) - \eta_1\left(\sqrt{\frac{s}{a_1}}\ell_1 + B_i\right)} \cdot T_f(s)$$

$$T_2 = \frac{B_i e^{-\sqrt{\frac{s}{a_1}}\ell_1}(\eta_2 - \eta_1)\left[e^{\sqrt{\frac{s}{a_2}}x_2} + e^{\sqrt{\frac{s}{a_2}}(2\ell_2 - x_2)}\right]}{\left(1 + e^{2\sqrt{\frac{s}{a_2}}\ell_2}\right)\left[\eta_2 e^{-2\sqrt{\frac{s}{a_1}}\ell_1}\left(-\sqrt{\frac{s}{a_1}}\ell_1 + B_i\right) - \eta_1\left(\sqrt{\frac{s}{a_1}}\ell_1 + B_i\right)\right]} \cdot T_f(s)$$

WHERE $\eta_1 = 2 - \left(1 + e^{2\sqrt{\frac{s}{a_2}}\ell_2}\right)\left(1 + \frac{k_1}{k_2}\sqrt{\frac{a_2}{a_1}}\right)$

$\eta_2 = 2 - \left(1 + e^{2\sqrt{\frac{s}{a_2}}\ell_2}\right)\left(1 - \frac{k_1}{k_2}\sqrt{\frac{a_2}{a_1}}\right)$

B_i : BIOT NUMBER

a : THERMAL DIFFUSIVITY

s : LAPLACE TRANSFORM

Numerical Calculation

Model : SUS 316 Base Metal(2) with INCONEL 718 Cladding(1)
Total Plate Thickness(t)= 10 mm

Clad Thickness (t_1) : 1 mm (t_1/t = 10%)
2 mm (t_1/t = 20%)

Temperature Amplitude (ΔT) : 100°C Max

Metal Properties : At 450°C

	k (Kcal/cm·s·°c)	a (cm /s)	β (1/°c)	E (Kg/cm)	ν
SUS 316	48.6×10^{-6}	0.0461	19.8×10^{-6}	1.67×10^{6}	0.298
INCONEL 718	43.0×10^{-6}	0.0504	15.6×10^{-6}	1.78×10^{6}	0.28

Numerical Calculation

Results:

A -- Calculated results assuming that the material is all SUS 316

B -- Calculated results assuming that the material is all INCONEL 718

(1) Temperature Distribution -- Fig. A3-4(b) and -5(b)

Clad temperature is nearly equal to B.

Base metal temperature is nearly equal to A

Temperature profile in the plate is approximated by the average of A and B.

(2) Stress Distribution -- Fig. A3-4(a) and -5(a)

Stress at clad surface is nearly equal to B

Stress at any point can be closely determined from A and B.

(3) Secondary Stress, Q -- Fig. A3-6 and -7

Q is larger in A than in B.

In the range $1 < B < 100$, Q becomes maximum at ω^* (non-dimensional angular frequency = $\sqrt{\frac{\omega}{a}\ell^2}$) from 1.8 to 2.8.

Q can be well determined by the average of A and B at all frequencies.

CALCULATION OF SECONDARY STRESS, Q

SECONDARY STRESS Q IS CALCULATED FROM THE EQUIVALENT LINEAR STRESS DISTRIBUTION (σ_{eq}) EQUAL TO THE MOMENT DUE TO THE STRESS DISTRIBUTION IN THE DIRECTION OF PLATE THICKNESS. (FIG. A3-3)

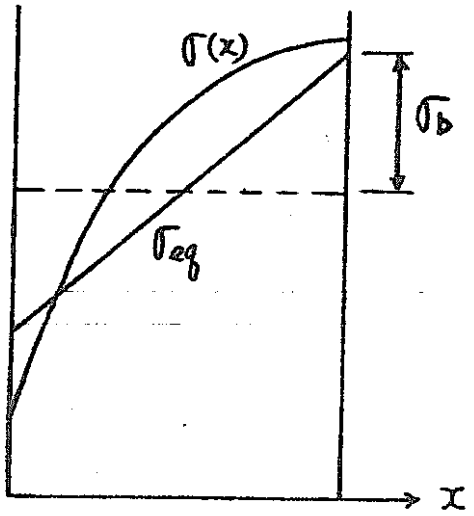

$$\sigma_{eq} = \frac{2\sigma_b}{\ell}\left(x - \frac{\ell}{2}\right)$$

$$M_{eq} = \int_0^{\ell}\left(x - \frac{\ell}{2}\right)\sigma_{eq}\,dx = \frac{\sigma_b}{6}\ell^2$$

FIG. A3-3 STRESS DISTRIBUTION

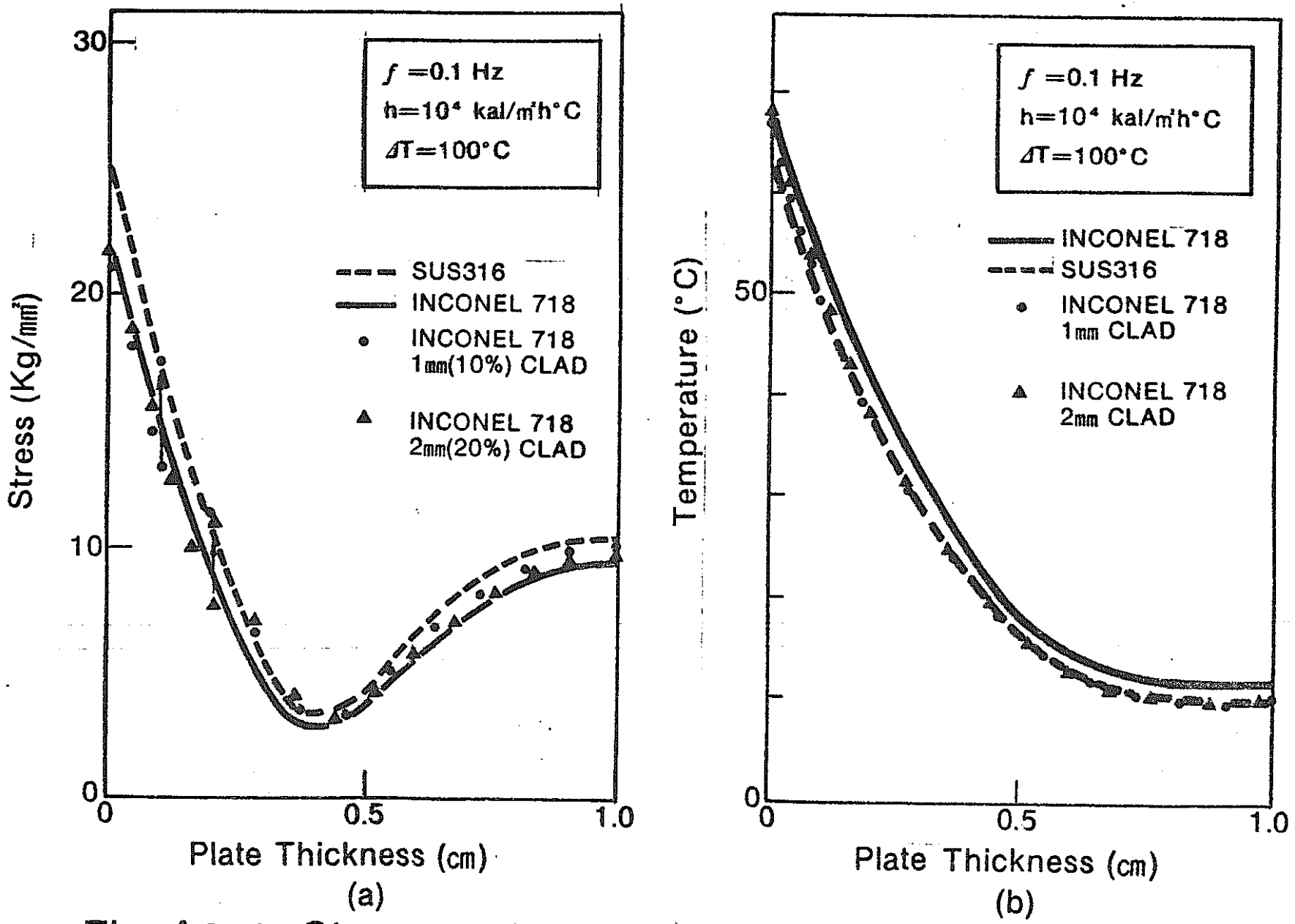

Fig. A3-4 Stress and Temperature Profile inside a Plate (f=0.1 Hz)

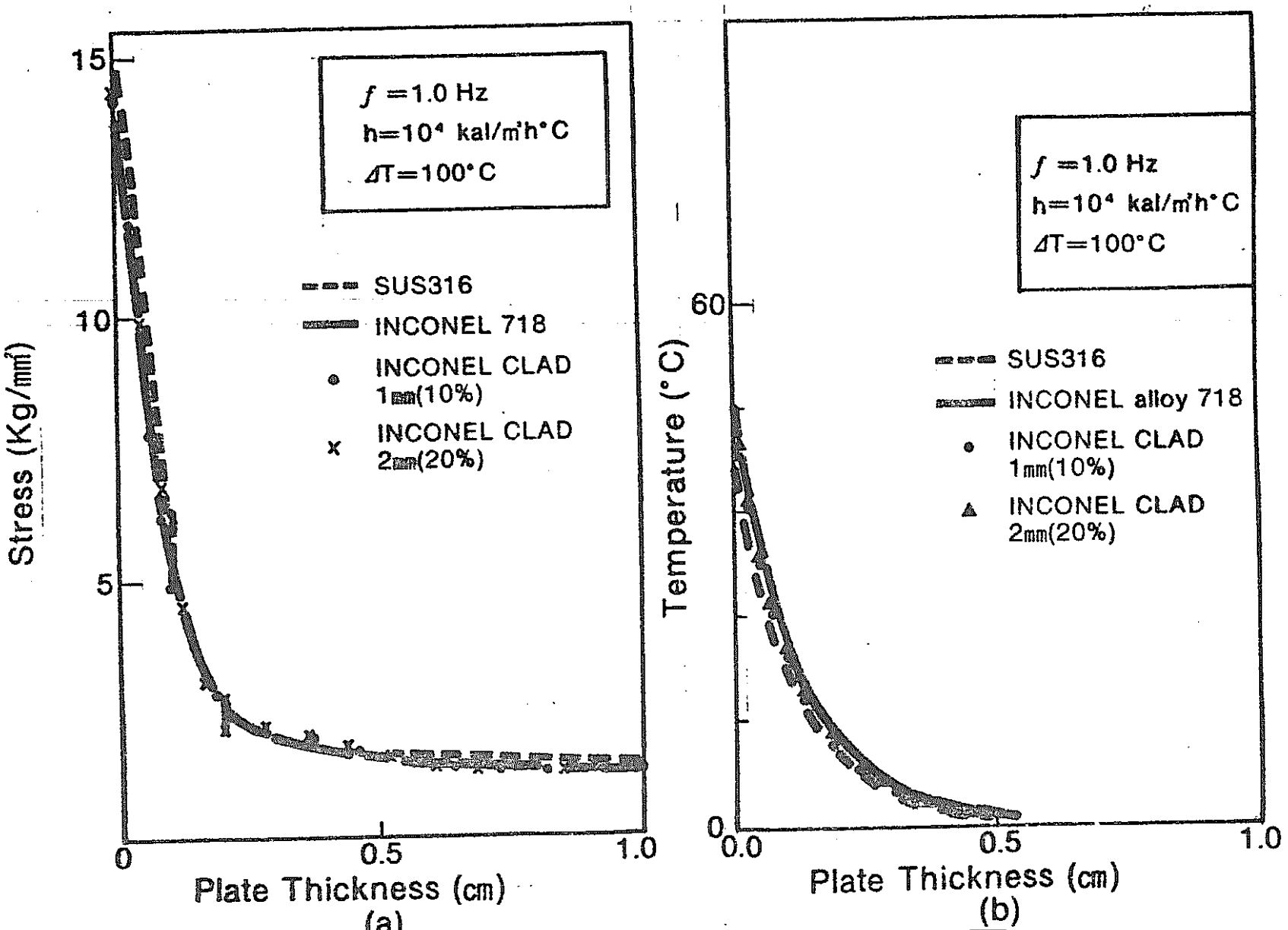

Fig. A3-5 Stress and Temperature Profile inside a Plate (f=1.0 Hz)

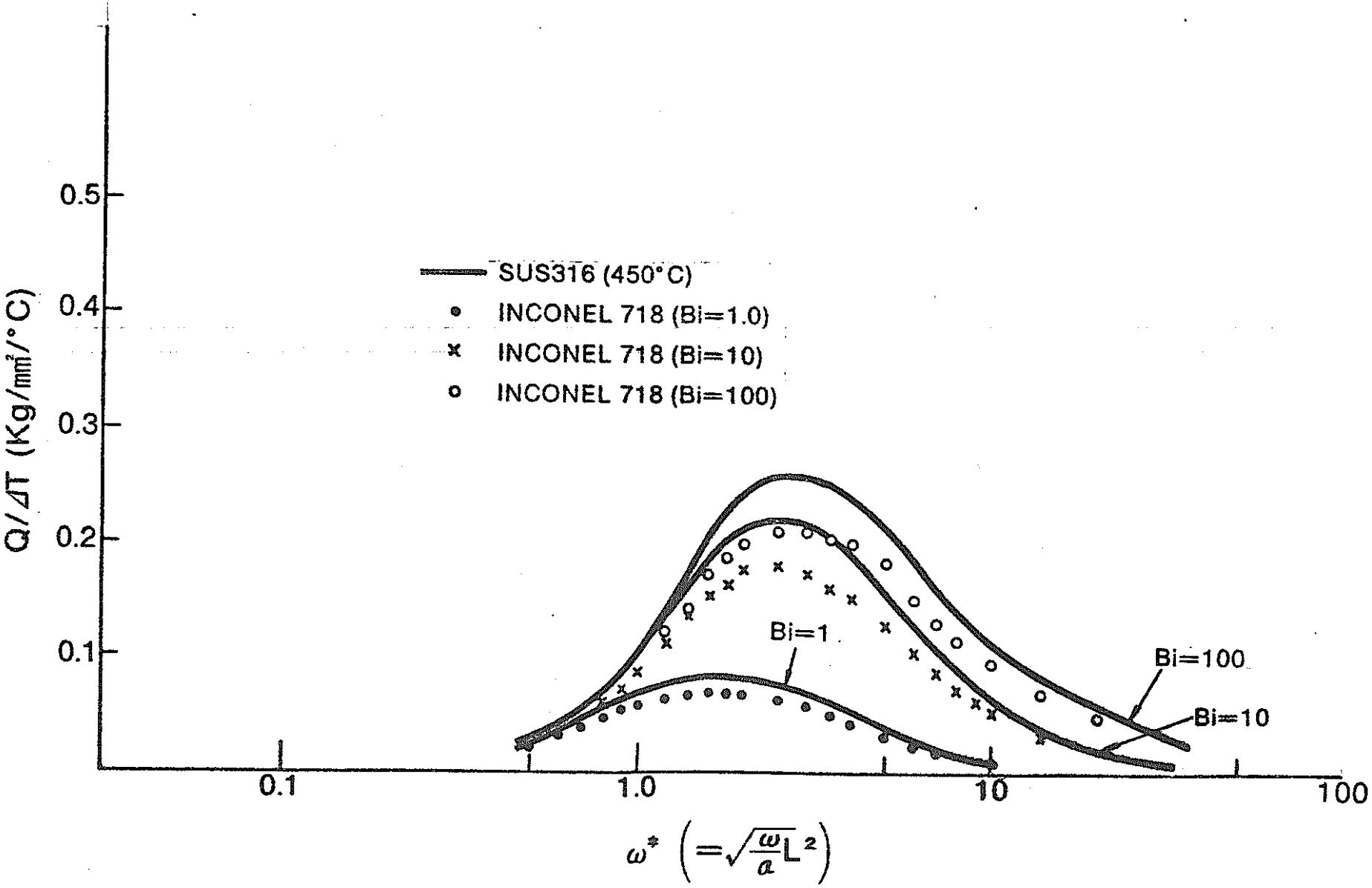

Fig. A3-6 Relationship between Secondary Stress and Parameters (Bi, ω^*, ΔT)

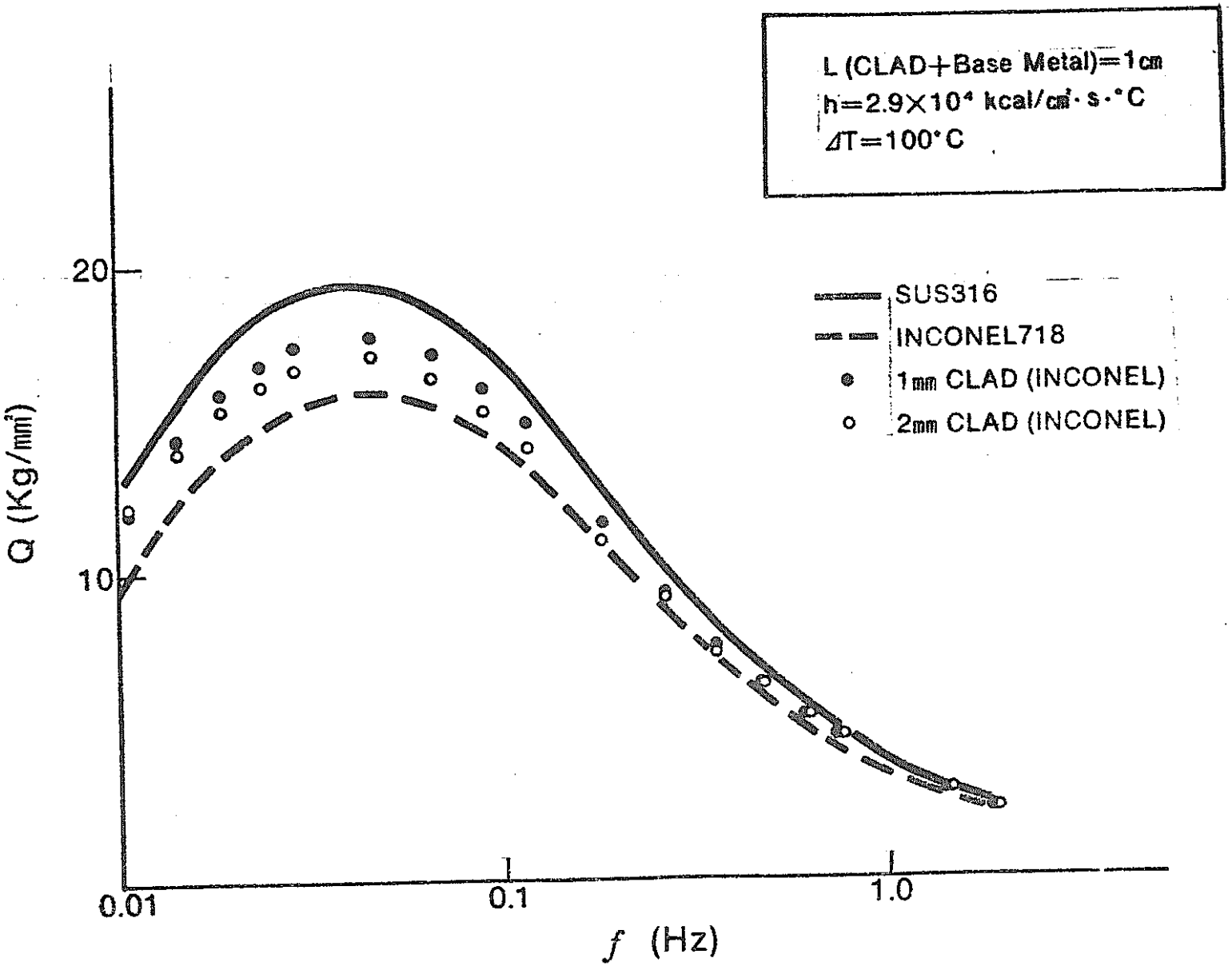

Fig. A3-7 Secondary Stress of the Plate with Clad

Stress Evaluation Charts

Objective:

To obtain maximum surface stress and secondary stress induced in the plate by fluid temperature fluctuation

Maximum Surface Stress Evaluation Chart -- Fig. A3-8 (SUS 316) and Fig. A3-9 (INCONEL 718)

Secondary Stress Evaluation Chart ------- Fig. A3-10 (SUS 316) Fig. A3-11 (INCONEL 718)

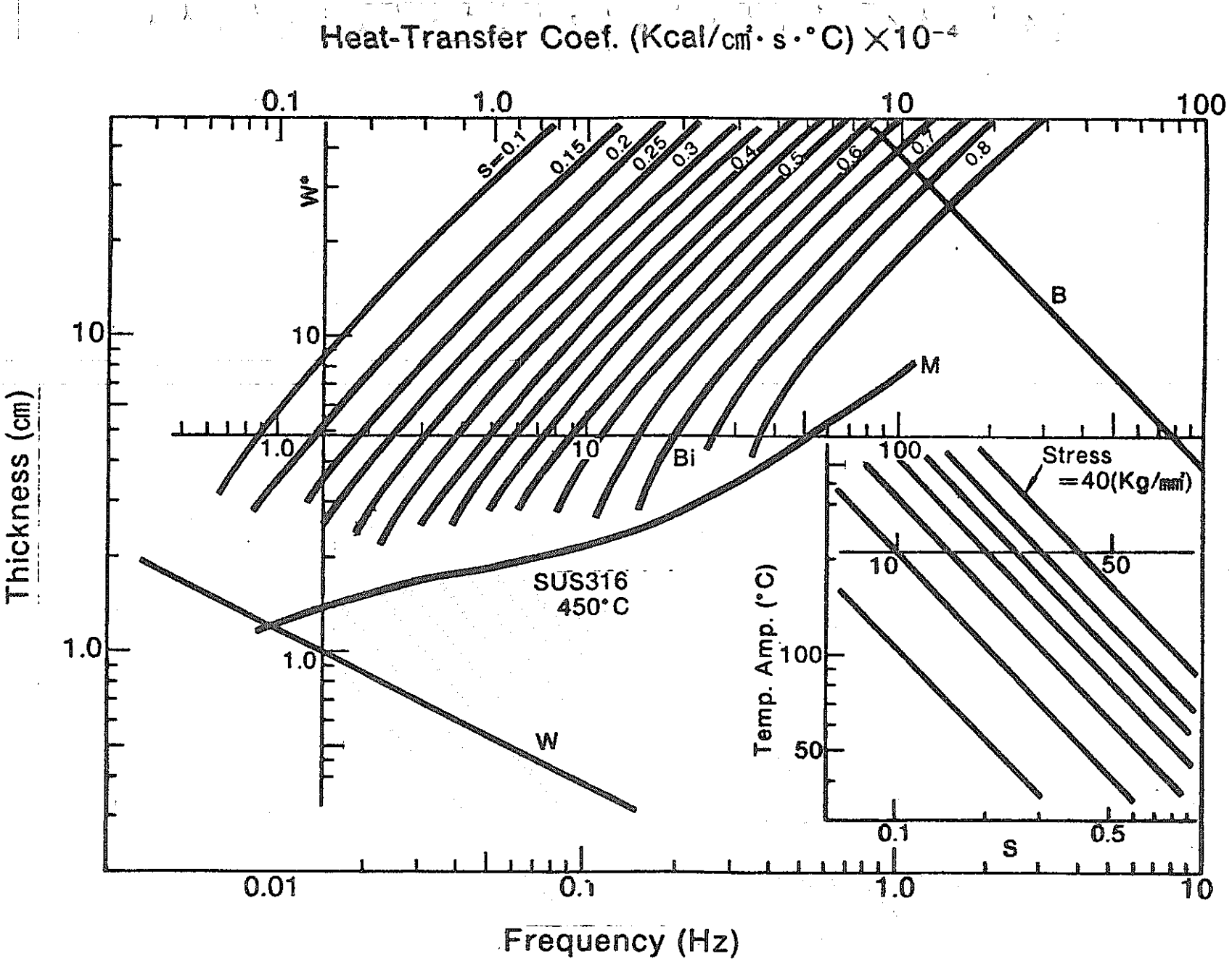

Fig. A3-8 Stress Chart (for SUS 316)

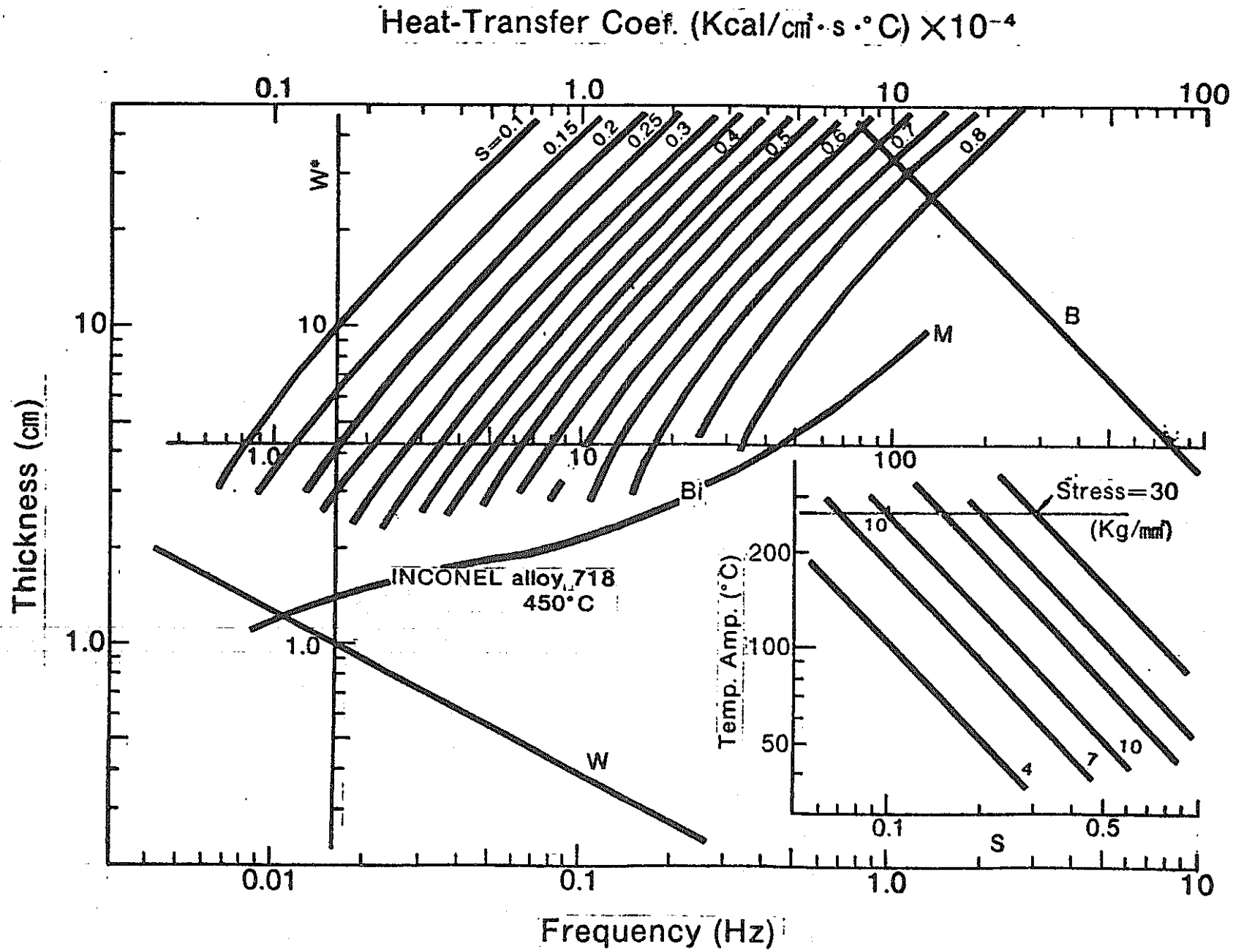

Fig. A3-9 Stress Chart (for INCONEL 718)

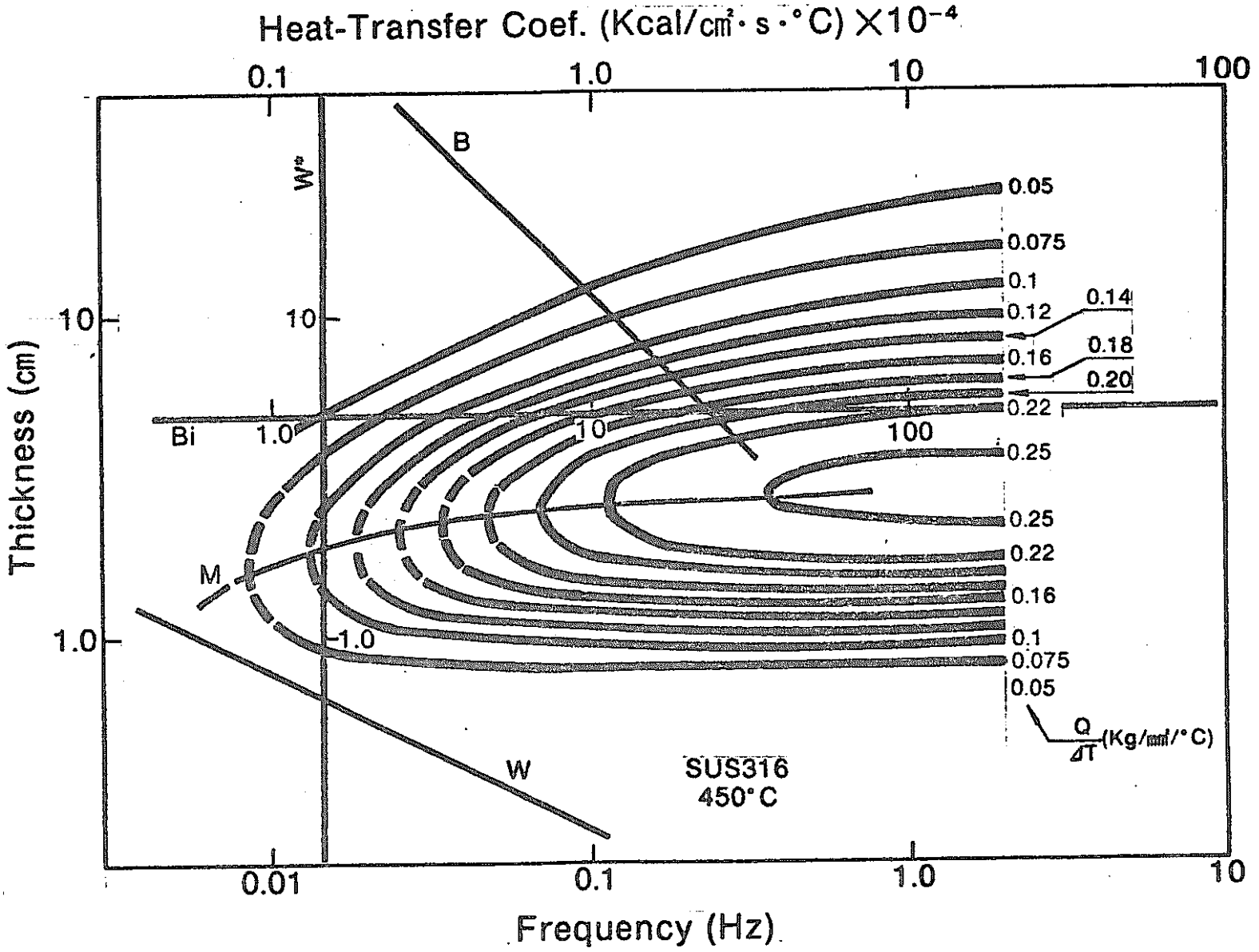

Fig. A3-10 Secondary Stress Chart (for SUS 316)

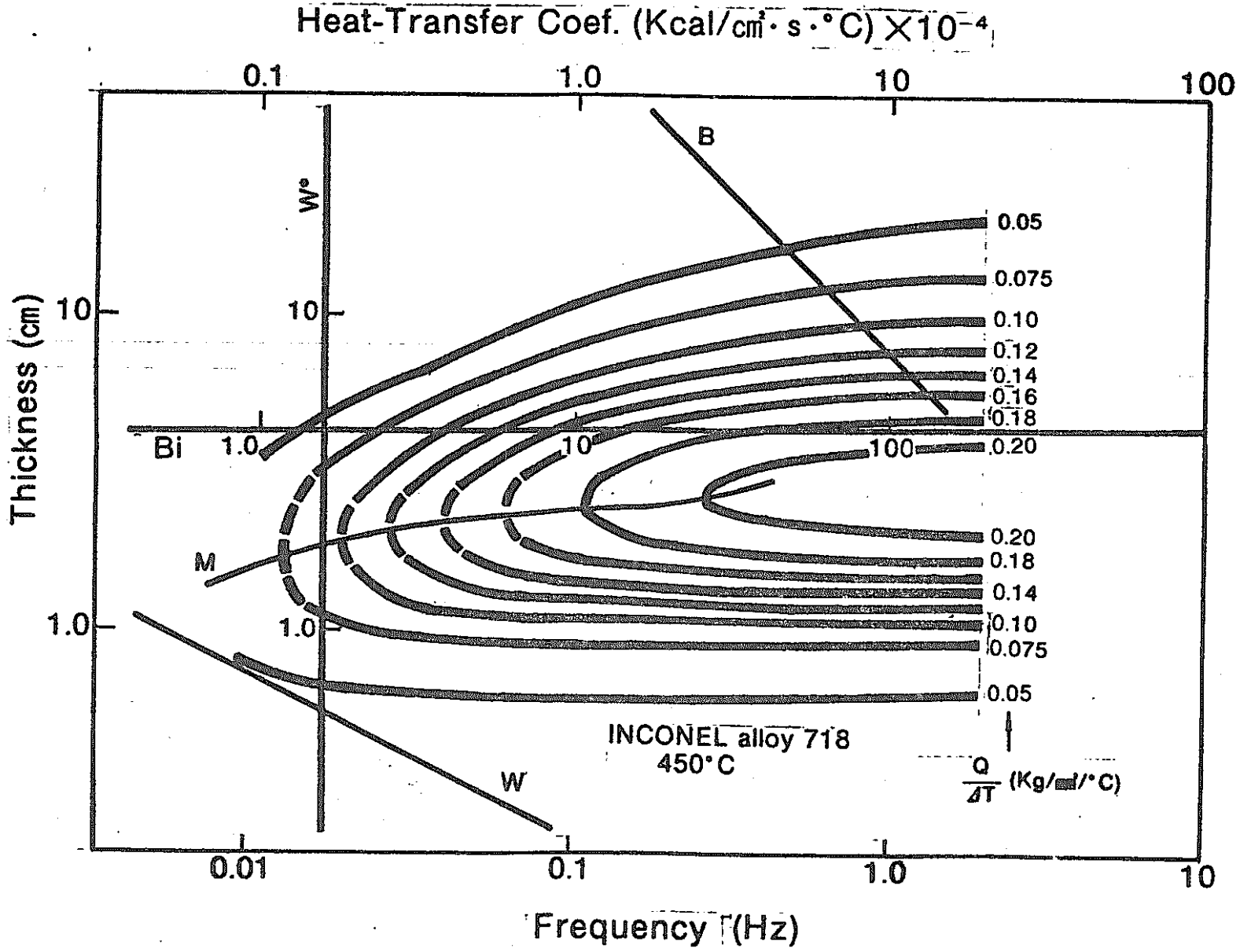

Fig. A3-11 Secondary Stress Chart (for INCONEL 718)

EXAMPLE:

GIVEN

PLATE THICKNESS : 1 CM

HEAT TRANSFER COEFF. : 10^4 KCAL/M^2H°C (=2.78 x 10^{-4} KCAL/CM^2S°C)

TEMPERATURE FLUCTUATION

AMPLITUDE : 100°C

FREQUENCY : 1.0 Hz

TO BE OBTAINED

MAXIMUM SURFACE STRESS

SECONDARY STRESS

SOLUTION

FROM FIG. A3-12, MAXIMUM SURFACE STRESS = 16-17 KG/MM^2

FROM FIG. A3-13, SECONDARY STRESS = 7.0 KG/MM^2

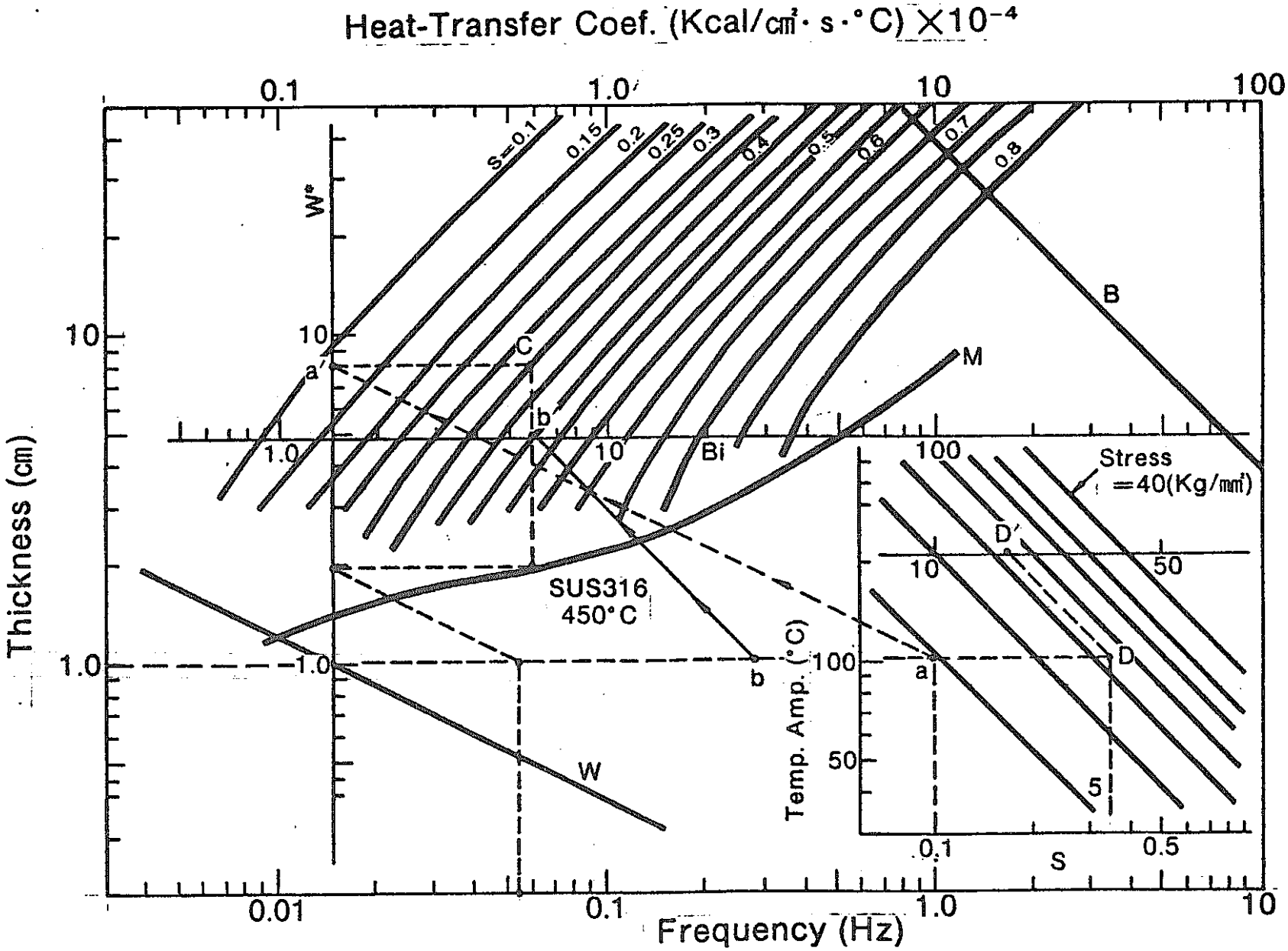

Fig. A3-12 Example to Calculate Surface Stress for SUS 316

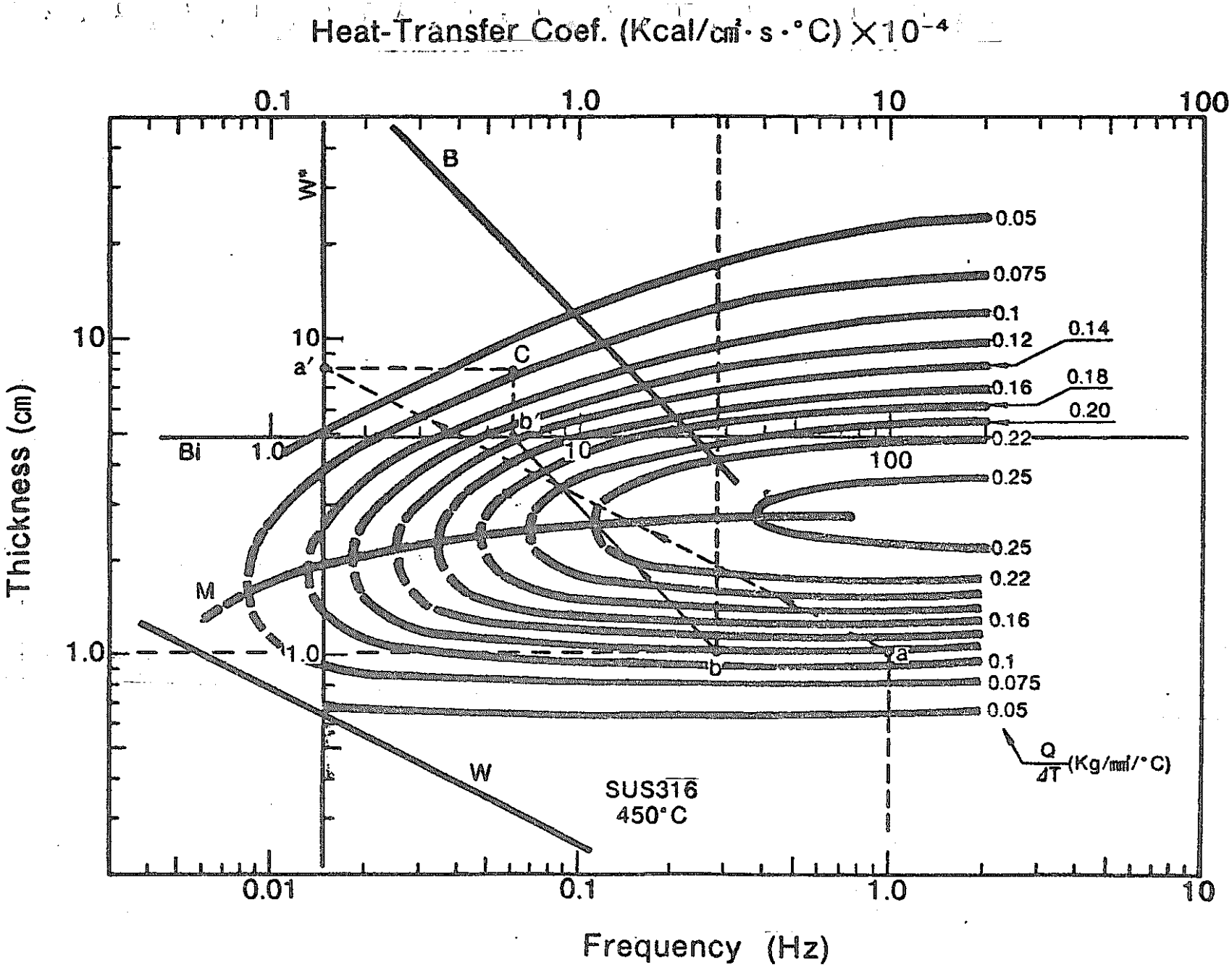

Fig. A3-13 Example to Calculate Secondary Stress for SUS 316

Stress Evaluation Using Stress Chart

1. Step 1
   1) Determine the point a from L and f.
   2) Draw from the point a a line parallel to the auxiliary line W and get a′, an intersecting point on the line W*.

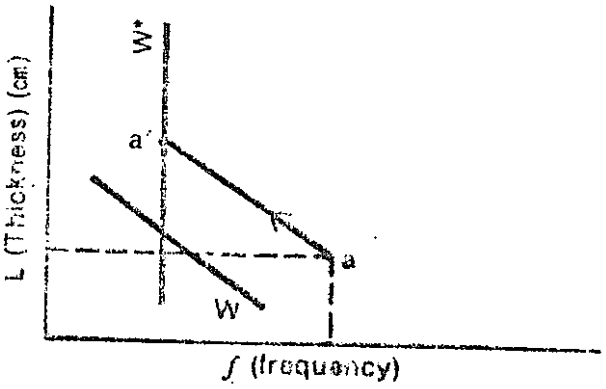

2. Step 2
   1) Determine the point b from L and h.
   2) Draw from the point b a line parallel to the auxiliary line B and get b′, an intersecting point on the line Bi.

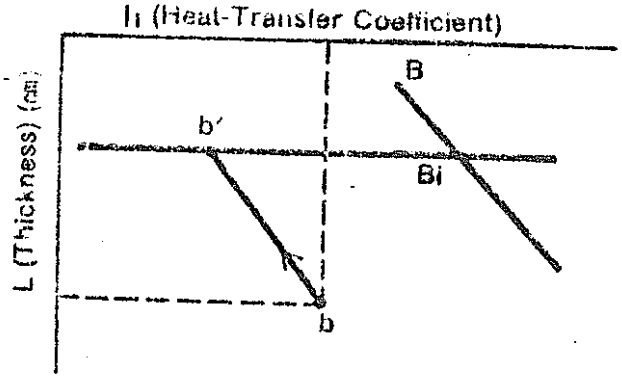

3. Step 3
   1) Determine the point C from points a′, b′ on the lines W*, Bi.
   2) Estimate the corresponding value of S from the group of S-lines.
   3) Calculate secondary stress for the given temperature fluctuation amplitude.

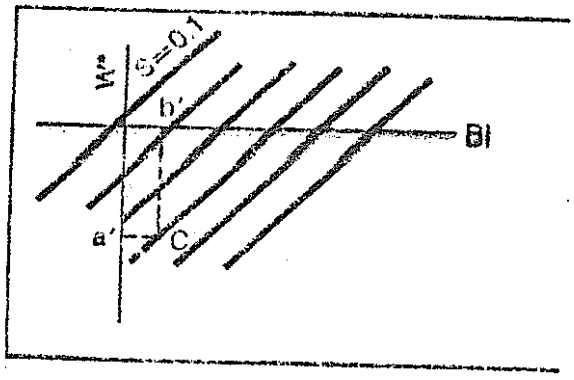

3') From the value of Sobtained in Step above and the given temperature amplitude, obtain a point D. Draw from D a line parallel to a group of straight lines to get an intersecting point D' with stress axis. This is the maximum surface stress.

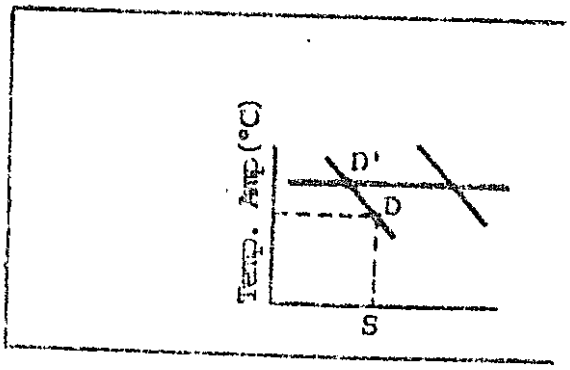

A-4 FUTURE TEST PLAN FOR THERMAL STRIPING

ABSTRACT

In order to provide detailed design data for the lower region of MONJU upper core structure (UCS), a thermal striping test in sodium is planned. A test model consists of a seven assembly full scale model of MONJU and the simulated UCS with flow straightener, instrument finger and thermal shield. Test is conducted in the Thermal Shock Test Loop at PNC-OEC with its test section modified. The objectives of the test are:

1) to obtain the correlation between the temperature fluctuation (its amplitude and frequency) and sodium velocity;
2) to obtain the correlation between the temperature fluctuation and the temperature difference of hot and cold sodium;
3) to locate the point of maximum strain range at the structural surface from the local temperature fluctuation data;
4) to compare the in-sodium test with the in-water test and to provide information on applicability of thermal striping conditions in water to sodium.

From the test results together with the separately obtained high cycle fatigue data from material tests, the structural integrity of the MONJU UCS is evaluated by the MONJU High Temperature Structural Design Standard.

THERMAL STRIPING TEST PLAN

1. BACK GROUND

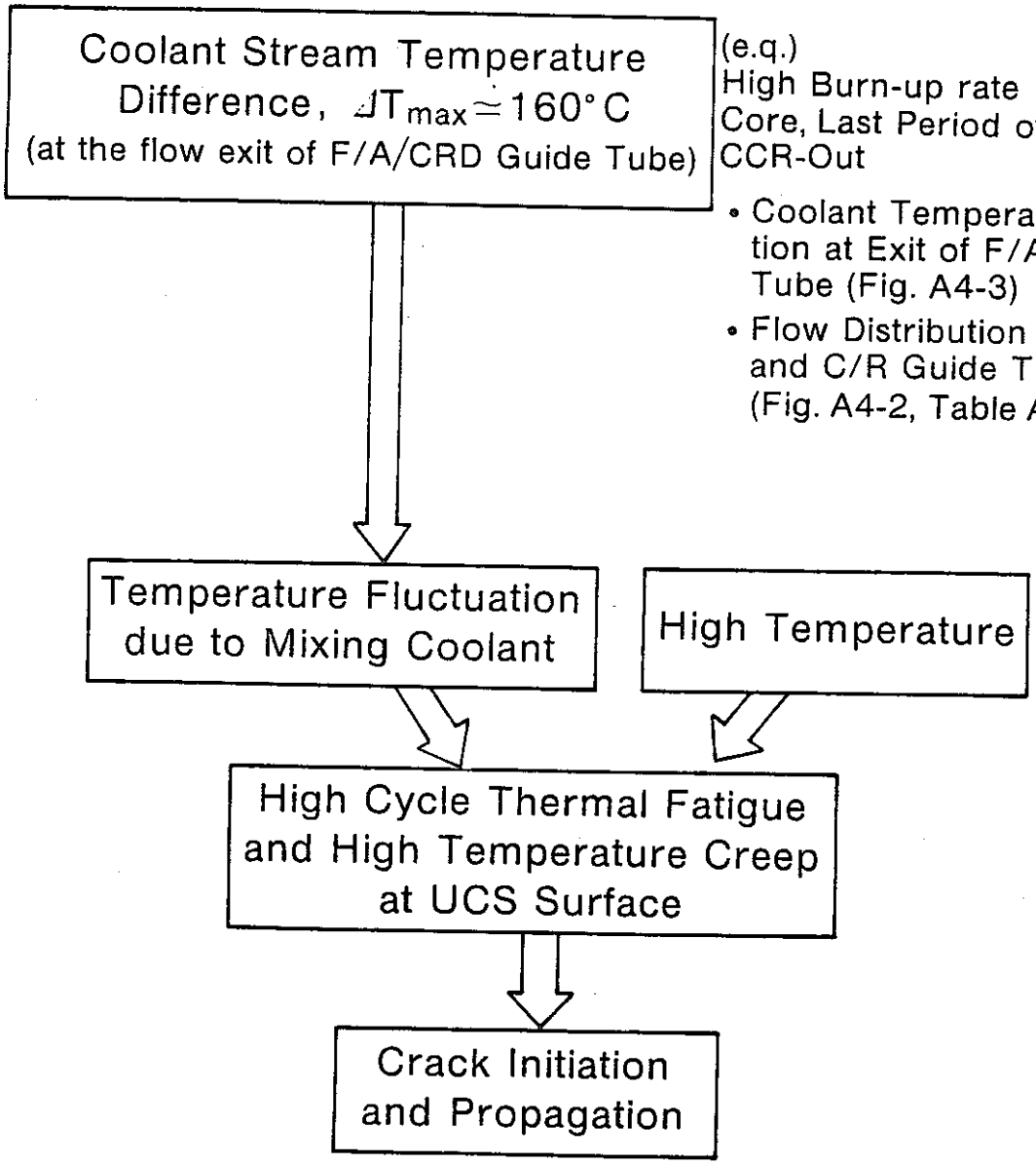

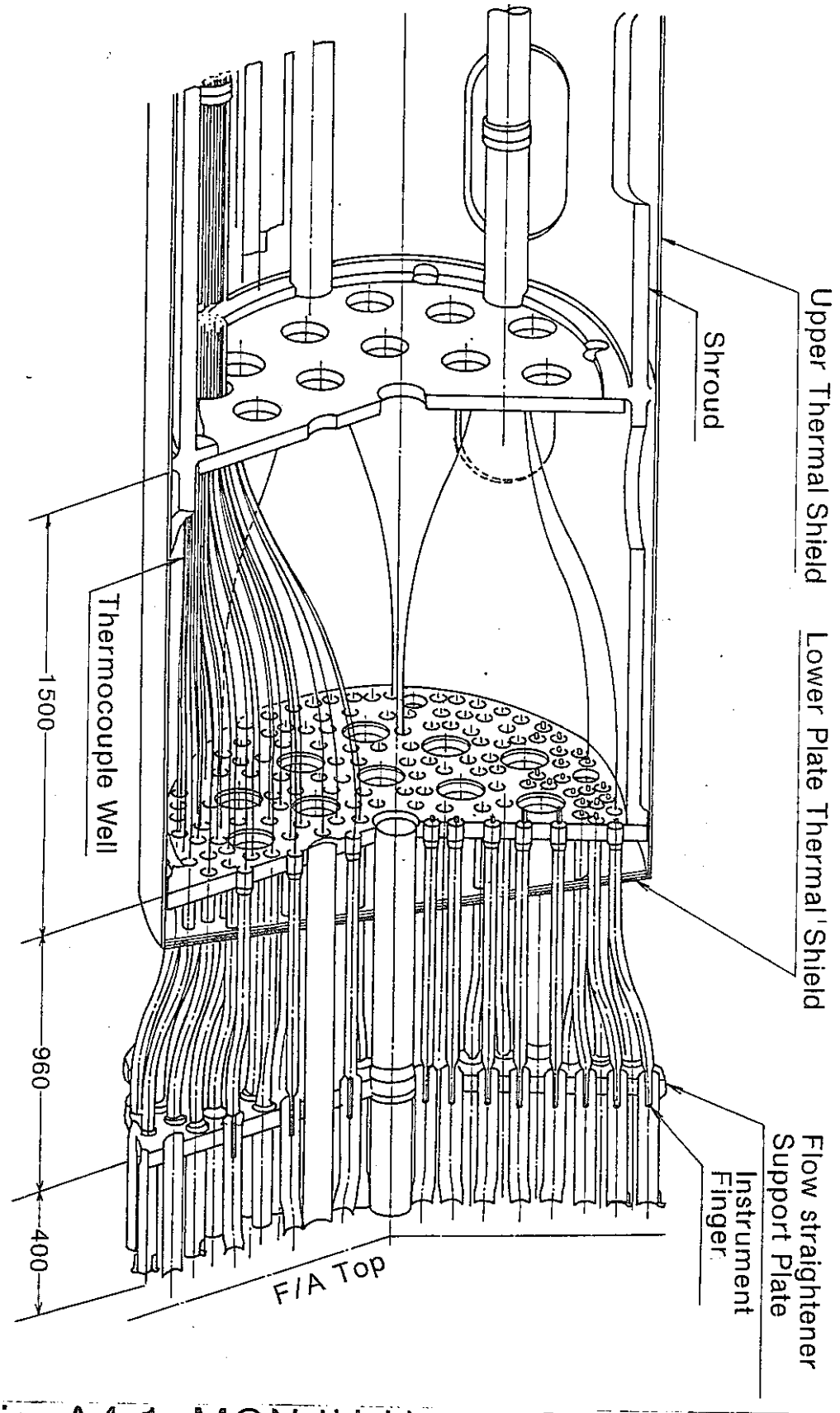

Fig. A4-1 MONJU Upper Core Structure

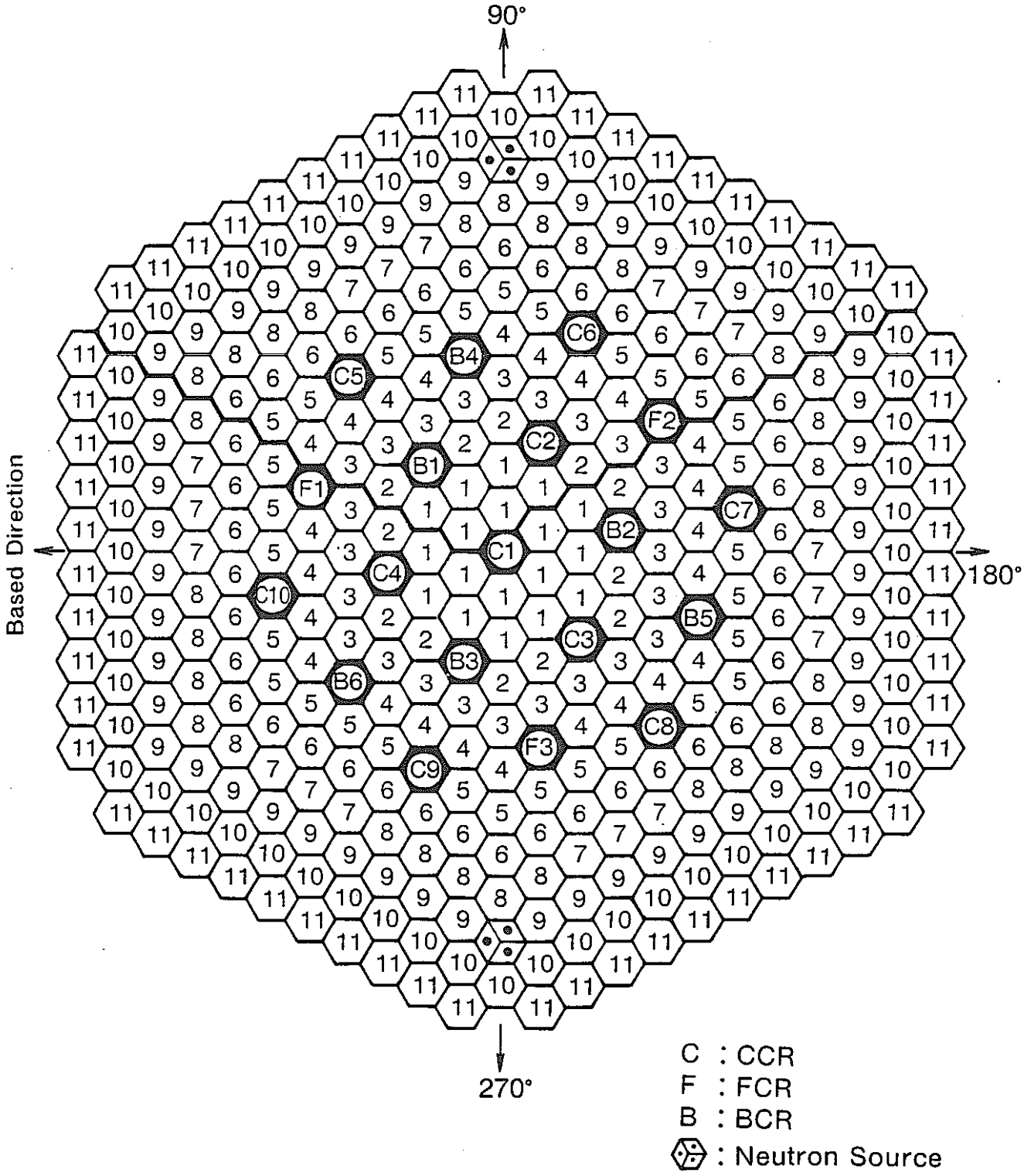

Fig. A4-2 Arrangement of Fuels and C/R Assemblies

Table A4-1 Flow Distribution in the F/A and C/R Guide Tube

	Flow Zone	No. of Assembly	Flow in Assembly (Kg/sec)	Flow in Each Zone (Kg/sec)
Core Zone (Ⅰ)	1	18	20.9	375.4
	2	12	19.6	234.7
	3	24	18.7	447.7
	4	24	17.4	416.6
	5	30	16.2	484.4
Core Zone (Ⅱ)	6	42	18.9	792.0
	7	18	15.9	285.2
	8	30	14.4	430.7
Blanket	9	52	4.6	237.1
	10	60	2.2	130.8
	11	60	1.0	59.6
Control Rod	CCR	10	11.0	110.3
	FCR	3	11.0	33.1
	BCR	6	3.0	18.1
Neutron Shield	12	282	0.16	45.3
	13	42	0.11	4.4
Neutron Source		2	3.0	6.0

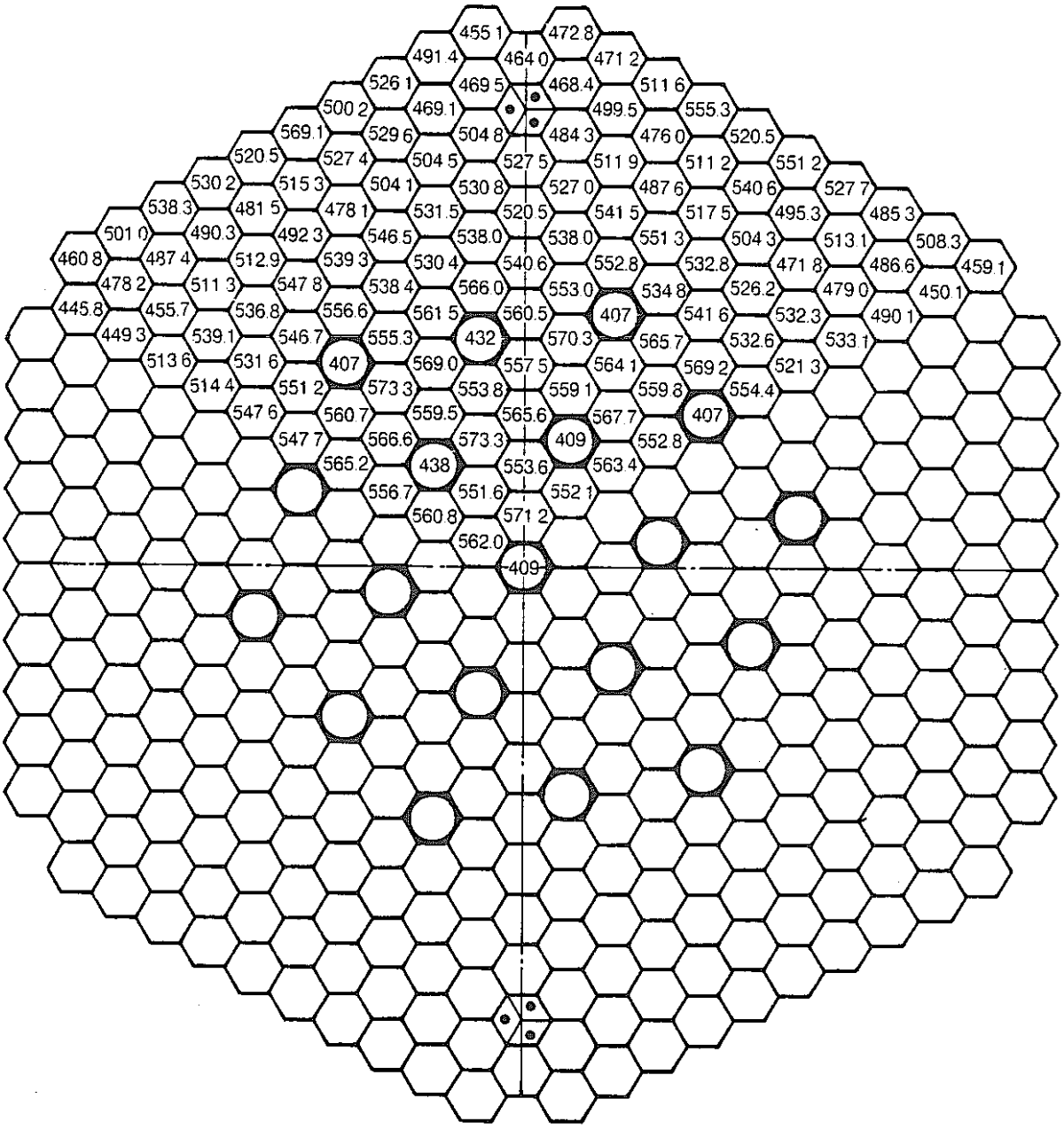

Fig. A4-3 Average Temperature Distribution of Mixed Coolant at F/A Exit (High Burn-up rate, Balanced Core, Last Period of No. 9 Cycle, CCR-Out)

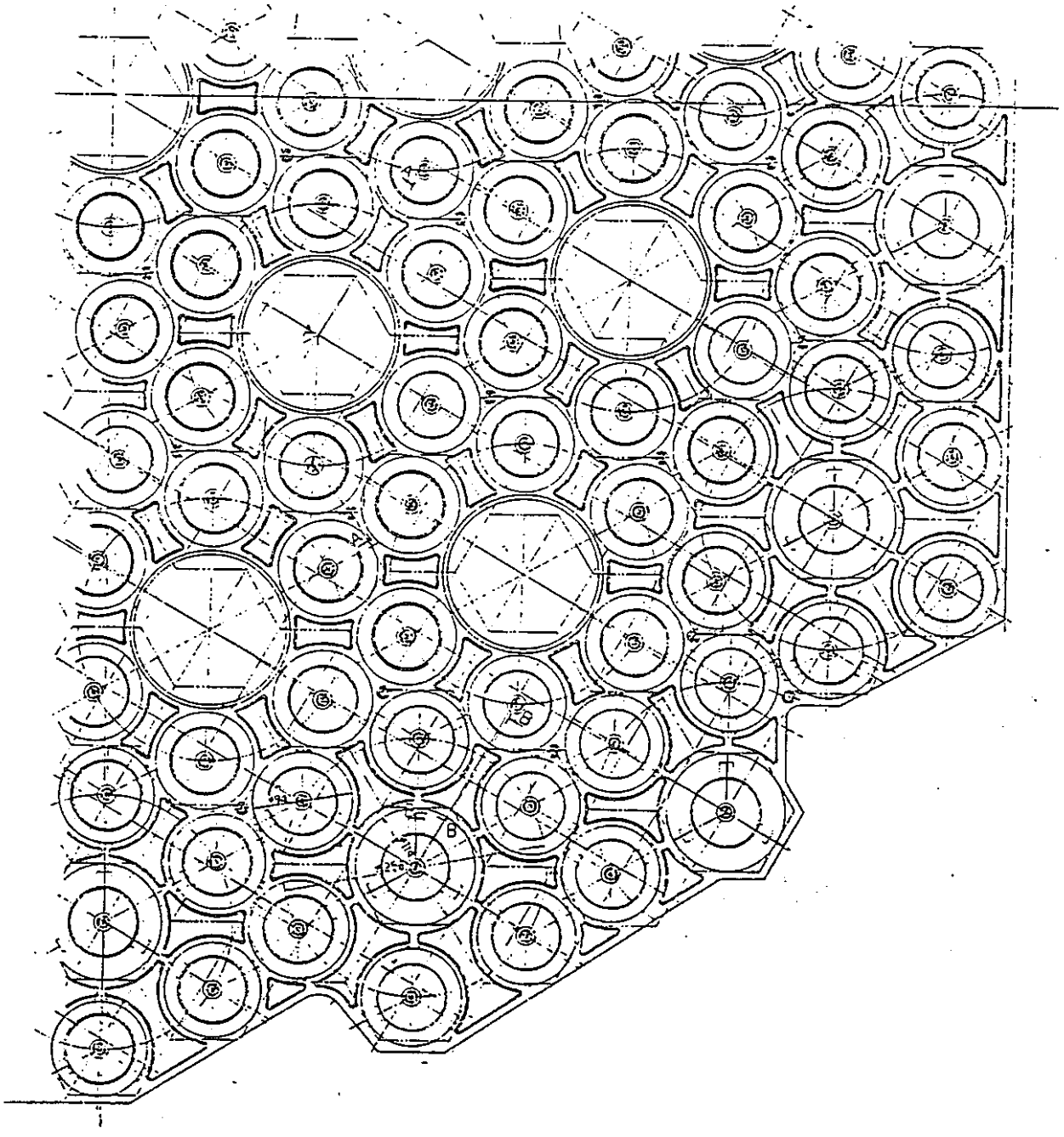

Fig. A4-4 MONJU UCS Flow straightener Support Plate

2. TEST PLAN

2.1 Purpose

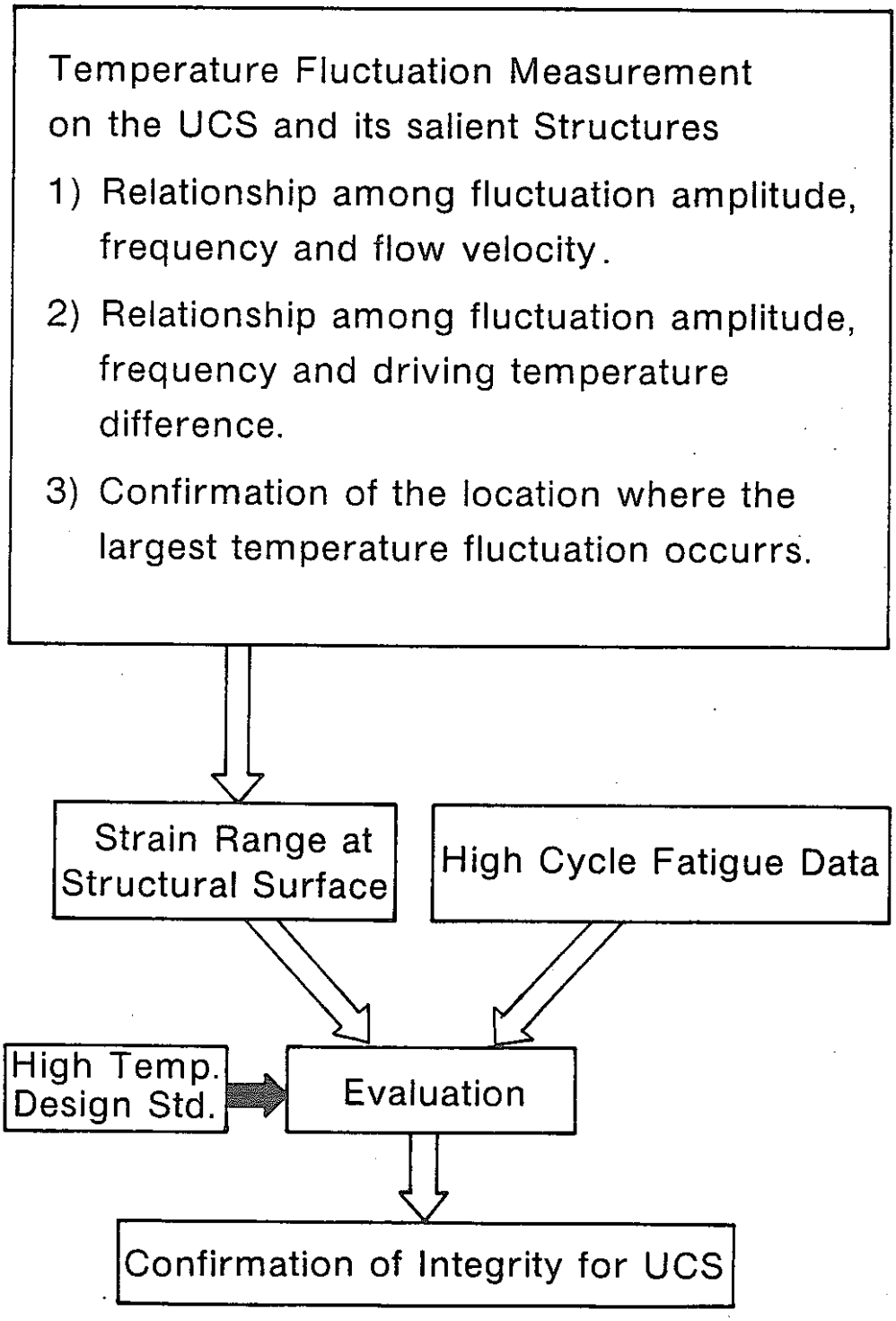

2.2 Overall Description

Test Model : MONJU Full Scale 7-Assembly Model

Test Facility : Thermal Shock Test Loop

Test Fluid : Sodium

Test Parameters : High and Low Temperature Difference
Flow Velocity

Instrument Sensor : C.A. Thermocouple

Measuring Points : Structural Surface Temperature
Sodium Temperature

Measuring Items : Temperature Fluctuation Amplitude
Frequency

2.3 Test Model

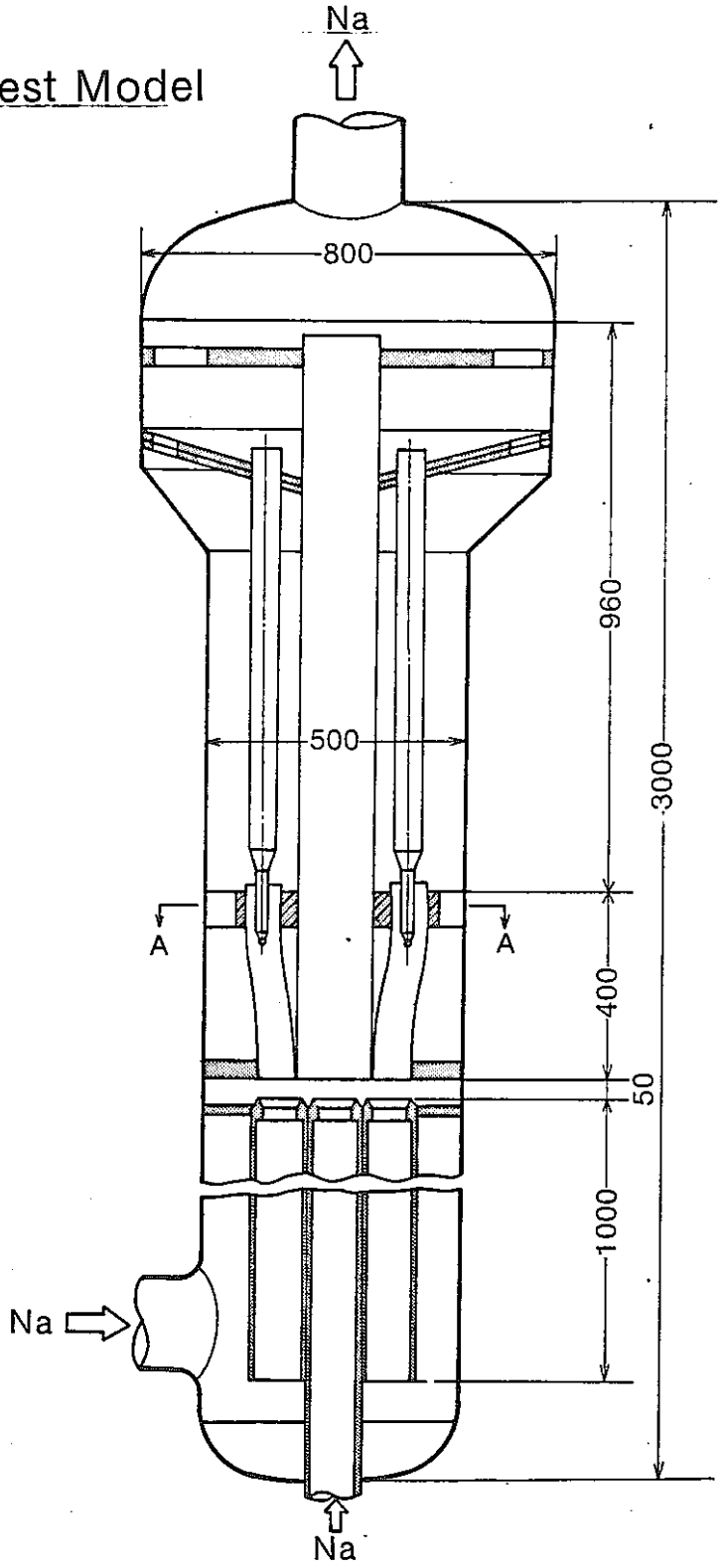

Fig. A4-5 Thermal Striping Test Model

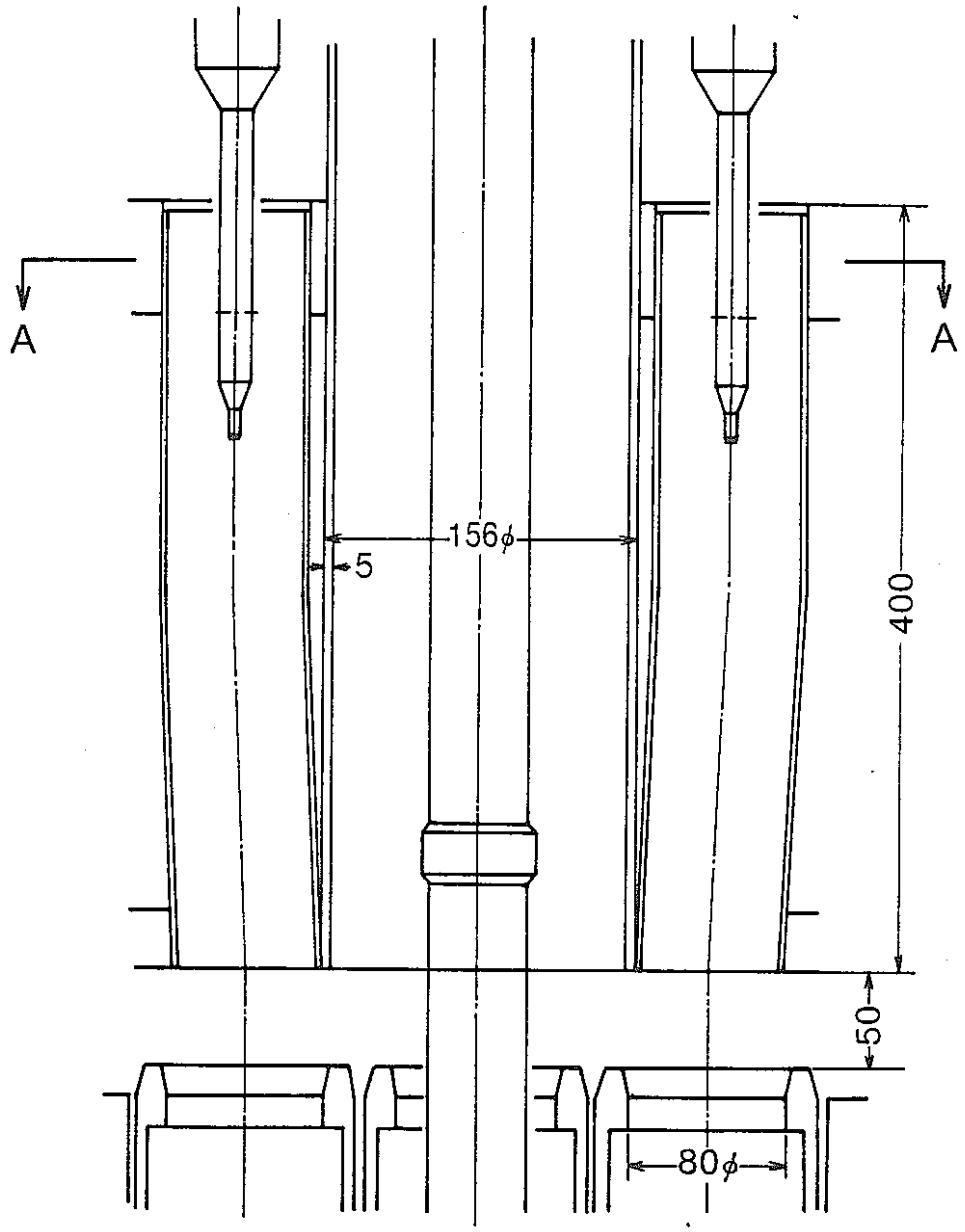

Fig. A4-6 Details of Flow Straigntener and Guide Tube

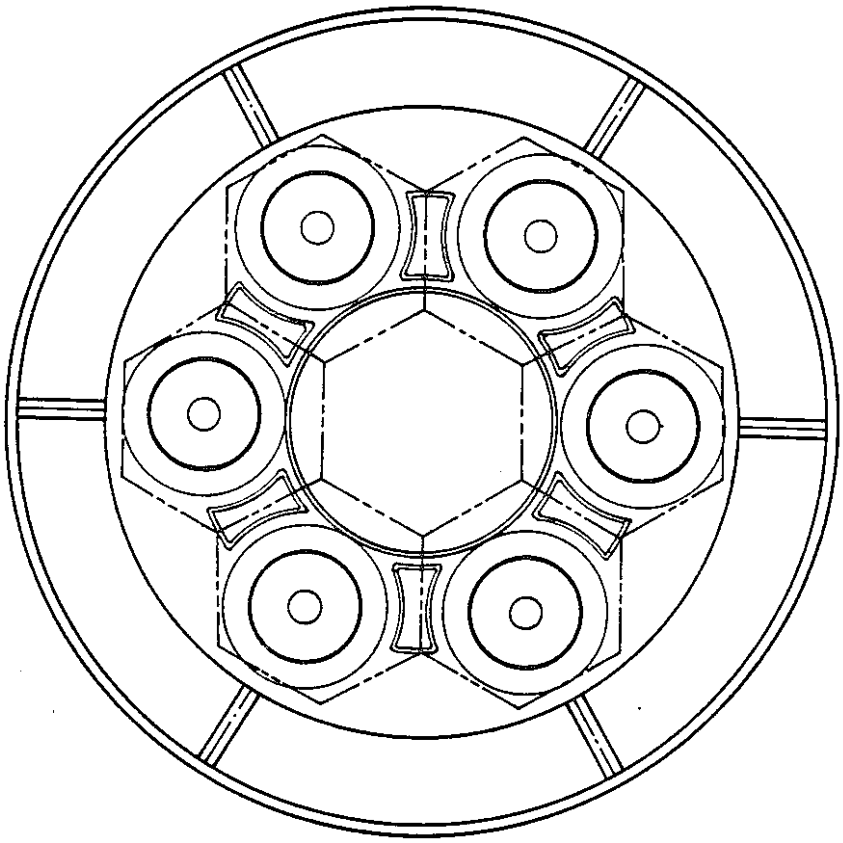

Two dotted line shows F/A

Fig. A4-7 Test Model (Section A-A)

2.4 Test Facility

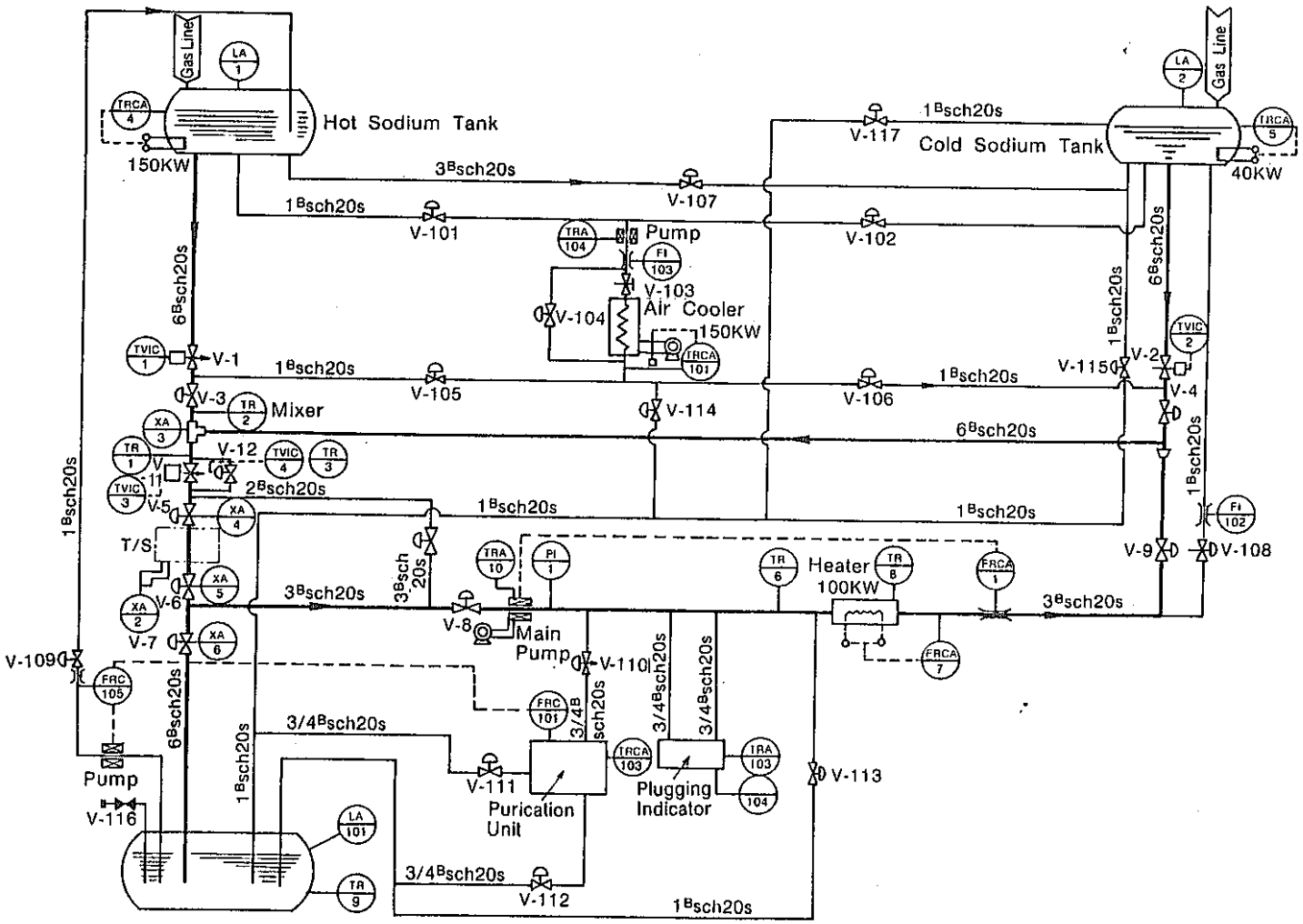

Thermal Shock Test Loop.

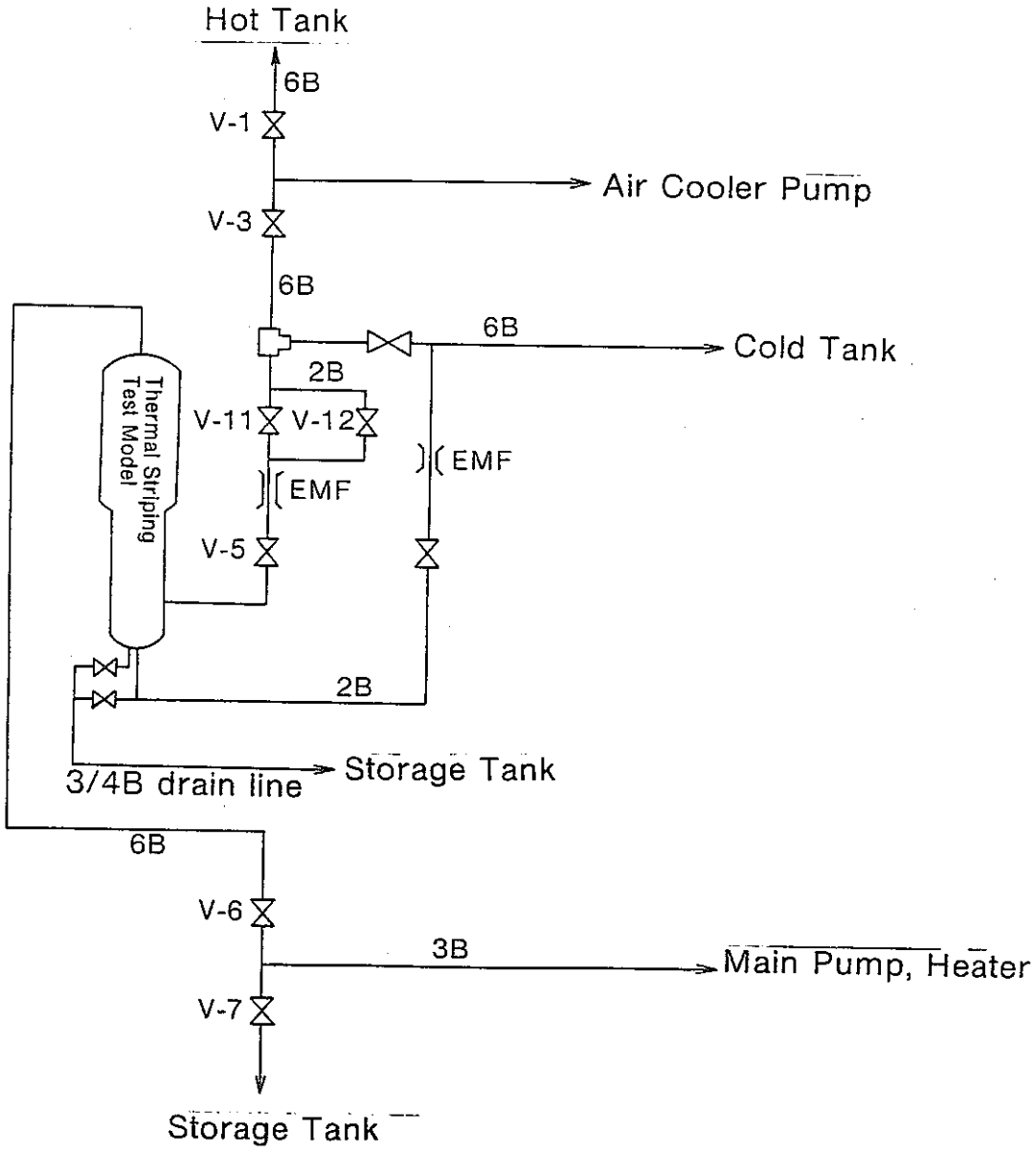

Fig. A4-8 Enlarged View of the Test Model in the TSTL

2.5 Test Condition

Reynolds No. (Inertial Force/Viscous Force)

$$Re = \frac{U \cdot L}{\nu}$$

Relative Reynolds No. $\equiv Re' = \frac{R}{R_o}$

$$Re' = \frac{U \cdot L}{\nu} \Big/ \frac{U_o \cdot L_o}{\nu_o}$$

$$= \frac{Q \cdot L}{S \cdot \nu} \Big/ \frac{Q_o \cdot L_o}{S_o \cdot \nu_o}$$

$$= \left(\frac{Q}{Q_o}\right) \left(\frac{S_o}{S}\right) \left(\frac{L}{L_o}\right) \left(\frac{\nu_o}{\nu}\right)$$

where U : Velocity

L : Characteristic length

ν : Kinematic viscosity

Q : Flow-rate

S : Flow cross-section

In the planned test (full scale, sodium)

$$Re' = \frac{Q}{Q_o}$$

Table A4-2 Test Conditions

		F/A	C/R
Flow	Model Q m³/min	0.025~1	0.0132~0.529
	MONJU Q_o m³/min	1.53	0.810
	Q/Q_o	0.0163~0.653	0.0163~0.653
Temperature	Model T°C	450~580	420~440
	MONJU T_o°C	450~580	420~440
	T/T_o	1	1
Relative Reynolds No. Re′		0.0163~0.653	0.0163~0.653

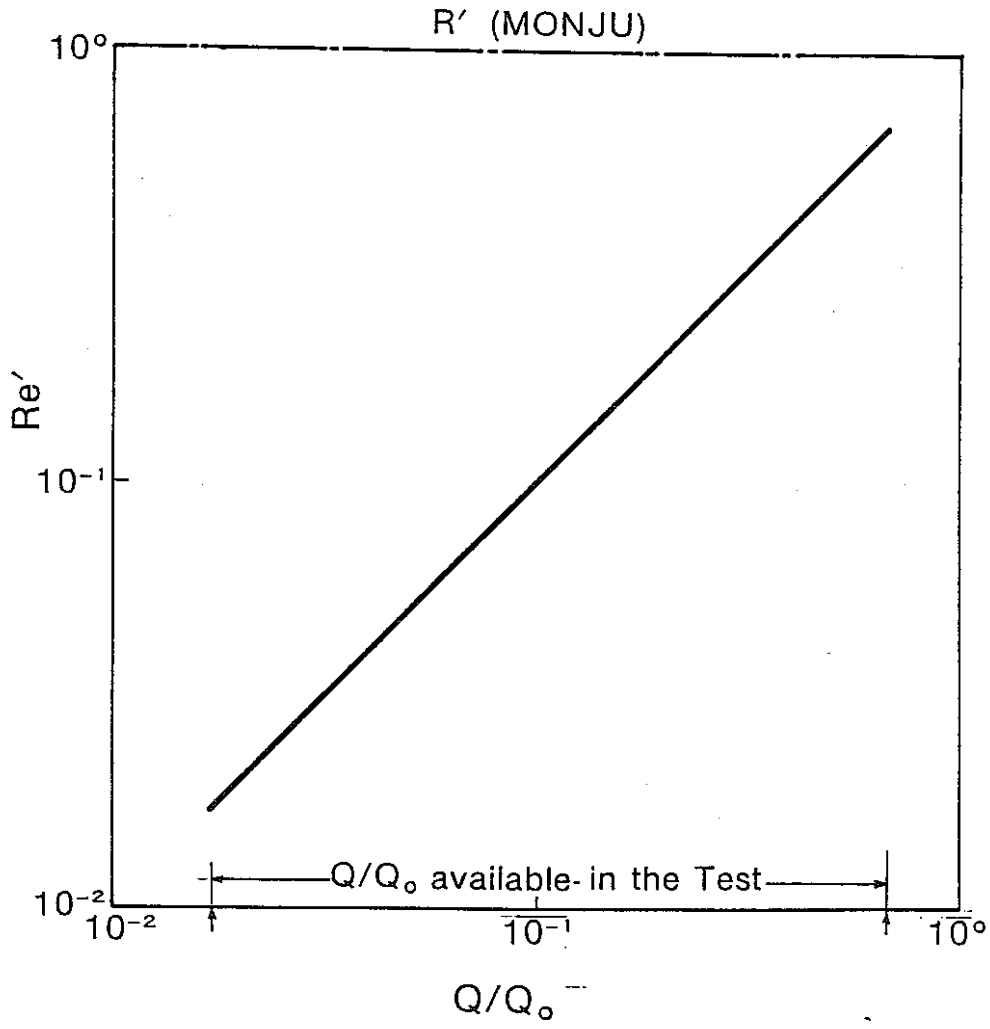

Fig. A4-9 Test Condition

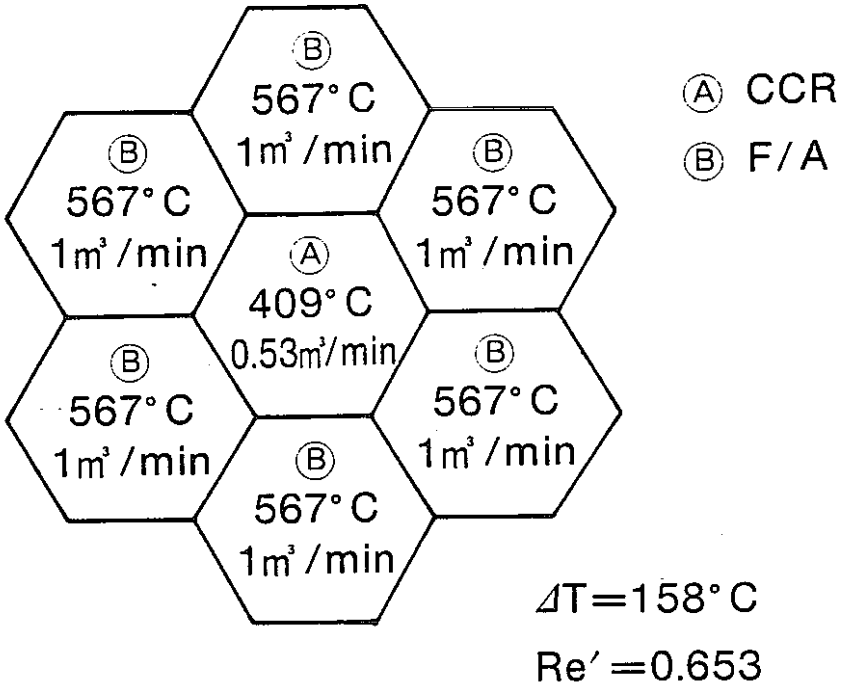

Fig. A4-10 Test Condition (one example)

PNC TN960 83-01

MONJU THERMAL STRATIFICATION DESIGN CONCEPT

OCTOBER, 1982

PNC / MONJU PROJECT

MONJU THERMAL STRATIFICATION DESIGN CONCEPT

ABSTRACT

An accurate evaluation for the thermal transient behavior in the outlet plenum of the MONJU reactor vessel is required to design components located in this region.

Due to flow coastdown and abrupt temperature decay following a reactor trip, thermal stratification was thought to occur in the MONJU reactor vessel upper plenum. Stratification aspects should be considered from the following two points of view :

1) Setting of upper plenum internal thermal transient conditions.
2) Treatment of the upper plenum behavior in the PTTA code.

This session deals with the design methodology for accommodating thermal stratification of the MONJU reactor vessel upper plenum.

1. Introduction

Due to flow costdown and abrupt temperature decay following a reactor trip, low-temperature, inertia-losing sodium enters a high-temperature sodium pool of the reactor vessel upper plenum. When the buoyancy effect due to density differnece overcomes the inertia force of the incoming fluid, the low-temperature sodium stagnates at the lower part of the upper plenum, resulting in so-called "thermal stratification." This phenomenon was thought to occur in the Monju reactor vessel upper plenum as well. However, since the plenum behavior during thermal transients had not been well characterized, an equivalent mixing volume approach was taken to give conservative outlet temperature transient predictions in the safety evaluation of the reactor,and the accurate treatment of the plenum behavior was carried into the detaled design stage.

As the stratification phenomenon has become clear through both experiment and analysis efforts, the axial temperature gradients due to the movement of the hot-cold interface and temperature flucuations in the vicinity of the interface have been found to cause not a least impact on the structural integrity of the reactor vessel.

Such being the case, the intensive design effort is under way to accommodate upper plenum thermal stratification. This paper deals with the design methodology for accommodating thermal

stratification of the Monju reactor vessel upper plenum.

2. Design Methodology

Stratification aspects of the Monju reactor vessel upper plenum design should be considered from the following two points of view:

1) Setting of upper plenum internal thermal transient conditions.
2) Treatment of the upper plenum behavior in the plant thermal transient analysis code.

Thermal transients of each component are to be set mainly through an analytical means using experimental results as references. Thus, the foregoing 1) is accomplished through analysis of a multi-dimensional thermal-hydraulic analysis code.

In the plant thermal transient analysis code, the reactor vessel outlet temperature prediction capabiligy plays an important role because the reactor vessel outlet temperature dictates the plant overall system temperature response. Thus, the reactor vessel upper plenum behavior have to be modelled to the degree that the outlet temperature prediction would give comparable results to those of the multi-dimensional analysis code results.

The entire perspective of the code verification and their design application is given in Fig. 1.

3. Code Development and Experimental Verification

3.1 Multi-dimensional thermal-hydraulic analysis code

A two-dimensional thermal-hydraulic analysis code, SKORT-II, has been developed for design purposes and vefified for 1/6-scale sodium test data. The code is now being put into practical use for reactor vessel upper plenum design application.

A similar two-dimensional code, NAGARE-2D, has also been developed independently from the SKORT-II code by the PNC for thermal-hydraulic analysis purposes. The verification of the NAGARE-2D code has been performed for various test data and being used as a cross-check code for the SKORT-II code.

There is another multi-dimensional thermal-hydraulic analysis code developed for design purpose. This code is called "THAUPR" and it is used for the design of the UCS. Test facility vs. code verification matrix is shown in Table 1.

3.2 Plenum Modelling of Plant Thermal Transient Analysis Code (PTTA Code)

An improved plenum model for the Plant Thermal Transient Analysis Code has been developed. The model of this code is not so detailed as those of the SKORT-II and NAGARE-2D codes. However, its plenum model has to be capable of predicting the reactor vessel outlet temperatures during thermal transients.

The temperature transient comparison to the experimental results is being performed for the experiments shown in Table 1.

4. Design Accommodation

Design work for accommodating thermal stratification is intensively under way with due consideration for the experimental and analytical results. Some of the water test results showed severe thermal stratification in the upper plenum near the top of the inner barrel and in the vicinity of the outlet nozzle region. This led to a concern that the similar conditions might exist in the prototype upper plenum. Thus, quantitative understanding of the severity of these regions is the imminent task entrusted to the design side. If these regions should actually be severe, some design modification to the reactor structures would be performed.

5. Future Work

Both the SKORT-II and plant thermal transient analysis codes have been verified for symmetric events and can be used for design purposes for these events. Therefore, in the design regime, analysis work for setting thermal transient conditions for symmetric events is going to start in the near future. In the R/D regime, future effort will be addressed to the development of three-dimensional codes which are capable of treating non-symmetric events such as "Failure of the Check Valve to Shut."

TABLE.1 CODE VERIFICATION PLAN

TEST \ CODE		DESIGN				CROSS CHECK
		SINGLE-DIMENSION	MULTI-DIMENSION			
		PLANT THERMAL TRANSIENT ANALYSIS CODE	SKORT-Ⅱ	THAUPR	NAGARE-2D	COMMIX
SODIUM	1/6-SCALE	○	○	△	○	△
	1/10-SCALE	△	△	△	△	△
WATER	1/1-SCALE (120°-SECTOR)	○	△	○	△	△
	1/6-SCALE*	△	△	△	△	△
	1/10-SCALE	△	△	—	△	—

* The 1/6-scale water testing was originally planned for non-symmetric events such as "Failure of the Check Valve to Shut." However symmetric tests have been added to understand the scale effects and ability for extrapotation.

** ○···Verification Completed △···Verification planned

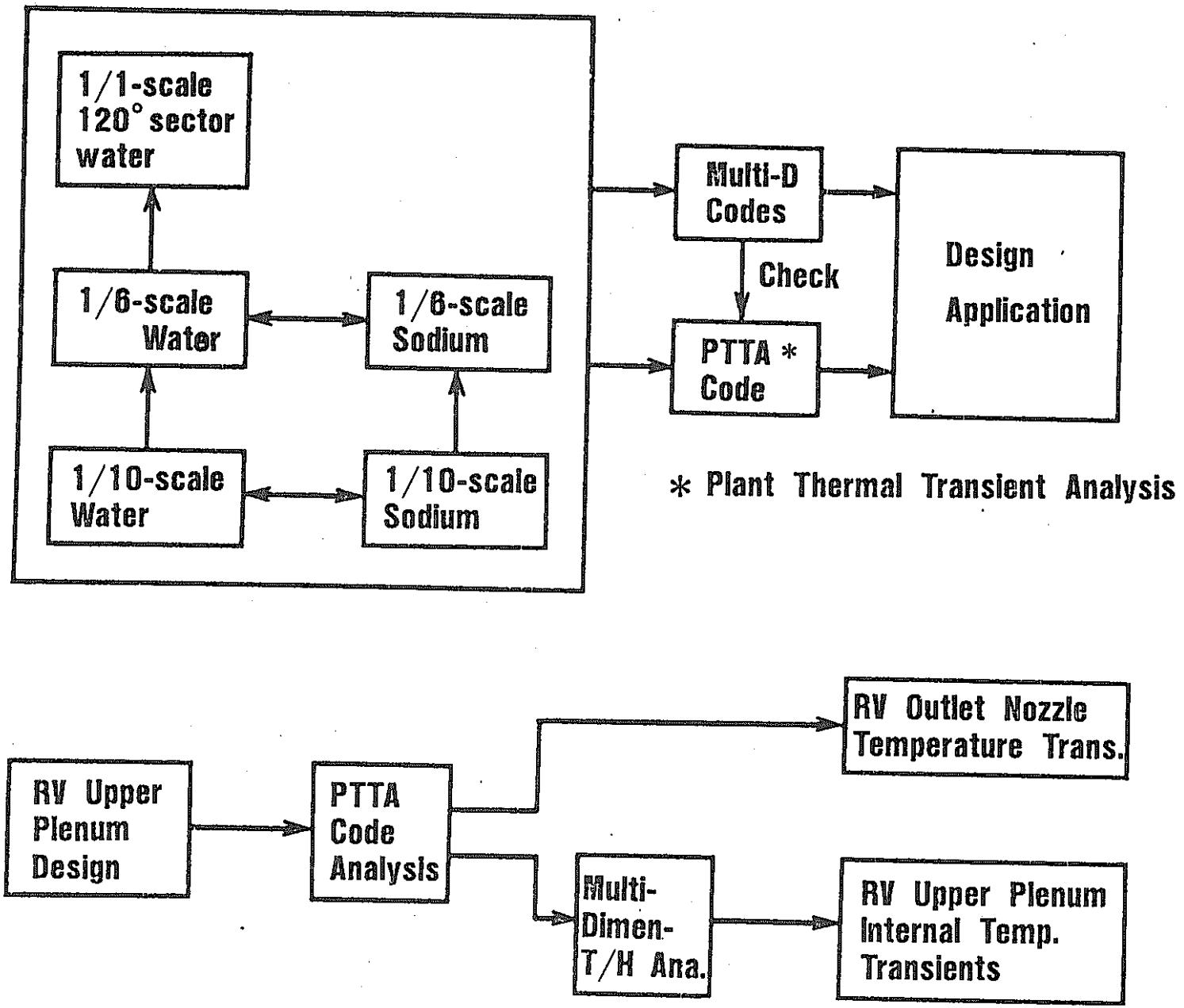

FIG.1 Code Verification and Design Application

B-2 THERMAL STRATIFICATION TEST PROGRAM FOR MONJU

ABSTRACT

The major effort in the study of thermal stratification with respect to the MONJU design has been directed to the reactor vessel upper plenum. Because of the prohibitive cost of performing a full scale sodium test, 1/6 and 1/10 scale models have been used with both sodium and water as test fluids. A 1/3 sector of a full scale water test has been performed as a final check of the influence of scale size. In parallel to the experimental work, an analytical method utilizing thermal hydraulic codes has been applied for the evaluation of the phenomenological study. This paper presents the overview of the thermal stratification test program within the framework of the MONJU Project.

THERMAL STRATIFICATION TEST PROGRAM FOR MONJU

1. OBJECTIVE

- Phenomenological Study of Thermal Stratification w.r.t. MONJU R/V Upper Plenum.
- Verification of Multi-dimensional Thermal Hydraulic Analysis Codes and Plant Thermal Transient Code.
- Evaluation of MONJU R/V Upper Plenum Design Accommodation During Reactor Thermal Transients.

2. PROGRAM PLAN

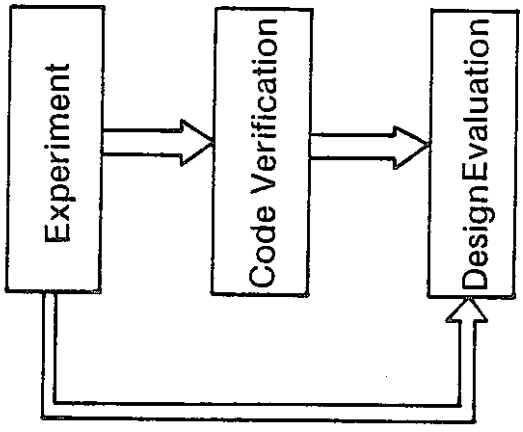

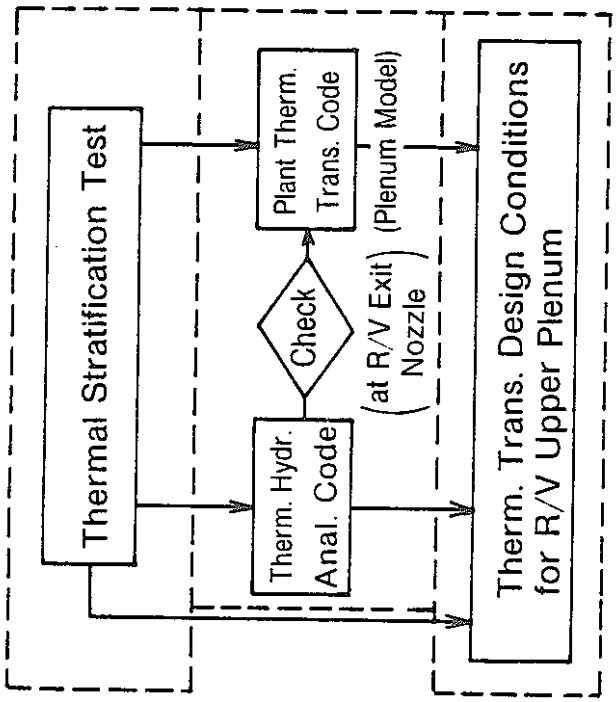

3. EXPERIMENT

3.1 Experimental Program

(a) Influence of scale size (⇑)

(b) Influence of fluid thermal properties (⟺)

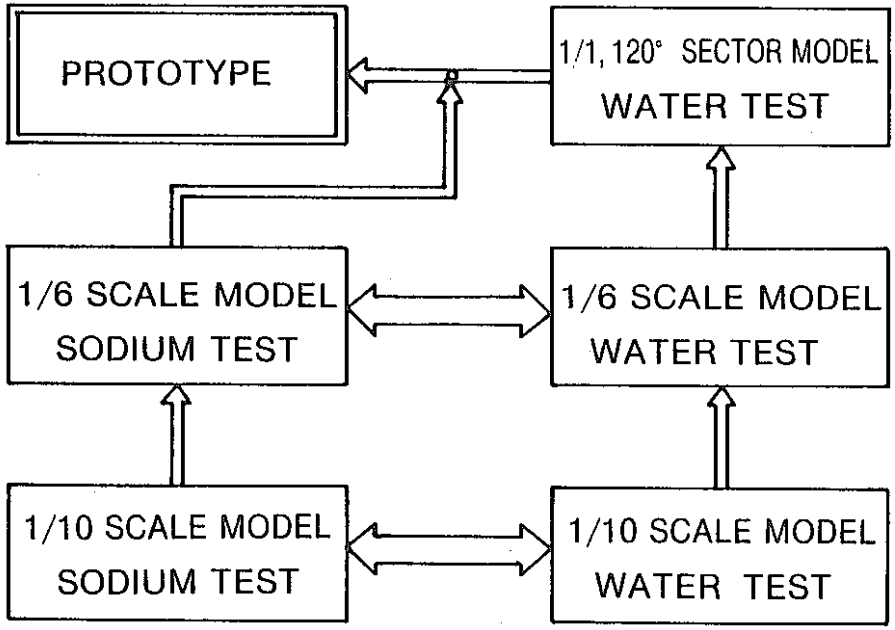

3.2 Description of the Phenomenon

3.2.1 Upper Plenum Flow Patterns During Steady State and Stratified Condition

Normal Operation

Transient Operation (Thermal Stratification)

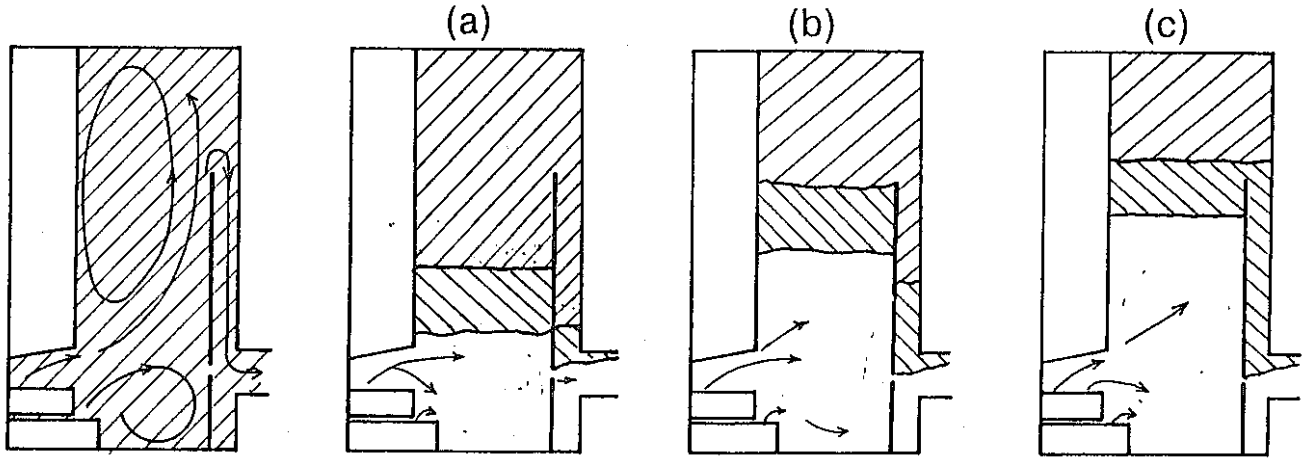

- Good Mixing
- Flow from Inner Barrel flow hole is very small

Cold Fluid Zone (Mixing Zone)

- Mixing Zone is small
- Large Percentage of flow is from Inner Barrel flow holes

Hot-Cold Transition Zone (Temperature Gradident Zone)

- Density Interface rising with Time (Mixing Zone Increasing)
- Flow from Inner Barrel flow holes increasing

Hot Fluid Zone

- Density Interface remains at top region of Inner Barrel

3.2.2 Similitude for the Physical Model

- $$Ri = \frac{\text{buoyant force}}{\text{inertial force}} = \frac{\Delta\rho/\rho}{U^2/g\cdot L} = \frac{\pi^2 g}{16}\cdot\frac{(\Delta\rho/\rho)\cdot L^5}{Q^2}$$

- $$Re = \frac{\text{inertial force}}{\text{viscous force}} = \frac{UL}{\nu} = \frac{4}{\pi}\frac{Q}{L\cdot\nu}$$

U = Core exit average flow velocity

L = Core diameter

Q = Core exit flow rate (Flow after coast-down)

g = gravitational acceleration

$\Delta\rho$ = not density change of incoming fluid

ρ = fluid density

ν = diffusivity of momentum

3.3 Test Procedure

3.3.1 Test conditions

(1) MONJU Scram condition

(2) Constant flow after scram

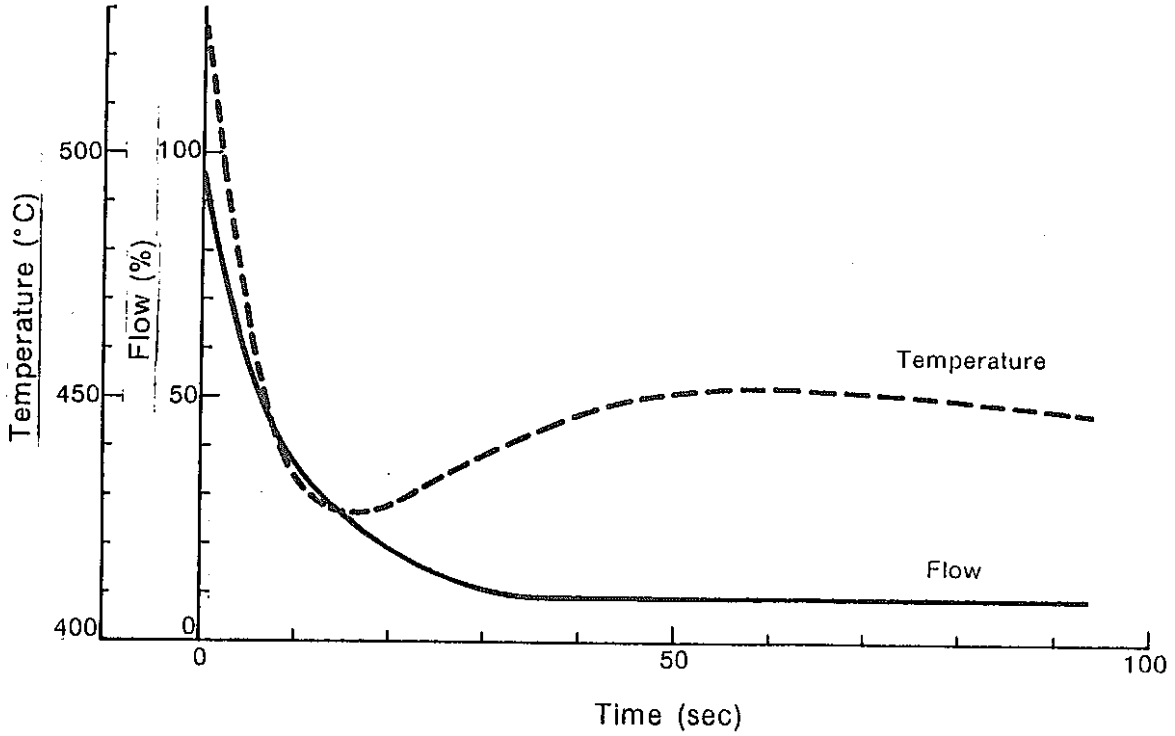

MONJU Thermal Transient Condition at Core Exit (Manual trip)

3.3.2 Comparison scheme of test results

- Relative Ri = Ri′ $= \dfrac{Ri}{(Ri)_M} = \dfrac{\Delta\rho/\rho}{(\Delta\rho/\rho)_M} \cdot \left(\dfrac{L}{L_M}\right)^5 \cdot \left(\dfrac{Q_M}{Q}\right)^2$

- Relative Re = Re′ $\dfrac{Re}{(Re)_M} = \dfrac{Q}{Q_M} \cdot \dfrac{L_M}{L} \cdot \dfrac{\nu_M}{\nu}$

- Non-dim. Time= t* $= \dfrac{1}{V} \int_{t_1}^{t} Q\,dt$

- Non-dim.Flow=% Flow $= Q/Q_o$

- Non-dim. Temperature $= \theta = \dfrac{T - T_C}{T_H - T_C}$

V=Upper plenum-fluid volume

t* =1, time to figuratively replace the total volume of upper plenum fluid with the incoming fluid from the core

Subscript

M : Value for MONJU

o : Total value

To compare data from different sources, select ones with Ri′ ≃1

3.4 Test Data of Importance

(1) Axial temperature distribution

(2) Time rate change of temperature at a point of interest

(3) Radial temperature distribution

(4) Per-cent flow from the inner barrel holes

(5) Temperature fluctuation

3.5 Data Evaluation

(1) Axi-symmetricalness of the phenomenon
(validity of 2-dim. analysis)

(2) Conditions for stratification initiation

(3) Rising speed of density interface
(or lower bound of thermally stratified zone)

(4) Mixing volume in the upper plenum

(5) Relation between the flow volume through flow holes and rising speed of the density interface

(6) Dissipation (or duration) time of thermal stratification

3.6 Test Models and Facilities

3.6.1 Data characteristics of various tests

Test Place	Scale	Test Fluid	Const. flow only	Q/Q_o	$T_H - T_C$ (°C)	Re′	Ri′	t* (max)	Remarks
PNC -OEC	1/6	Na		0.05 ~1.0	160	0.6 ~0.03	0.01 ~4.11	3	Flow coast-down also possible
	1/10	Na	○	0.1	40~100	0.03~ 0.015	0.25 ~0.83	1	Initially, stagnant sodium in the plenum
MHI	1/10	Water		0.1	26	0.007	0.83	28	Flow coast-down
MAPI	1/6	Water		0.1	67	0.022	1	2	Flow coast-down
TOSHIBA	1/1 120° Sector	Water brine	○	0.54 ~1.23	31 ~40	3.3	0.25 ~1.35	0.7	

3.6.2 Descriptions of Test Models and Facilities.

(1) $\frac{1}{6}$ Scale, Sodium (PNC-OEC)

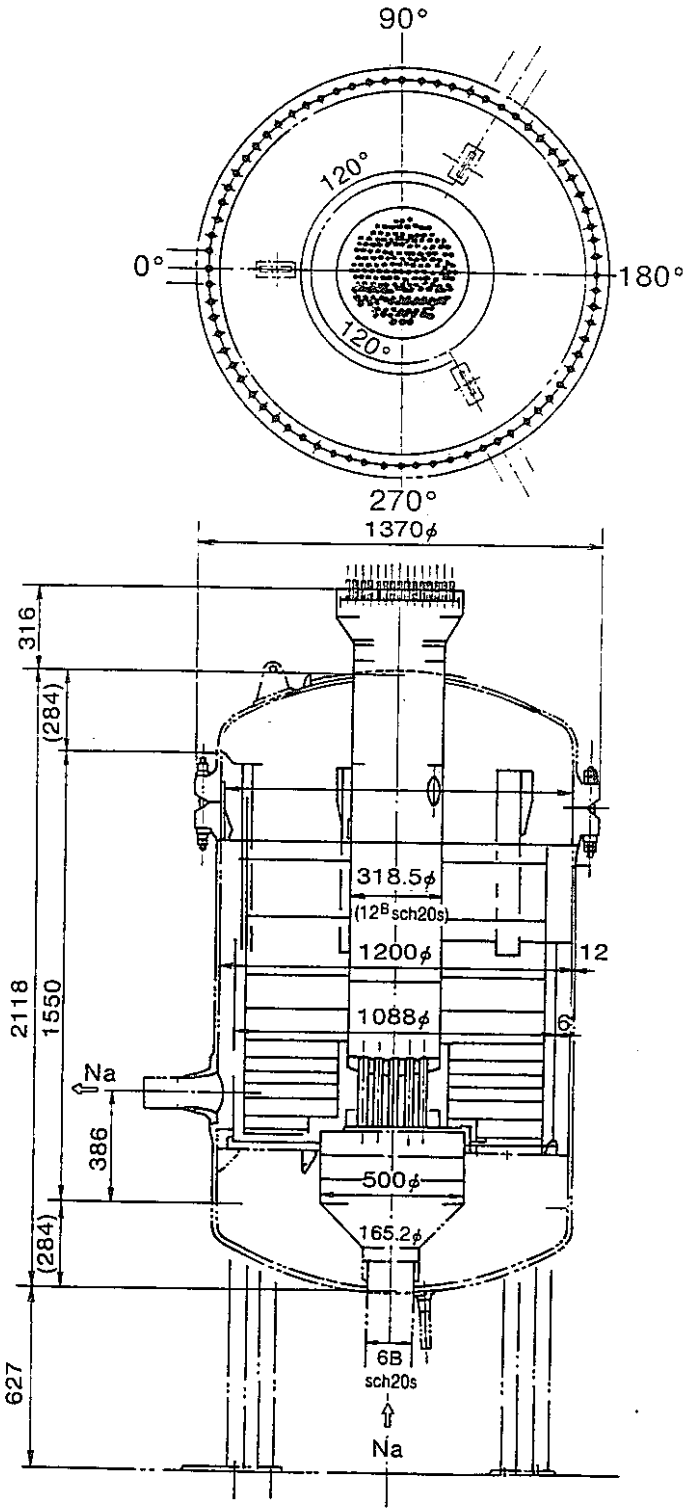

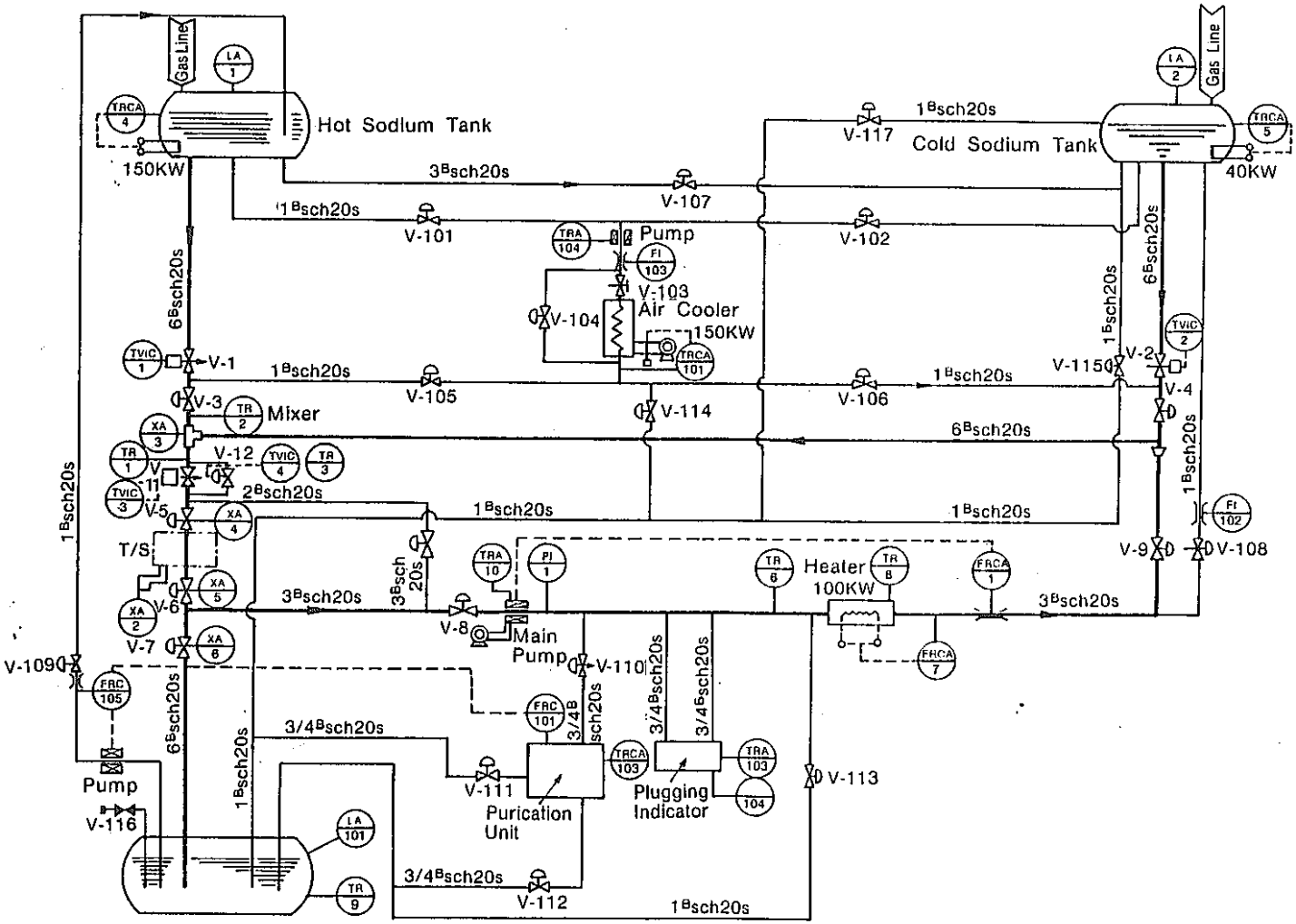

Thermal Shock Test Loop.

(2) $\frac{1}{10}$Scale, Sodium (PNC)

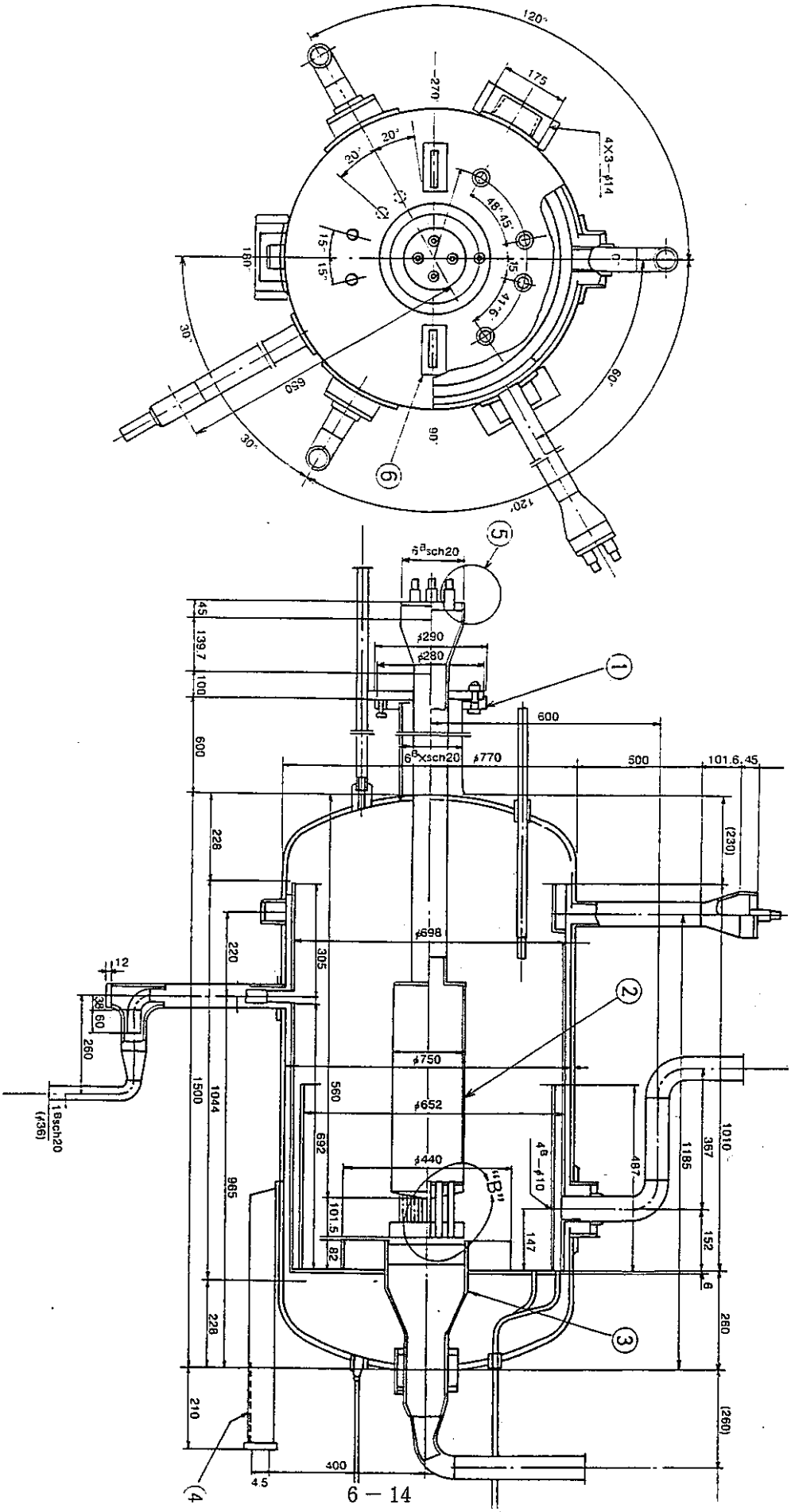

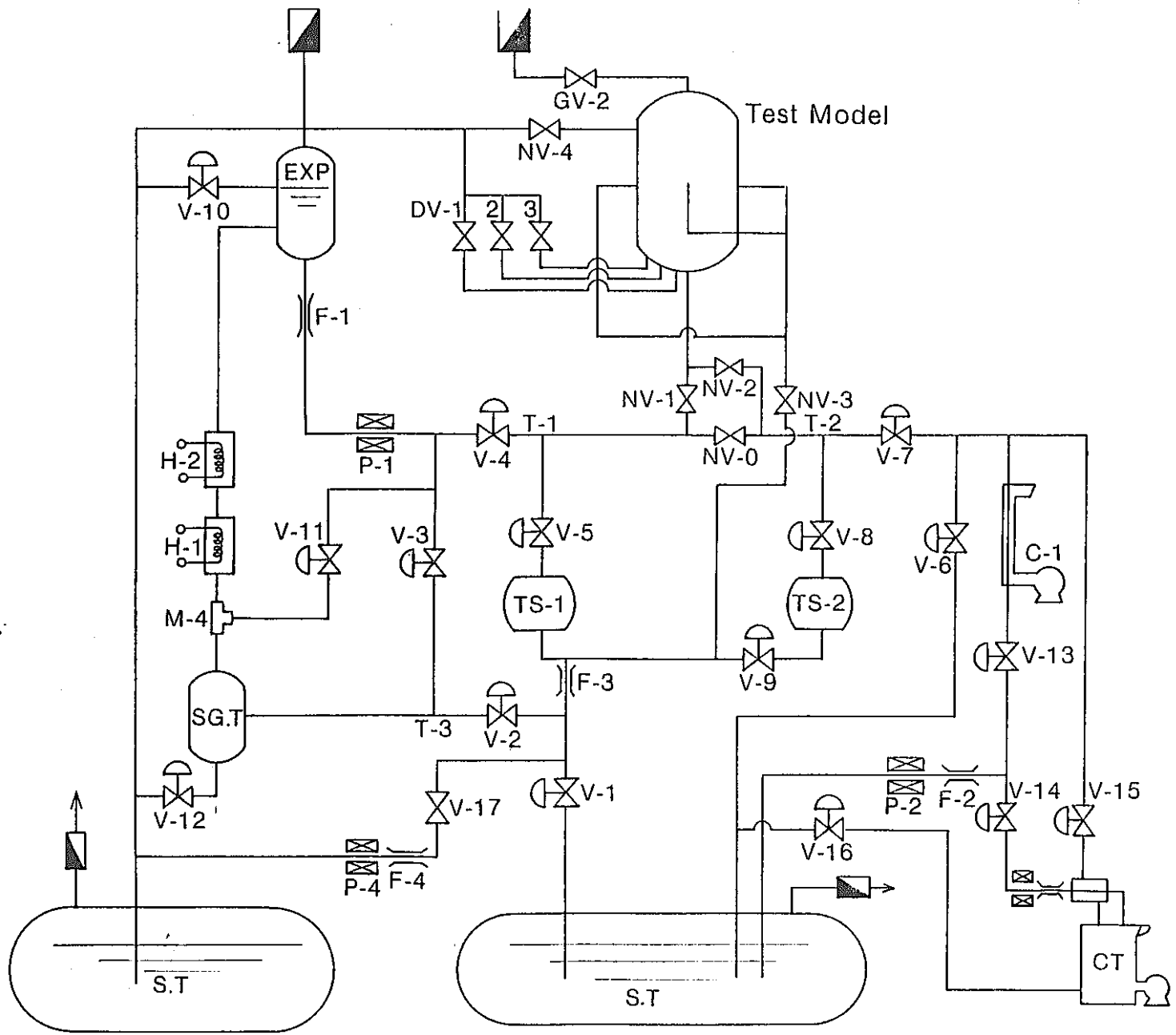

Small Thermal Shock Test Loop

(3) $\frac{1}{6}$ Scale, Water (MAPI)

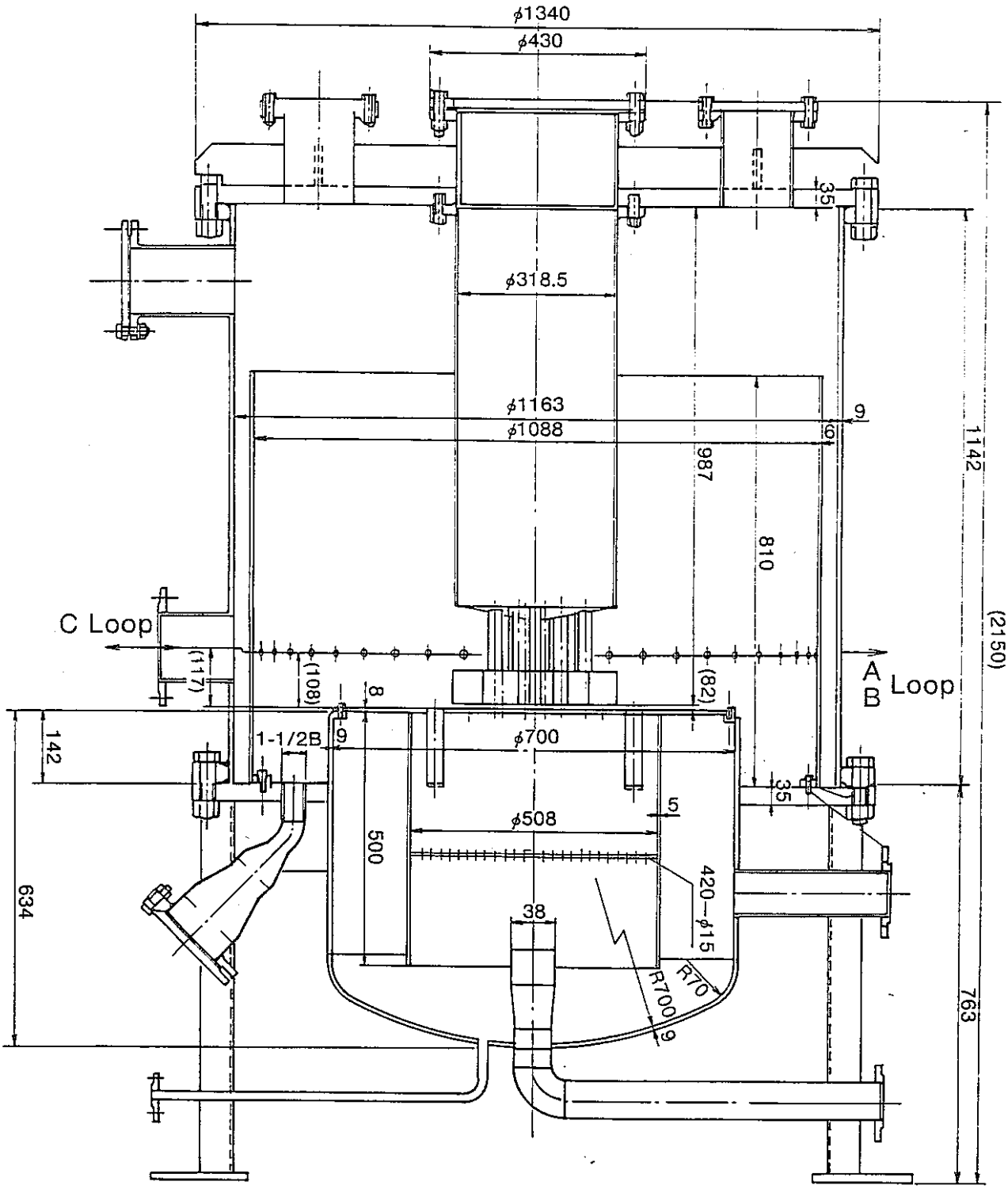

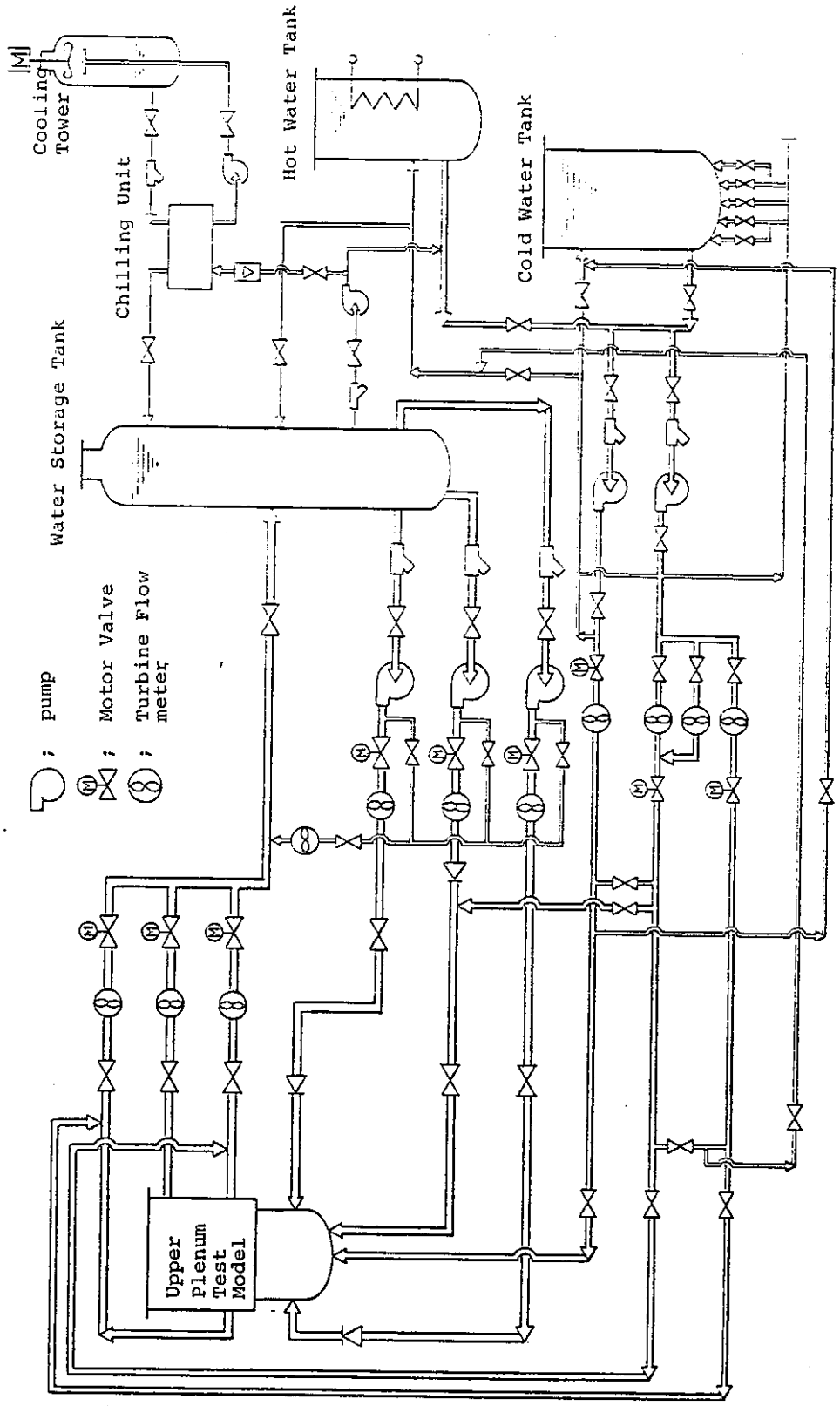

1/6 SCALE, WATER TEST LOOP

(4) $\frac{1}{10}$Scale, Water (MHI)

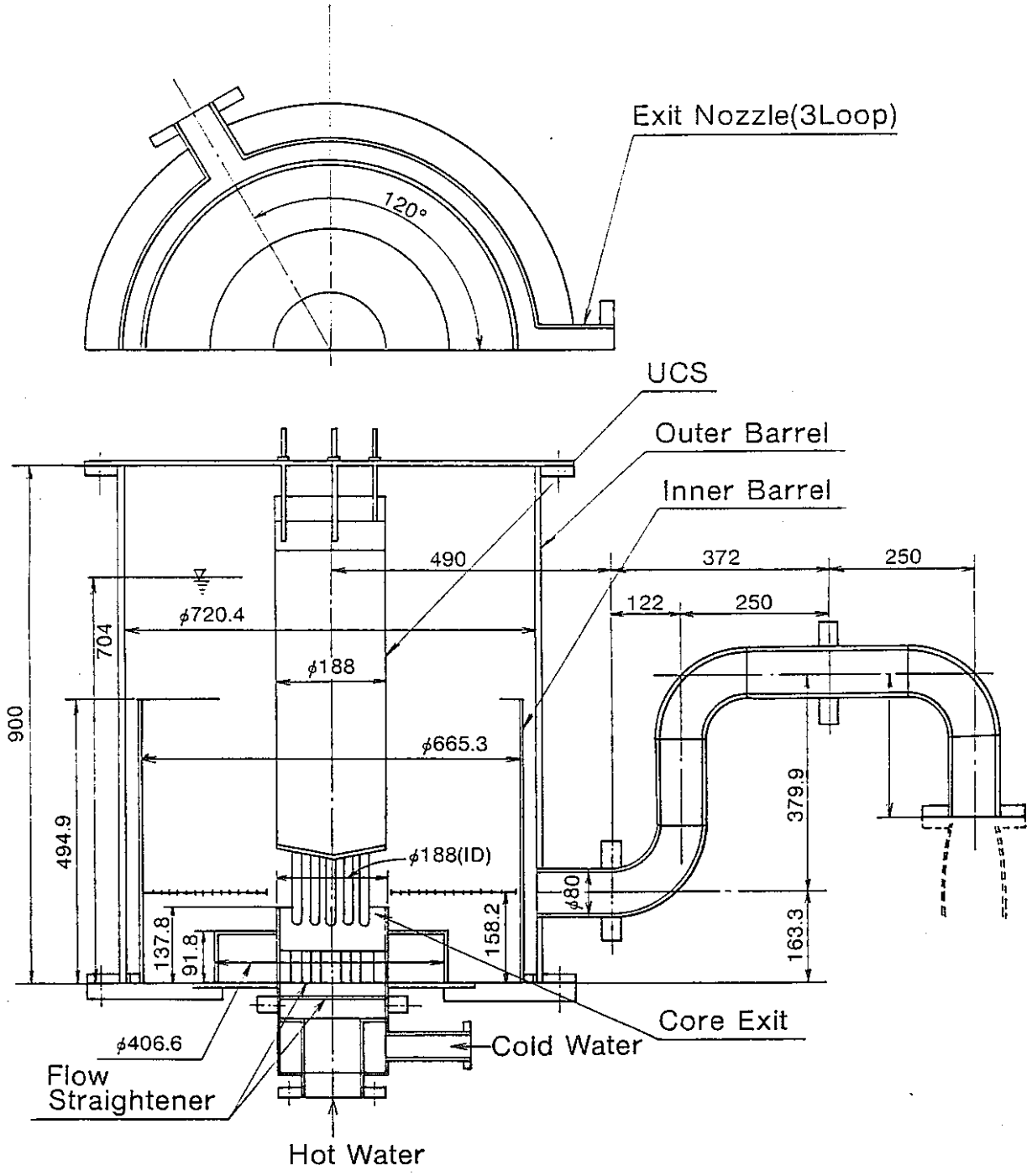

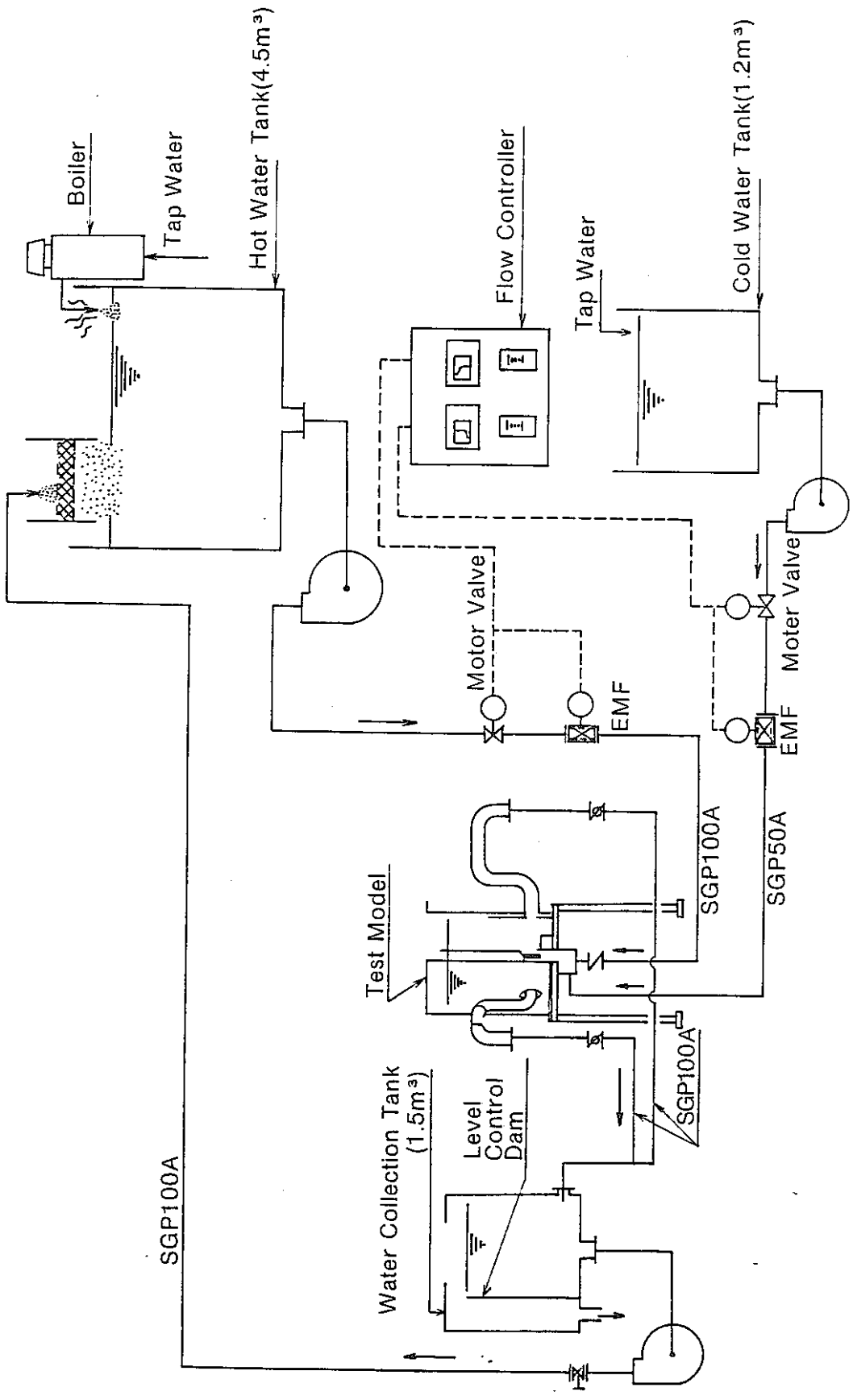
Boiler
Tap Water
Hot Water Tank(4.5m³)
Flow Controller
Tap Water
Cold Water Tank(1.2m³)
Motor Valve
EMF
EMF
Moter Valve
SGP100A
SGP50A
Test Model
SGP100A
Level Control Dam
Water Collection Tank (1.5m³)
SGP100A

3.7 Thermal Stratification Test Schedule.

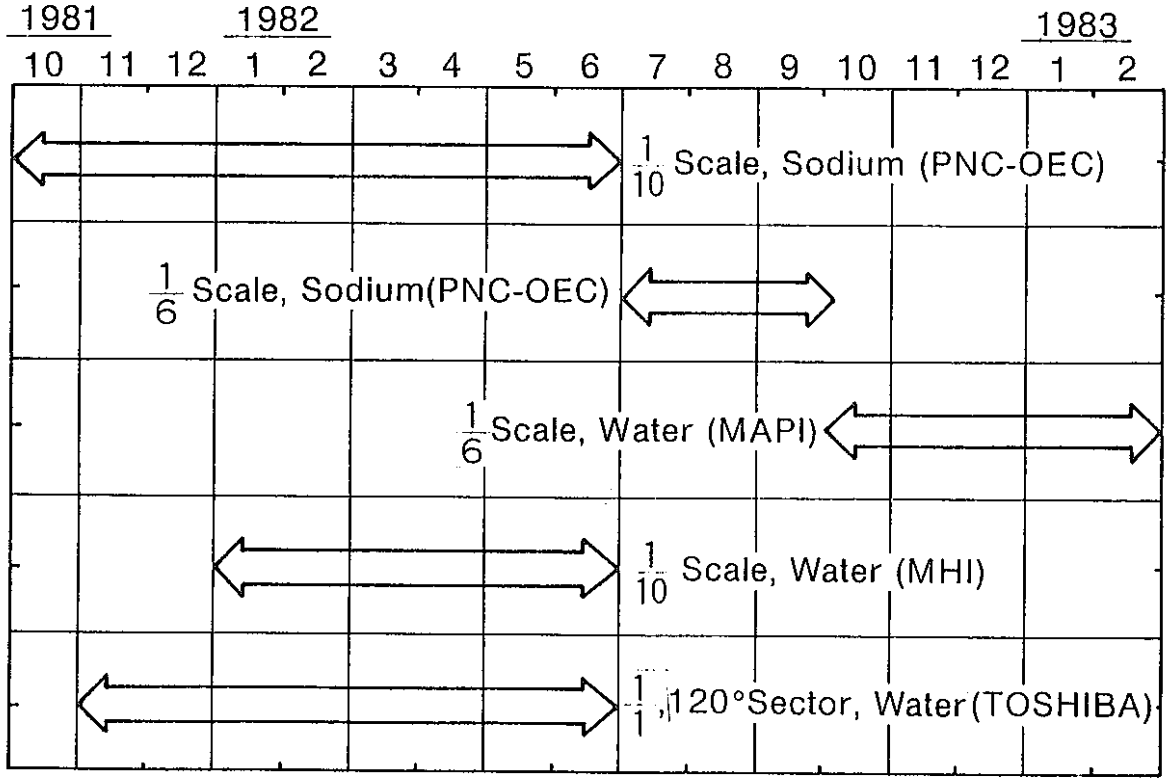

4. CODE VERIFICATION

4.1 Thermal Hydraulic Analysis Code

—Setting of upper plenum thermal transient conditions

4.1.1 MONJU design code : SKORT-Ⅱ

4.1.2 Cross-check code : NAGARE

4.2 Plant Thermal Transient Code

—Treatment of the upper plenum behavior in the plant thermal transient analysis

(prediction of R/V exit nozzle temperature)

4.3 Code Verification Program

Test Model		Thermal Hydraulic Analysis Code	Plant Thermal Transient Analysis Code
Sodium	$\frac{1}{6}$	Completed	Completed
	$\frac{1}{10}$	In Plan	In Plan
Water	$\frac{1}{1}$ (120°-Sector)	In Plan	Completed
	$\frac{1}{6}$	In Plan	In Plan
	$\frac{1}{10}$	In Plan	In Plan

B-3 SODIUM THERMAL STRATIFICATION TEST

WITH A 1/6 MODEL OF MONJU OUTLET PLENUM

ABSTRACT

The transient temperature behavior after a normal reactor scram was studied in a 1/6 scale model of the reactor upper plenum of MONJU using sodium as a test fluid. Effects of variations in Richardson number (ratio of buoyancy/inertia forces) were evaluated. The relative Richardson number, R_i^* (ratio of R_i of model/MONJU at 10% coast-down flow) was used as the measure for comparison.

Thermal stratification was observed in the region $R_i^* > 0.2$. In the presence of stratification, the sodium temperature in the upper plenum showed an almost linear distribution in the axial direction without a clearly defined stratification interface. At $R_i^* = 1$, the sodium mixing condition in the plenum was unexpectedly good, with the effective mixing volume being around 60%.

Sodium Thermal Stratification Test with a 1/6 Model of MONJU Outlet Plenum

Table B3-1 Test Conditions

Case	Test No.	Q/Q_o	$T_H - T_C$ (°C)	Re′	Ri′	t* (max)	Remarks
Case Ⅰ	14	0.05	160	0.0315	3.54	3	Const. at Low Flow
Case Ⅱ	21	1.0	160	0.58	0.011	3	Normal Operation Flow
Case Ⅲ	19	1.0～0.05	160	0.57～0.029	0.0116～4.11	3	Coast-down Flow

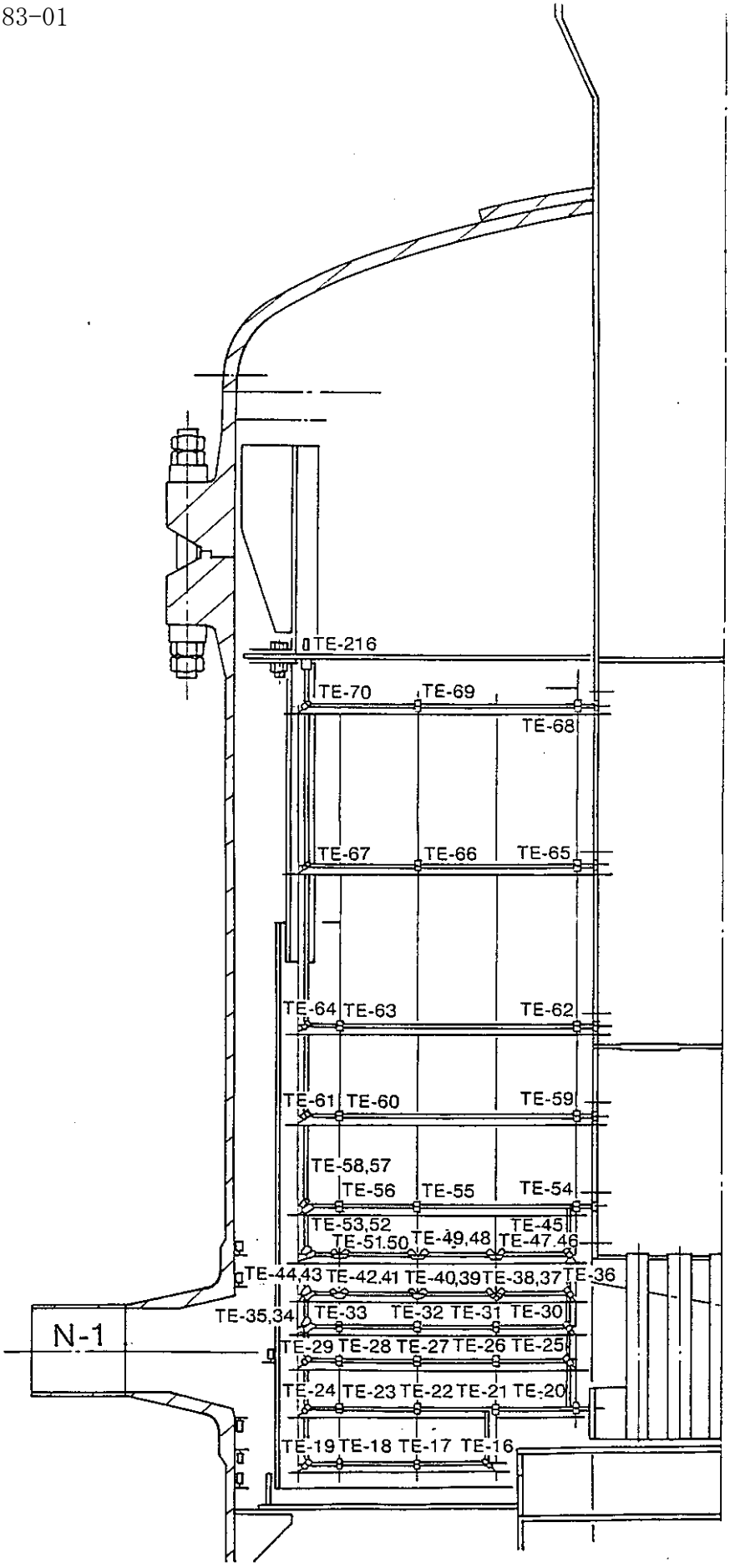

Fig. B3-1 Thermocouple Installation (0°C, Nozzle 1-direction)

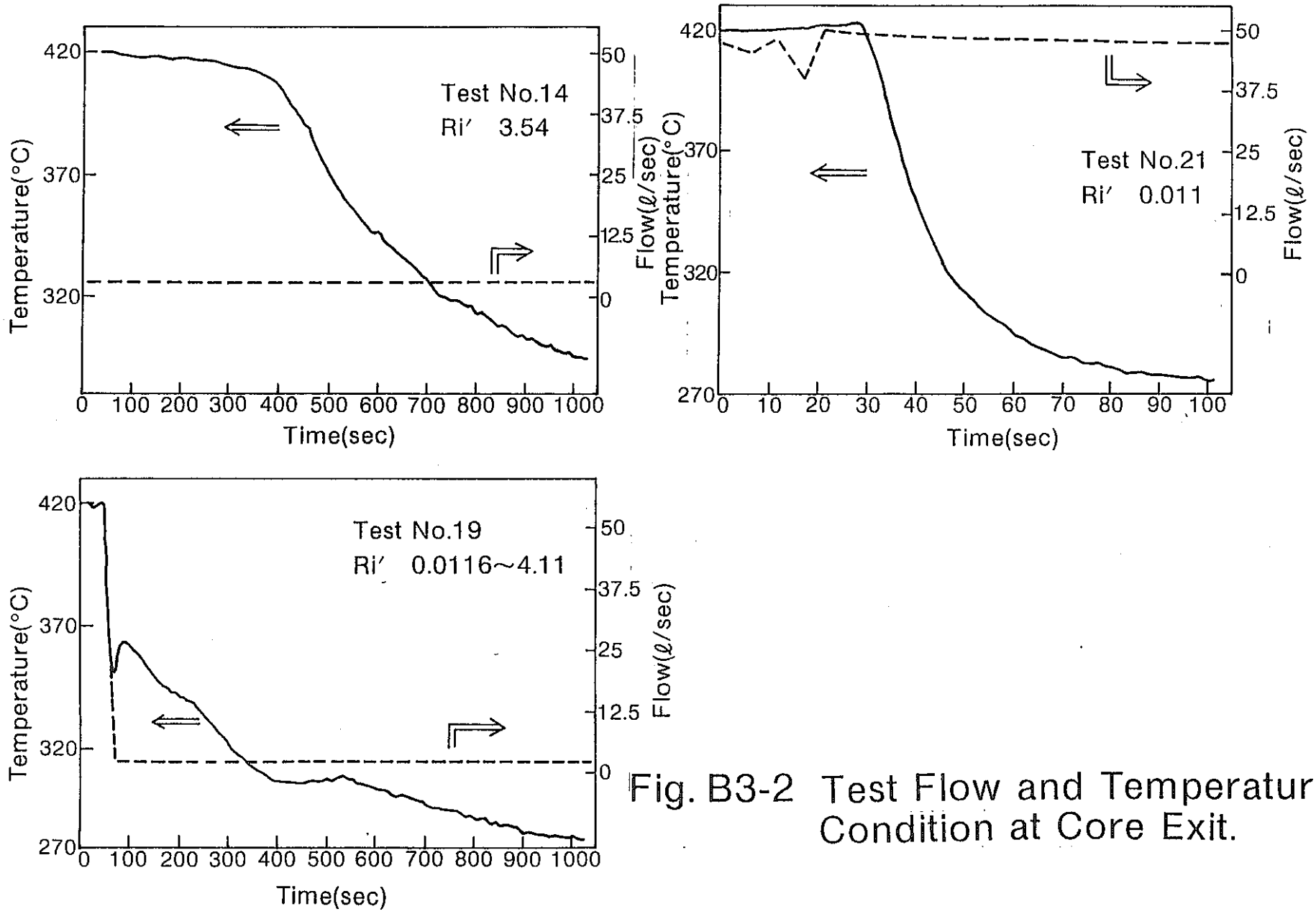

Fig. B3-2 Test Flow and Temperature Condition at Core Exit.

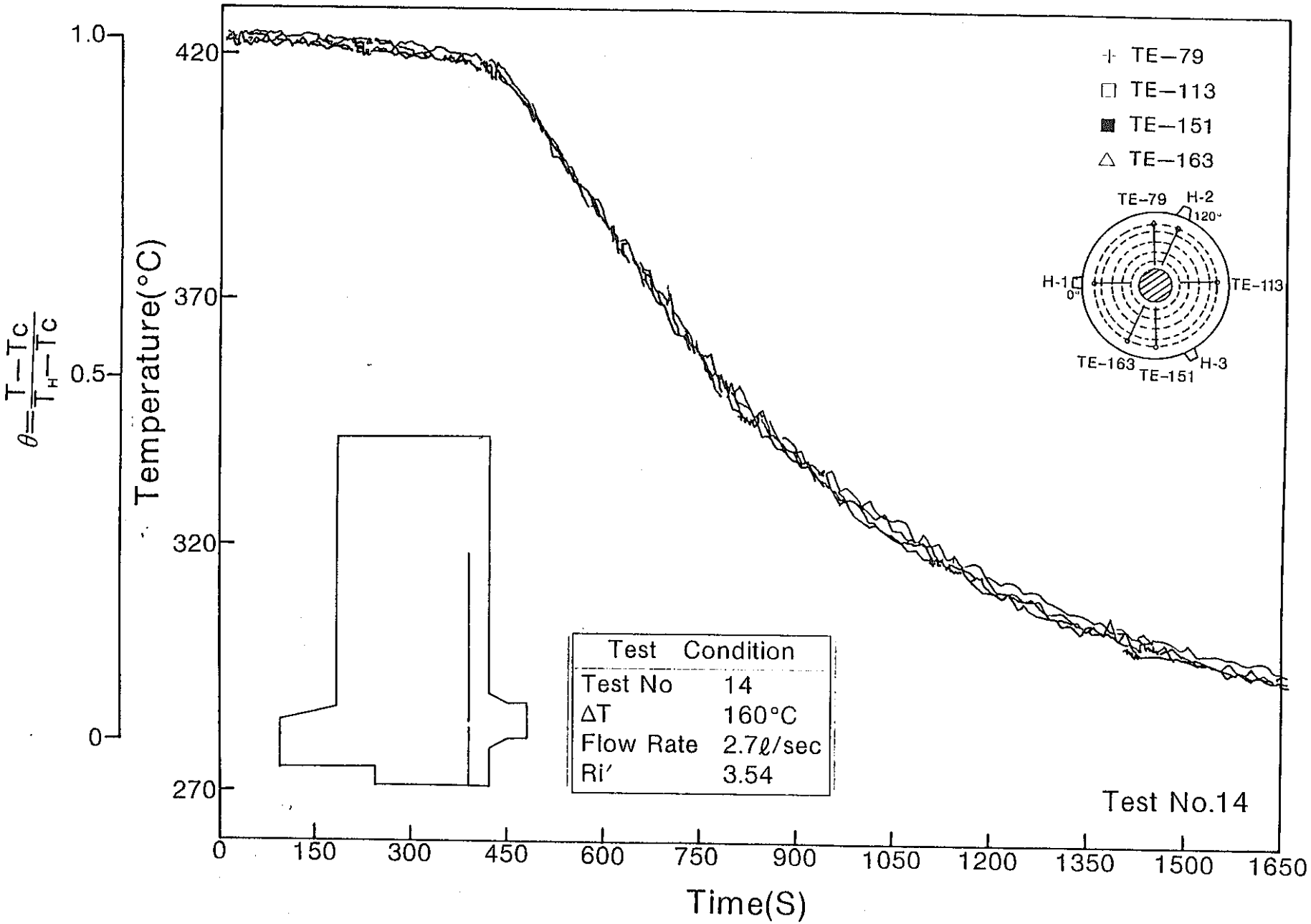

Fig. B3-3 Symmetricalness of Test Data.

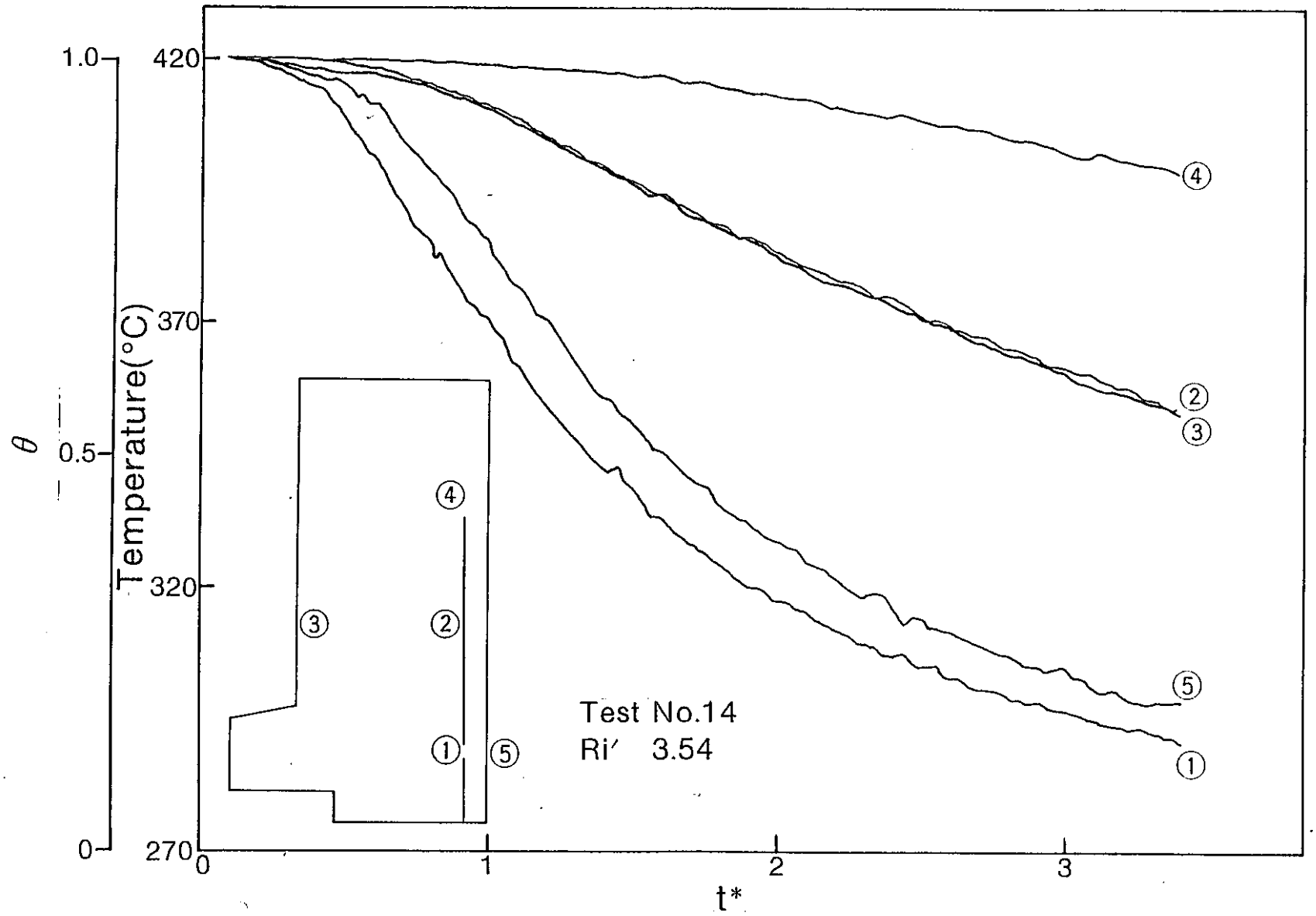

Fig. B3-4 Time-rate Change of Temperature at Points of Interest (Test No.14)

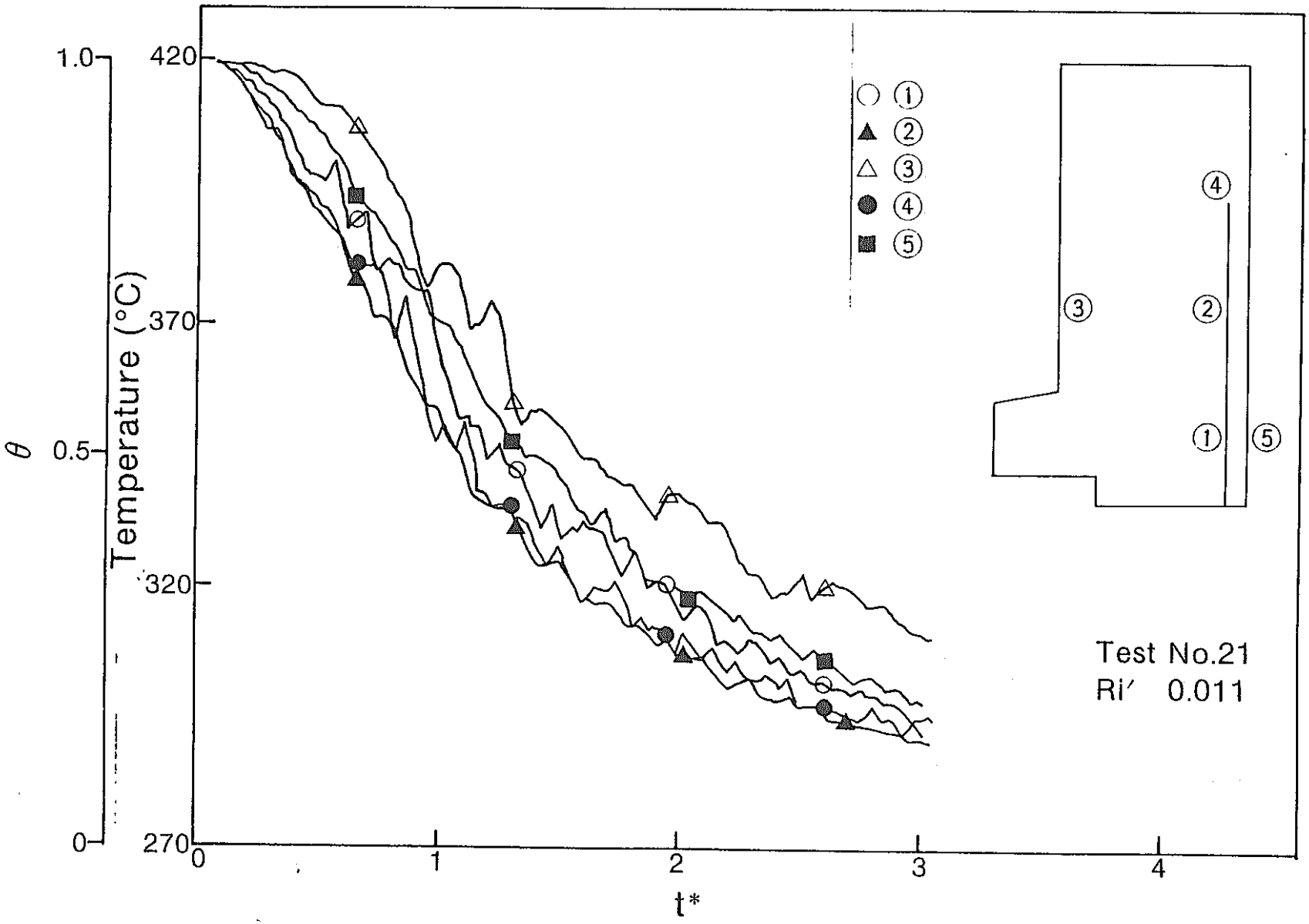

Fig. B3-5 Time-rate Change of Temperature at Points of Interest (Test No.21)

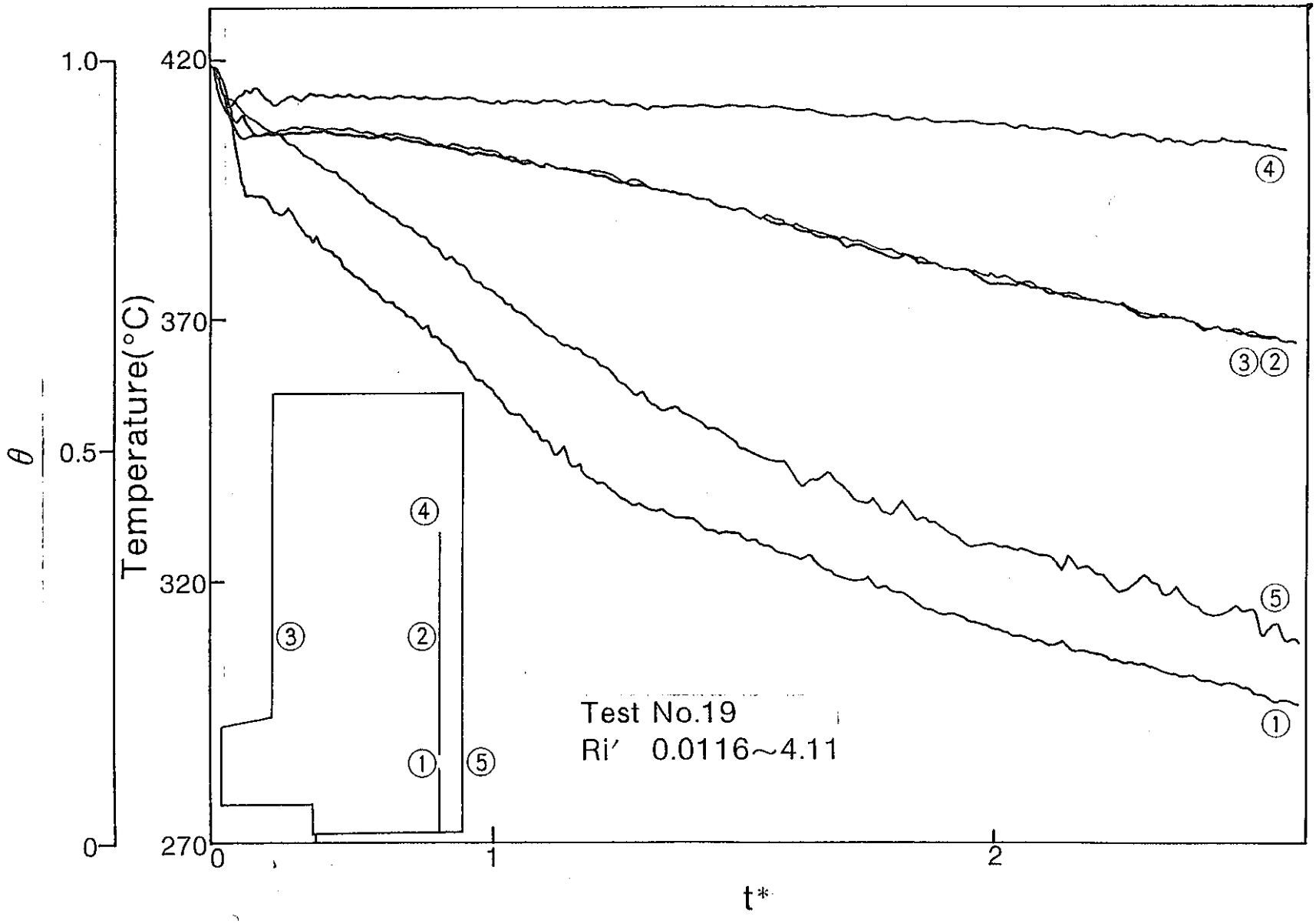

Fig. B-3-6 Time-rate Change of Temperature at Points of Interest (Test No.19)

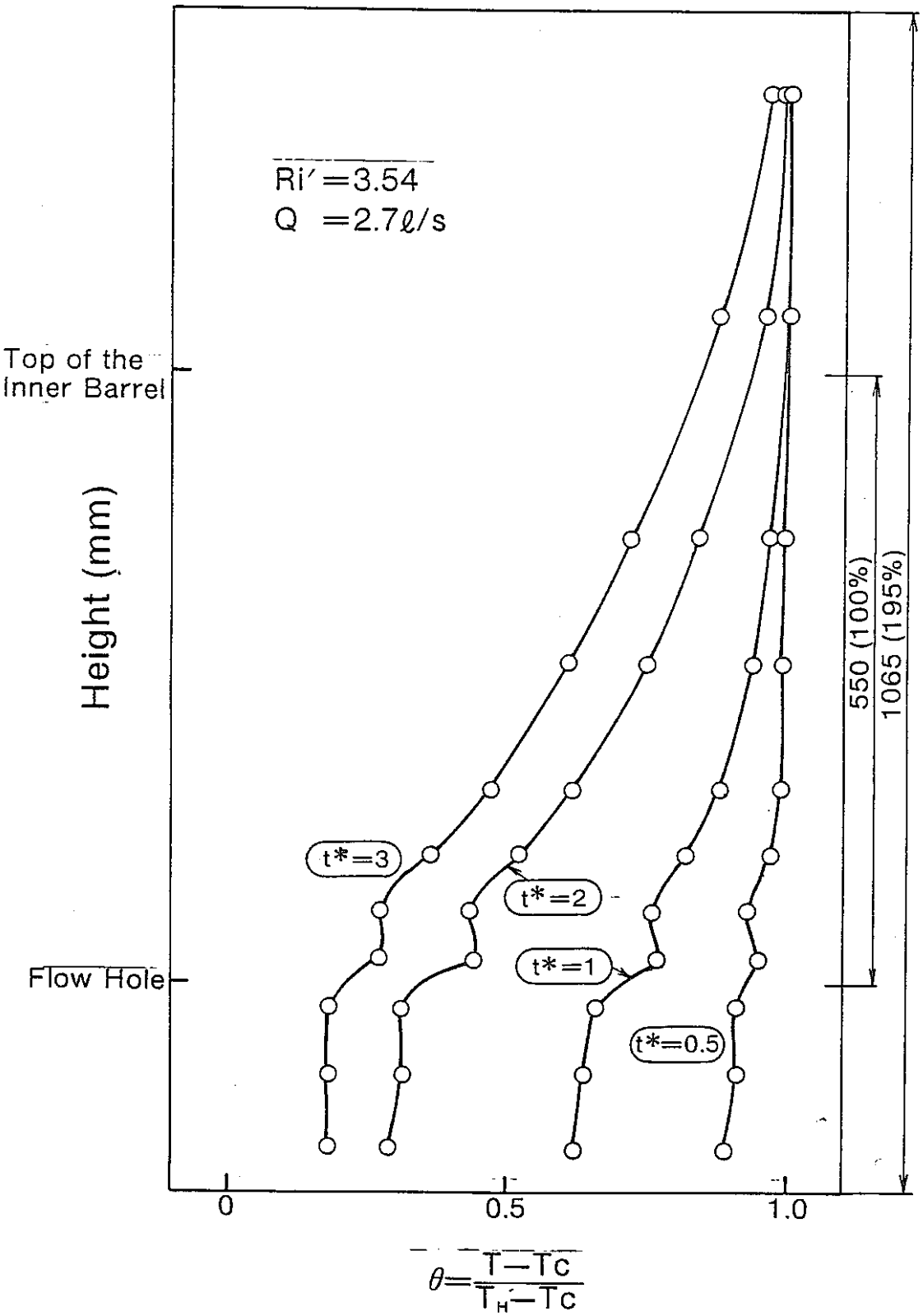

Fig. B3-7 Axial Temperature Distribution (Test No.14)

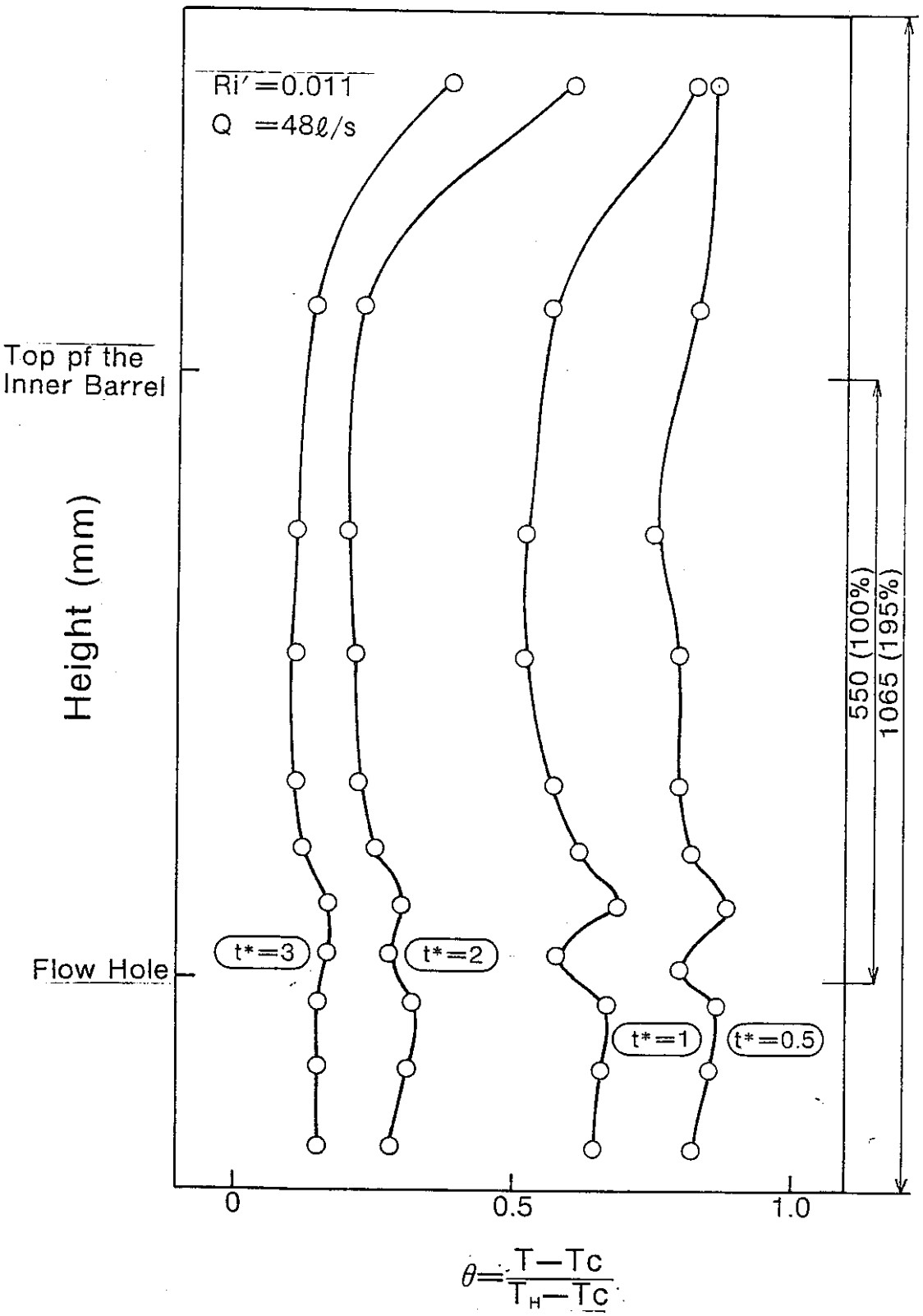

Fig. B3-8 Axial Temperature Distribution (Test No.21)

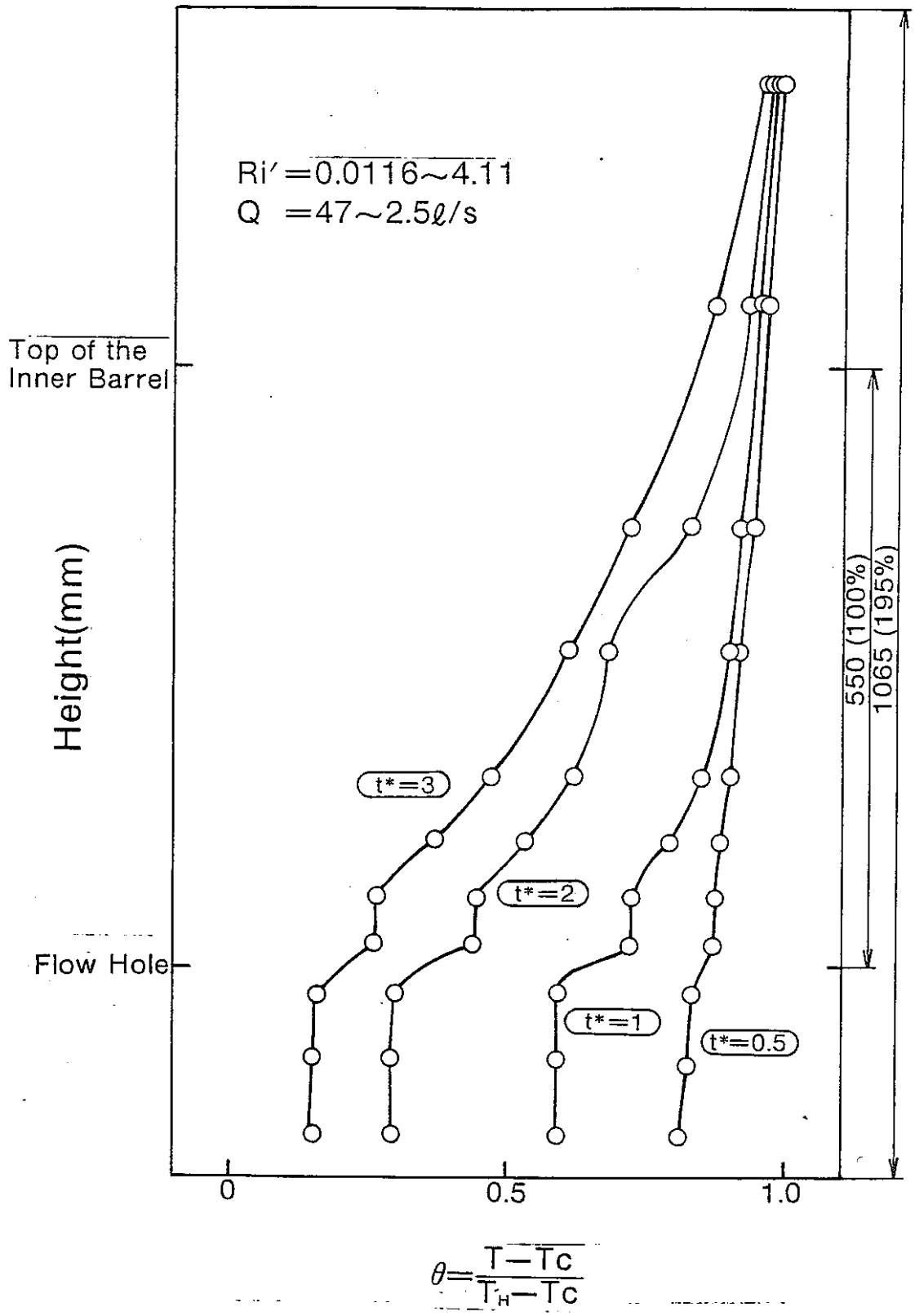

Fig. B3-9 Axial Temperature Distribution (Test No.19)

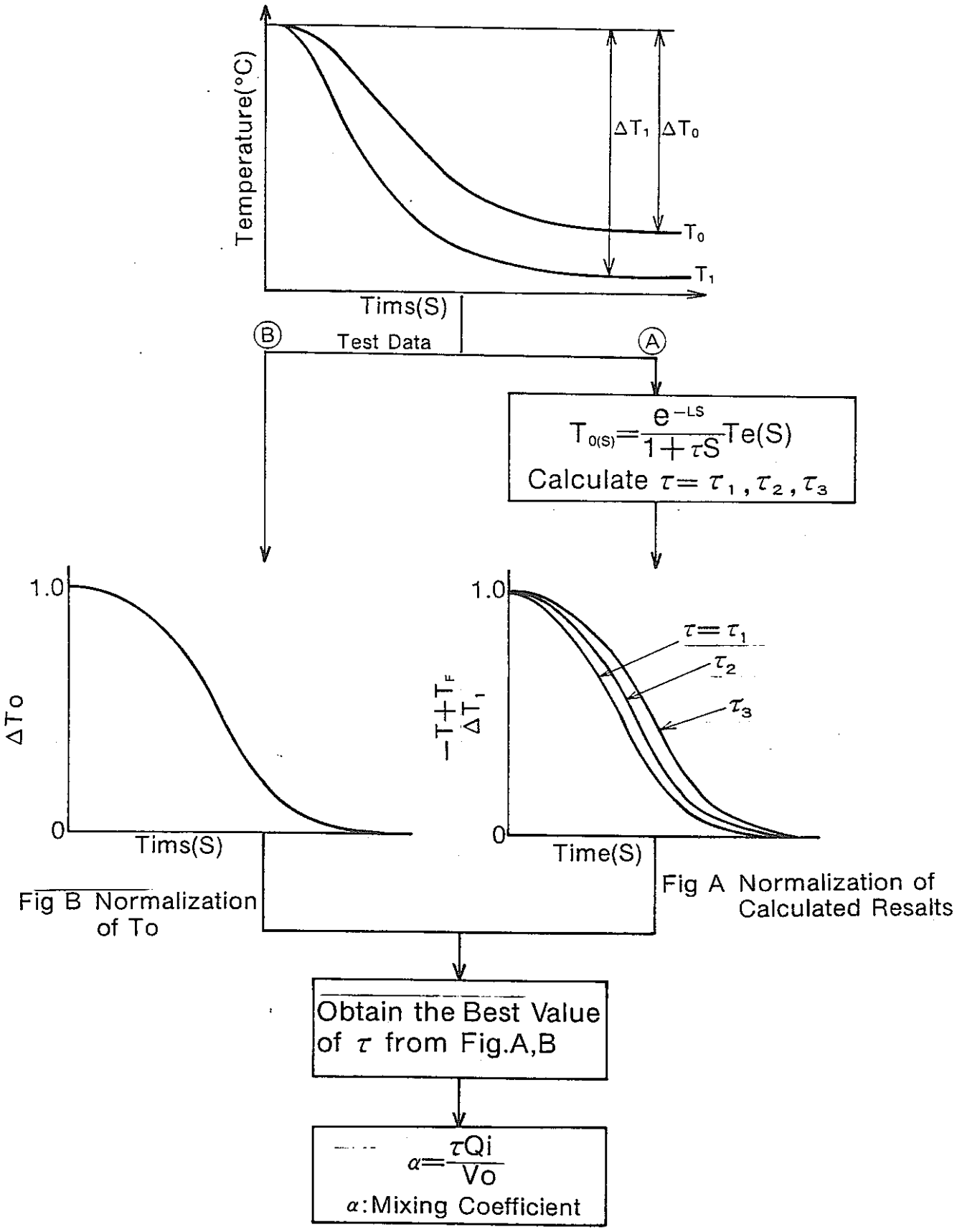

Fig. B3-10 Evaluation of Mixing Coefficient from Primary Delay Time and Dead Time.

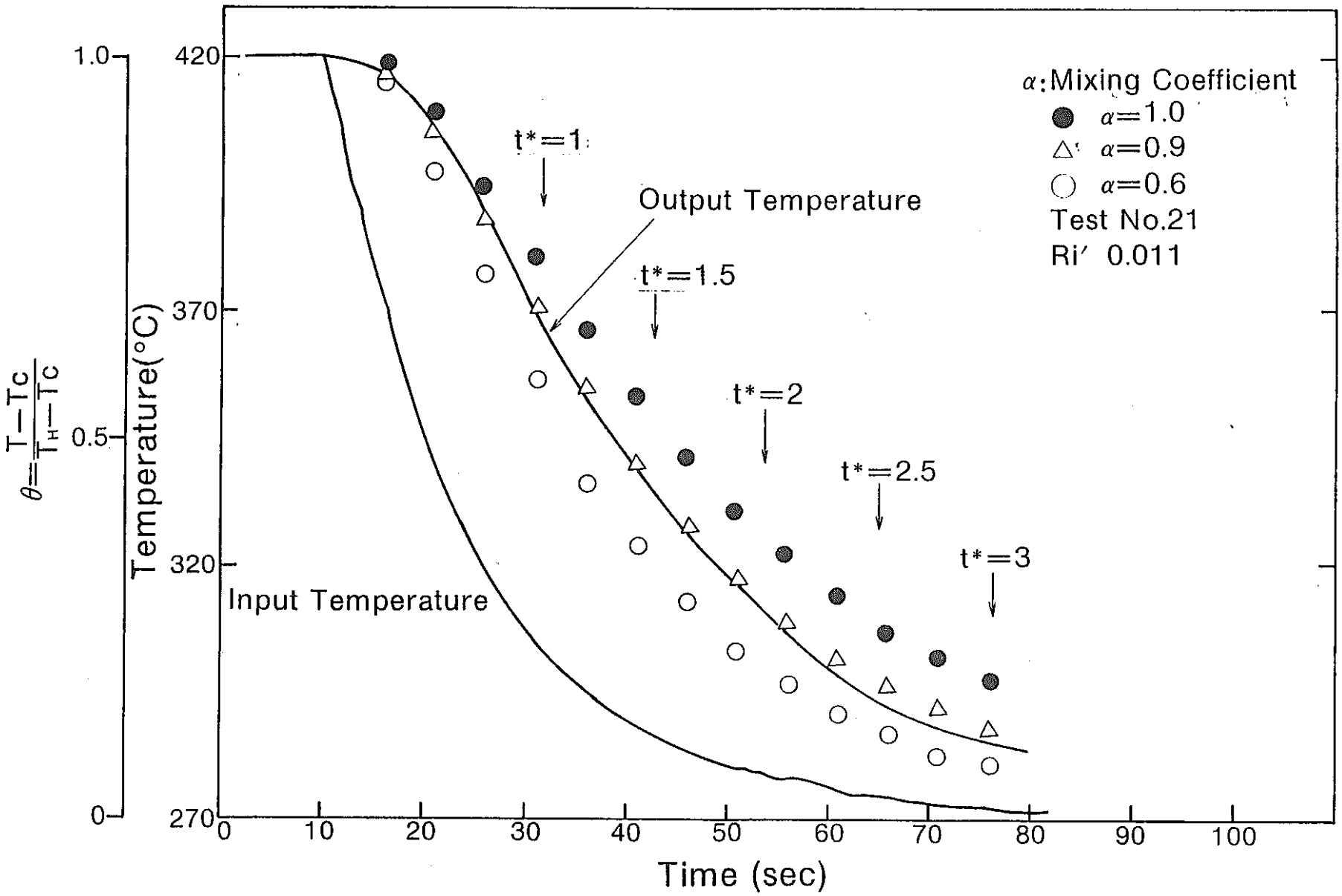

Fig. B3-11 Evaluationof Mixing Coefficient.

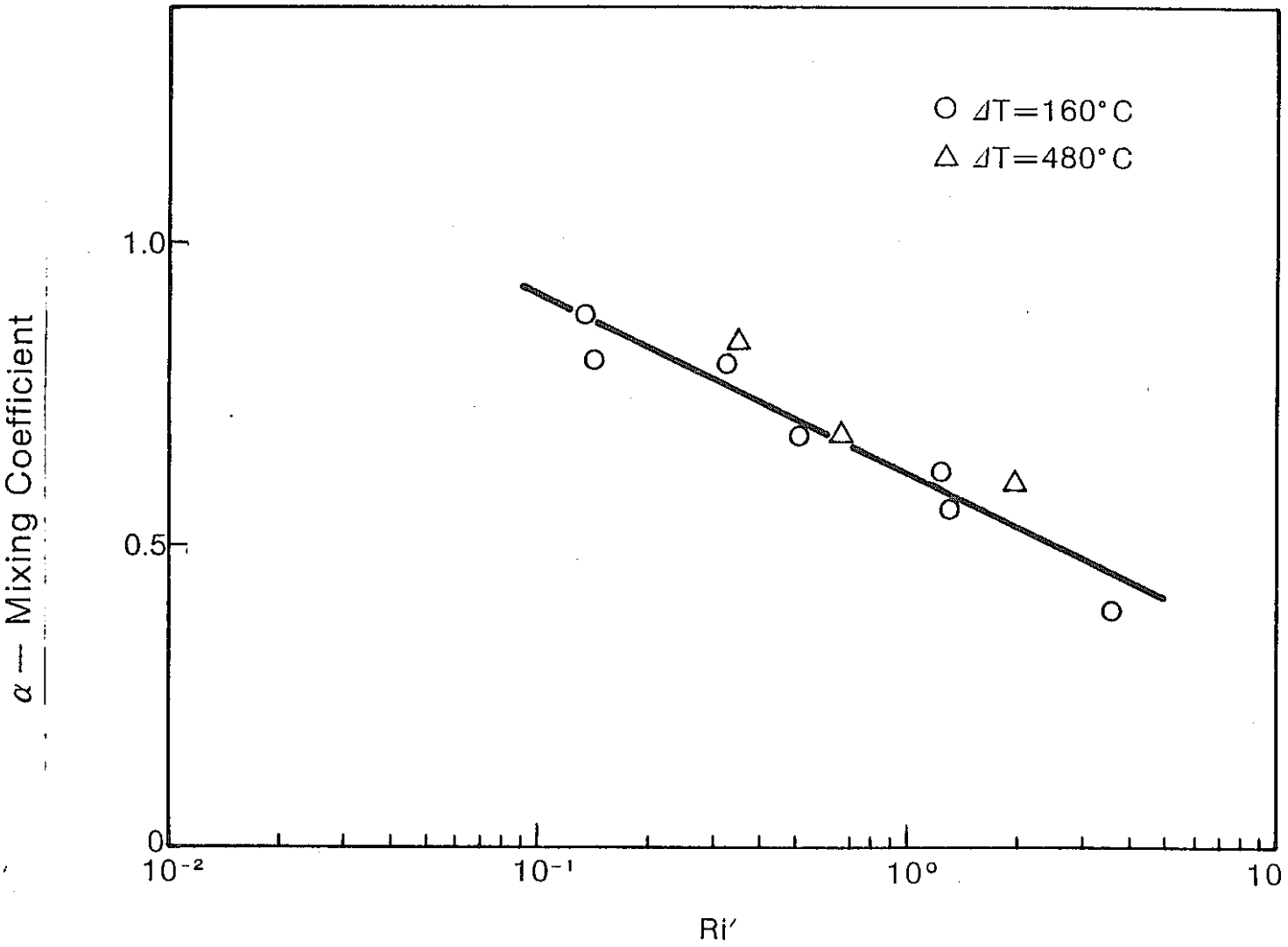

Fig. B3-12 Relation between Mixing Coefficient evaluated from Primary Delay Time and Relative Richardson Number

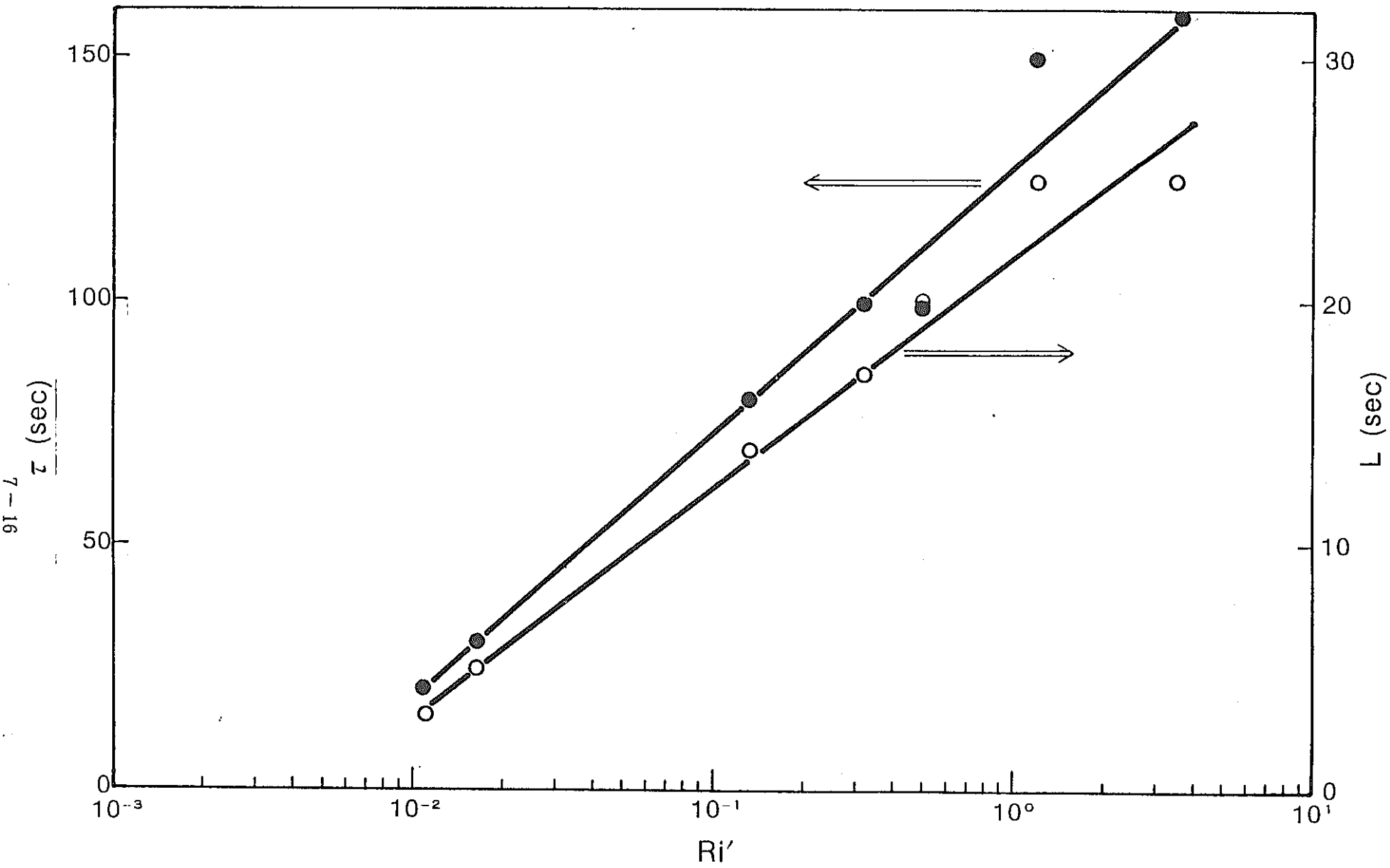

Fig. B3-13 Ri′-dependency of τ (Primary delay time constant) and L (dead time constant)

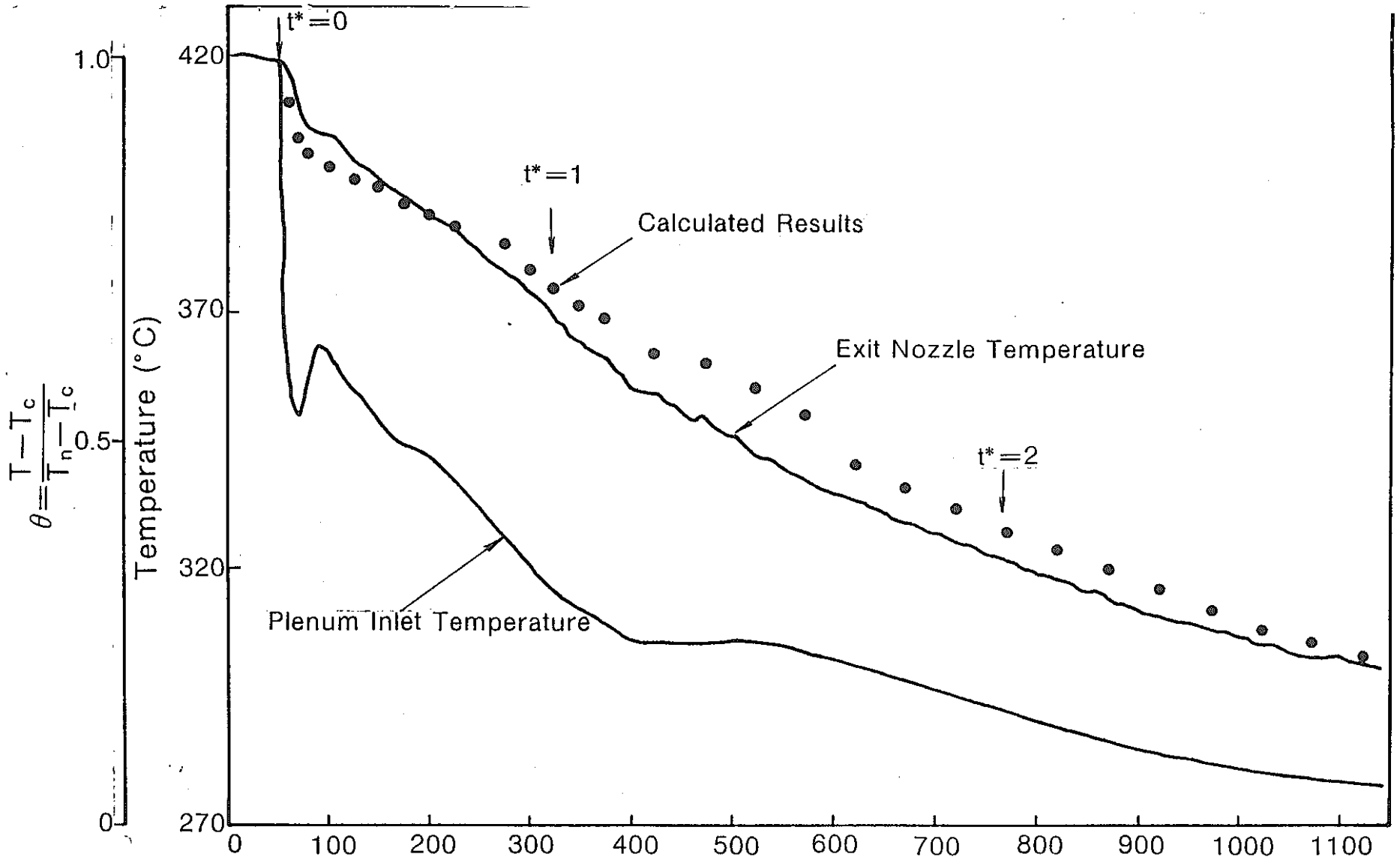

Fig. B3-14 Evaluation of Transient Temperature from the Calculated τ and L obtained from the Steady State Data

Evaluation Method

$$T_F \cdot X + T_A(Q-X) = T_O \cdot Q$$

$$X = \frac{Q(T_O - T_A)}{T_F - T_A}$$

T_F : Temp. at Flow holes	(°C)
T_A : Temp. in the annulus	(°C)
T_O : Temp. at the exit nozzle	(°C)
Q = Flow volume entering the Plenum	(ℓ/s)
X : Flow volume through flow holes	(ℓ/s)

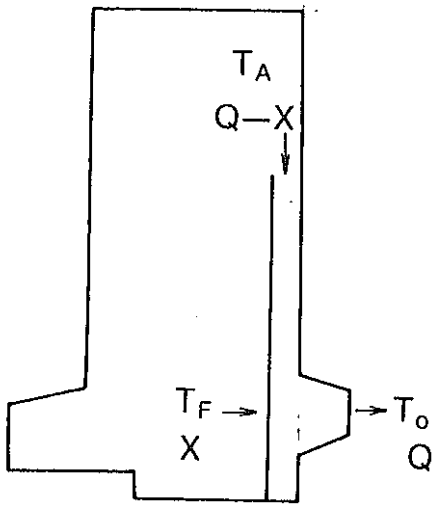

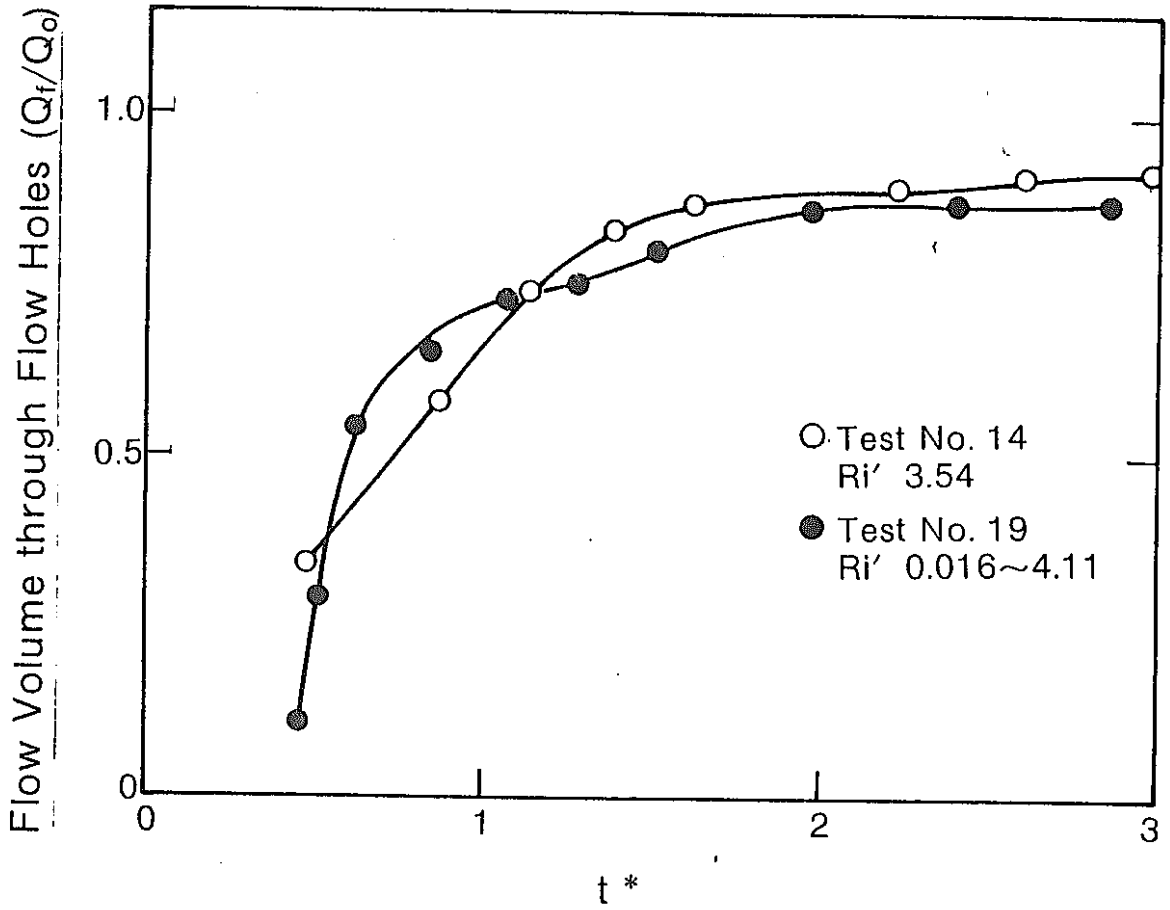

Fig. B3-15 Flow Volume through Flow Holes

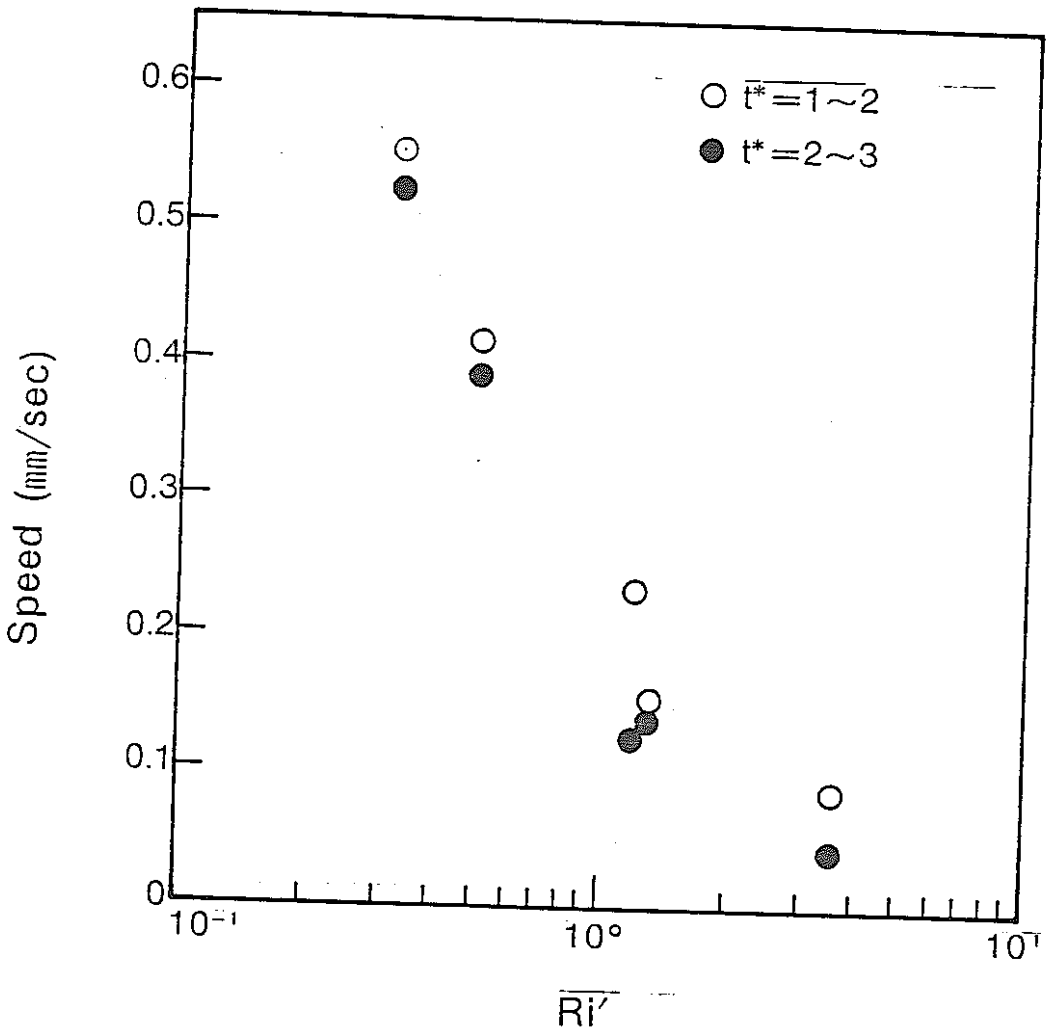

Fig. B3-16 Rising Speed of Density Interface Obtained from the Average Plenum Temperature

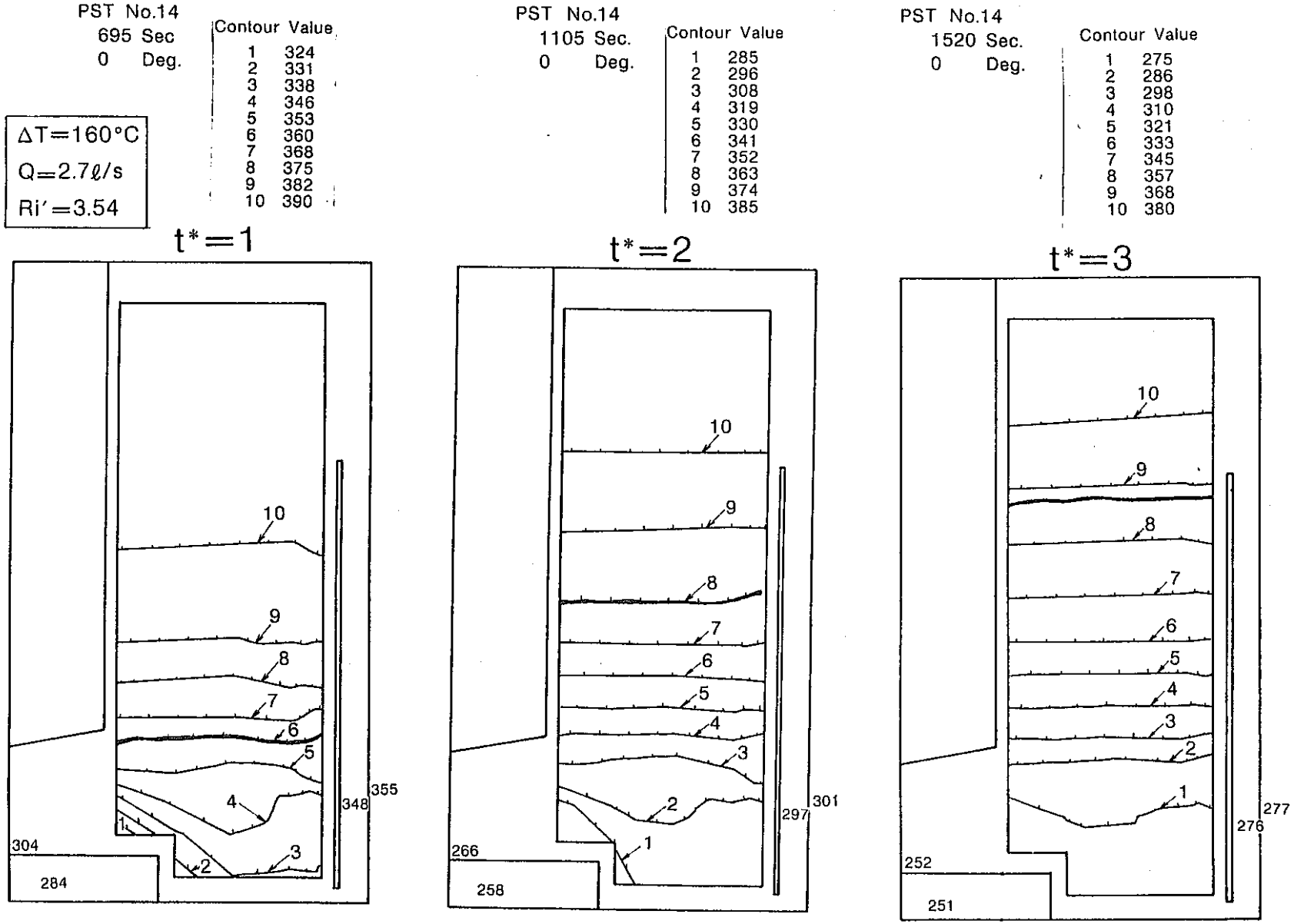

Fig. B3-17 Change-in-time of Iso-thermal Lines (Test No.14)-Stratification Present

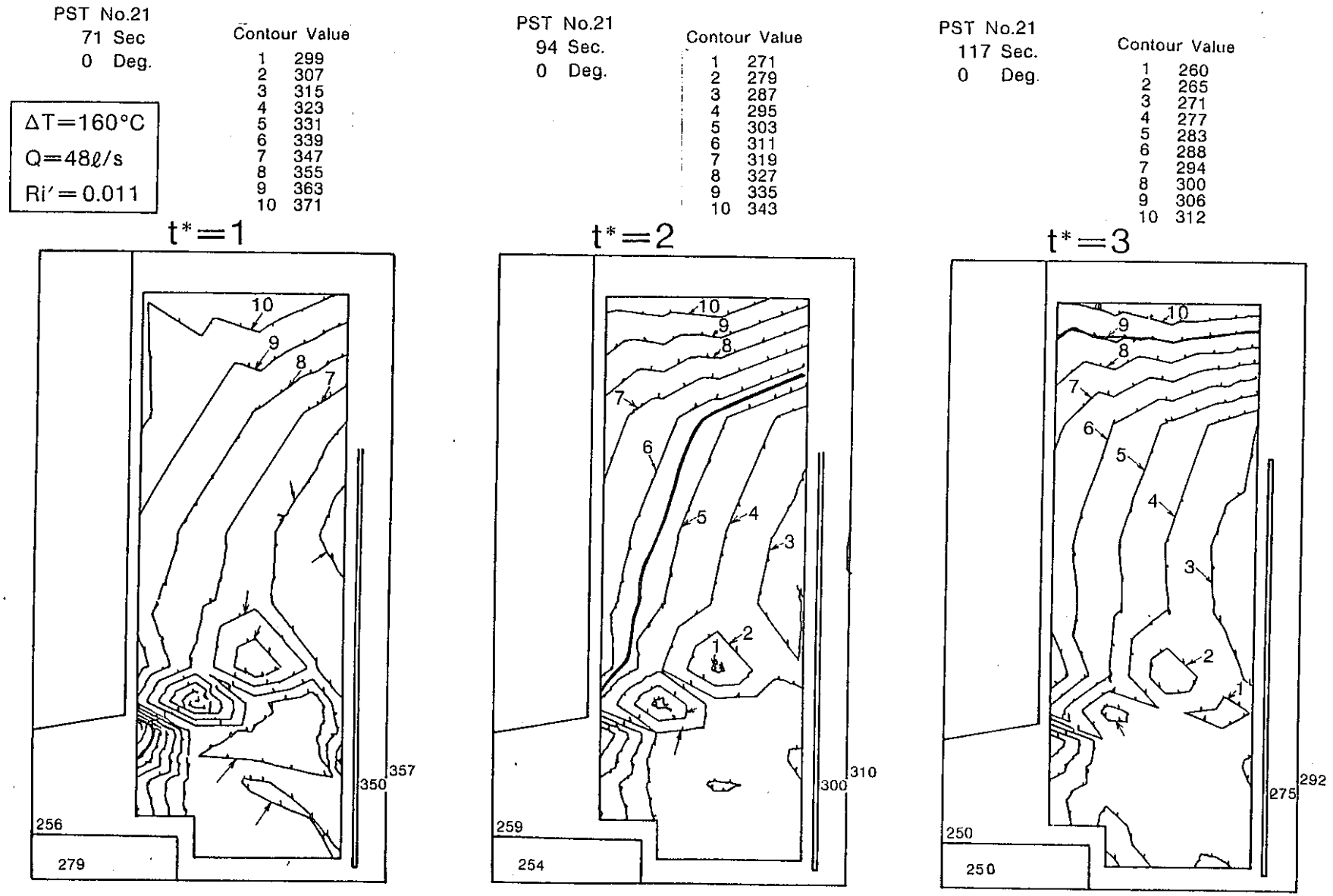

Fig. B3-18 Change-in-time of Iso-thermal Lines (Test No.21)-Stratification Absent

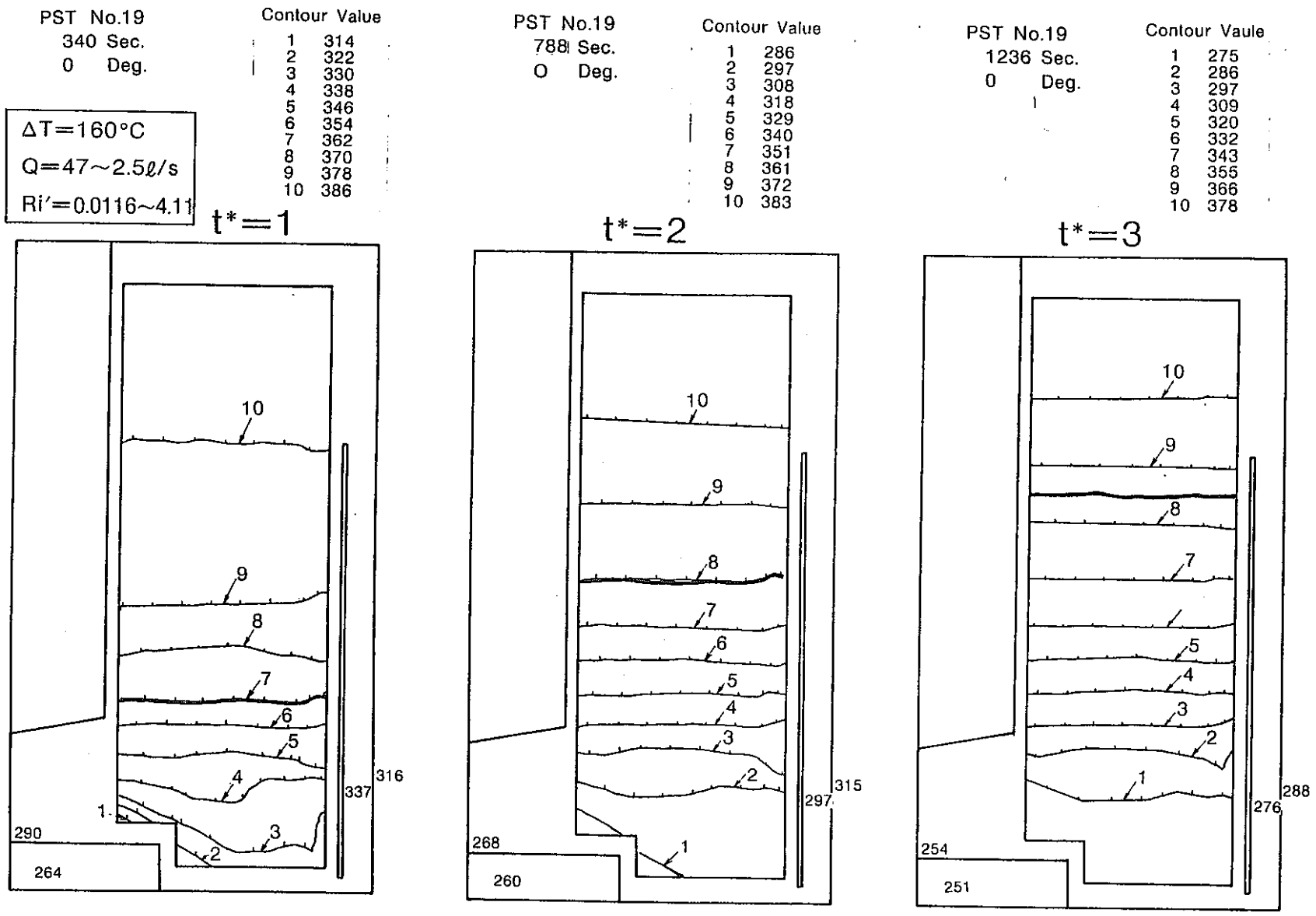

Fig. B3-19 Change-in-time of Iso-thermal Lines (Test No.19)-Stratification Present

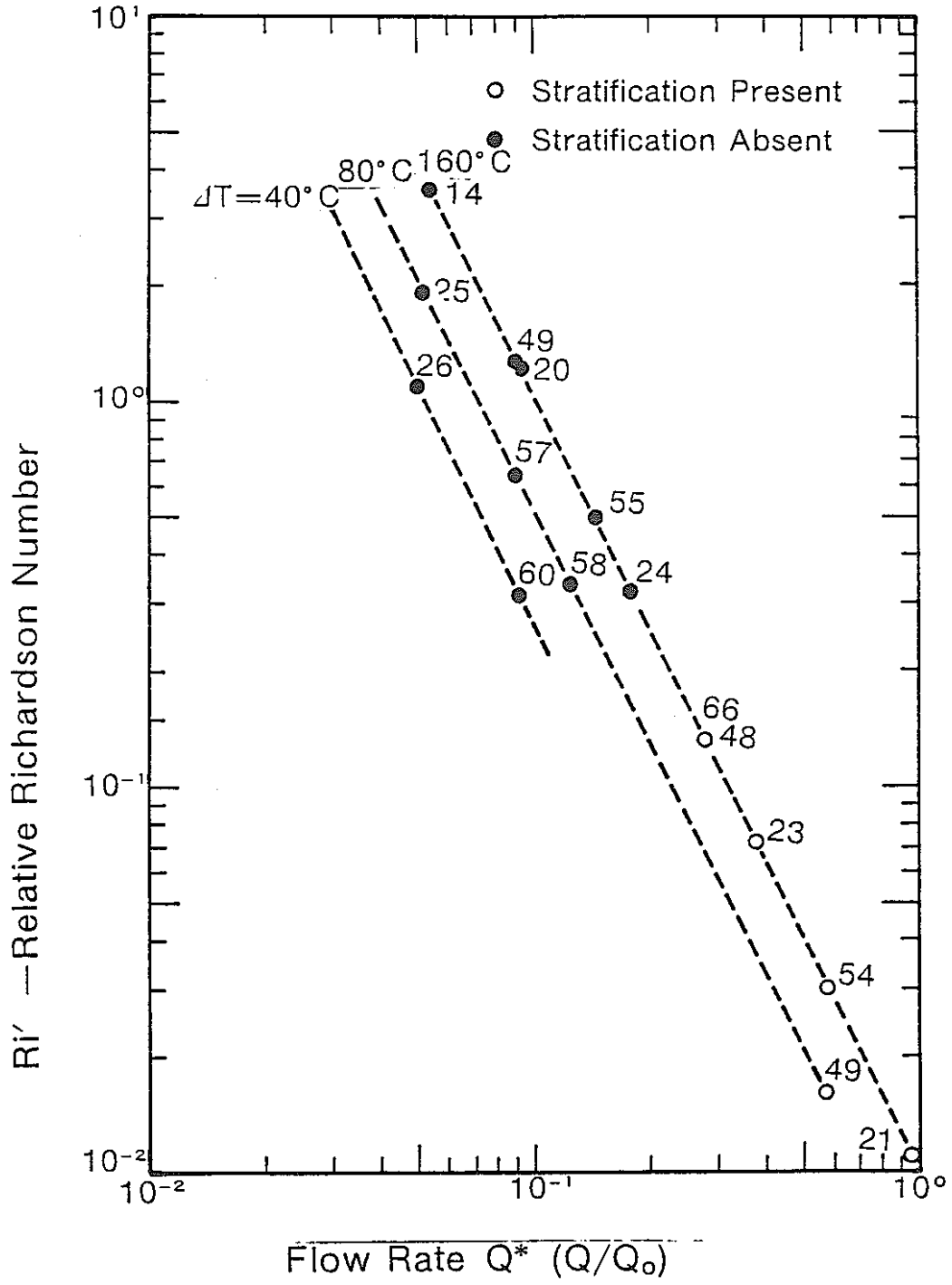

Fig. B3-20 Stratification Map

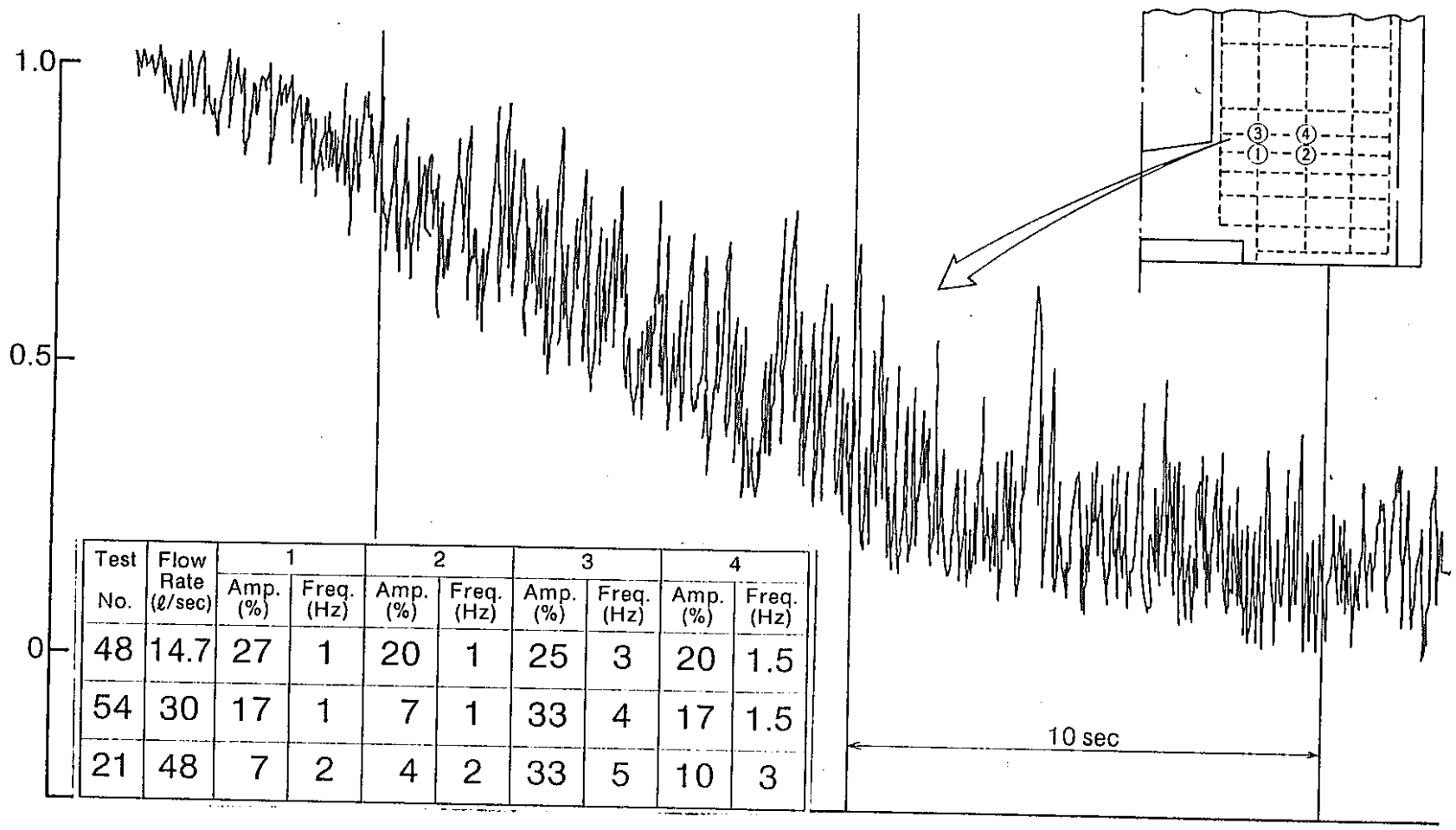

Test No.	Flow Rate (ℓ/sec)	1		2		3		4	
		Amp. (%)	Freq. (Hz)	Amp. (%)	Freq. (Hz)	Amp. (%)	Freq. (Hz)	Amp. (%)	Freq. (Hz)
48	14.7	27	1	20	1	25	3	20	1.5
54	30	17	1	7	1	33	4	17	1.5
21	48	7	2	4	2	33	5	10	3

Fig. B3-21 Temperature Fluctuation in the Upper Plenum.

Water thermal stratification test with a full-scale 1/3 sector model of Monju outlet plenum (TOSHIBA)

Abstract

It is expected that stratification would occur in an LMFBR outlet plenum under scram transient which is initiated by loss of electrical power and so on. These temperatures must be known in order to design the reactor vessel and the upper plenum internals.

It is, therefore, of great importance to clarify the stratification phenomena under various transient conditions. This report deals with experimental studies on the stratification phenomena in an LMFBR outlet plenum.

In the experiments, stratified flow was simulated using water, hot water and brine. It was required then that buoyancy effects were simulated properly. Test conditions were determined based on the relative Richardson number.

From the experimental results we conclude the following ;

1) Thermal stratification occured in the outlet plenum of 1/3 sector full scale mock up test model, under $Ri' = 0.25 \sim 1.35$ and $Re' = 0.28 \sim 0.58$.

2) The velocity for density interface rising up depends on leak flow-rate through the flow holes.

3) After scram, thermal fluctuation was measured at various elevations in the plenum as follows ;

at lower end of UCS

f = 1/5 Hz, Amp. = 30% of initial difference in temperatures (I.D.T)

at lower part of UCS

f = 1/30 Hz, Amp.= 10% of I.D.T

at outlet nozzle

f = 1/5 Hz, Amp.= 25% of I.D.T

where

Amp. is peak to peak amplitude

4) Between the reactor vessel and inner barrel density interface stayed at the outlet nozzle.

The experimental test section has been modeled analytically by the axisymetric computer code THAUPR. In general THAUPR predictions agree well with the experimental data.

Objectives

1. Thermal Stratification in the "Monju" Outlet Plenum.

2. Rising Velocity, Temperature Gradiant and Temperature Fluctuation at hot - cold interface.

3. Flow rate through the flow holes of the inner barrel.

4. Analysis with THAUPR code.

Table B4-1 The stratification test conditions

Test No.		Flow (Qm^3/min)	Plenum Temp. (T_H °C)	Inlet nozzle Temp. (T_C °C)	Re'	Ri'	Remarks
Monju		9.98	529	400	1	1	
1 - 1		5.35	59	22	0.24	1.35	
1 - 2		5.35	54	20	0.23	1.17	
1 - 3		7.09	54	23	0.31	0.63	
1 - 4		11.68	54	20	0.49	0.25	
1 - 5		11.79	57	21	0.52	0.27	
2 - 1		11.37	58	23	0.51	0.69	γ_{Nacl} = 1018 kg/m³
2 - 2		12.30	63	23	0.58	1.35	γ_{Nacl} = 1061 kg/m³

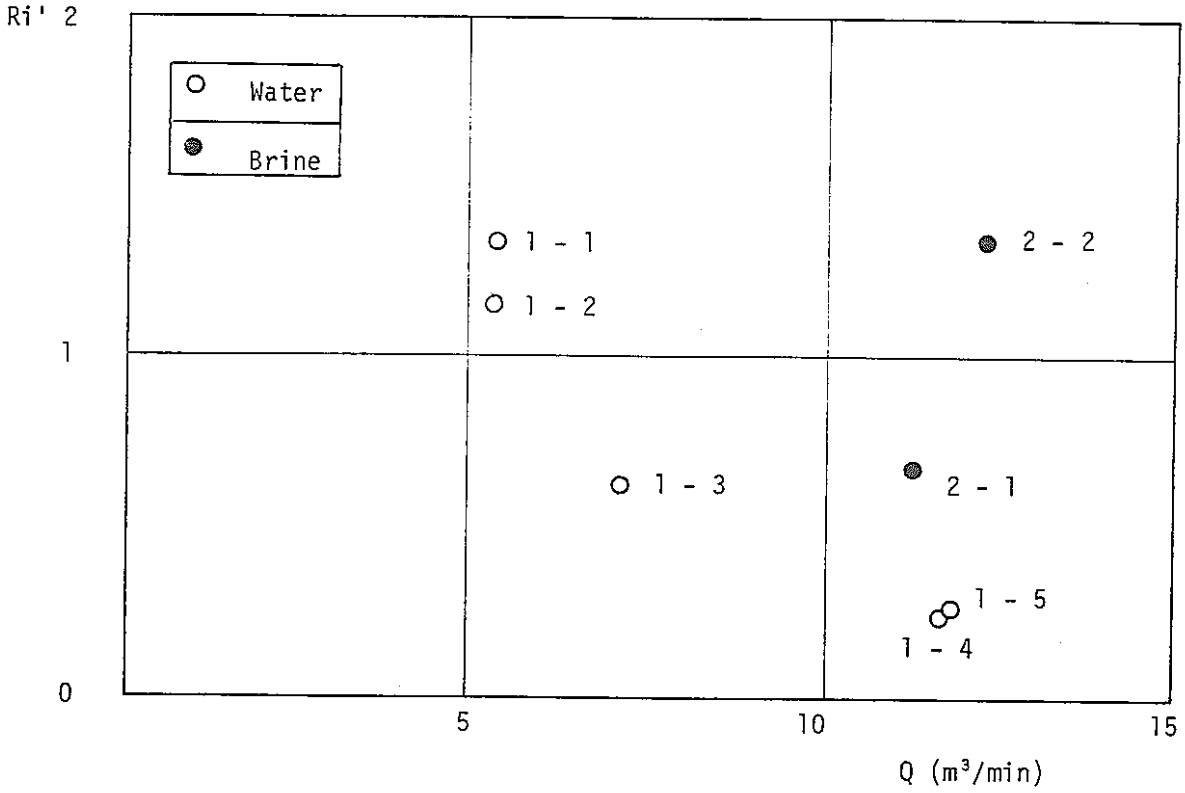

Fig. B4 -1 Test conditions

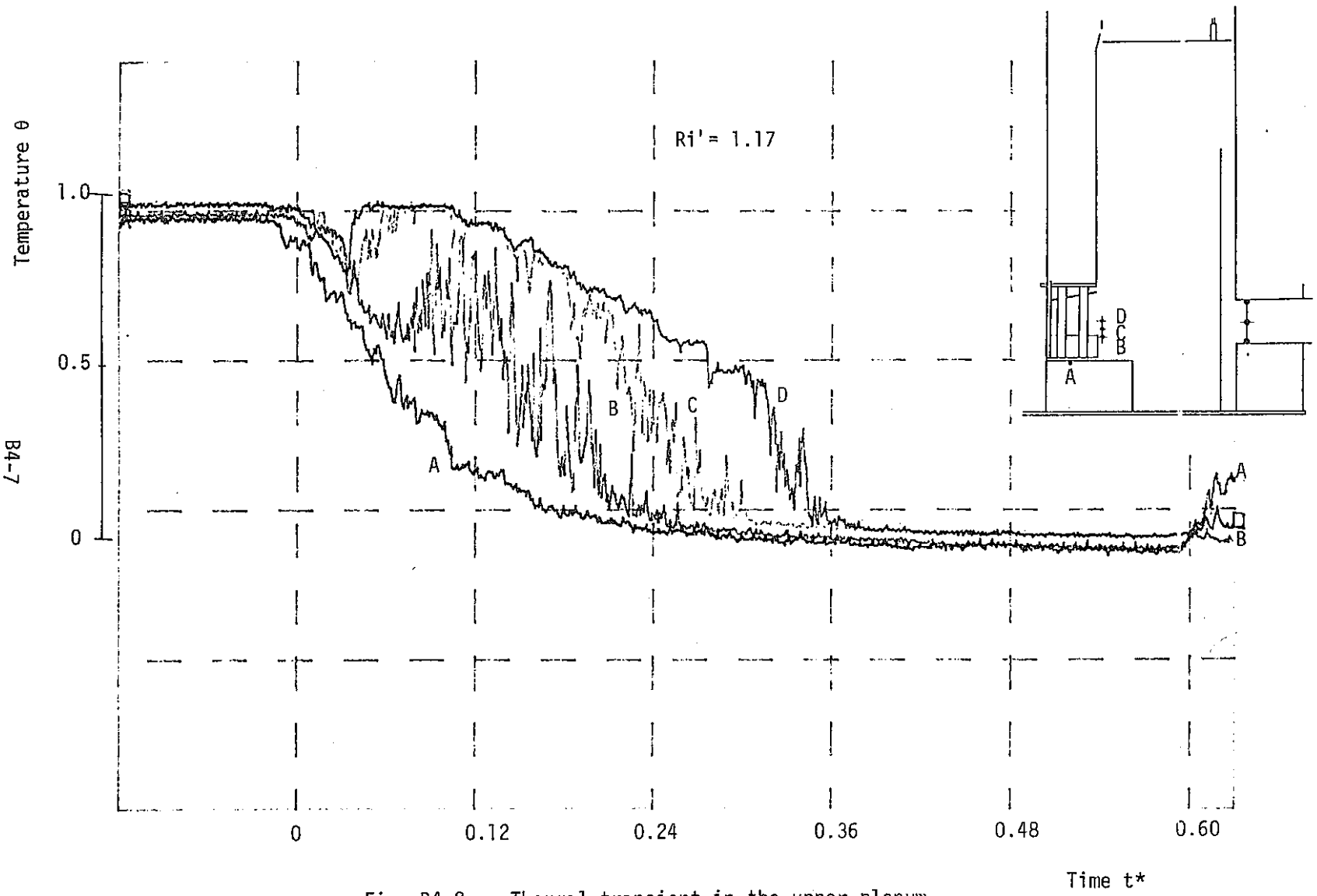

Fig. B4-2 Thermal transient in the upper plenum

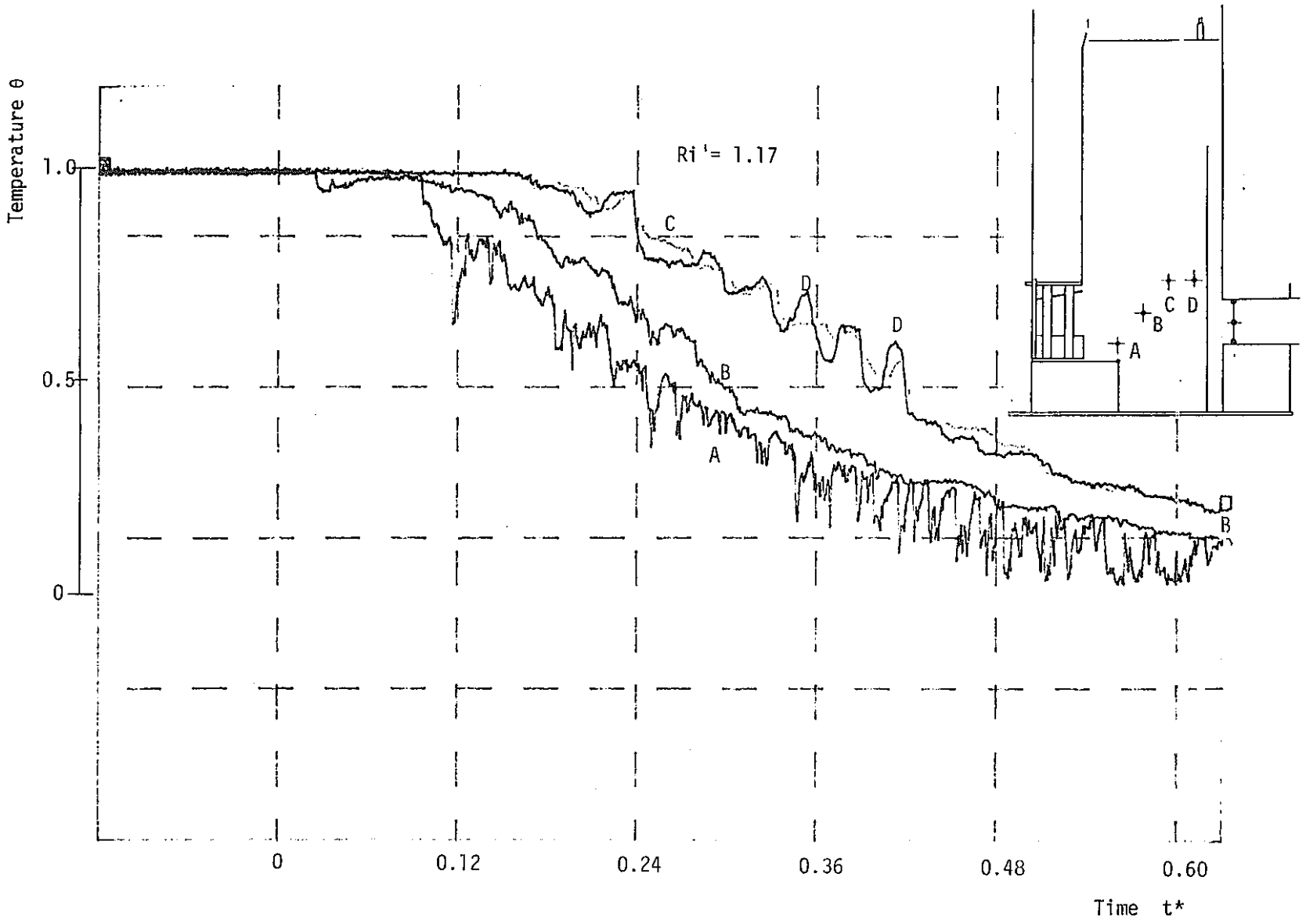

Fig. B4-3 Thermal Transient in the upper plenum

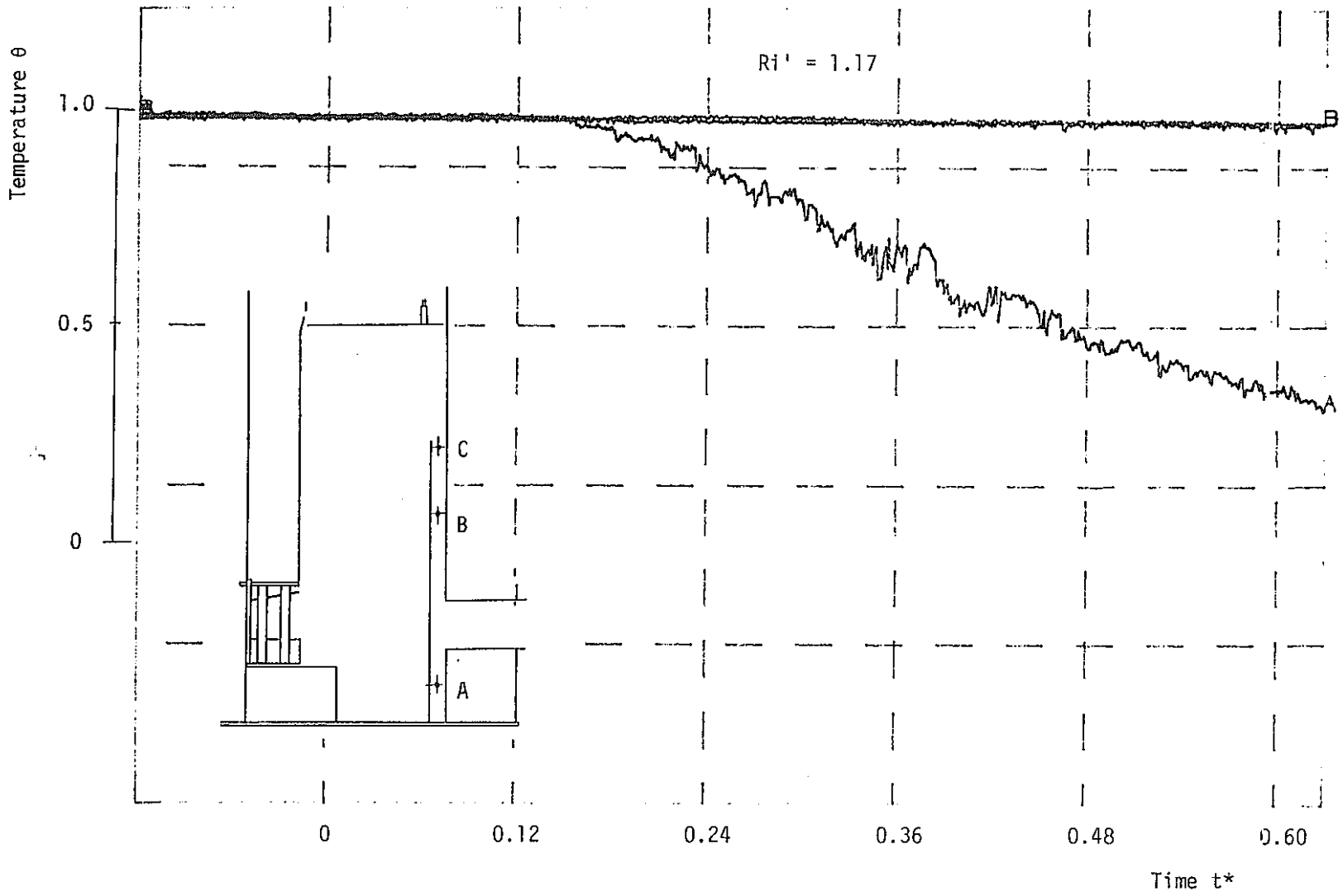

Fig. B4-4 Thermal Transient in the upper plenum

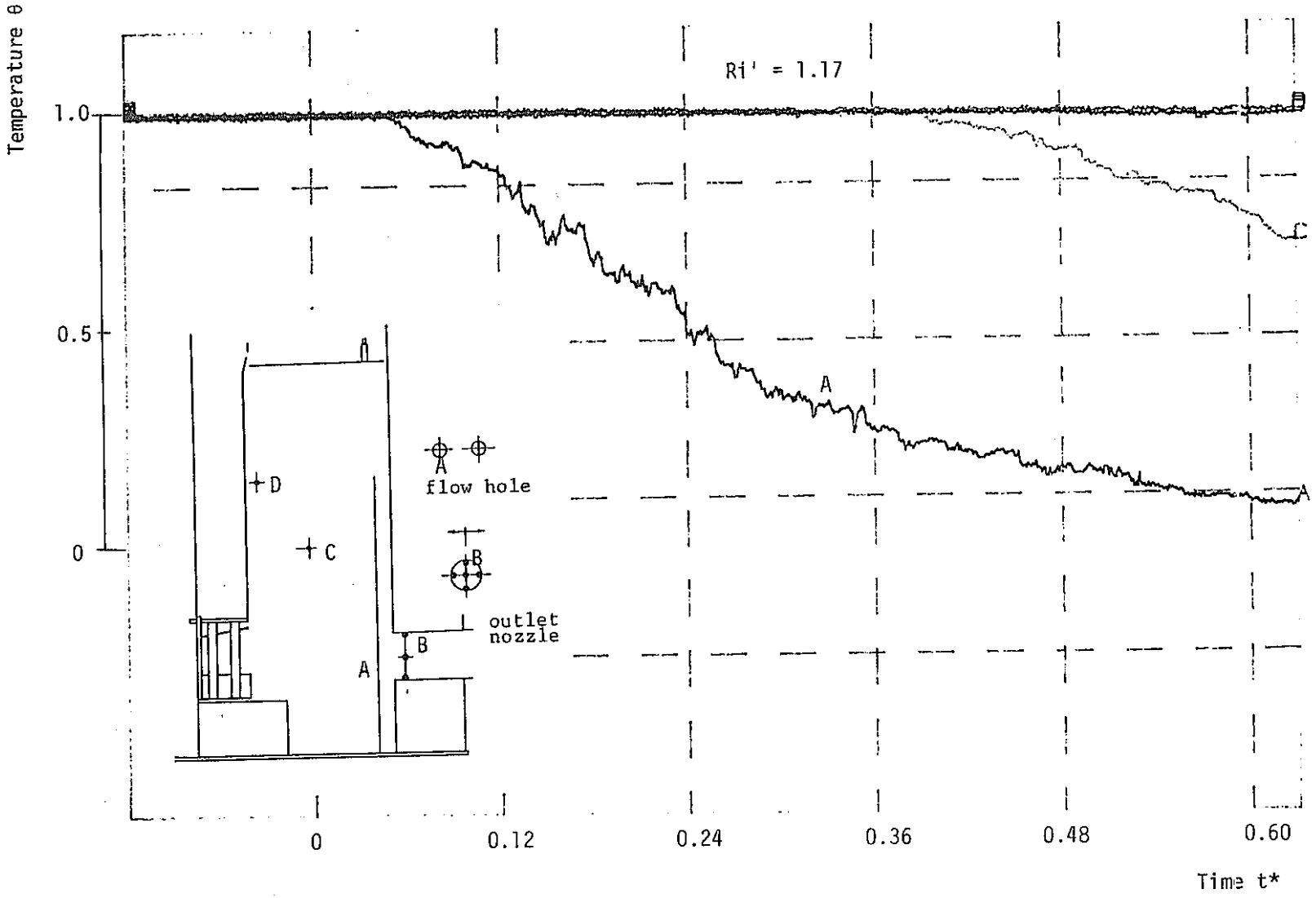

Fig. B4-5 Thermal Transient in the upper plenum

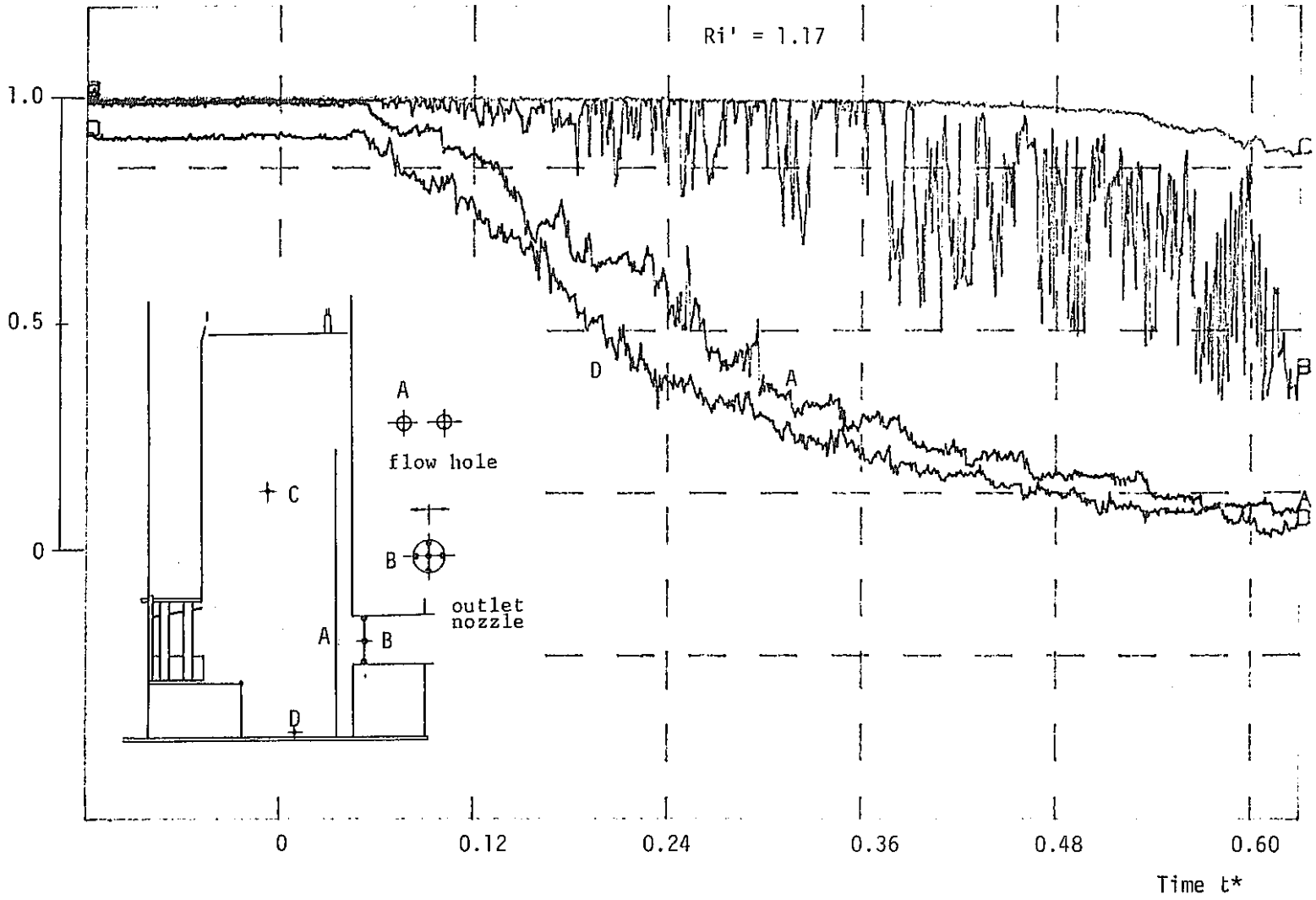

Fig. B4-6 Thermal Transient in the upper plenum

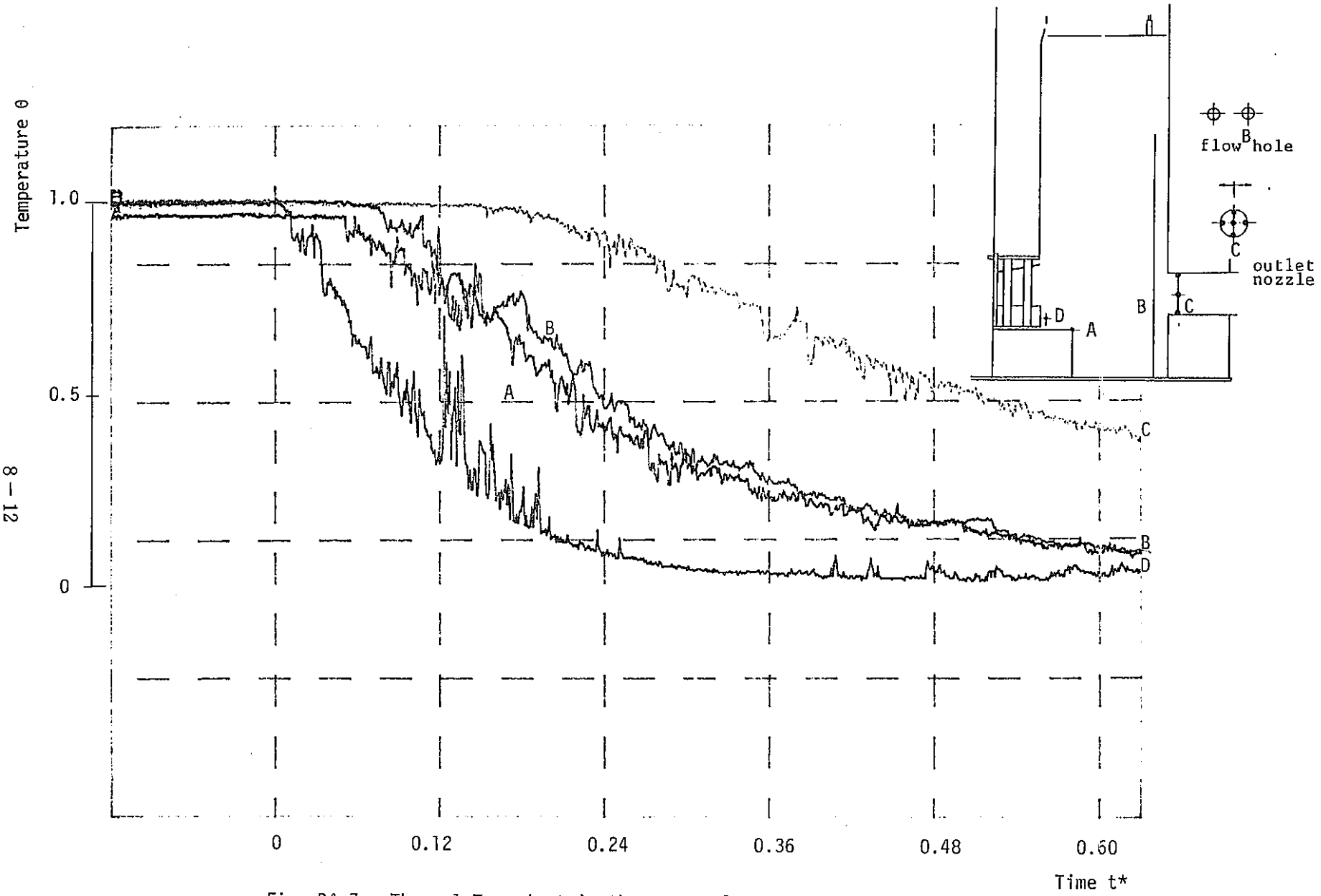

Fig. B4-7 Thermal Transient in the upper plenum

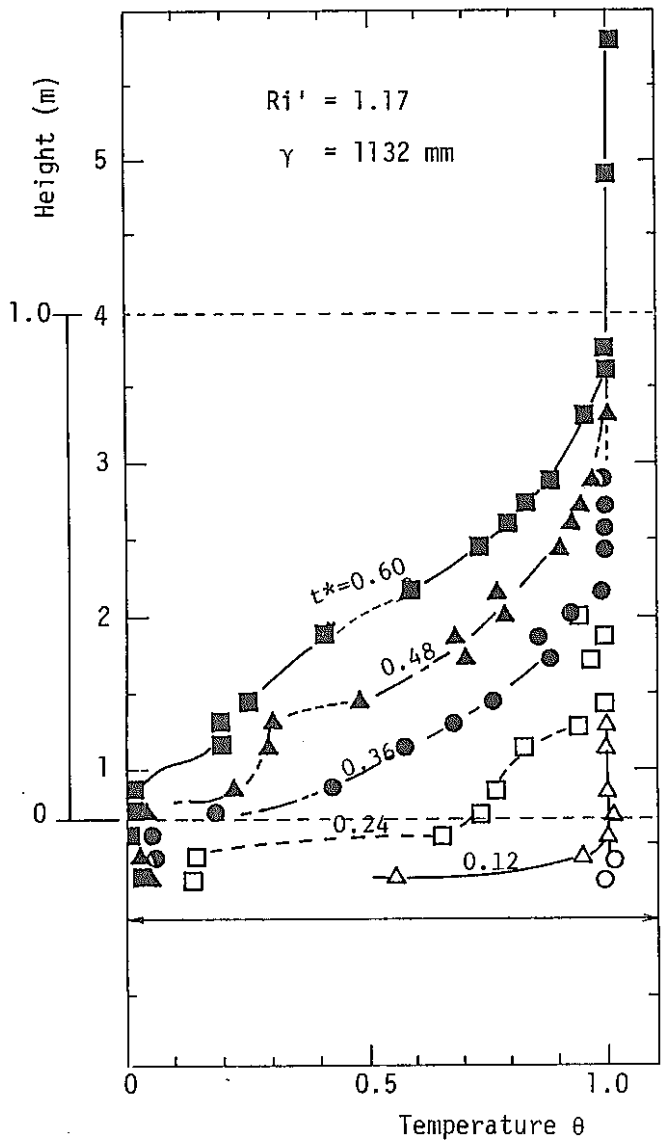

Fig. B4-8 Axial temperature profiles in the upper plenum

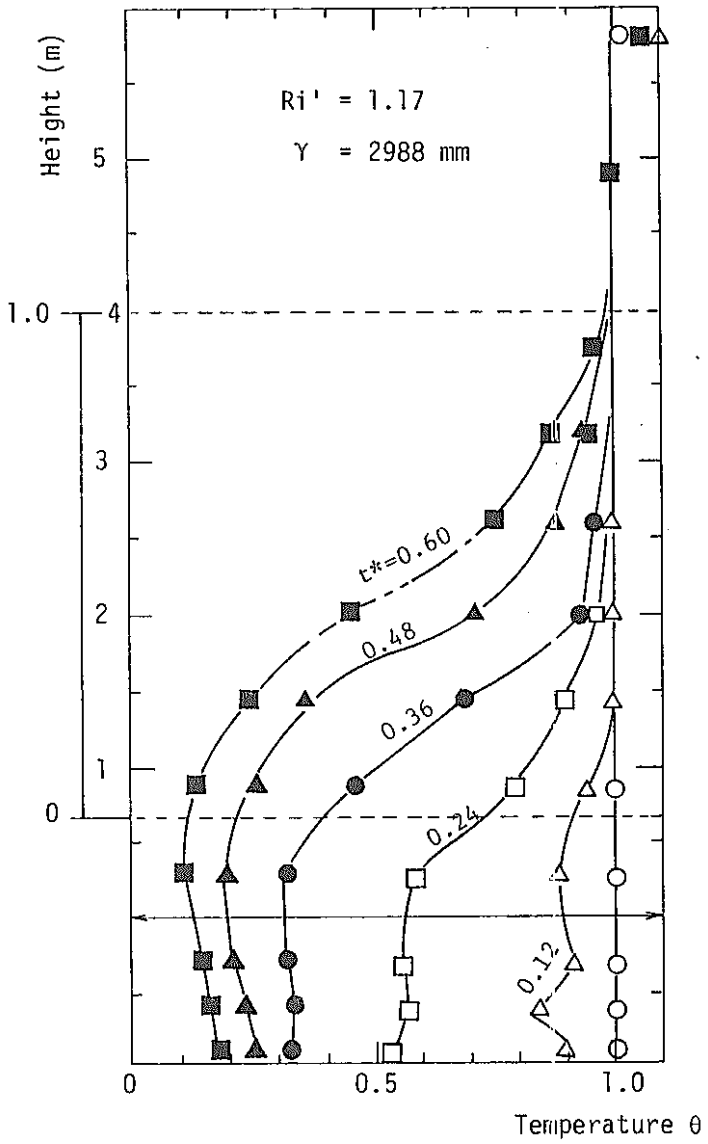

Fig. B4-9 Axial temperature profiles in the upper plenum

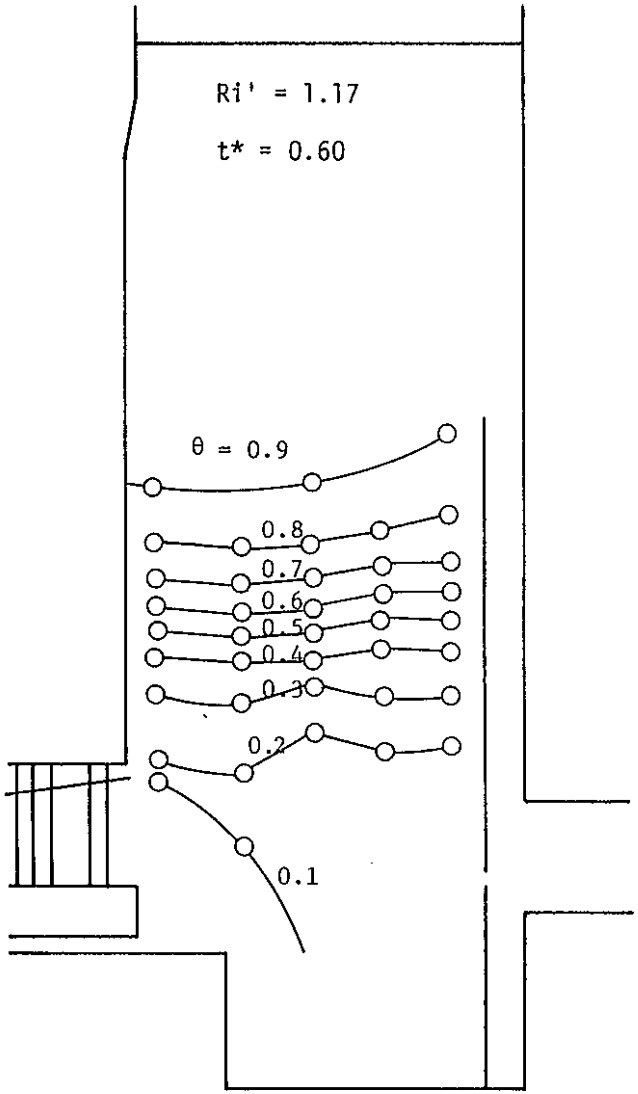

Fig. B4-10 Isothermal lines in the upper plenum

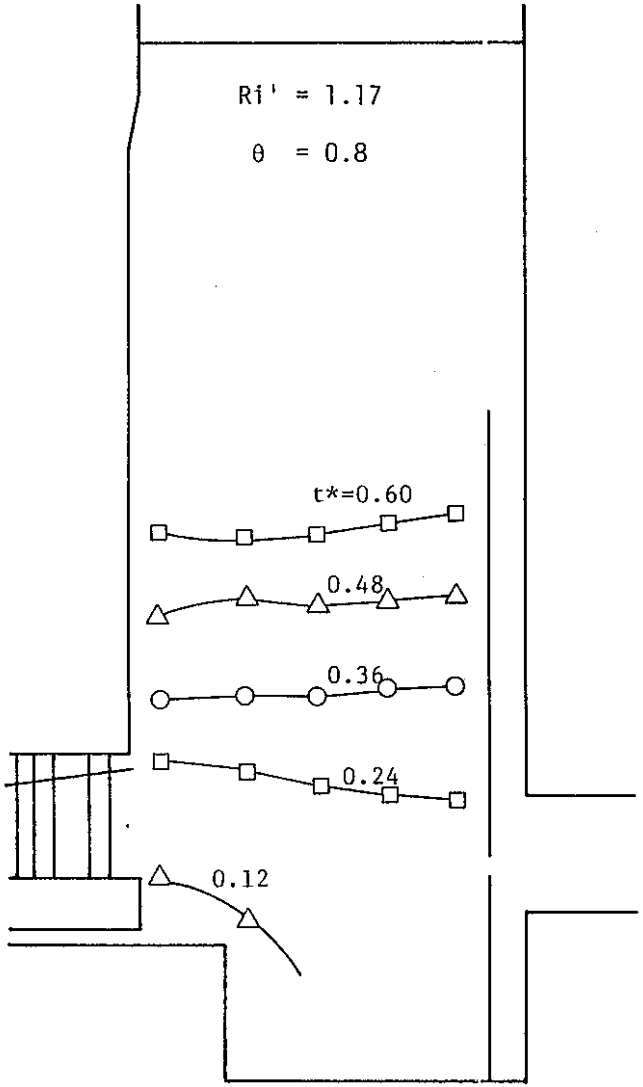

Fig. B4-11 Transient behavior for density interface

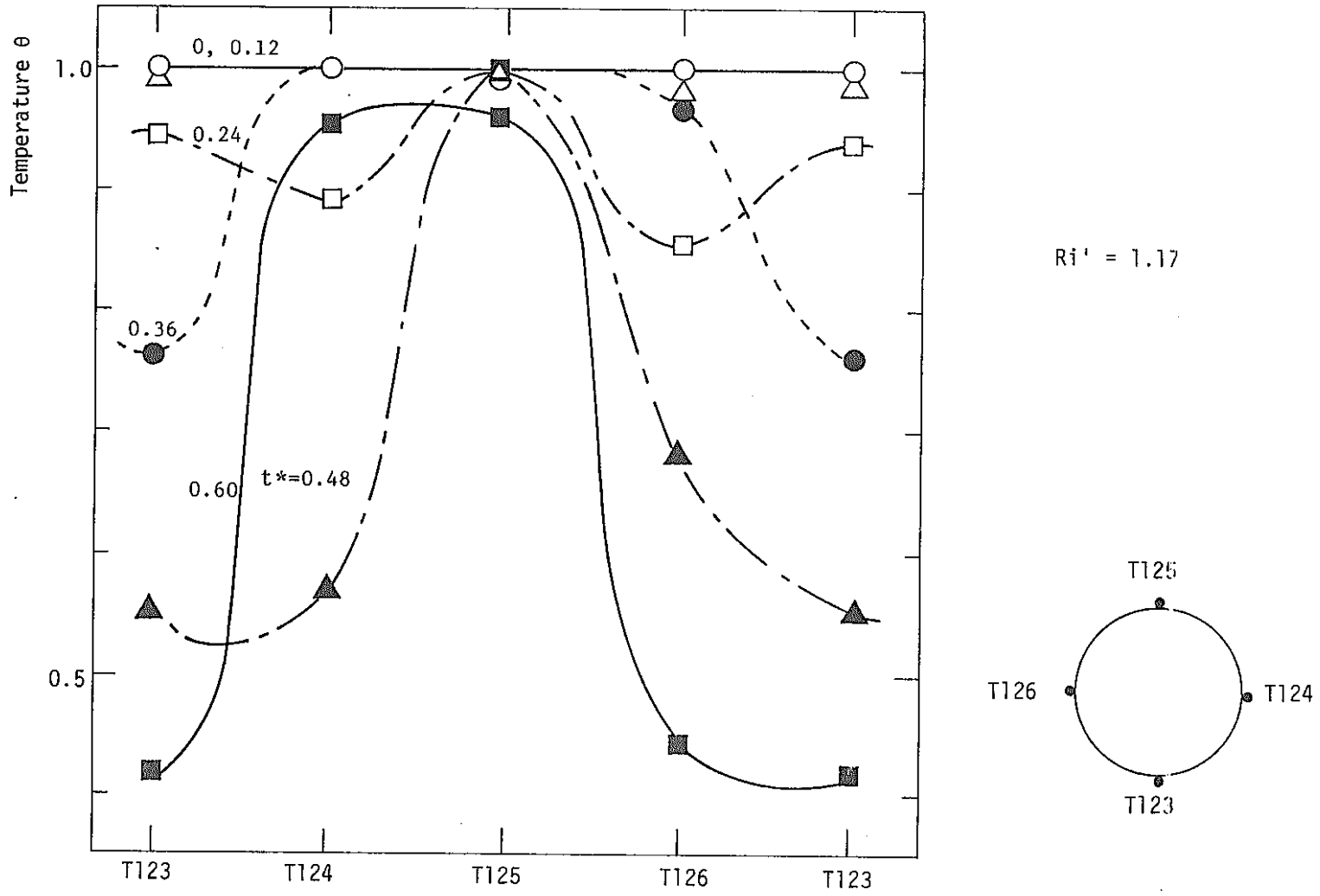

Fig. B4-12 Circumferential temperature profiles at the outlet nozzle

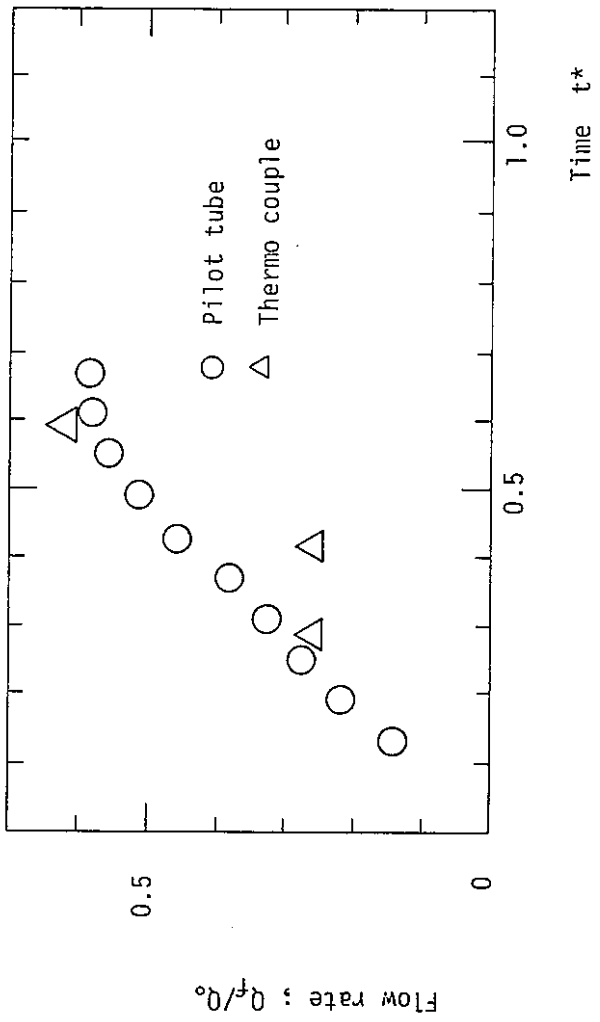

Fig. B4-13 Transient behavior for the ratio of coolant flow through the flow hole

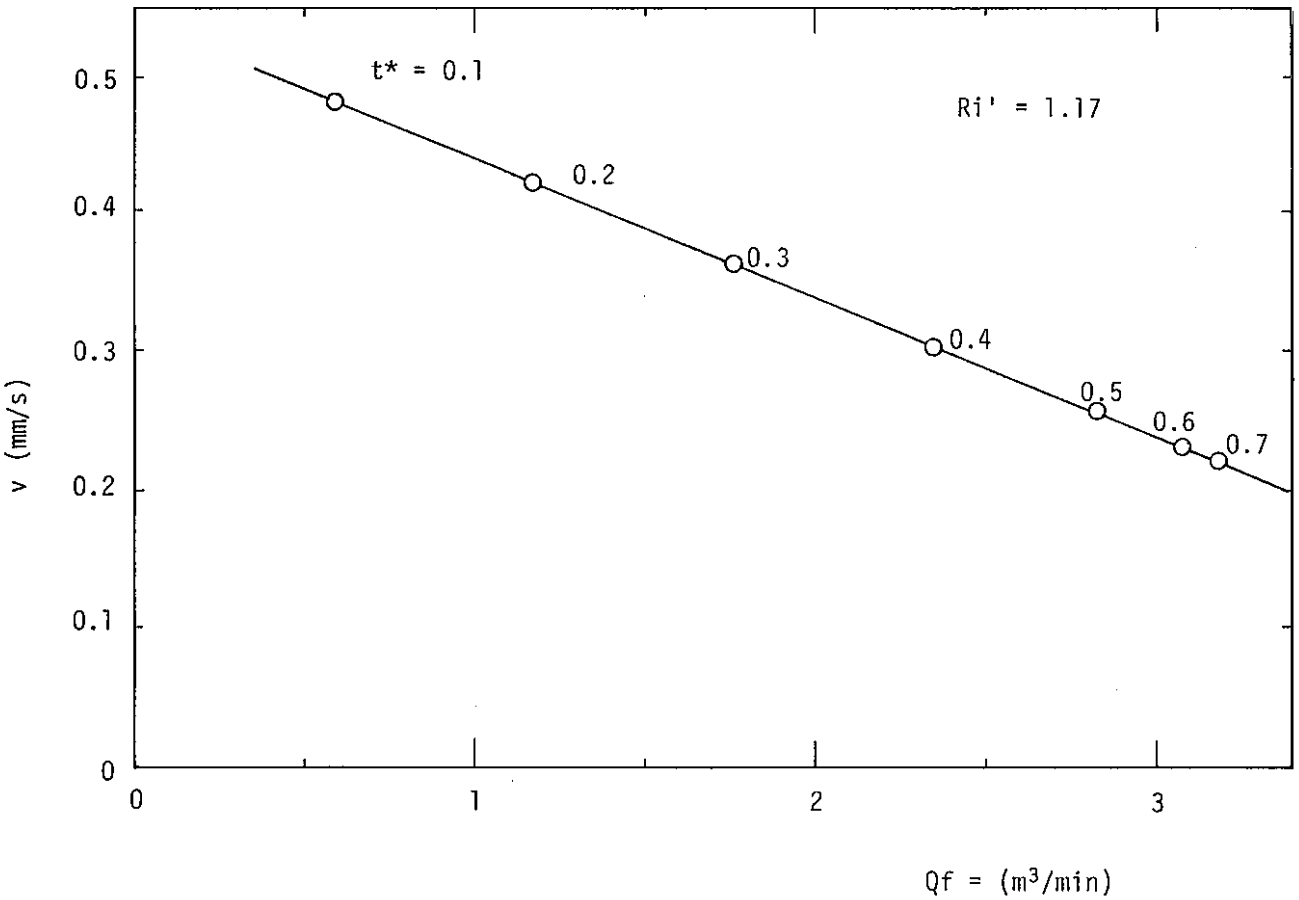

Fig. B4-14 Rising velocity of Density interface Vs coolant flow rate through flow holes

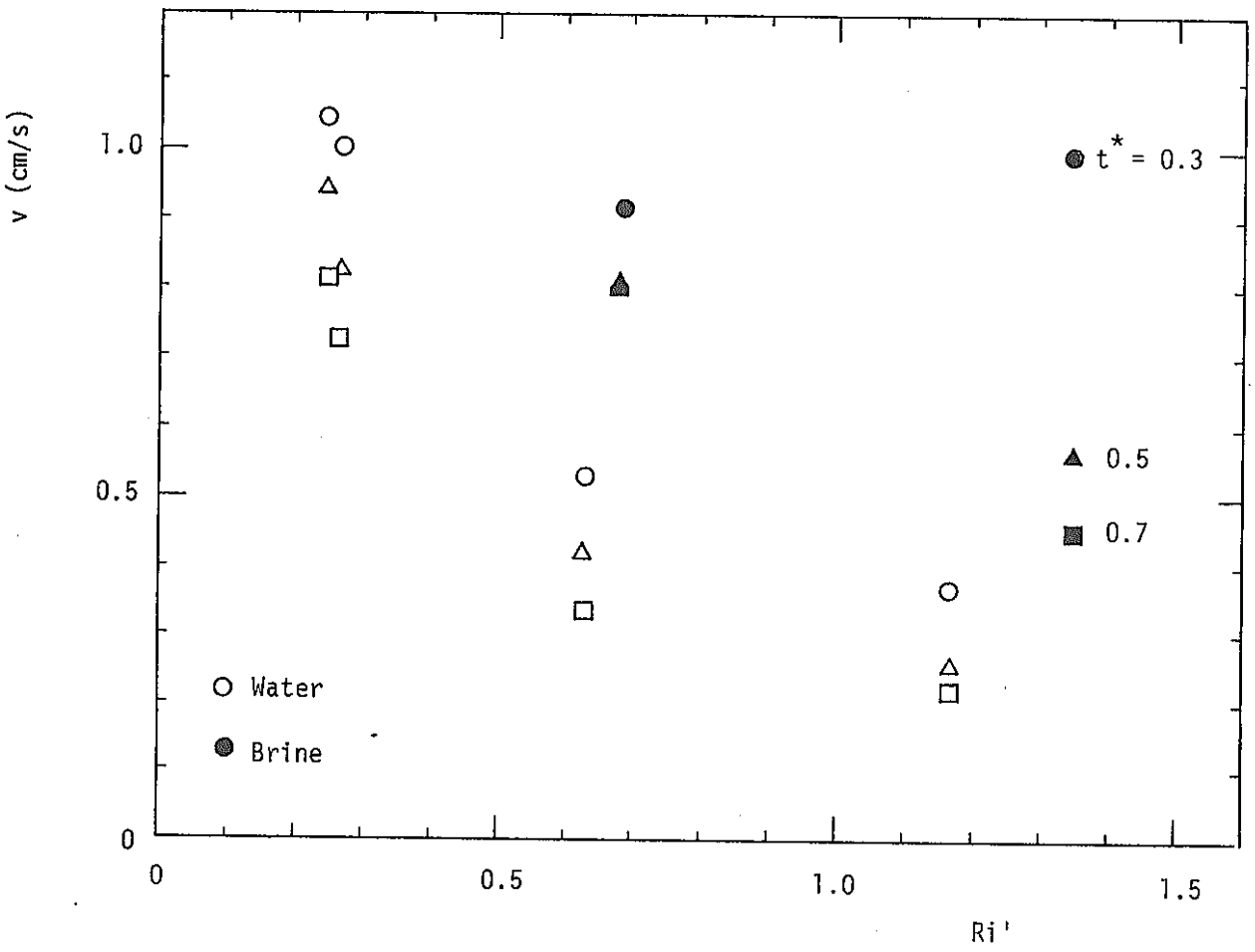

Fig. B4-15 Rising velocity of density interface Vs relative Richardson number

Table B4-2 Temperature fluctuation characteristic

Test case	A		B		C		Ri'	Flow rate Q (m^3/min)
	%	Hz	%	Hz	%	Hz		
1-1	±25	0.22	±24	0.21	±8	0.02	1.35	5.35
1-2	±25	0.15	±19	0.15	±11	0.02	1.17	5.35
1-4	±17	0.08	± 6	0.15	±3	0.01	0.25	11.68
1-5	±15	0.05	±20	0.15	±9	0.01	0.27	11.79
2-1	±23	0.13	±23	0.17	±11	0.01	0.69	11.37
2-2	±18	0.12	±22	0.19	±3	0.03	1.35	12.30

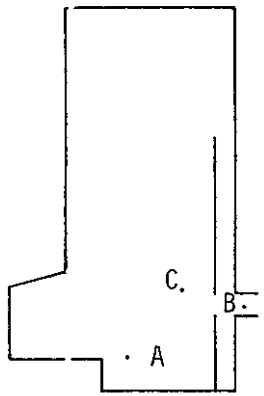

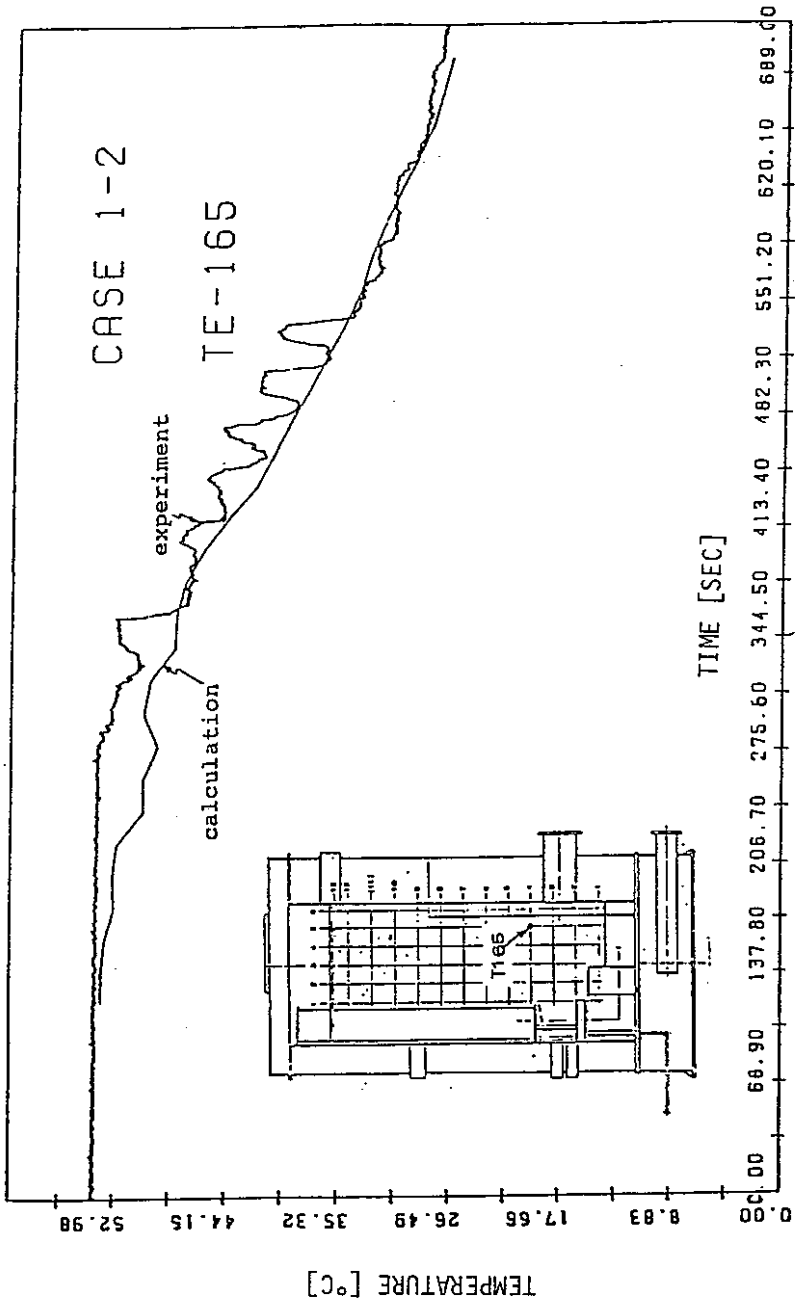

Fig. B4-16 Comparison of experimental data and analytical results

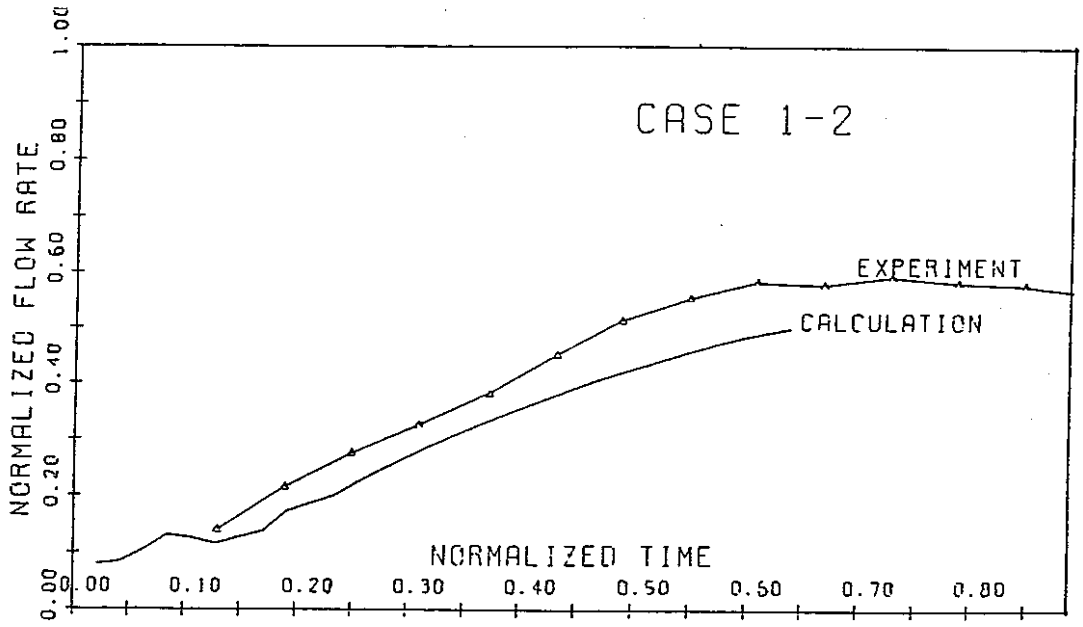

Fig. B4-17 Comparison of flow rate of flow hole for experiment and calculation

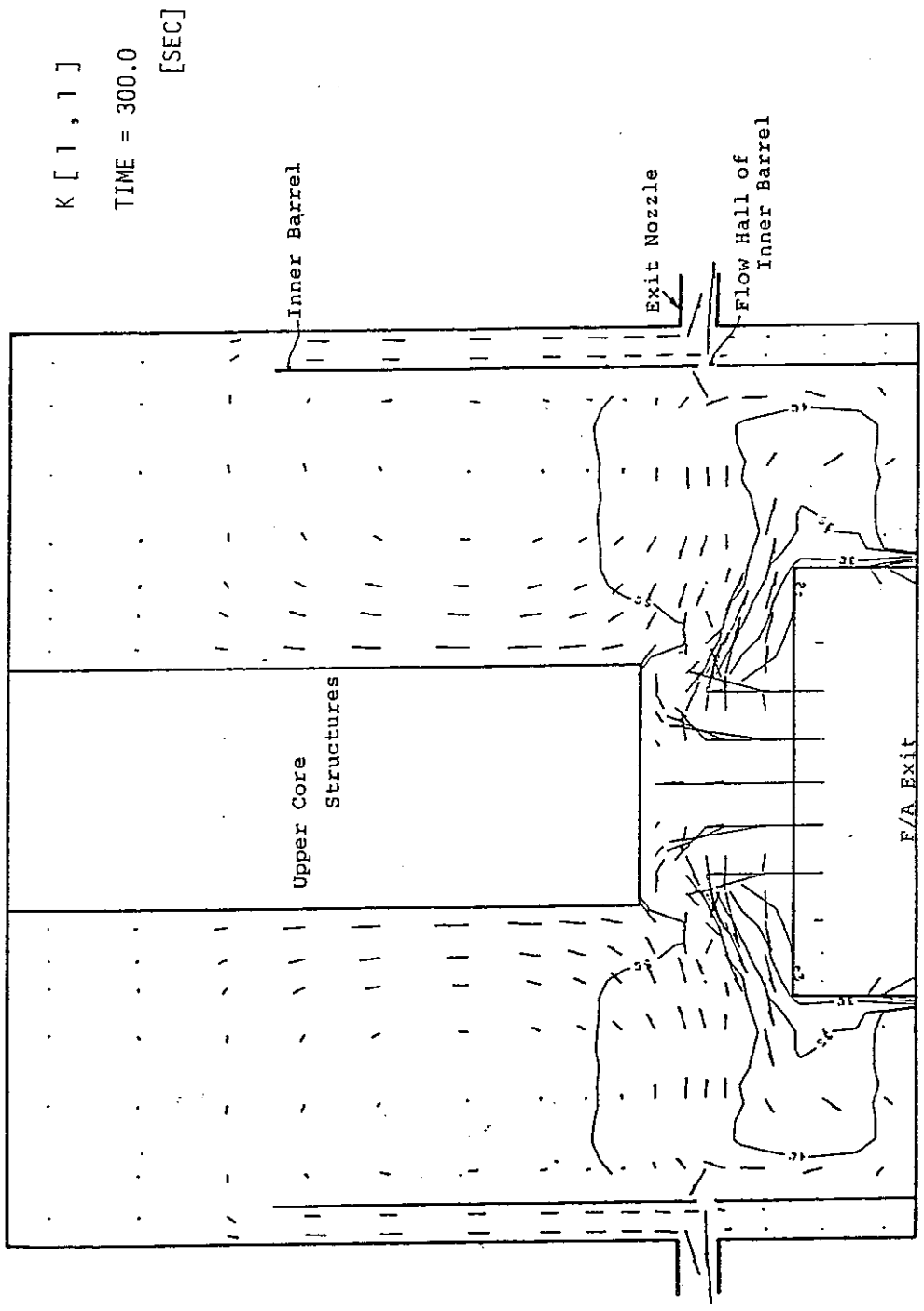

Fig. B4-18 Flow velocity distribution

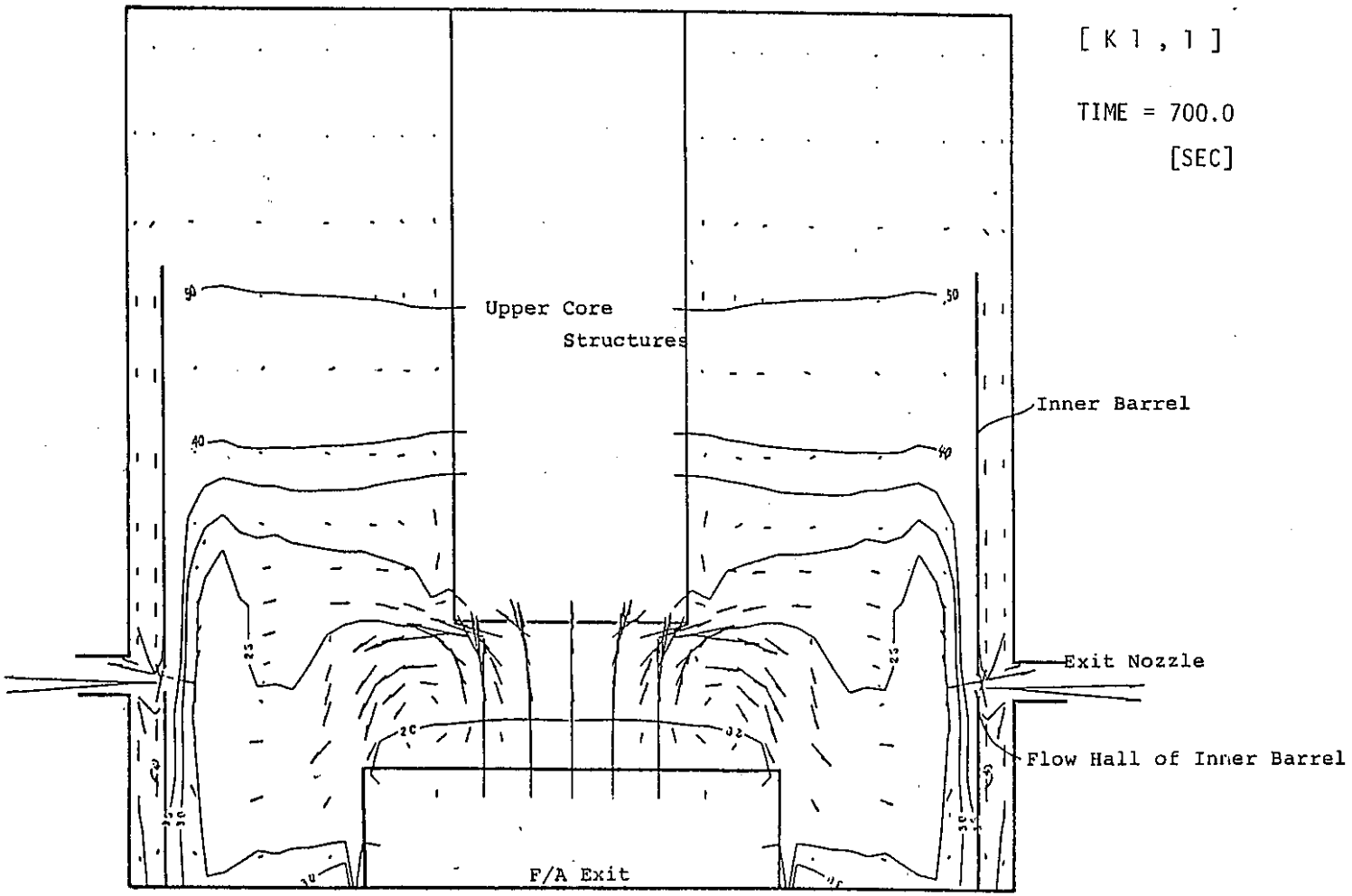

Fig. B4-19 Flow velocity distribution

Concluding remarks

1. Thermal stratification occured in the outlet plenum of full scale 1/3 sector test model using water, under $Ri' = 0.25 \sim 1.35$ and $Re' = 0.28 \sim 0.52$.

2. Coolant flow hole rate increases as the density interface goes up to the top of the inner barrel.

3. Rising velocity of density interface depends on coolant flow rate through flow holes.

4. Temperature fluctuation occured after scram. The location of the temperature fluctuation changed from time transients throughout test.

5. Good agreement is obtained between experimental results and THAUPR with regard to flow rate through flow holes, rising velocity of density interface and onset time for thermal stratification.

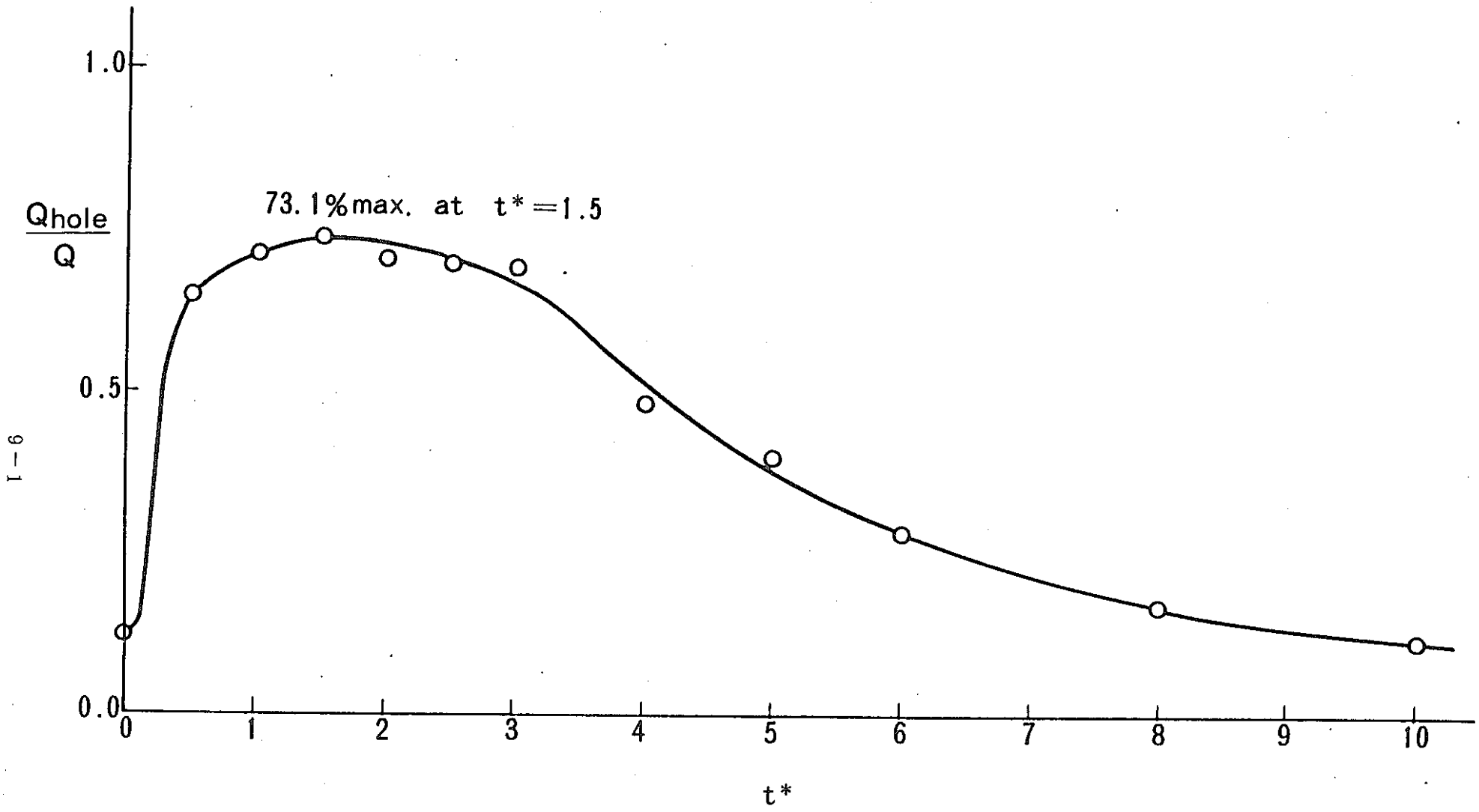

Fig. B5-15 Flow Volume through Flow Holes

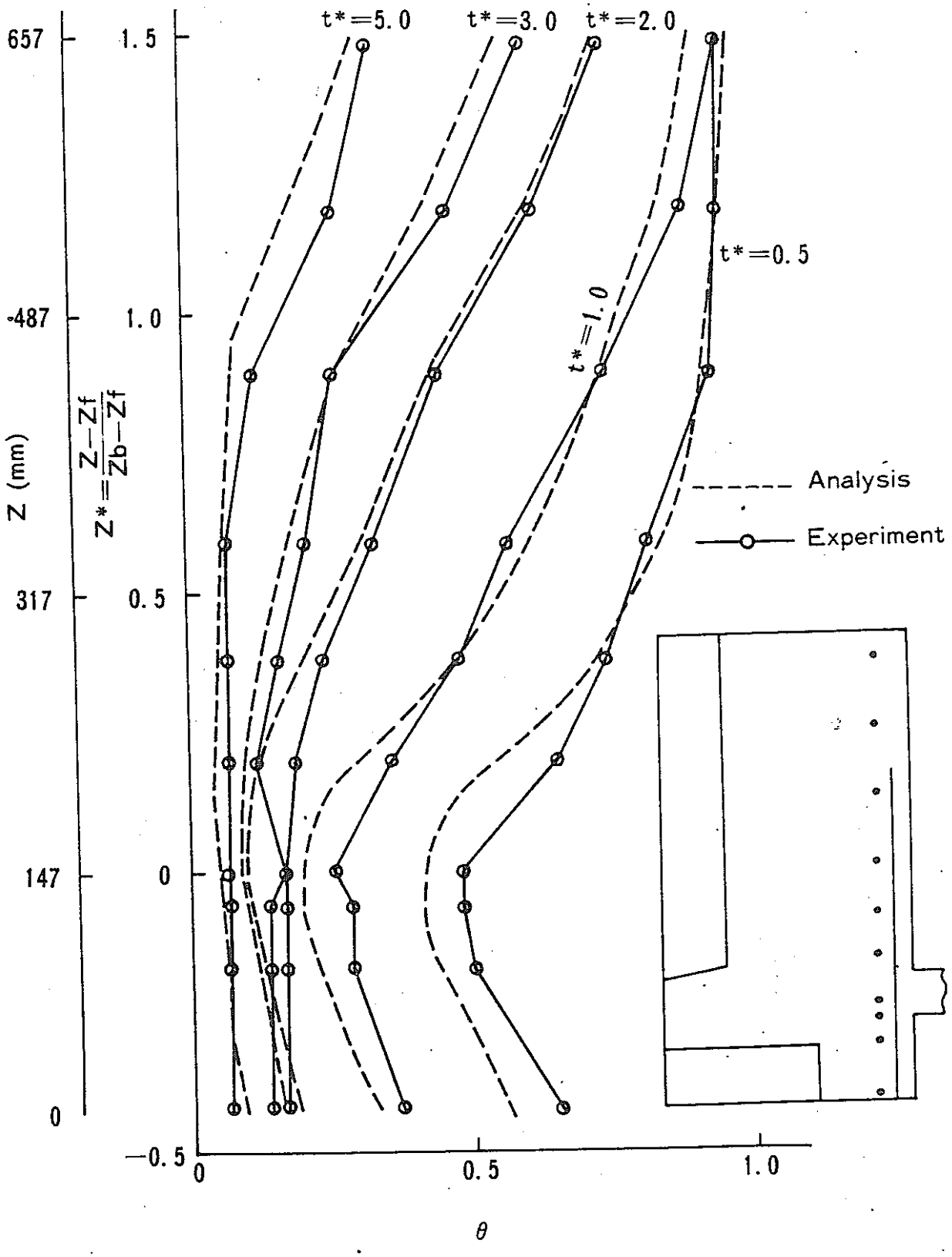

Fig. B5-14 Axial Temperature Distribution

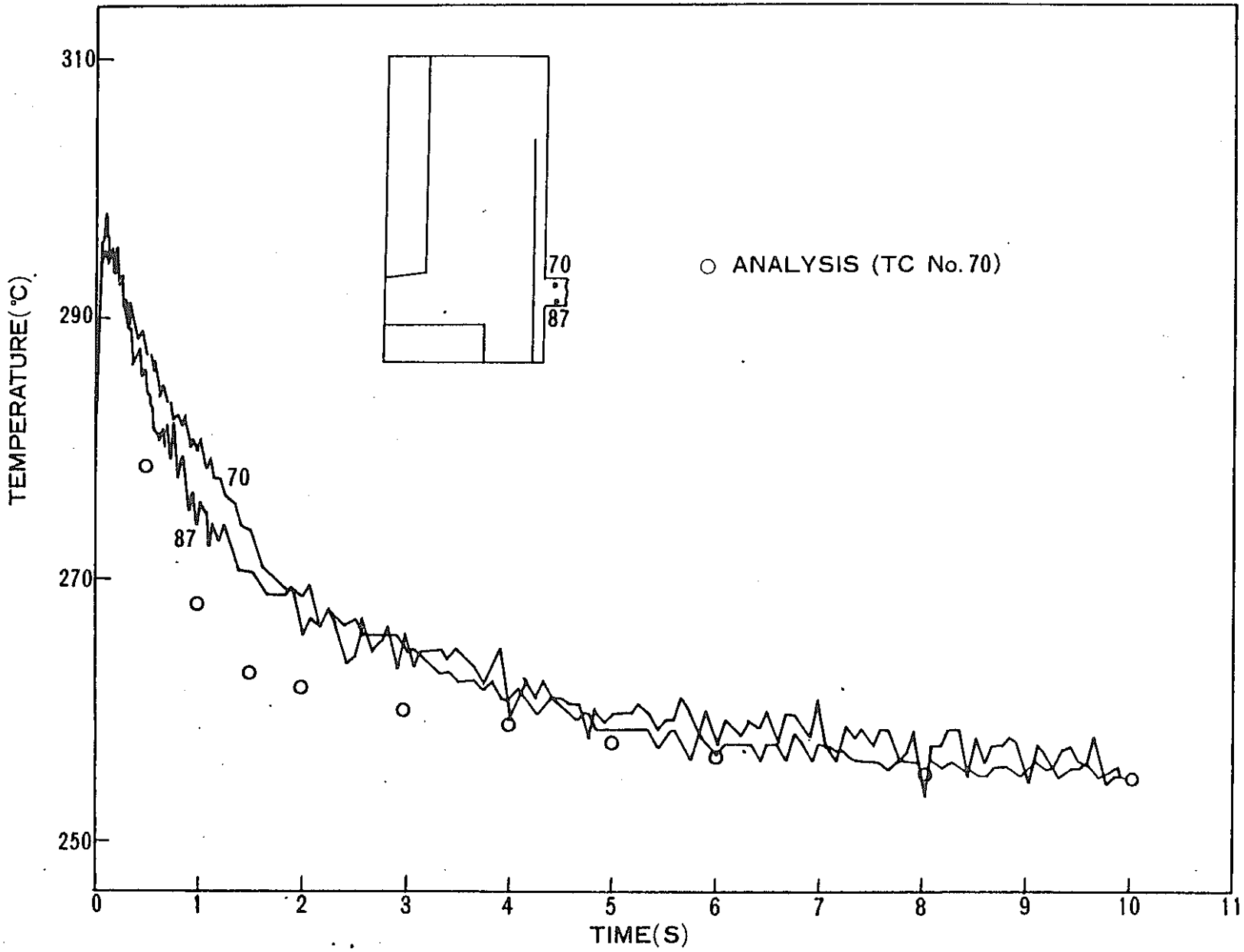

Fig. B5-13 Temperature Change in Time

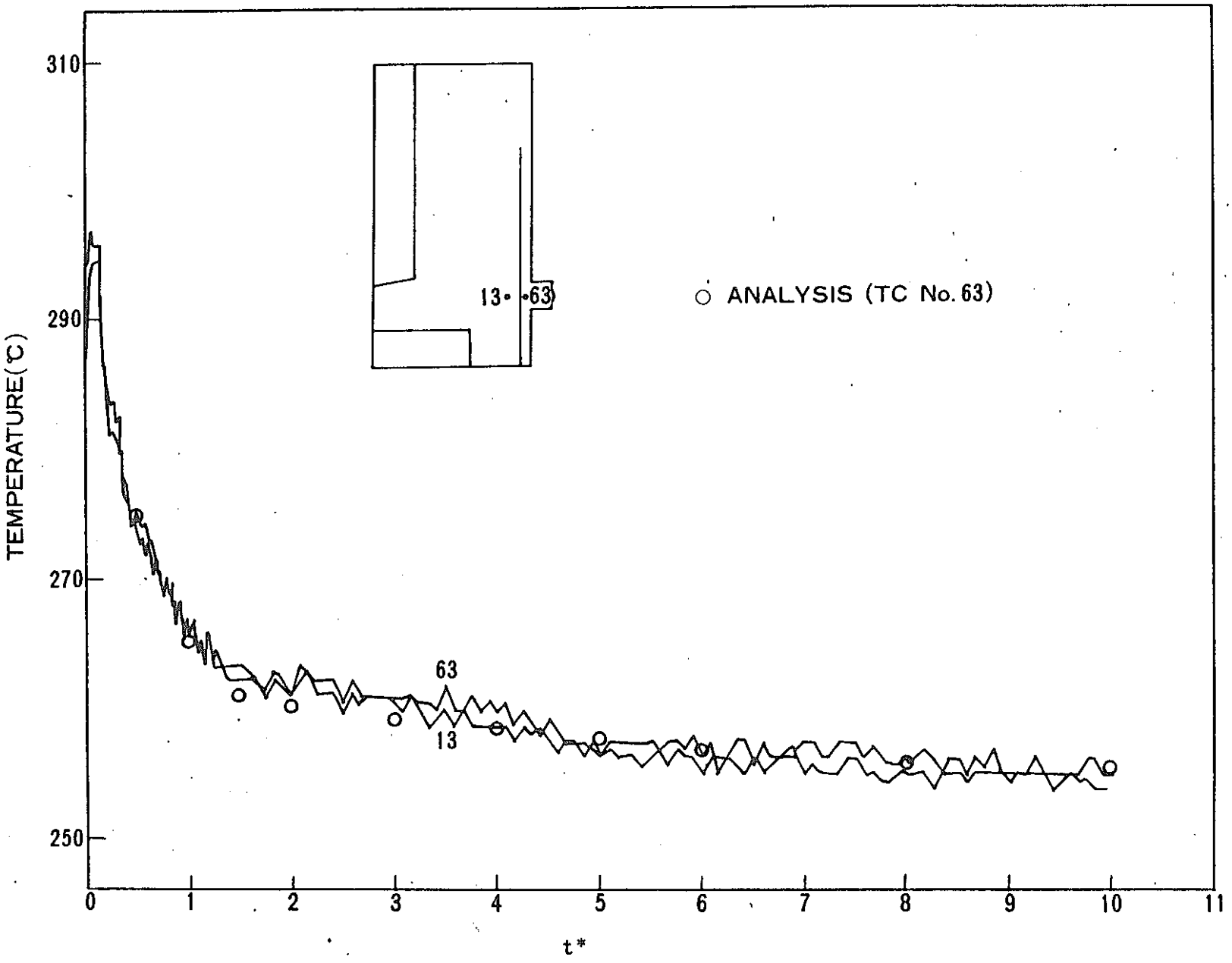

Fig. B5-12 Temperature Change in Time

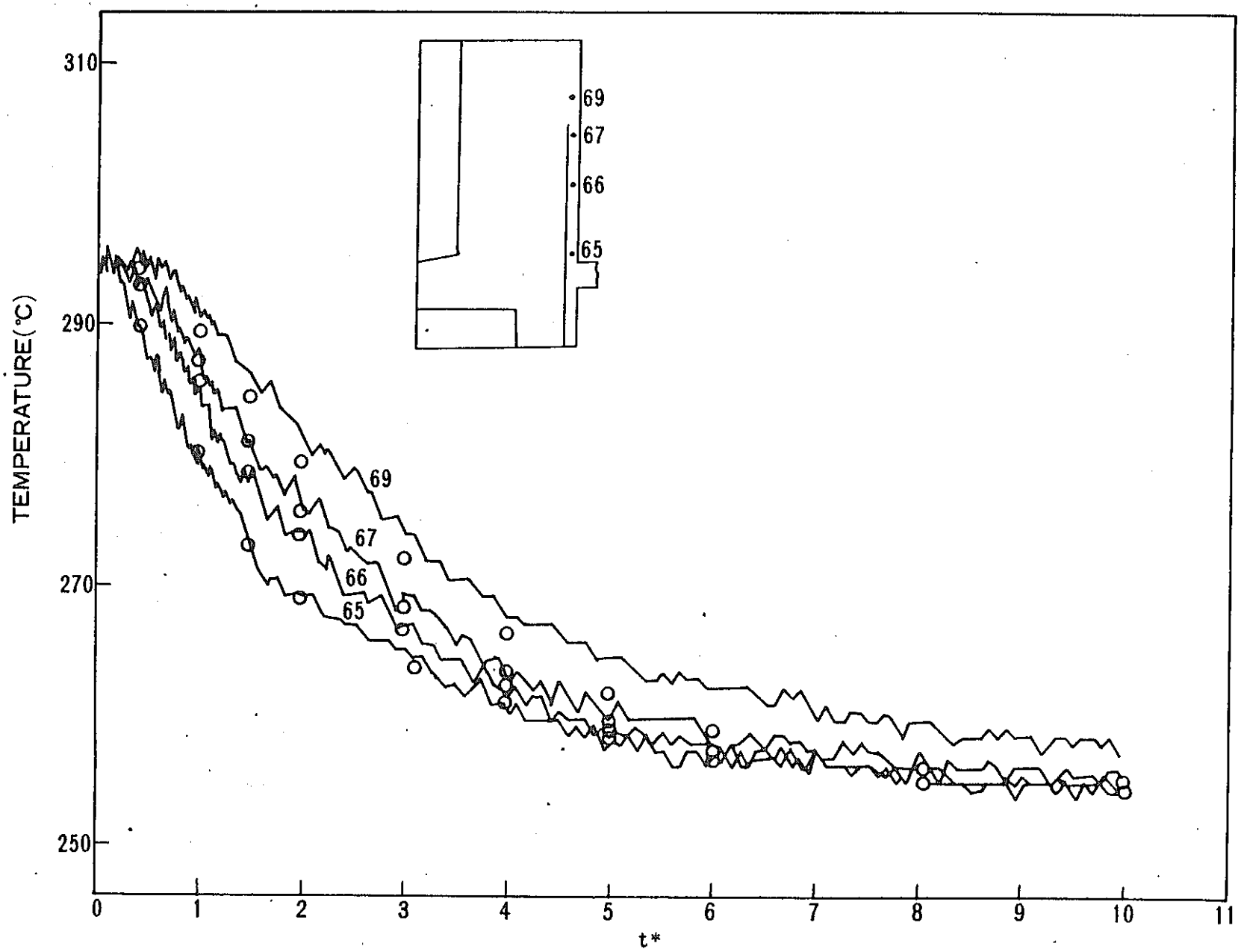

Fig. B5-11 Temperature Change in Time

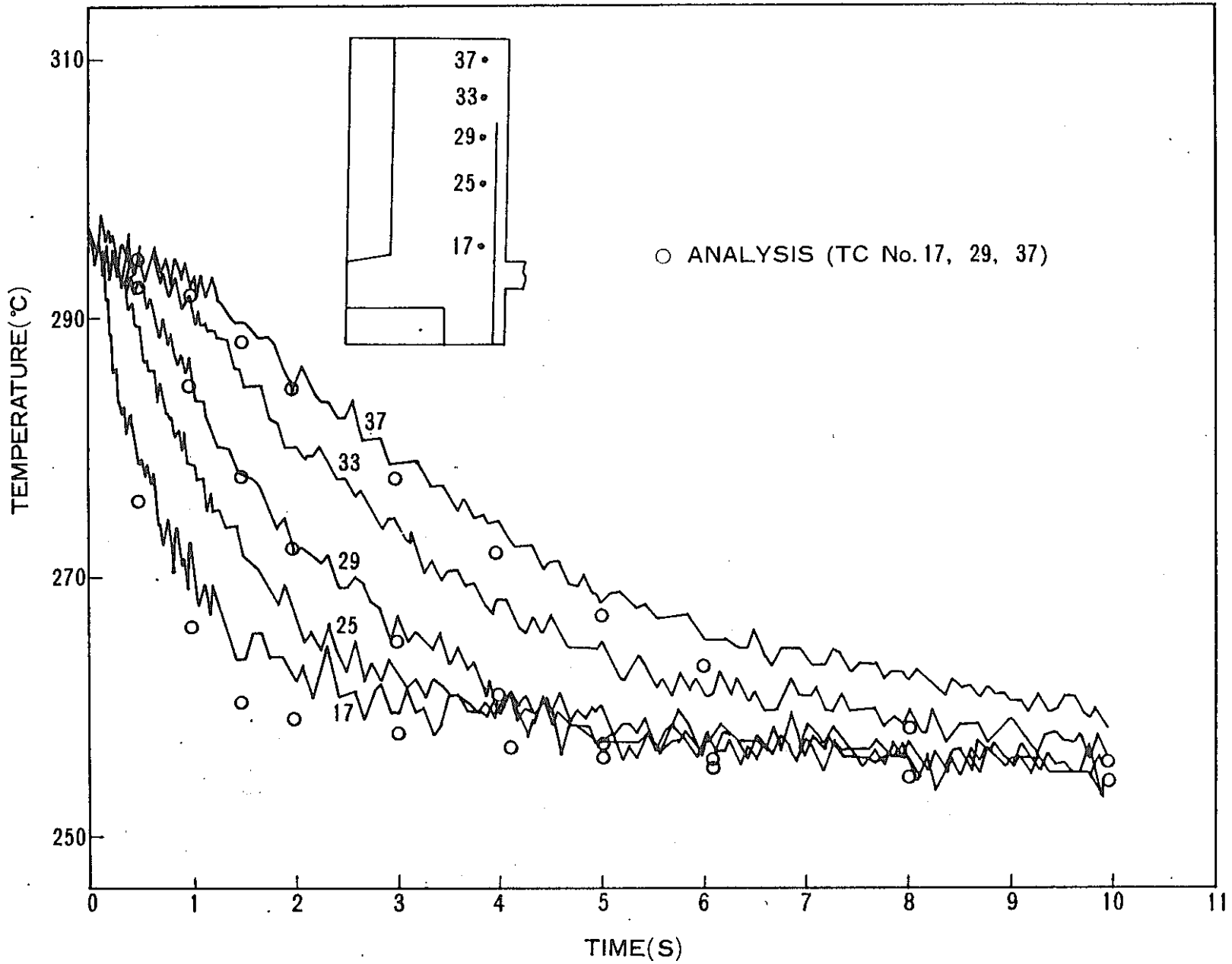

Fig. B5-10 Temperature Change in Time

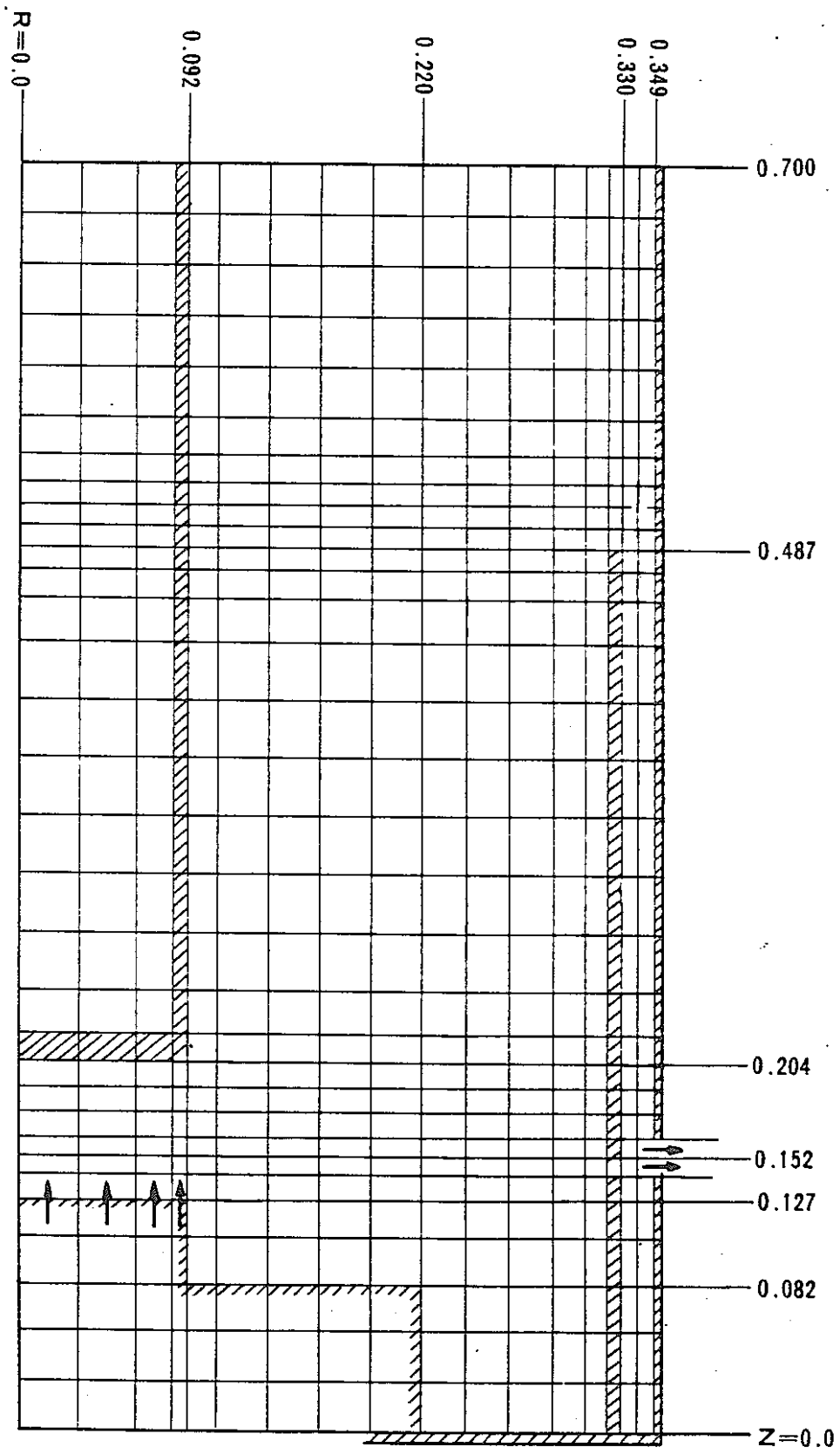

Fig. B5-9 Mesh Arrangement

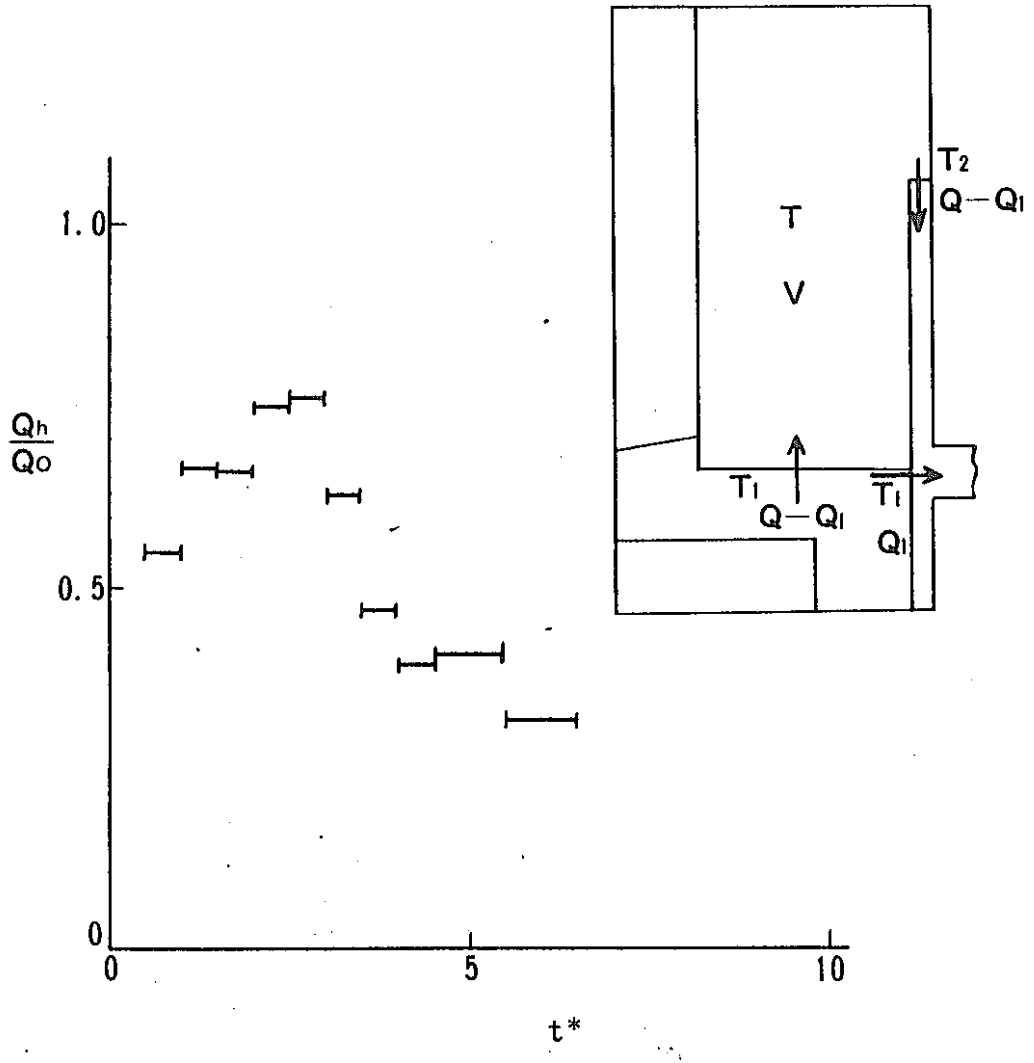

$$V\ \{T(t+\Delta t)-T(t)\}$$

$$=(Q-Q_1)\cdot\int_{t}^{t+\Delta t}\{T_1\ (t)-T_2(t)\}\cdot dt$$

$$\frac{Q_1}{Q}\fallingdotseq 1-\frac{V\cdot\Delta T}{Q(\widetilde{T}_1-\widetilde{T}_2)\cdot\Delta t}$$

Fig. B5- 8 Flow Volume through Flow Holes

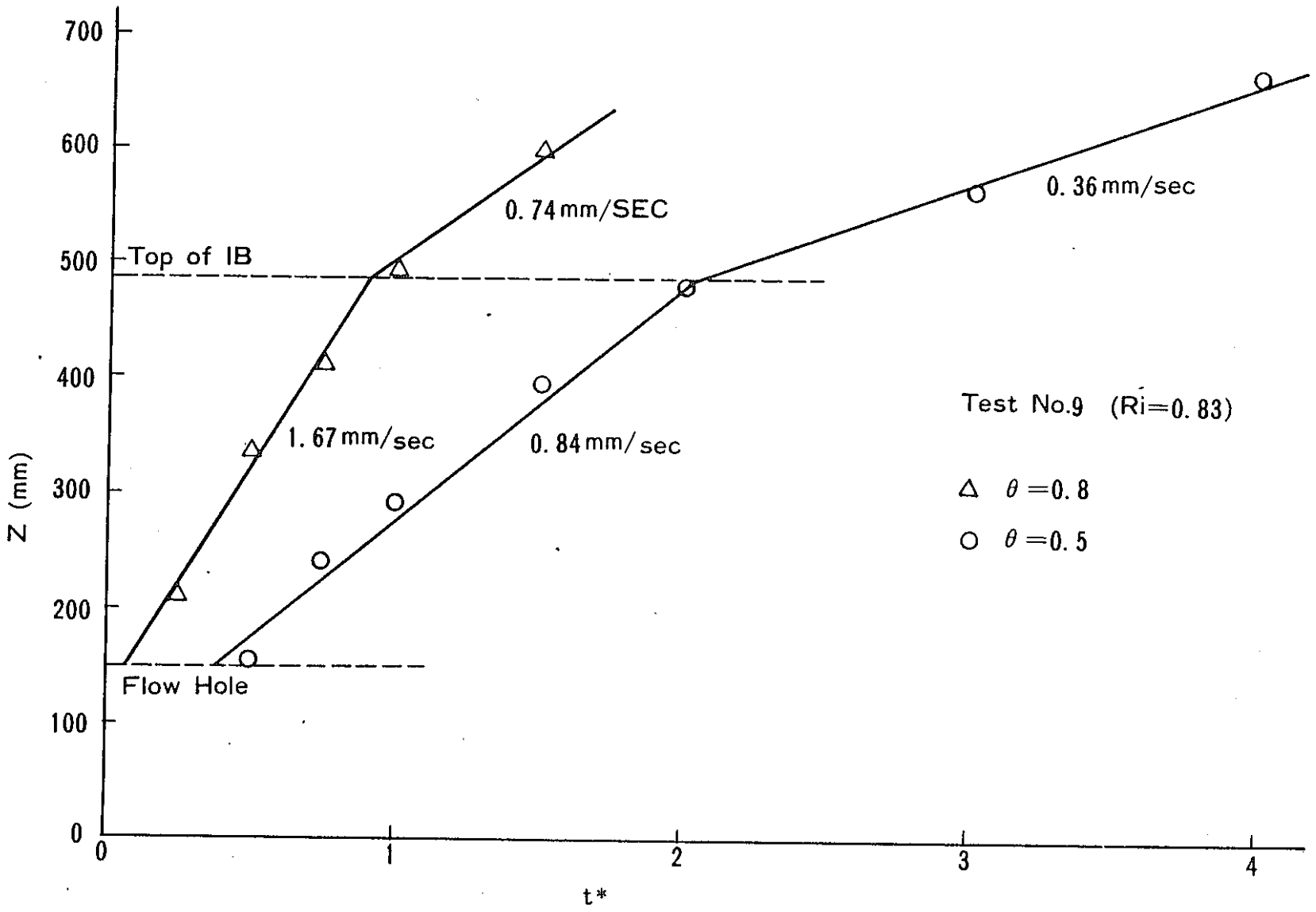

Fig. B5-7 Rising Speed of Density Interface

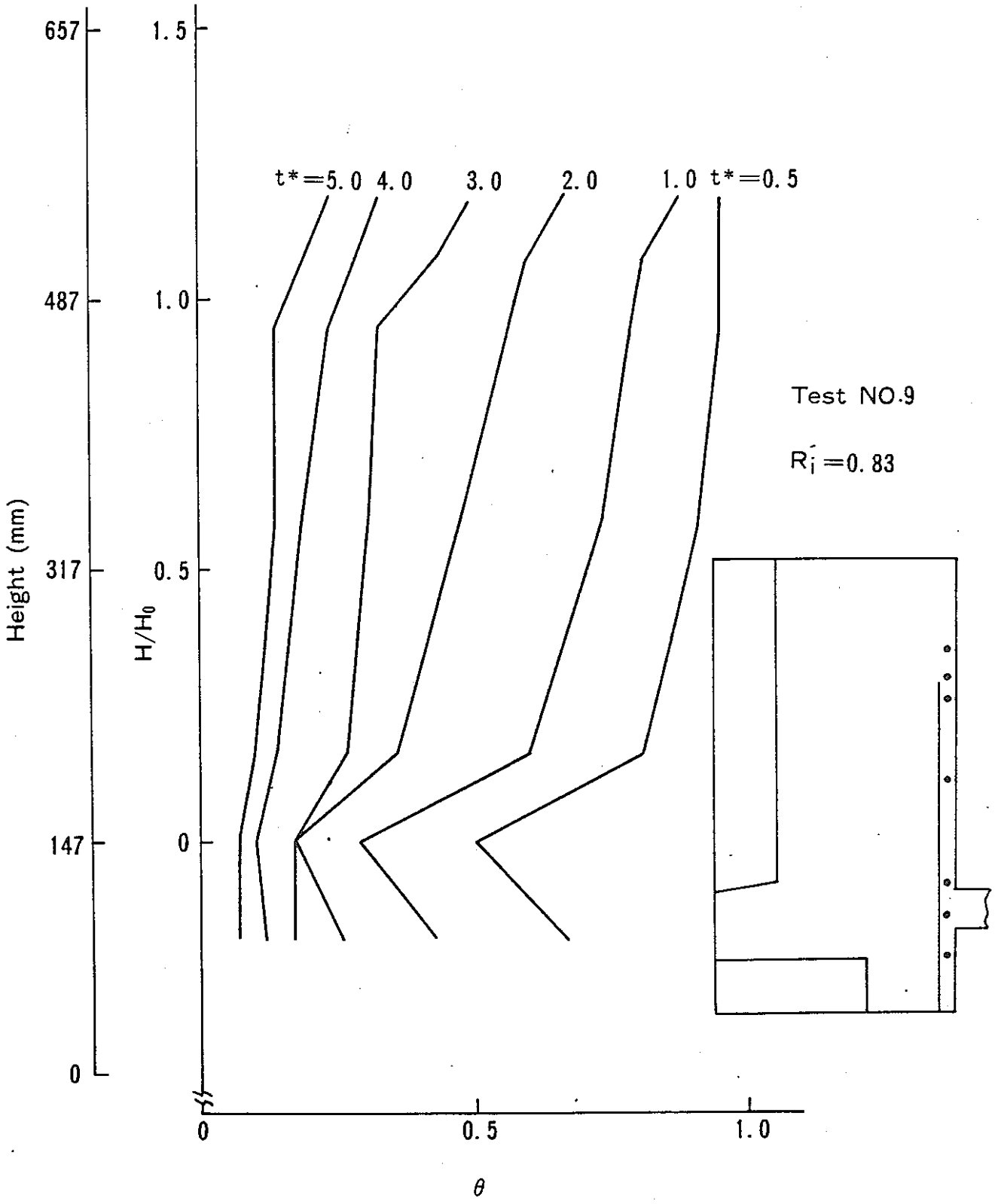

Fig. B5- 6 Axial Temperature Distribution

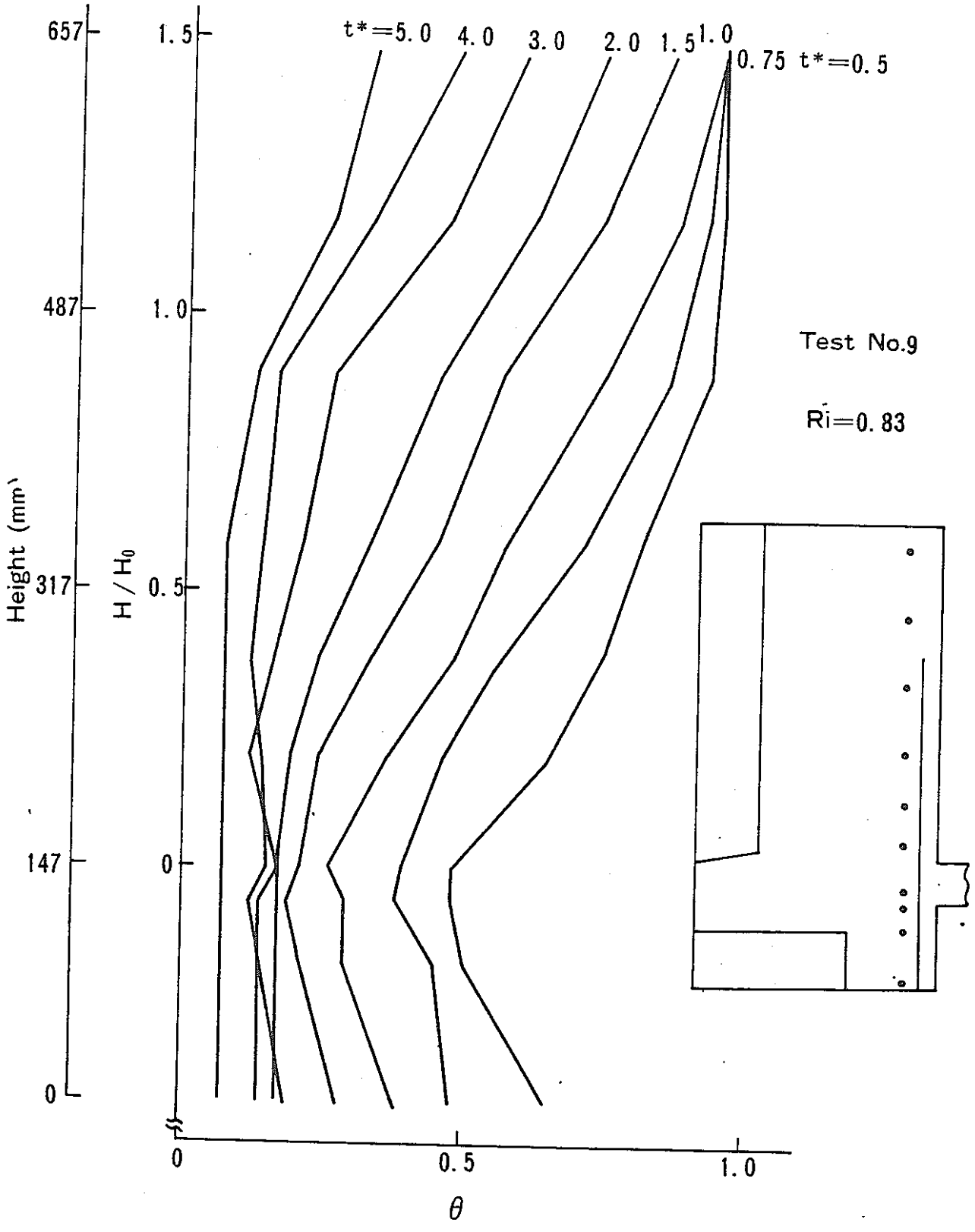

Fig. B5-5 Axial Temperature Distribution

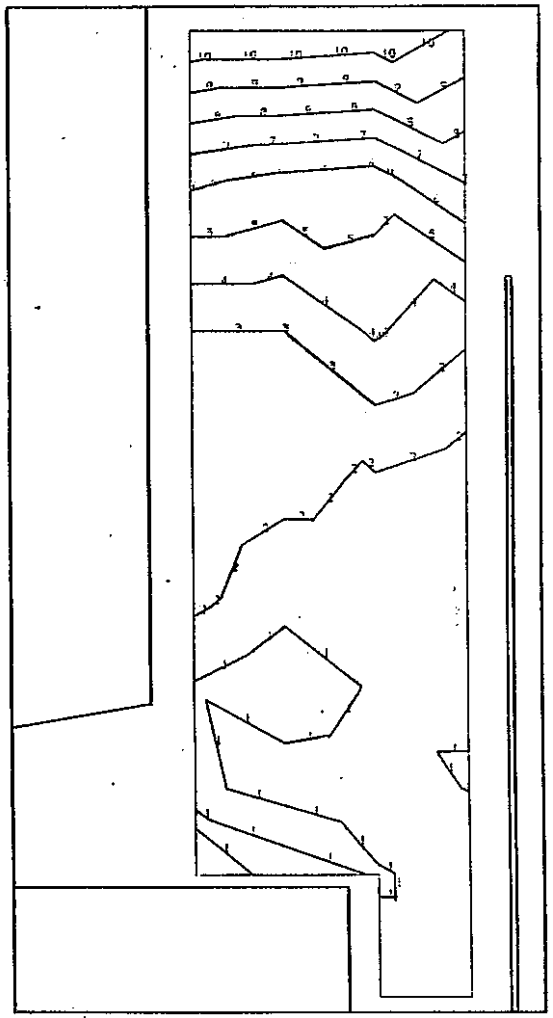

t* =5

1	256
2	258
3	259
4	260
5	261
6	263
7	264
8	265
9	267
10	268

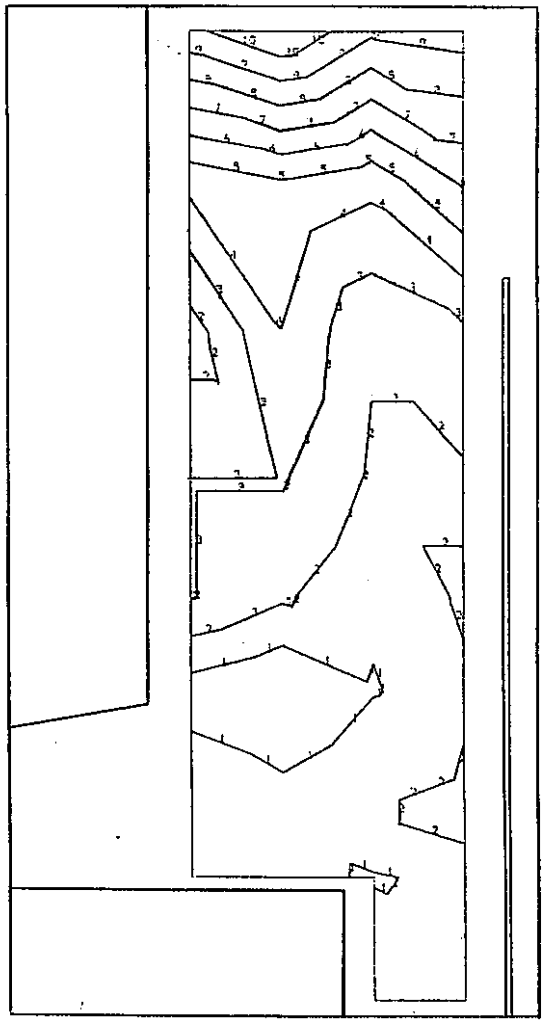

t* =7

1	255
2	256
3	257
4	258
5	259
6	260
7	261
8	262
9	263
10	264

FIG. B5-4 (CONTINUED)

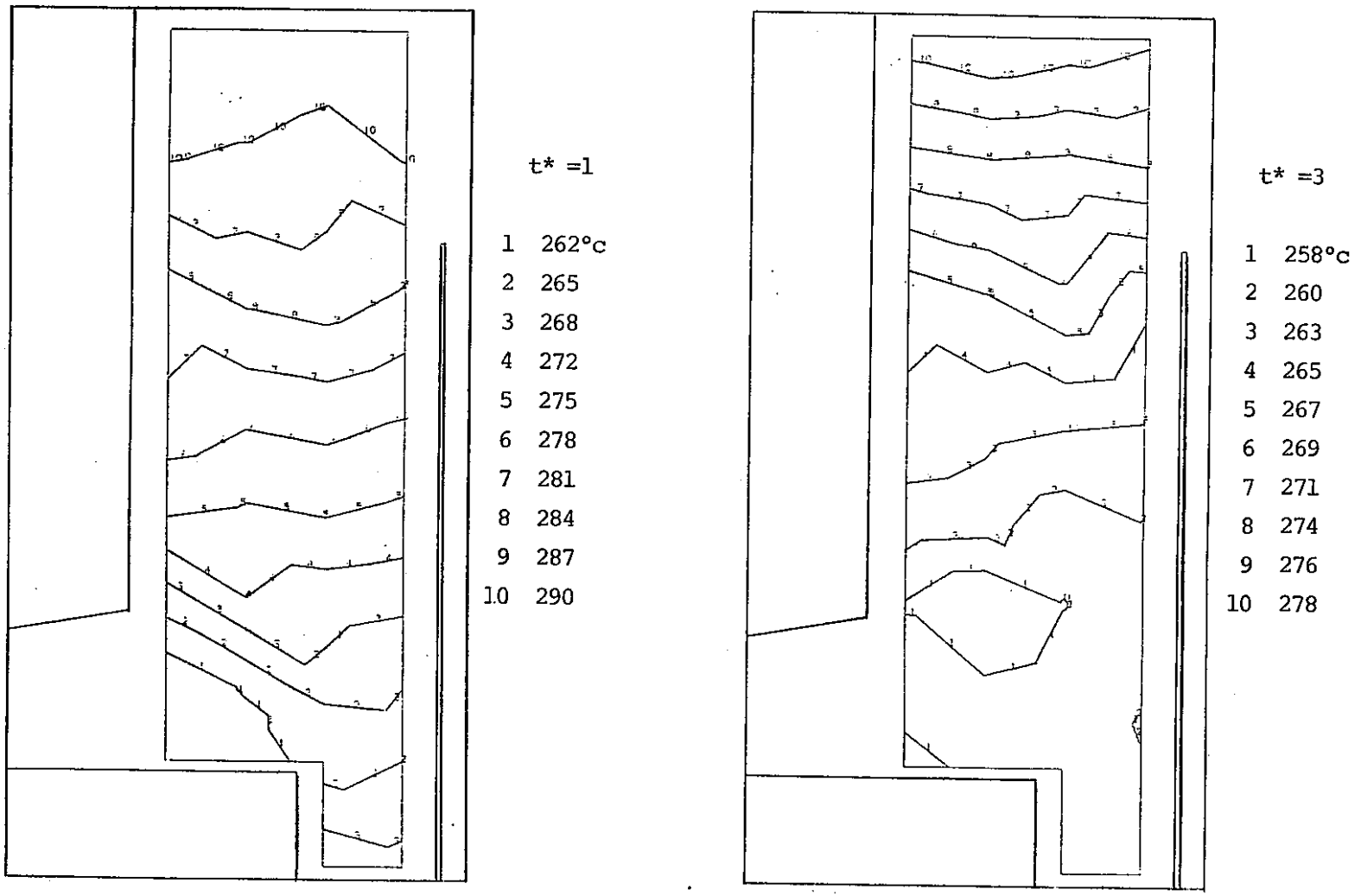

FIG.B5-4 MEASURED TEMPERATURE CONTOUR LINES IN THE UPPER PLENUM

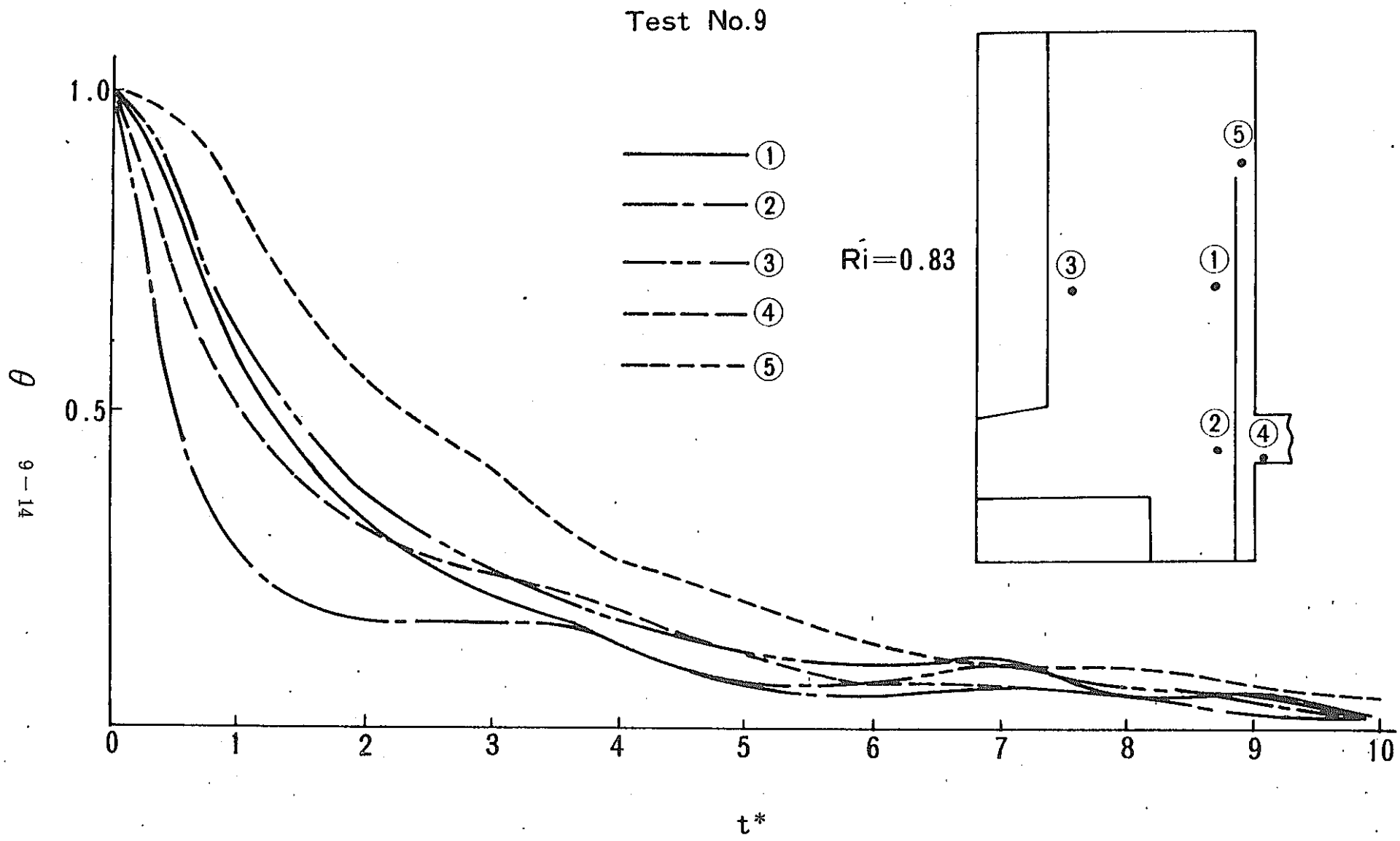

Fig. B5-3 Temperature Change in Time

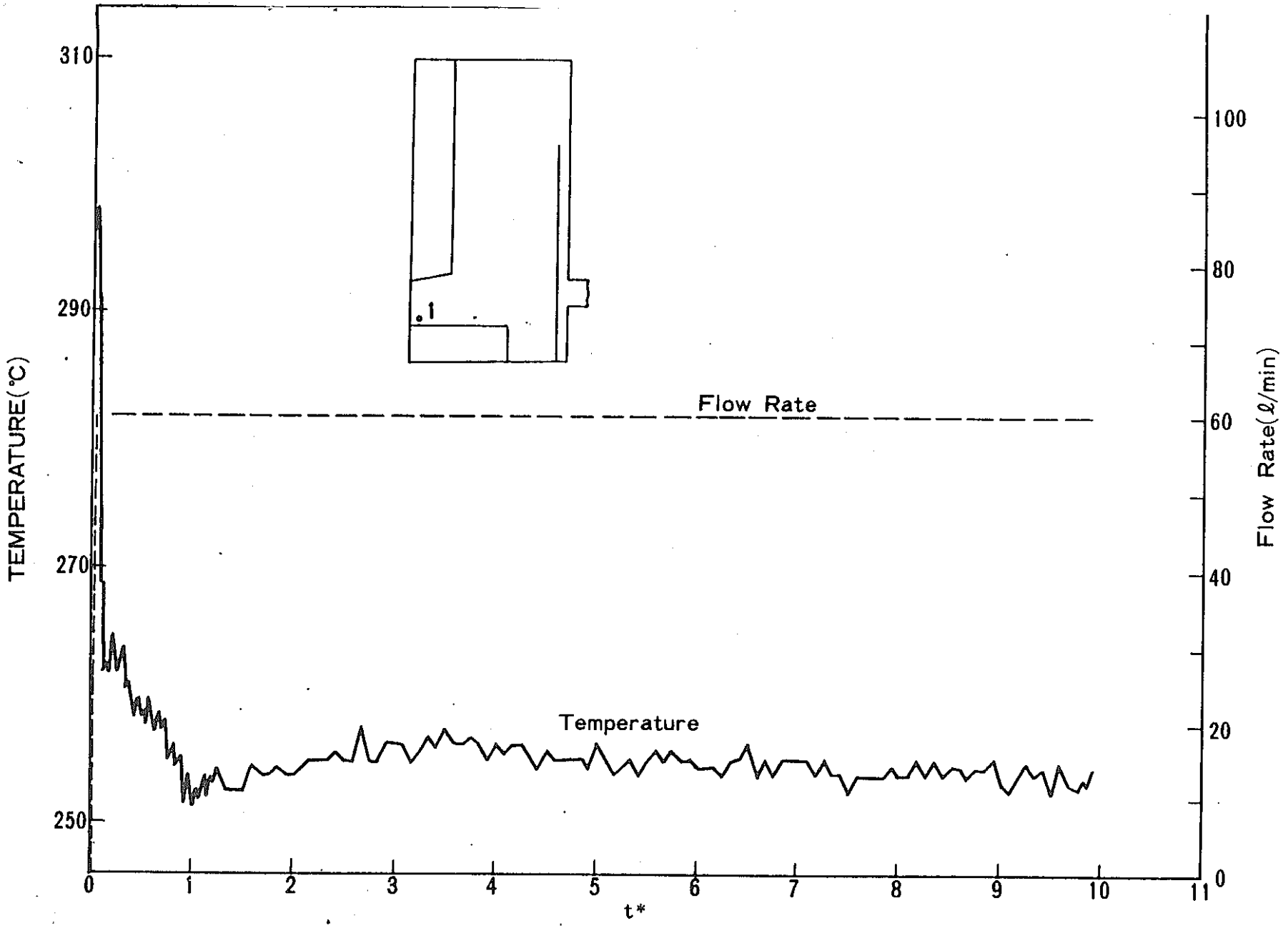

Fig. B5-2 Temperature and Flow Transients at Core Exit

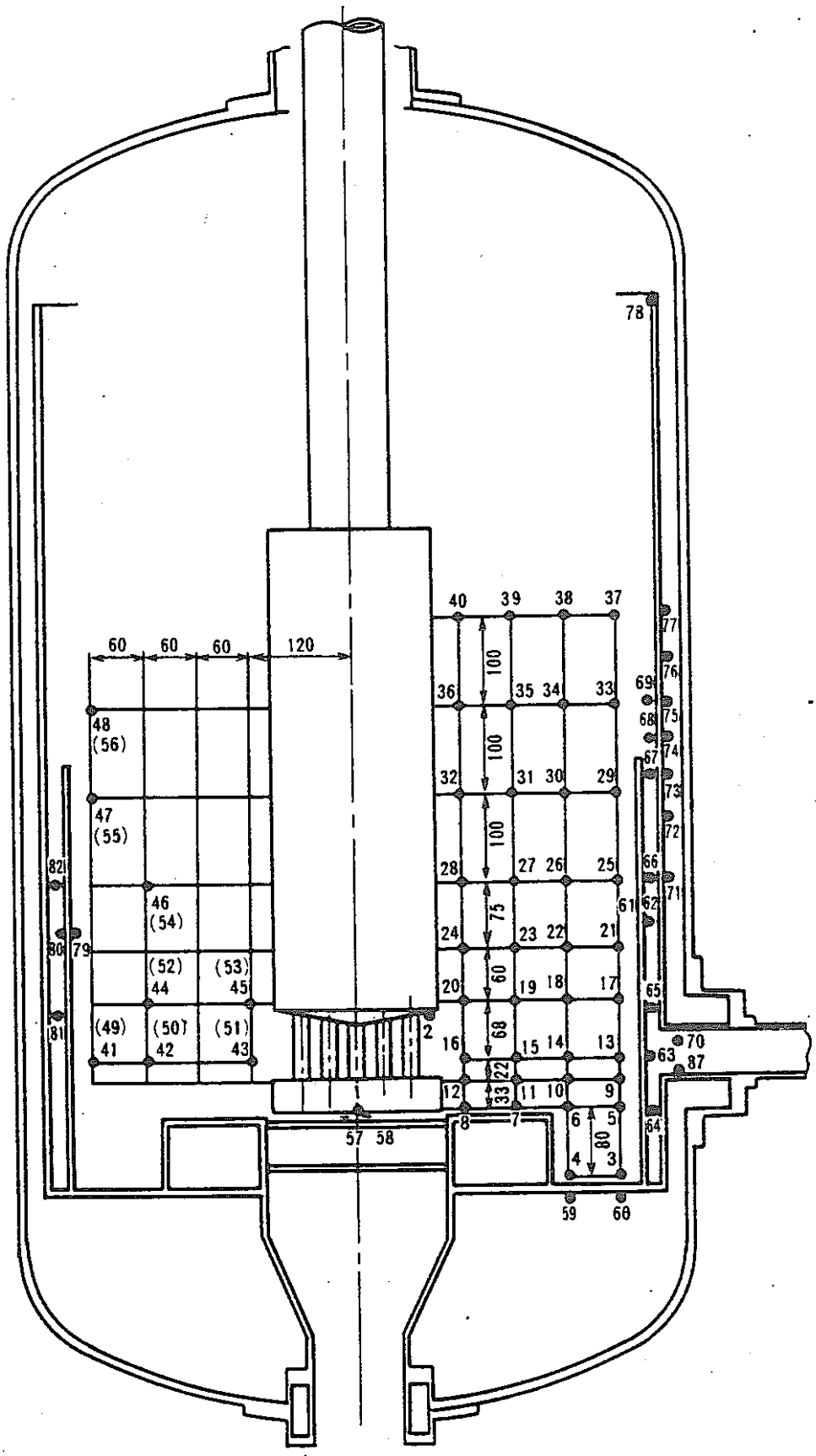

Fig. B5-1 Thermocouple Installation

COMPARISON OF THRMAL STRATIFICATION IN SODIUM & IN WATER WITH 1/10 MODELS

PNC/DOE REACTOR THERMAL-HYDRAULIC PERFORMANCE SPECIALISTS MEETING

OCTOBER , 1982

PRESENTED BY

K. OKADA

MITSBISHI HEAVY INDUSTRIES, LTD.
KOBE SHIPYARD & ENGINE WORKS
ADVANCED NUCLEAR PLANT ENGINEERING DEPARTMENT

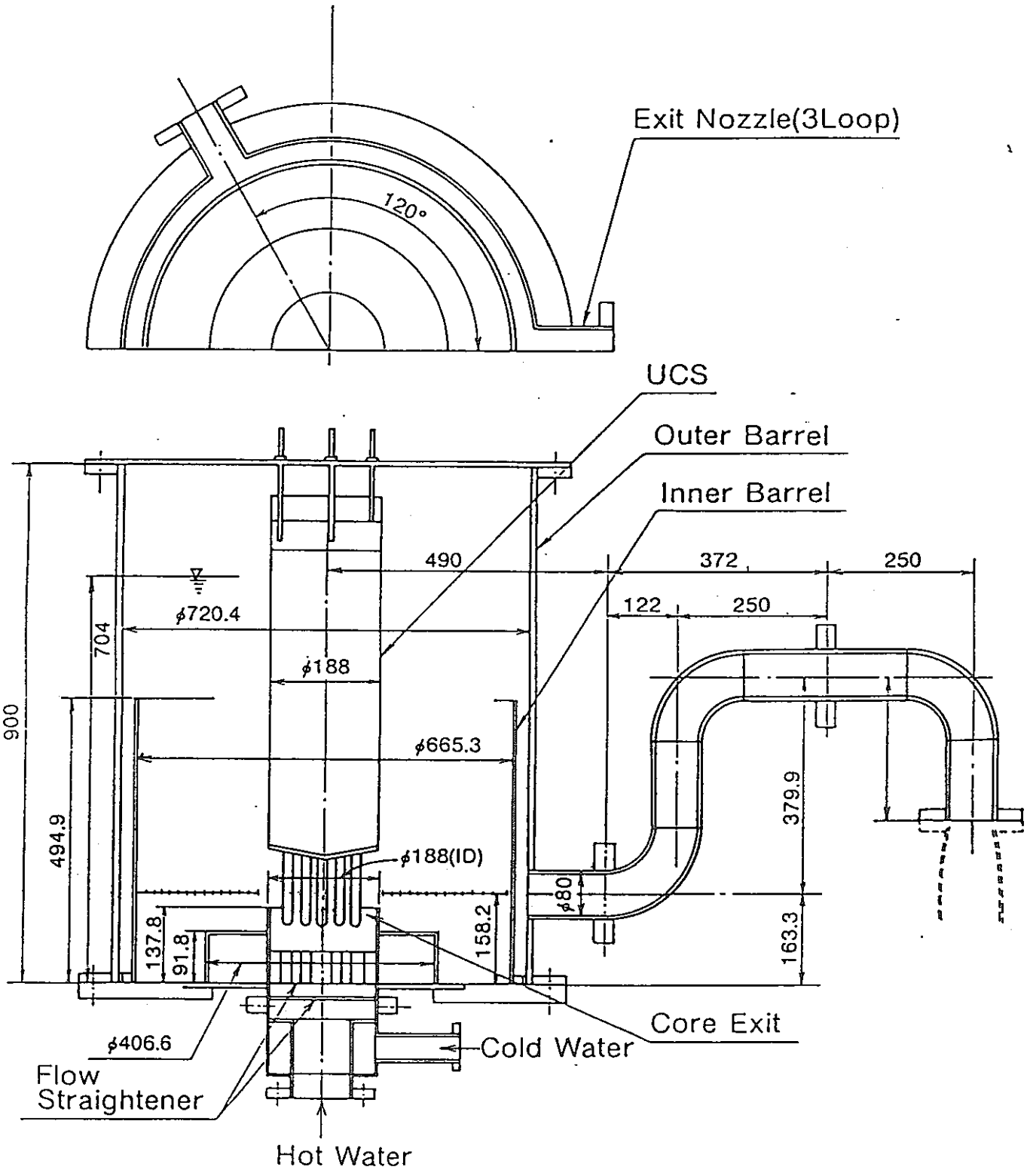

Fig B6-1

1/10 Scale Model Of "MONJU" Upper Plenum

	MONJU	1/10 Scale Model (Water)	1/10 Scale Model (Sodium)
θh (°C)	529	50	296
θc (°C)	419	24	254
Flow Rate (nominal operation)	15.36×10^{6} (Kg/hr)		
Flow Change	100%→9.5% (≒30sec)	0→9.5% (60 ℓ/min)	0→9.5% (60 ℓ/min)
Diameter of Core ExiT (De) (m)	1.788	0.188	0.188
Velocity of Core Exit (V) (m/s)	0.19	0.036	0.036
$\frac{\rho c-\rho h}{\rho C}$	0.031	0.011	0.011

Table B6-1(1/2) Condition of Thermal Stratification

	MONJU	1/10 Scale Model (Water)	1/10 Scale Model (Sodium)
Re $\left(\frac{V \cdot De}{\nu}\right)$	1.1×10^{6} (1.0)	7.5×10^{3} (0.007)	1.56×10^{4} (0.015)
Pr $\left(\frac{\nu}{a}\right)$	4.9×10^{-3} (1.0)	6.33 (1.3×10^{3})	6.46×10^{-3} (1.32)
Pe $\left(\frac{V \cdot De}{a}\right)$	5.2×10^{3} (1.0)	4.75×10^{4} (9.13)	1.01×10^{2} (0.019)
Ri $\left(\frac{\frac{\rho c - \rho h}{\rho c} \cdot g \cdot De}{V^2}\right)$	15.1 (1.0)	12.5 (0.83)	12.5 (0.83)

Table B6-1 (2/2) Condition of Thermal Stratification

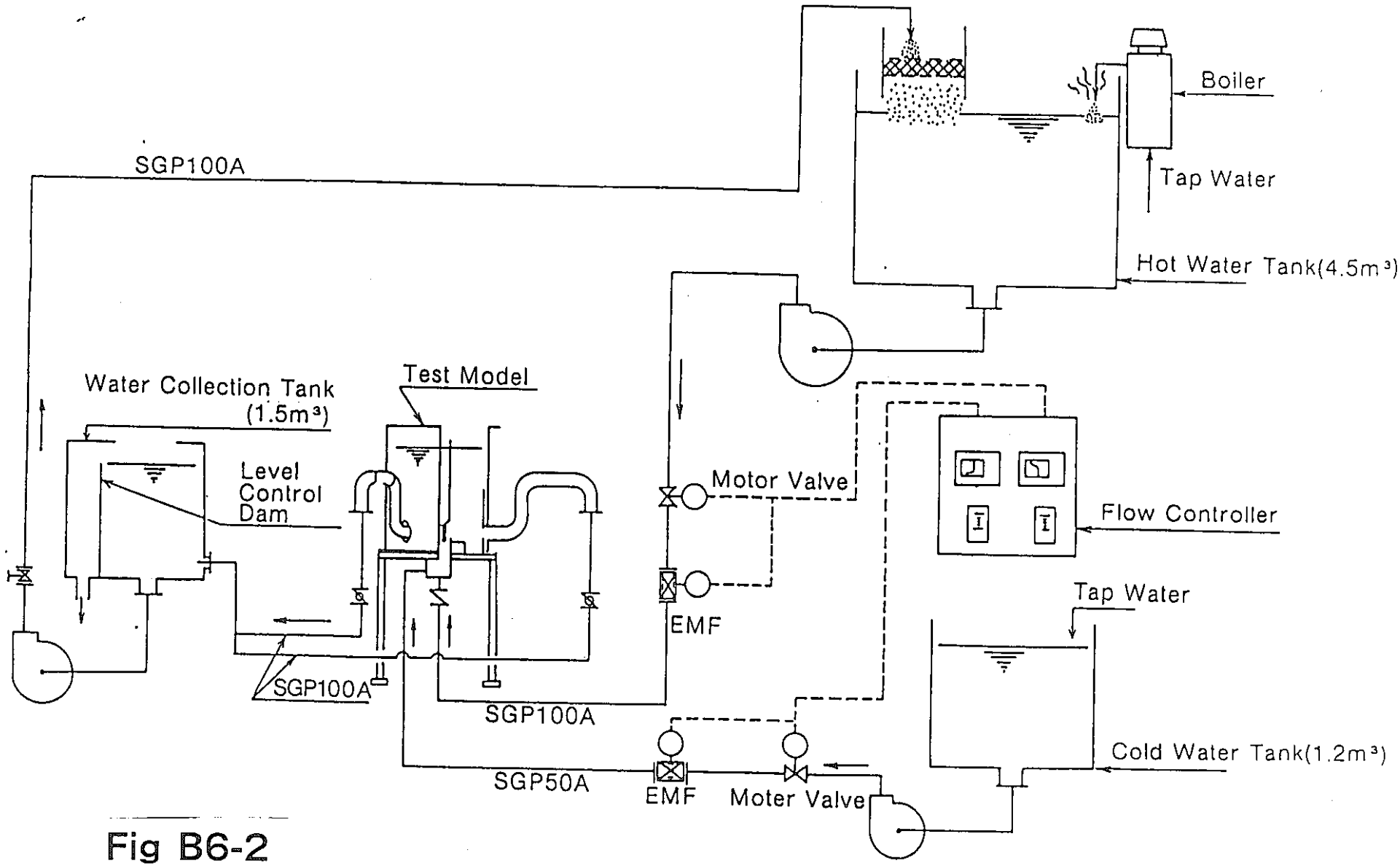

Fig B6-2

Test Loop Of 1/10 Scale Model(Water)

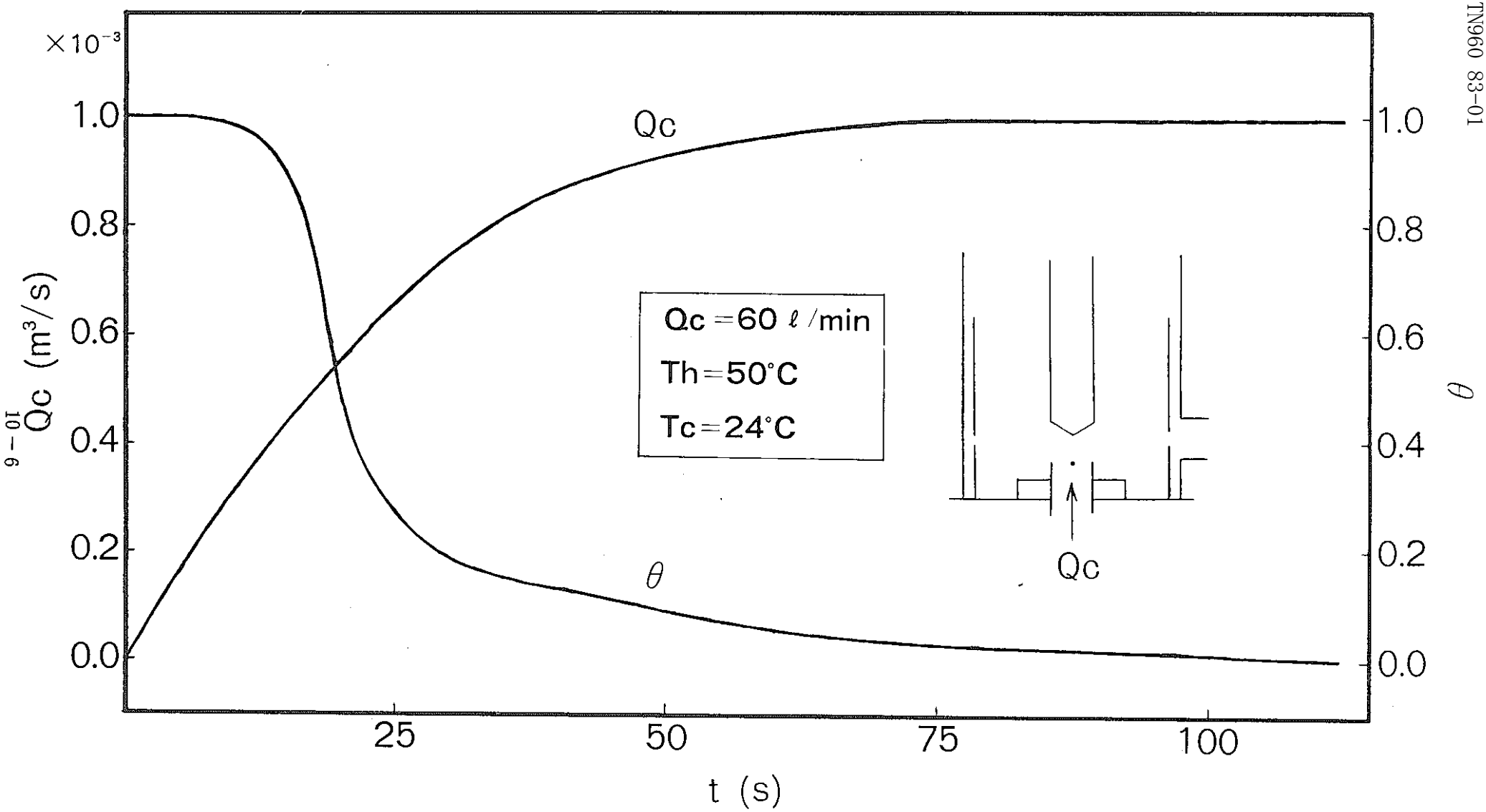

Fig B6-3 Flow and Temperature Transition from Core Exit

Fig B6-4
Thermo-Couple Position

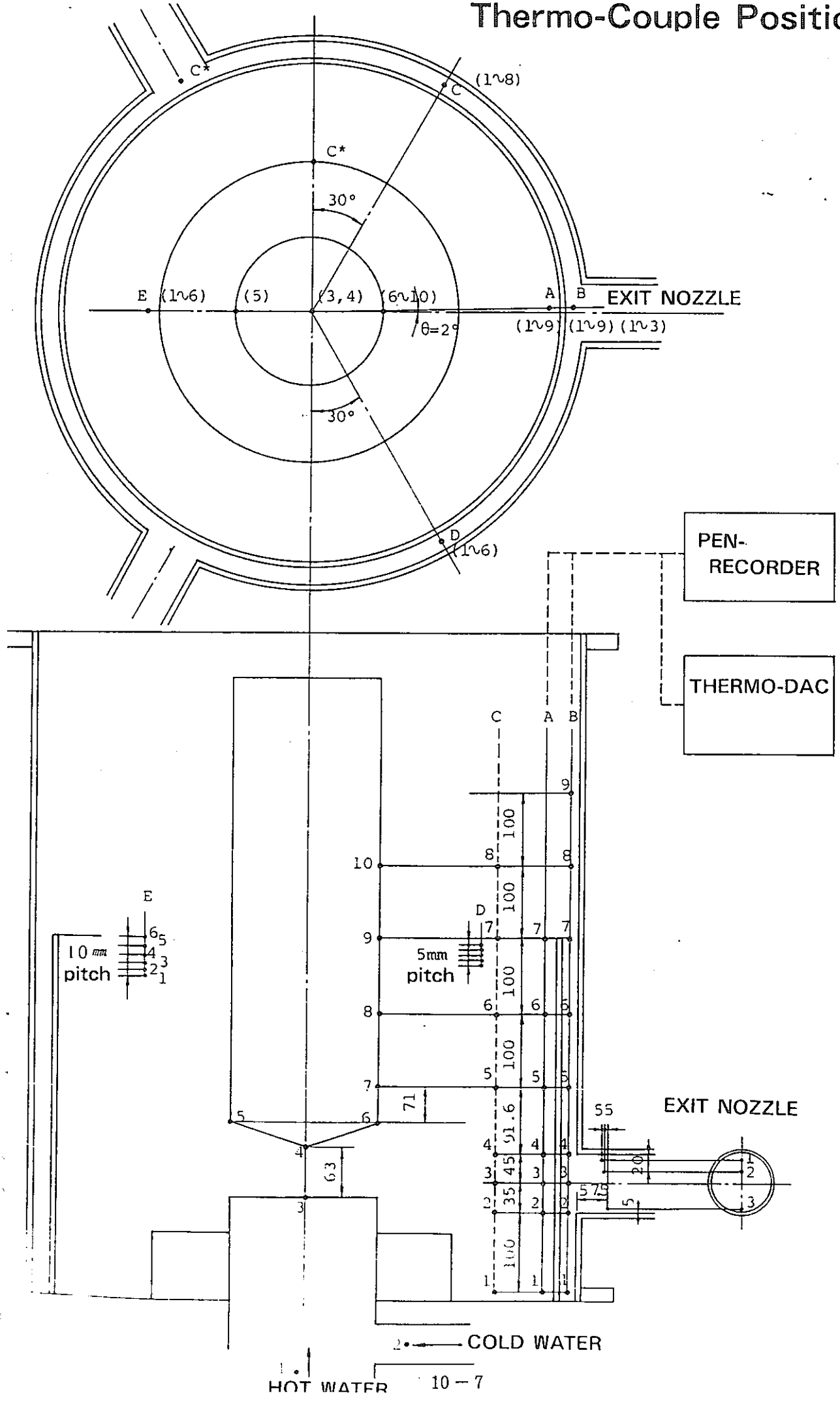

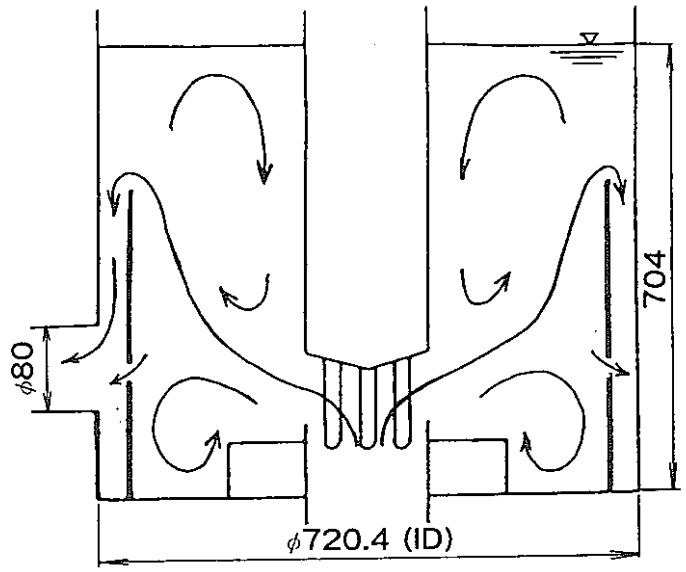

1. IN NORMAL OPERATION

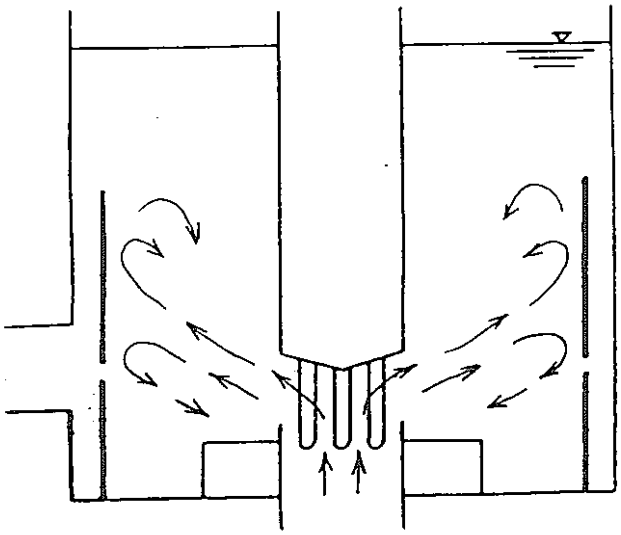

2. AFTER POURING COLD WATER

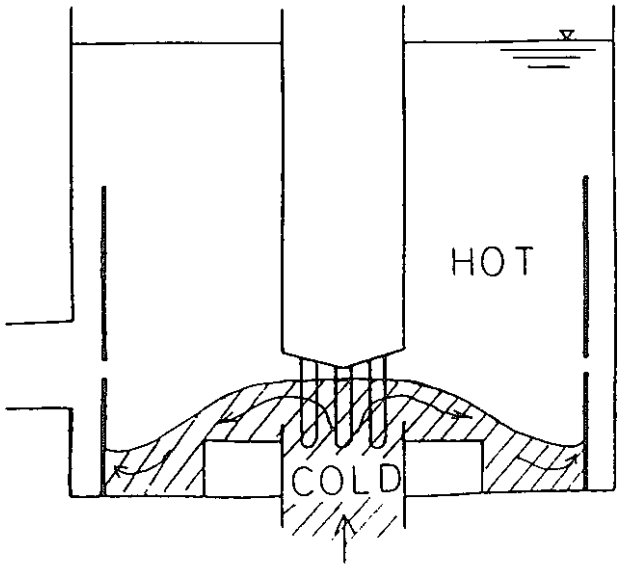

3. THERMAL STRATIFICATIO

Qc=60 ℓ/min
Th=50°C
Tc= 24°C

Fig B6-5 (1/2) Flow Pattern

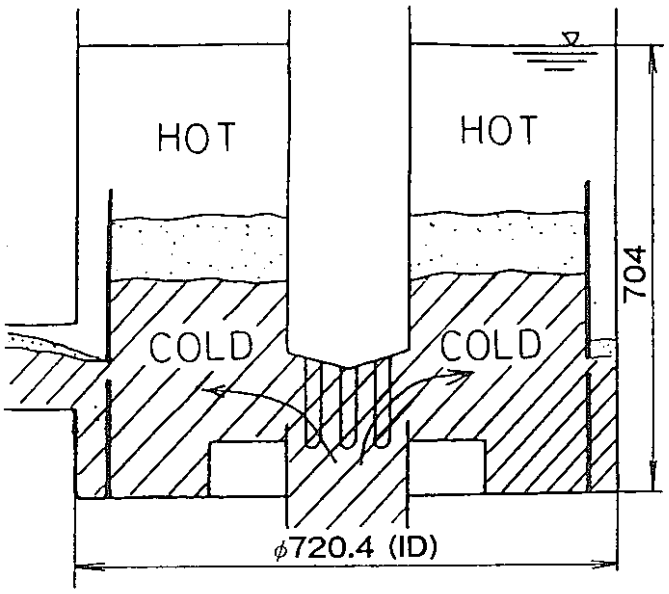

4. THERMAL STRATIFICATION (STEP 1)

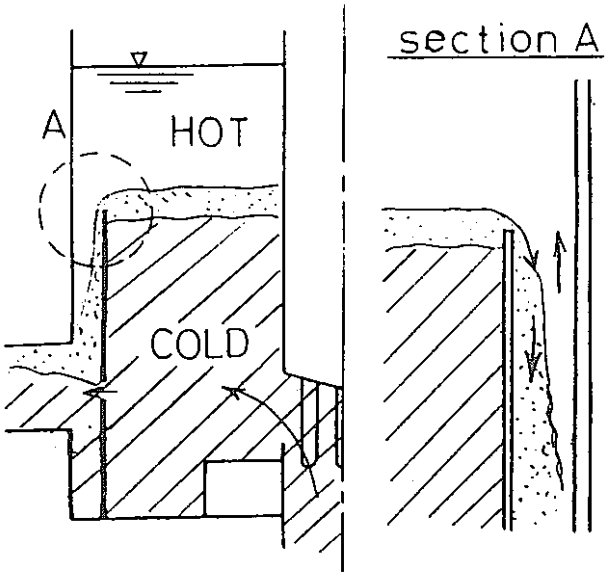

5. THERMAL STRATIFICATION

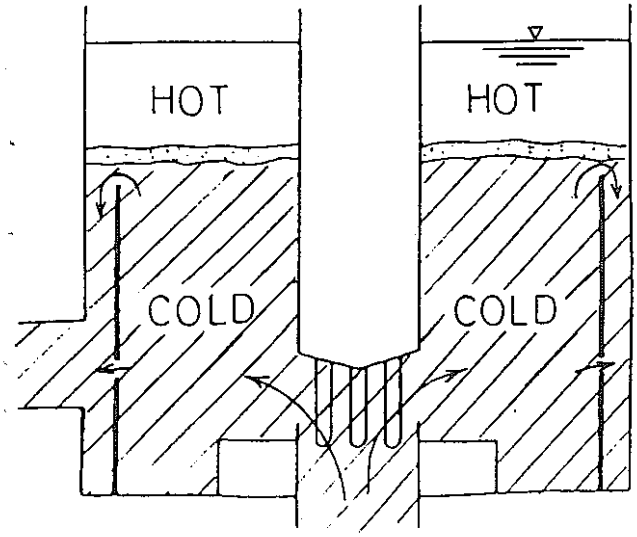

6. THERMAL STRATIFICATION (STEP 2)

Qc=60 ℓ/min
Th=50°C
Tc=24°C

Fig B6-5 (2 2) Flow Pattern

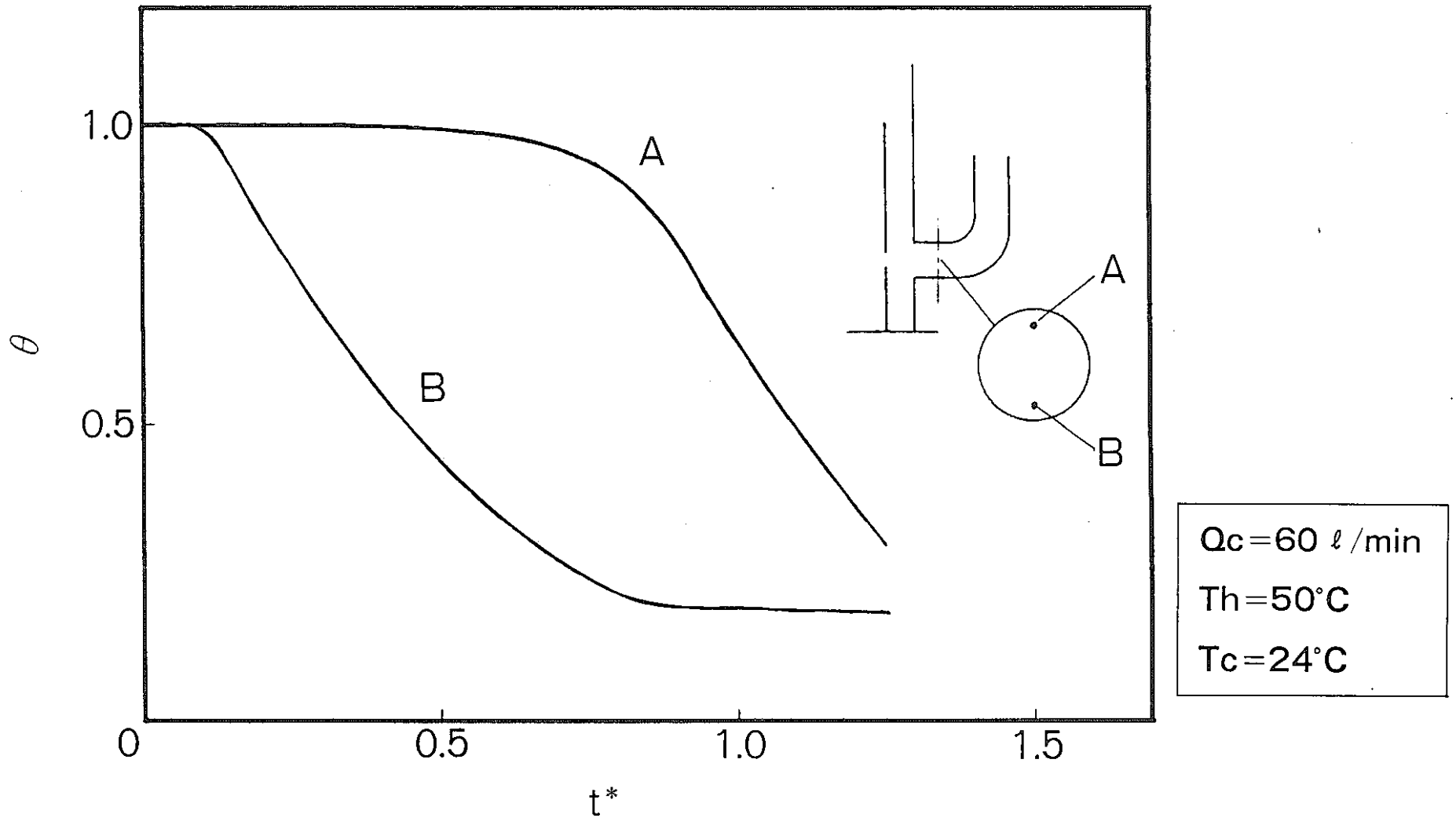

Fig B6-6 Temperature Transition in the Exit Nozzle

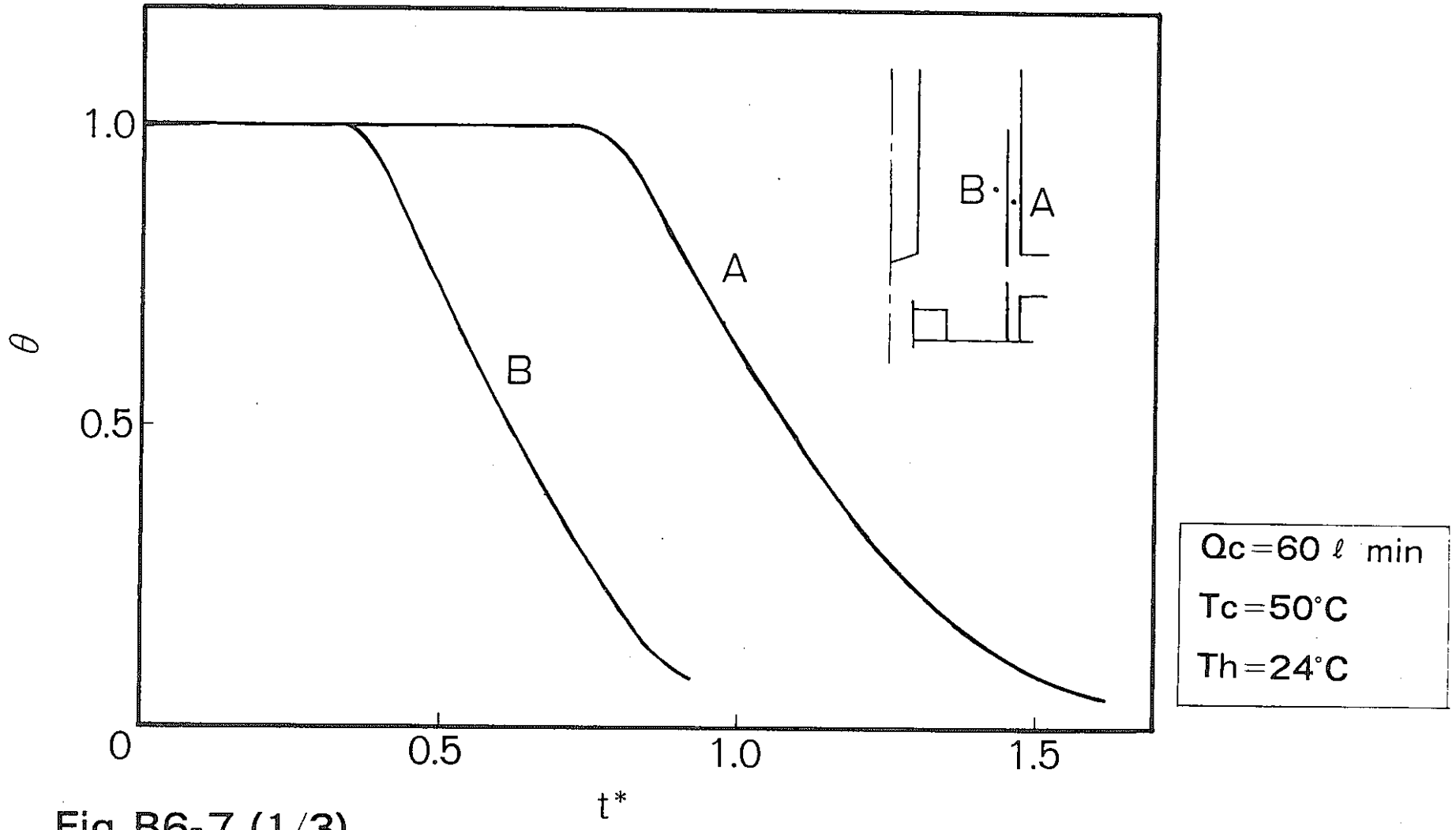

Fig B6-7 (1/3)

Temperature Transition in the Upper Plenum

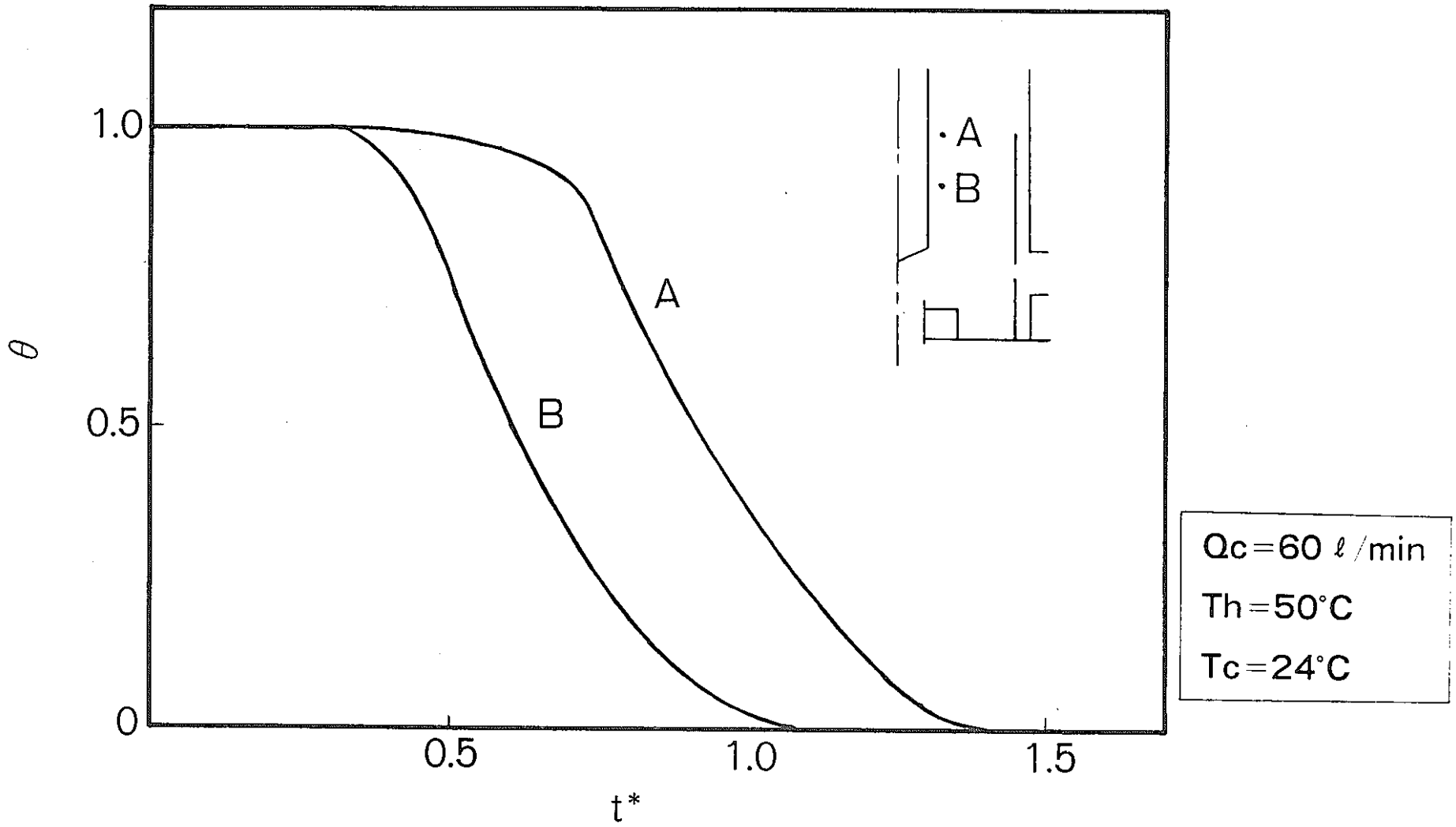

Fig B6-7 (2/3)

Temperature Transition in the Upper Plenum

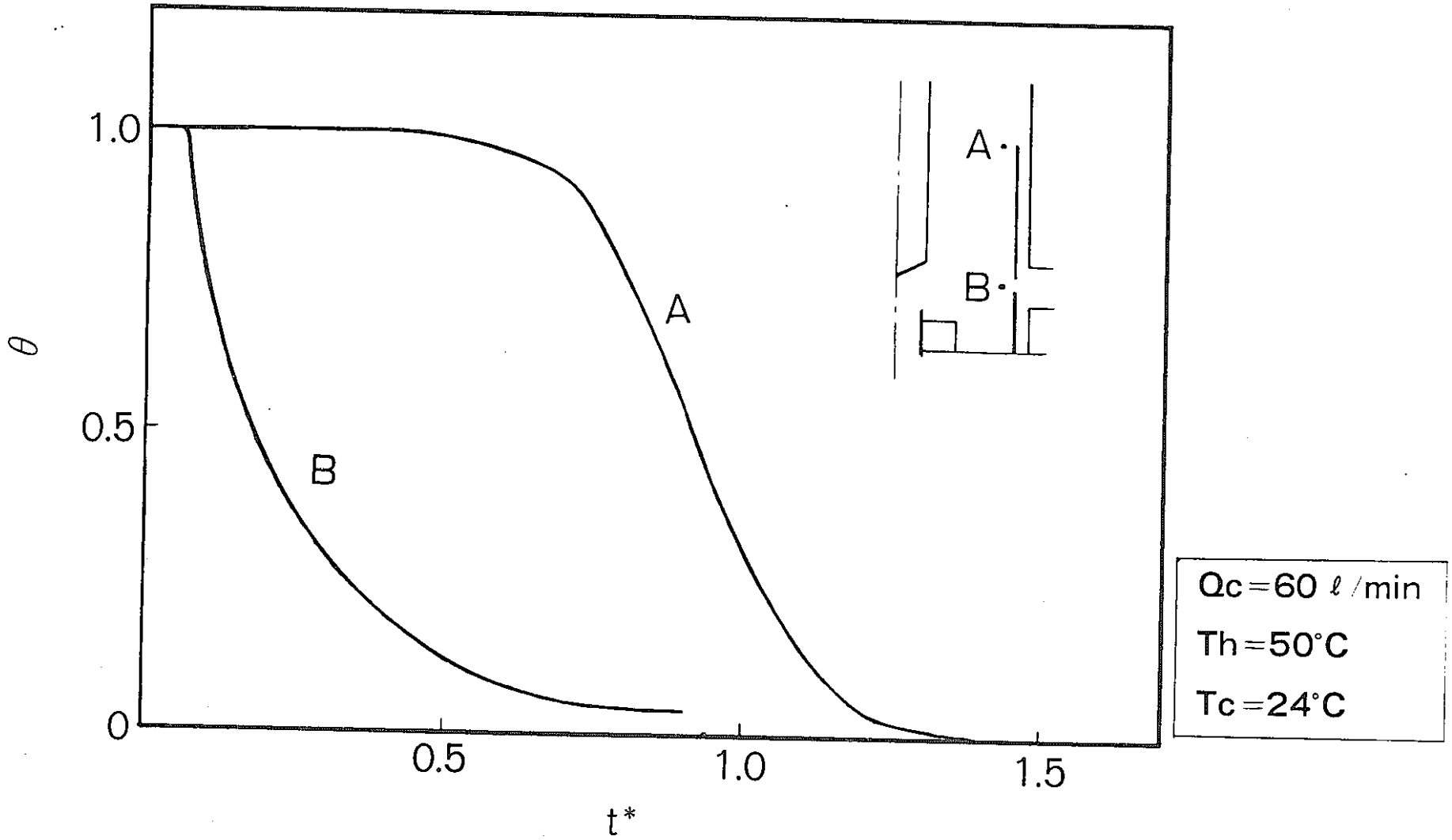

Fig B6-7 (3/3)

Temperature Transition in the Upper Plenum

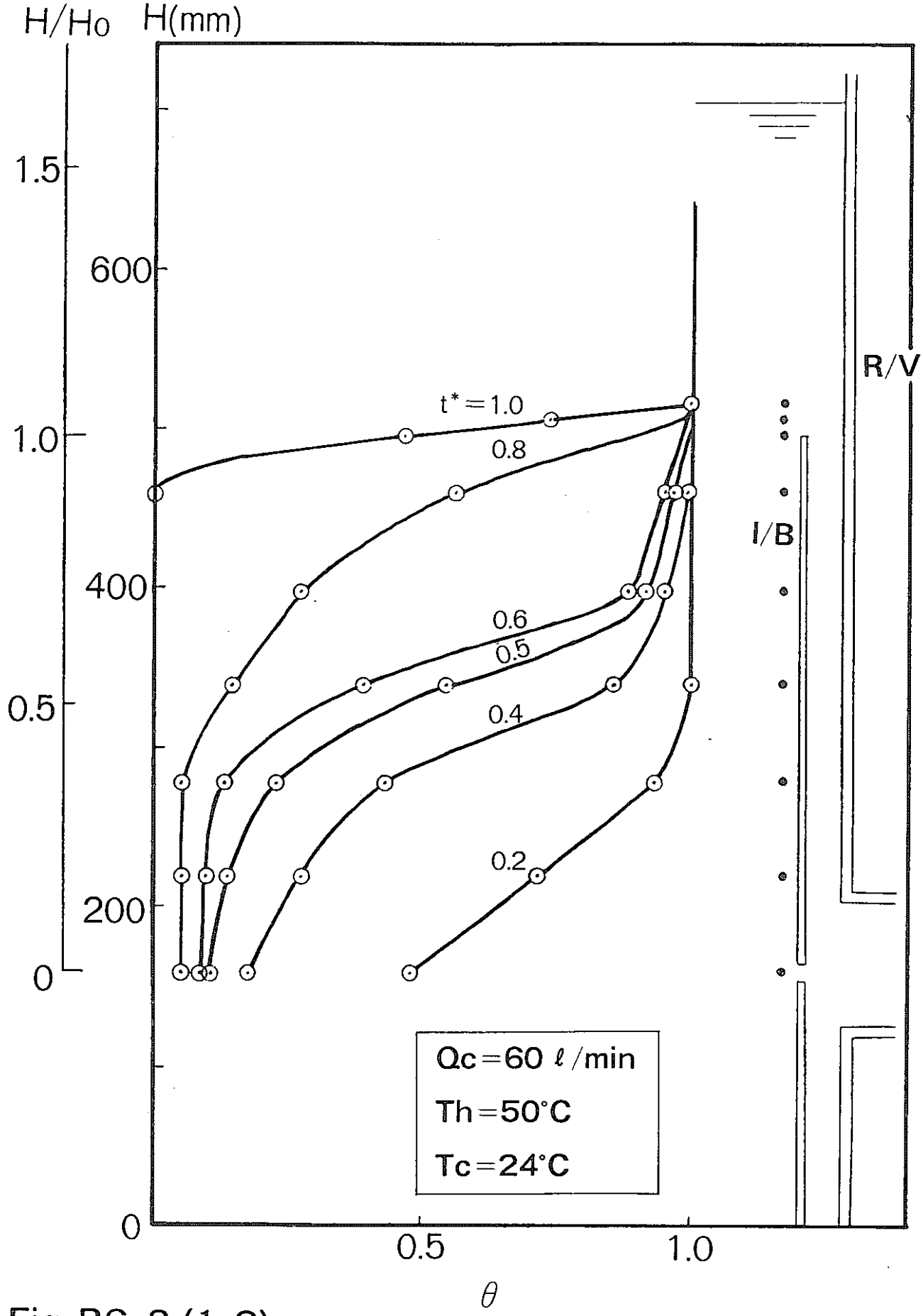

Fig B6-8 (1 2)

Axial Temperature Profile in the Upper Plenum

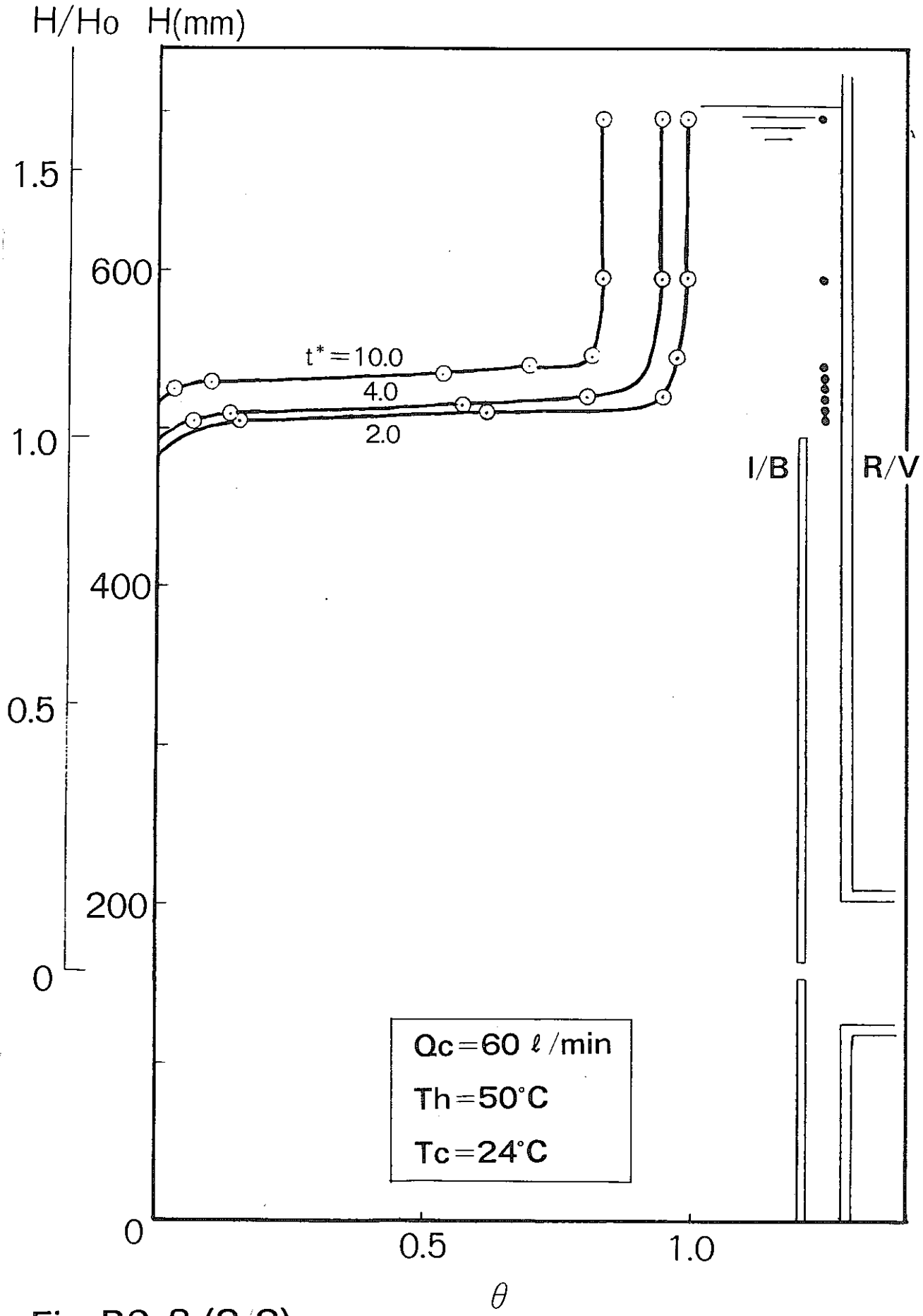

Fig B6-8 (2/2)

Axial Temperature Profile in the Upper Plenum

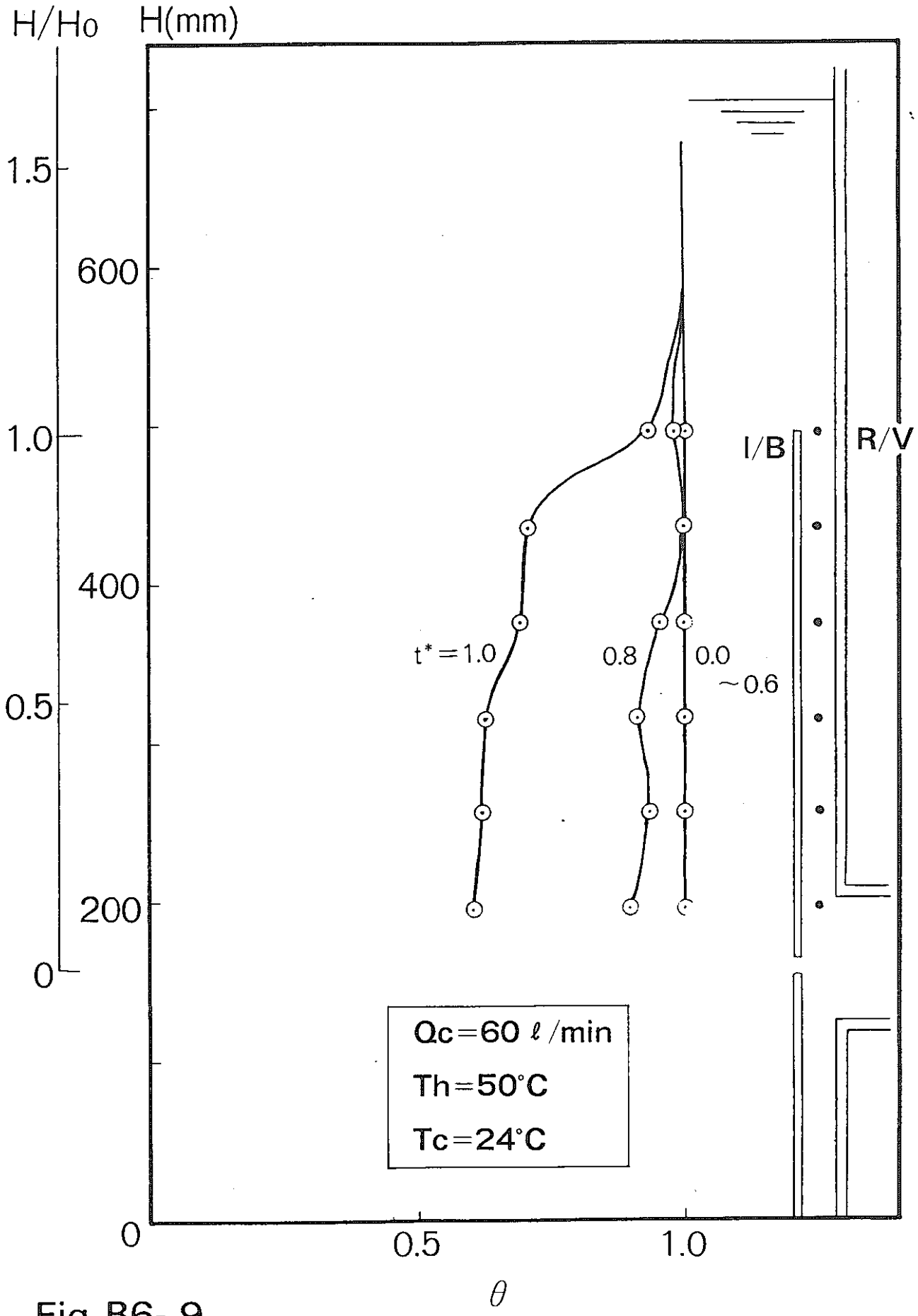

Fig B6- 9

Axial Temperature Profile in the Annulas Part

OUTLET NOZZLE			ANNULUS PART			UPPER PART OF I/B		
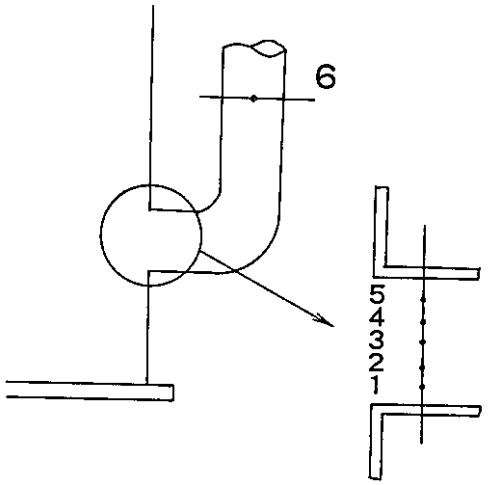			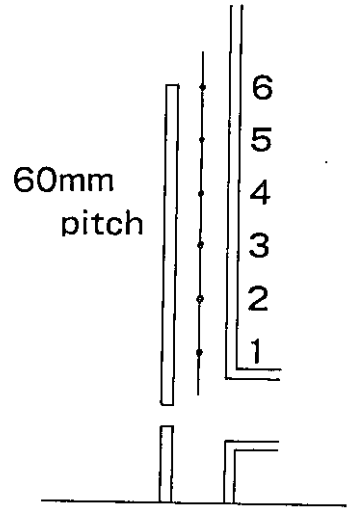			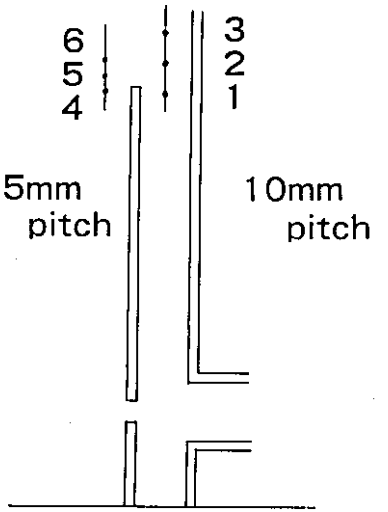		
	$\frac{\triangle Tmax}{Th-Tc}$(%)	f(Hz)		$\frac{\triangle Tmax}{Th-Tc}$(%)	f(Hz)		$\frac{\triangle Tmax}{Th-Tc}$(%)	f(Hz)
1	7.5	1.00	1	13.2	0.17	1	—	—
2	20.7	2.50	2	11.3	0.50	2	37.7	0.50
3	53.7	2.00	3	7.5	0.17	3	37.7	0.17
4	73.5	1.10	4	7.5	0.17	4	—	—
5	67.8	2.50	5	18.8	0.50	5	35.8	0.04
3	24.5	0.80	6	39.6	0.21	6	60.3	0.29

Table B6-2 Temperature Variation And Frequency

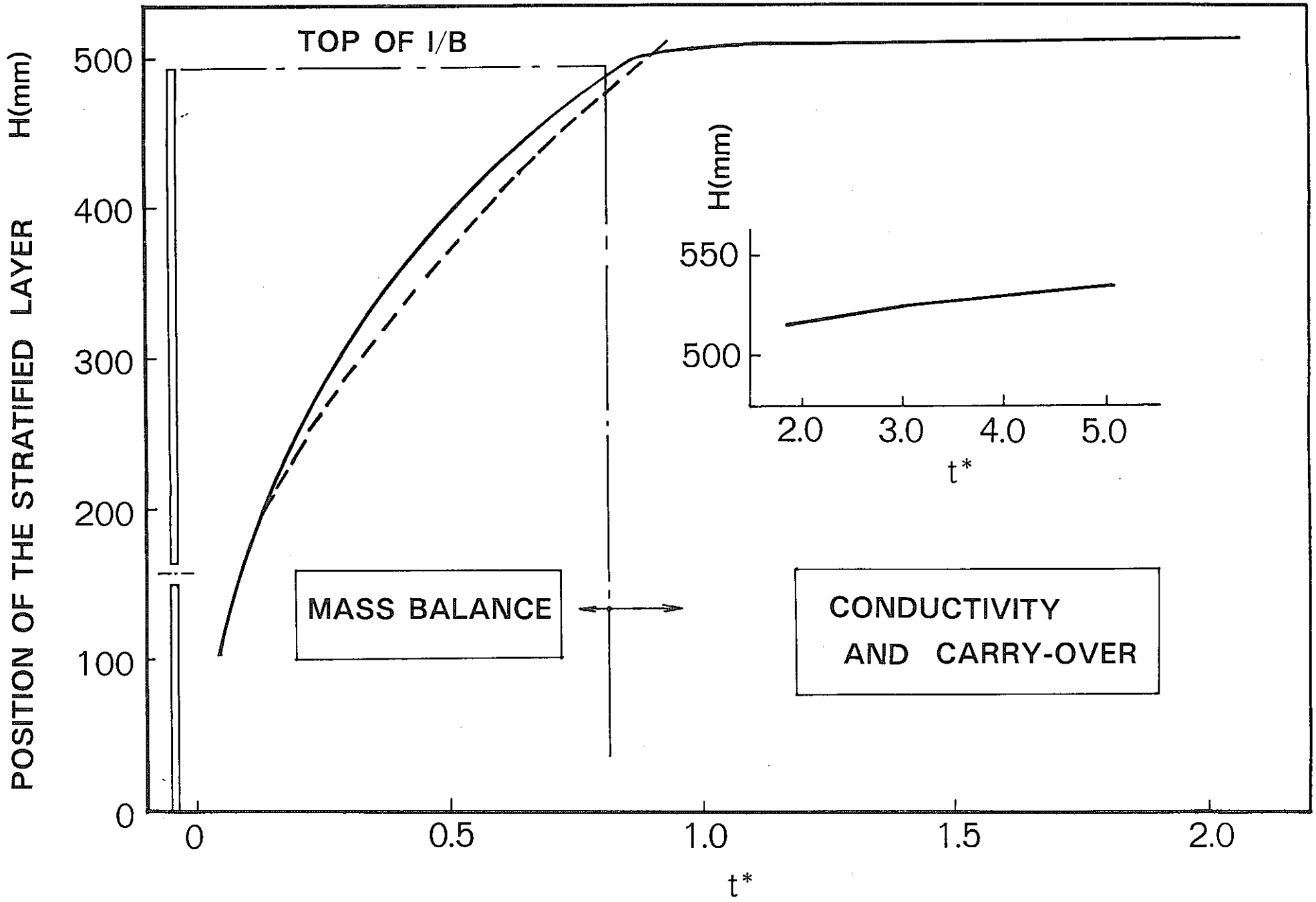

Fig B6-10 Rising Rate Of The Stratified Layer

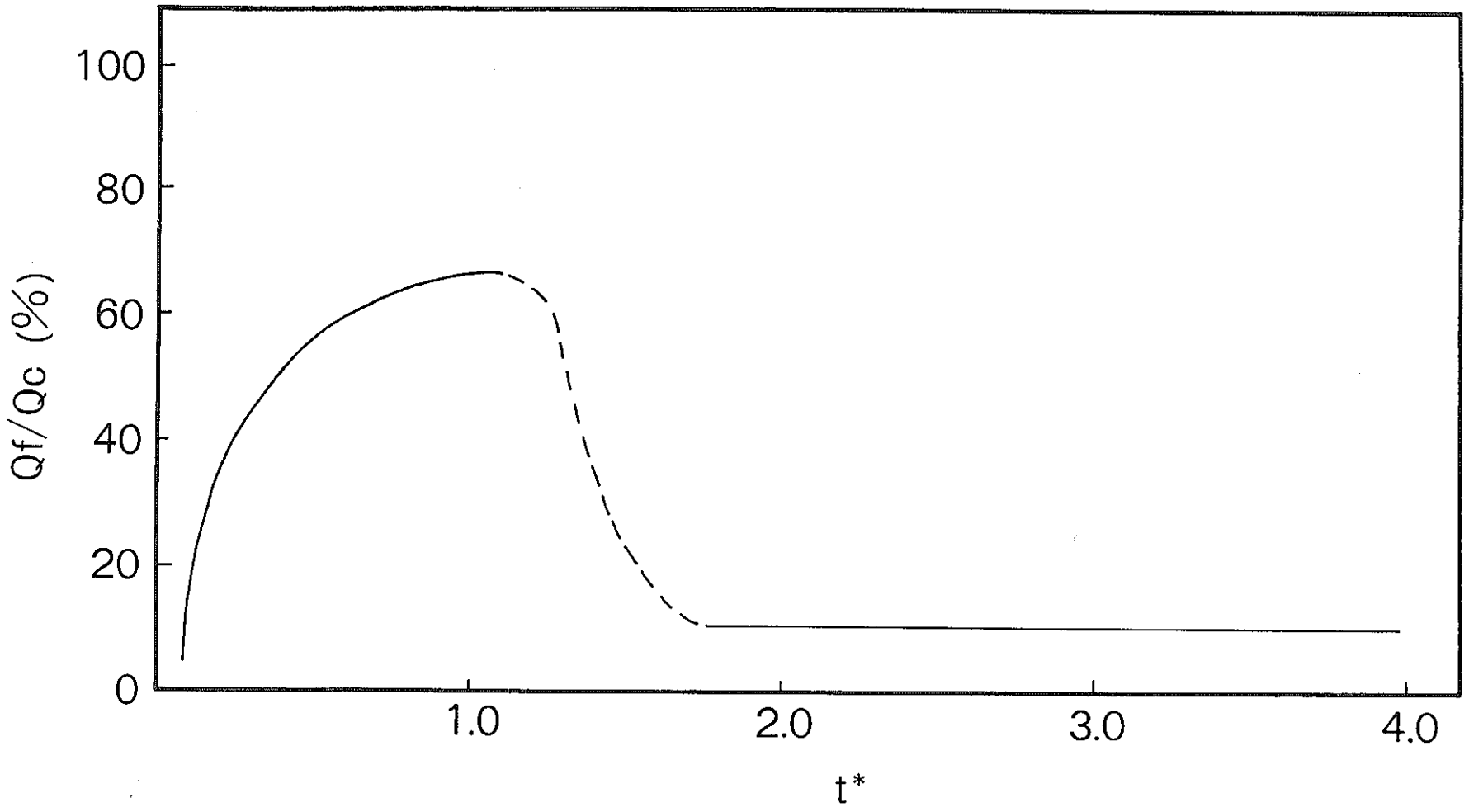

Fig B6-11 Flow Rate Transition
Through The Flow Holes Of I/B

1/10 Scale Model (Water)	1/10 Scale Model (Sodium)
(I) $t^*=0\sim1.0$ ● Stratified Zone Rising in I/B ● in I/B : $d\theta/dh \fallingdotseq 0.15°C/mm$, $dh/dt \fallingdotseq 2mm/sec$ ● in Exit Nozzle : $\triangle\theta\,max \fallingdotseq 0.8$, Duration : $t^*=0\sim1.0$ ● above I/B : $\theta \fallingdotseq 1.0$	(I) $t^*=0\sim1.0$ ● Axial Temperature Prifile Rising ● in I/B : $d\theta/dh \fallingdotseq 0.07°C/mm$, $dh/dt \fallingdotseq 1\sim1.5mm/sec$ ● in Exit : $\triangle\theta max \fallingdotseq 0.1\sim0.2$, Duration : $t^*=0\sim1.5$ ● above I/B : $\theta \fallingdotseq 0.9\sim1.0$

Table B6-3(1/2) Comarison of Experimental Results

1/10 Scale Model (Water)	1/10 Scale Model (Sodium)
(II) $t^*=1.0\sim$	(II) $t^*=1.0\sim$
● Density Interface Rising above I/B	● Axial Temperature Profile Rising
● in I/B, in Exit Nozzle : $\theta \fallingdotseq 0\sim0.1$ (nearly uniform)	● in I/B above I/B : $d\theta/dh \fallingdotseq 0.05\sim0.07$°C/mm, $dh/dt \fallingdotseq 0.5\sim1.0$mm/sec
● above I/B : $d\theta/dt \fallingdotseq 1\sim2$°C/mm ($\triangle h \fallingdotseq 10\sim20$mm), $dh/dt \fallingdotseq 1\sim2$mm/min	● in Exit Nozzle : $\triangle\theta \fallingdotseq 0$ (nearly uniform)
● Density Interface did not disappear at $t^*=28$	● Thermal Stratification disappeared at $t^*=5.0$

Table B6-3(2/2) Comparison of Experimental Results

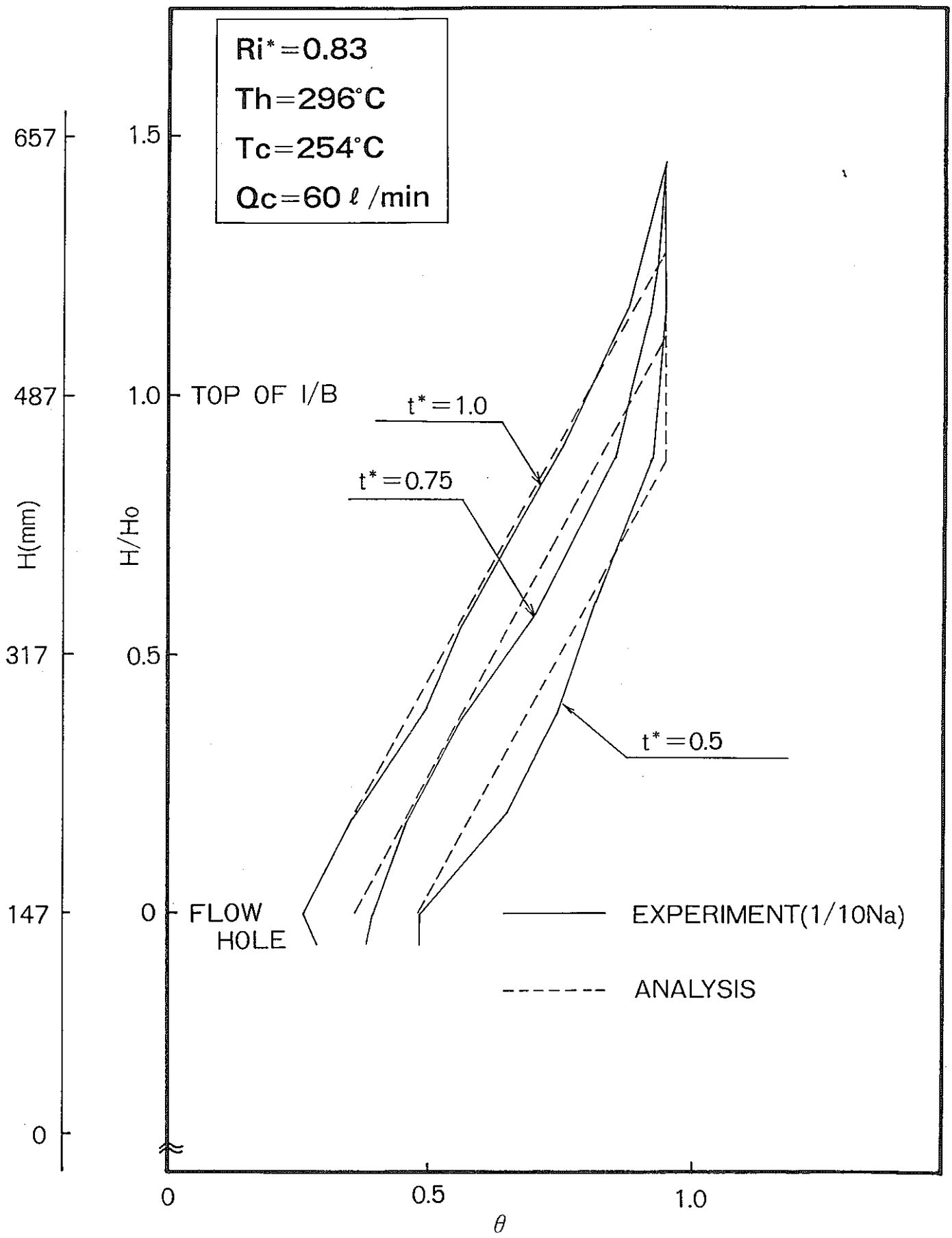

Fig 6-12

Estimation Of Stratified Zone Rising Rate In I/B(1/10Na)

1/10 Scale Model (Water)	1/10 Scale Model (Sodium)
(I) Stratifisd 「Layer」 Rising in I/B	(I) Stratified Zone Rising in I/B
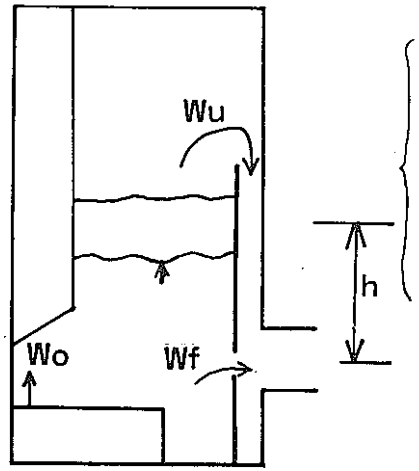 Ap : area in I/B Af : area of Flow Holes n : number of Flow Holes S : pressure 「Loss」 factor	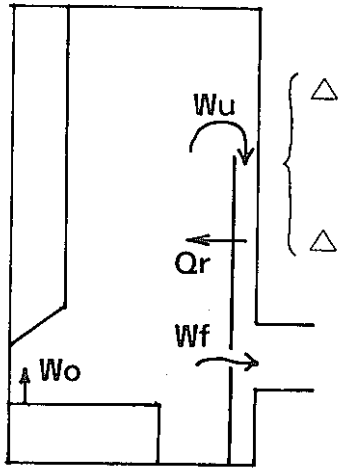 △θp : axial temperature difference in I/B △θu : difference in annulas part
Mechanism	Mechanism
mainly [Mass Balance]	[Mass Balance]+[Axial Heat Conduction] −[Heat Exchange through I/B]
Rising Rate	Rising Rate
$\frac{dh}{dt}=\frac{Wo}{Ap}-\frac{n\cdot Af}{Ap}\sqrt{\frac{\triangle\gamma\cdot 2g\cdot h}{\gamma c\cdot S}}$	$(dh/dt)i=\frac{(Wu)i}{Ap}\left(1-\frac{(\triangle\theta u)i}{(\triangle\theta p)i}\right)$

Table B6-4(1/2) Comparison of Thermal Stratification Mechanism

1/10 Scale Model (Water)	1/10 Scale Model (Sodium)
(II) Density Interface Rising above I/B 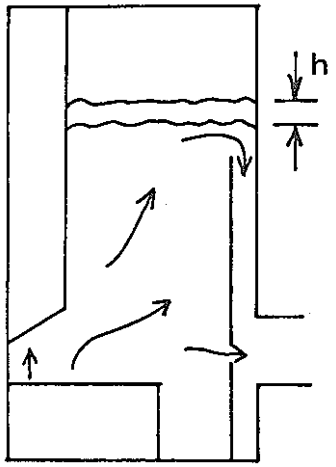 **Mechanism** [Axial heat Conduction] +[Carry-Over by Flow] **Rising Rate** h or dh/dt Function [a/v, Pe……]	(II) Axial Temperature Profile Change above I B 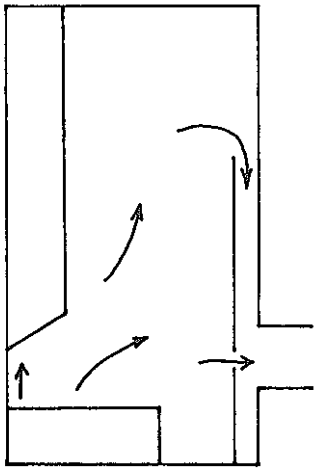 **Mechanism** mainly [Axial Heat Conduction]

Table B6-4(2/2) Comparison of Thermal Stratification Mechanism

B-7 ANALYTICAL EVALUATION OF THERMAL STRATIFICATION

ABSTRACT

A two-dimensional thermal hydraulic analysis code, SKORT-II, has been developed for MONJU design purposes. A similar code, NAGARE, developed independently from SKORT-II by PNC, has been used as an evaluation tool for experimental works and also for cross-check purpose of SKORT-II. These analytical codes must be verified by various thermal transient test data before successfully being applied to predict thermal stratification behavior in MONJU reactor vessel upper plenum.

This paper reports the results of evaluation and comparison by SKORT-II and NAGARE on the sodium thermal stratification test with a 1/6 model of MONJU outlet plenum.

ANALYTICAL EVALUATION OF THERMAL STRATIFICATION

1. CODE VERIFICATION

1.1 Code — Thermal Hydraulic Analysis Code

- "Monju" Design Code; SKORT-II
- Cross-check Code; NAGARE

1.2 Objective

To verify the code using the thermal transient simulation test data of the scale-down model for the reactor upper plenum-specifically,

1) to confirm the analytical technique used in the code

2) to select the proper values for turbulant parameters (ε_M, ε_H) to simulate correctly the stratification phenomenon.

1.3 Method

- Experimental verification using mainly 1/6–scale sodium model test

- Scale effect (values of ε_M, ε_H, mesh size)

  → Confirm by water test series

- Coolant property effect (water and sodium)

  → Water and sodium tests with the models of same scale

- Coherency check of analytical results against experimental data by comparing the temperature response at various points in the plenum.

1.4 CONDITIONS FOR ANALYSIS (1/6–SCALE SODIUM MODEL TEST)

	NAGARE			SKORT-II		
TEST NO.	14	21	19	14	21	19
FLOW (ℓ/sec)	2.7	48	47 – 2.5	2.7	48	47 – 2.5
$\varepsilon_M = \varepsilon_H$	100	2000	2000 – 100	0		
α_2 ($\frac{Kcal}{m^2 h \cdot c}$)	2000	900	900 – 2000	2000		
Plenum Inlet Condition	Average Value			Experimental Data		
Flow Hole Area	Actual Area			Actual Area		
Exit Nozzle Area	Actual Area			Actual Area		
ThermalCapacity of Structure	Not Considered			Not Considered		

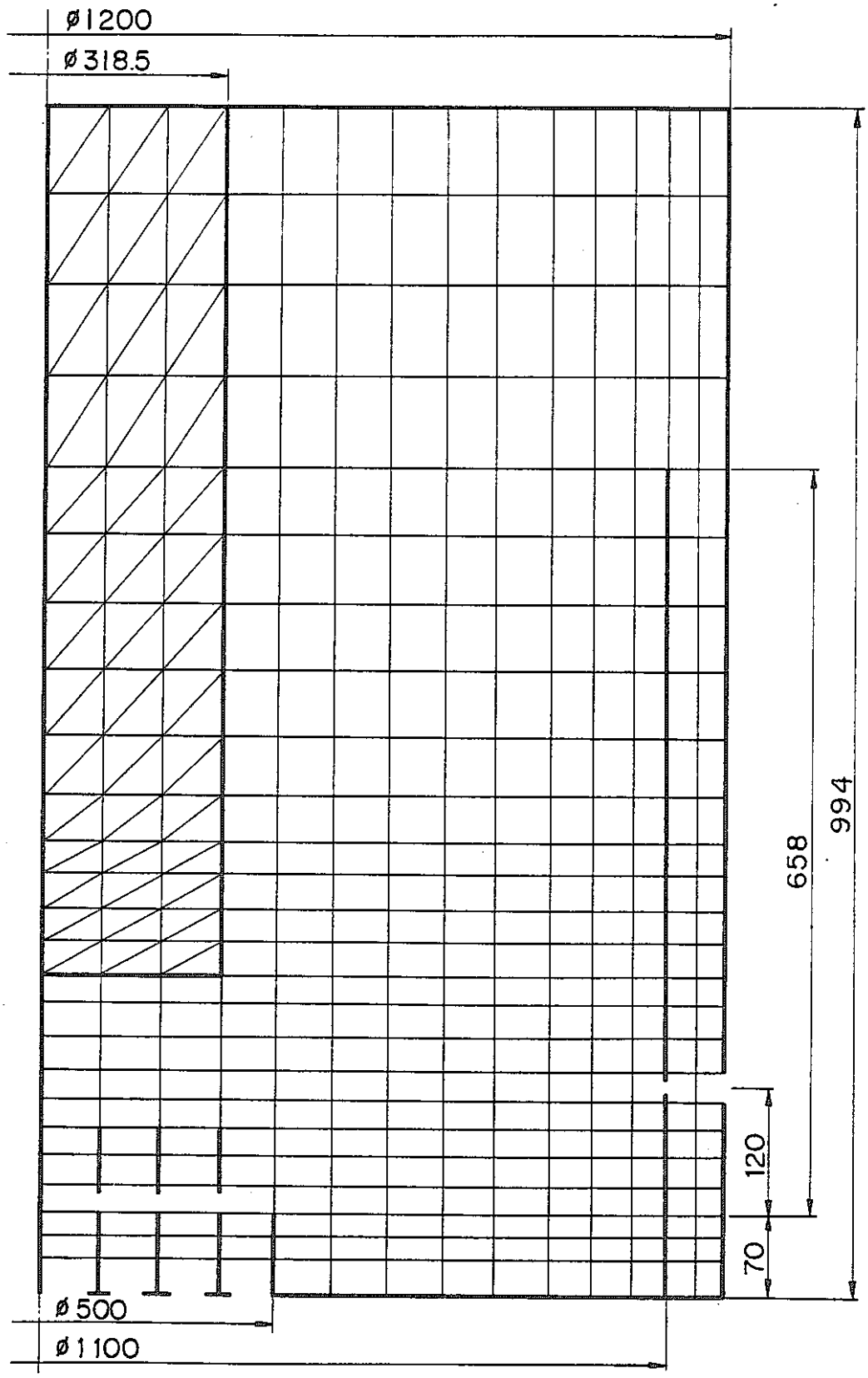

Fig. B7-1a ANALYTICAL MESH ARRANGEMENT

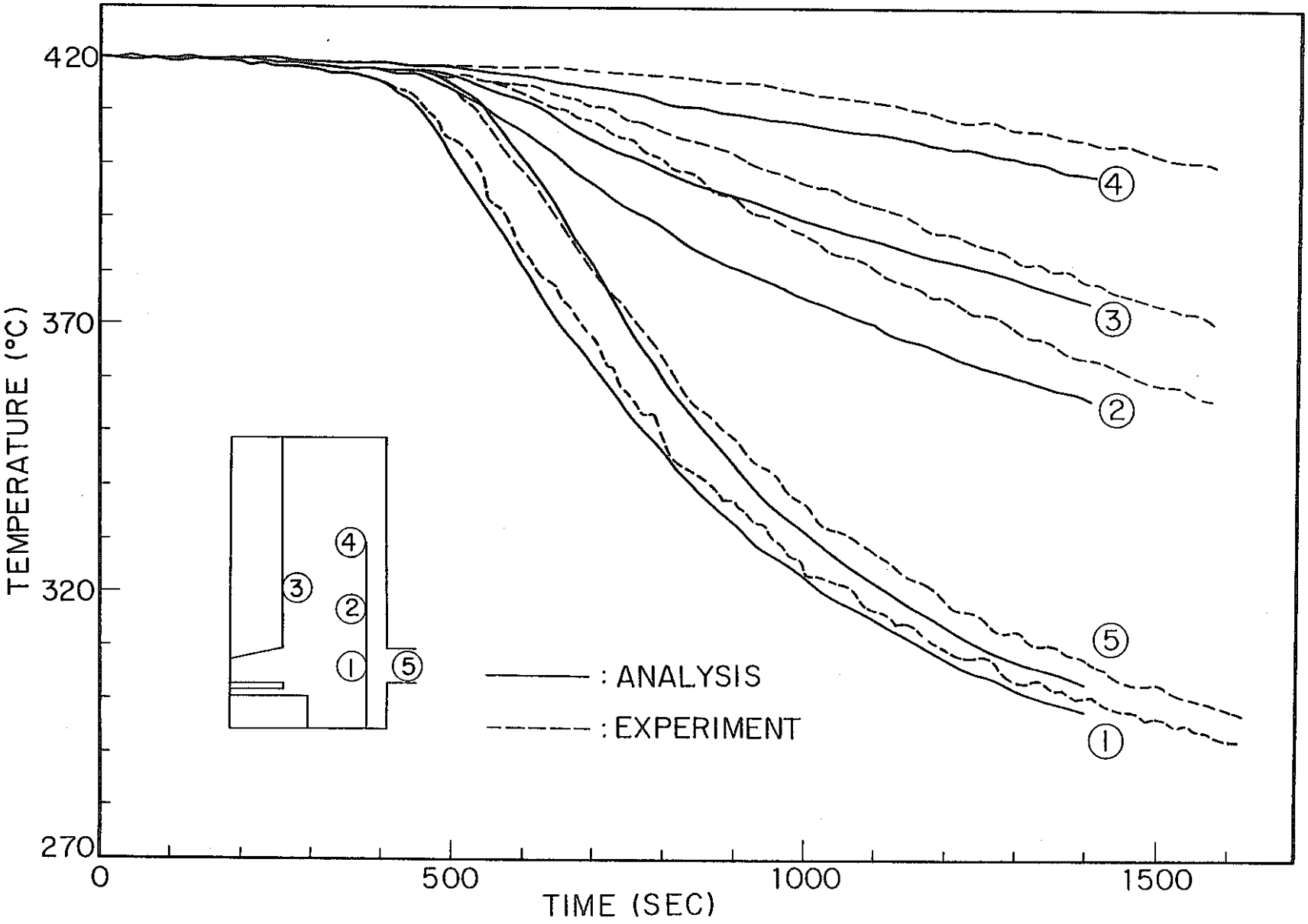

Fig-B7-2a TIME VARIATION OF TEMPERATURE (TEST No.14)

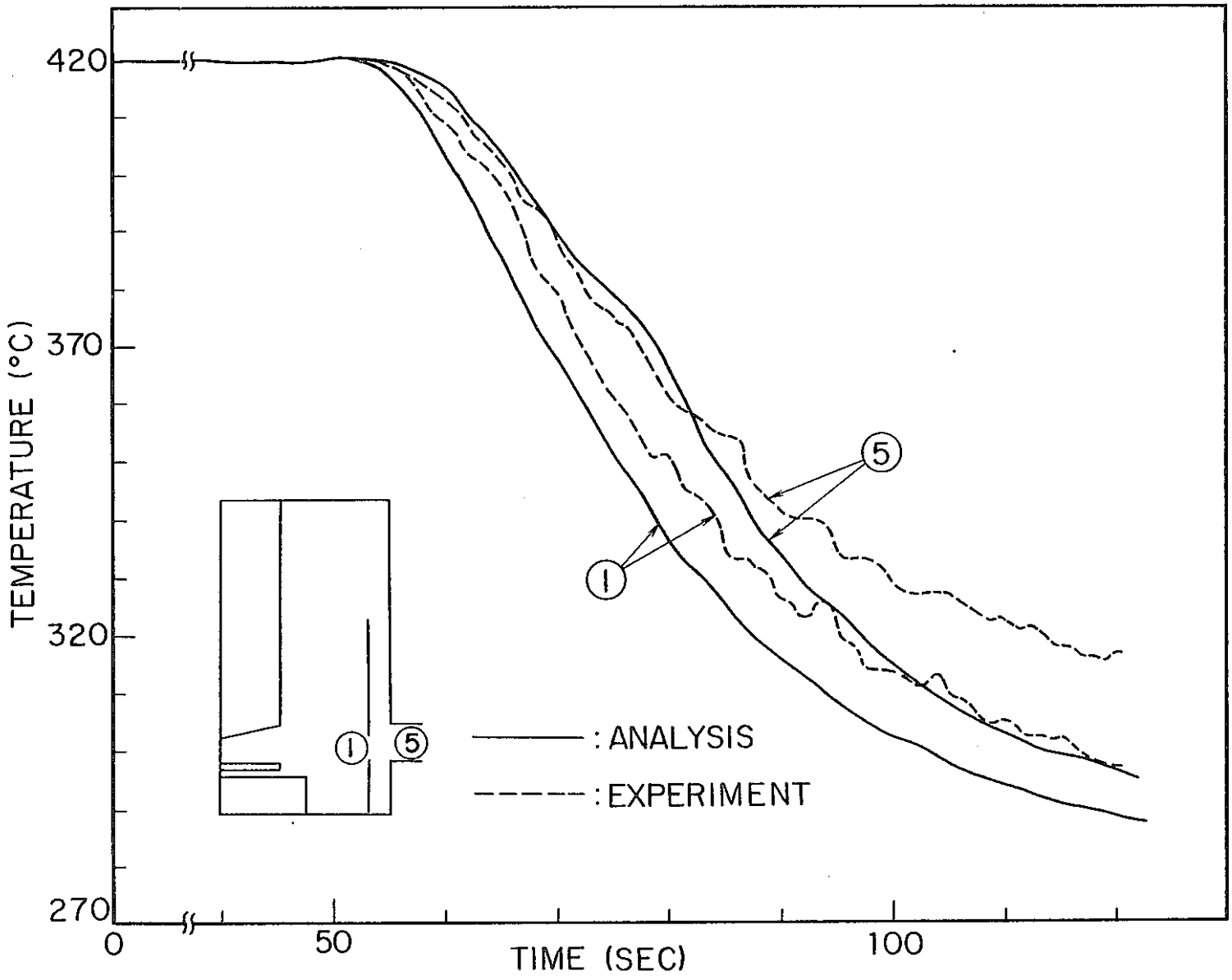

Fig-B7-3a TIME VARIATION OF TEMPERATURE (TEST No.21)

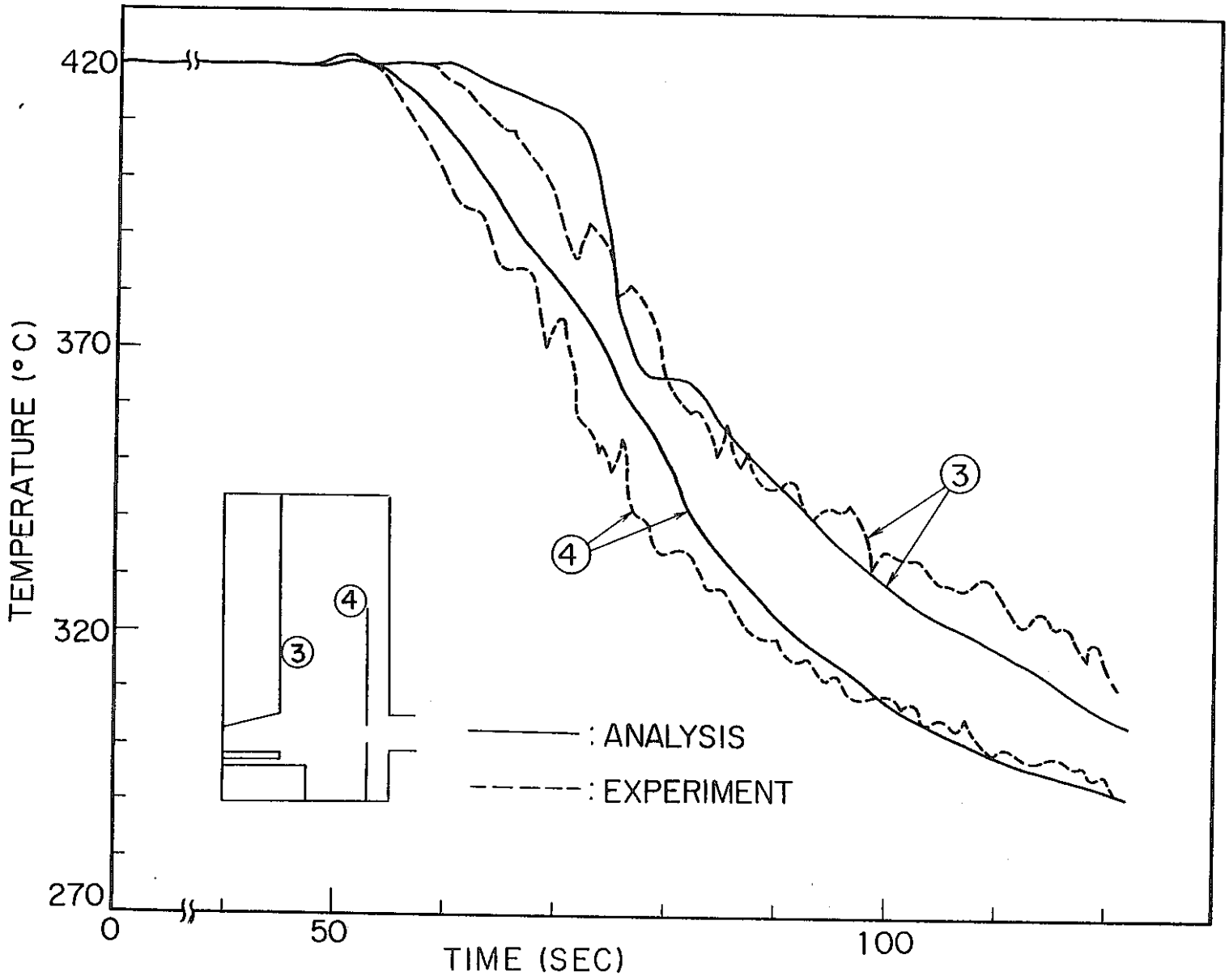

Fig-B7-4a TIME VARIATION OF TEMPERATURE (TEST No.21)

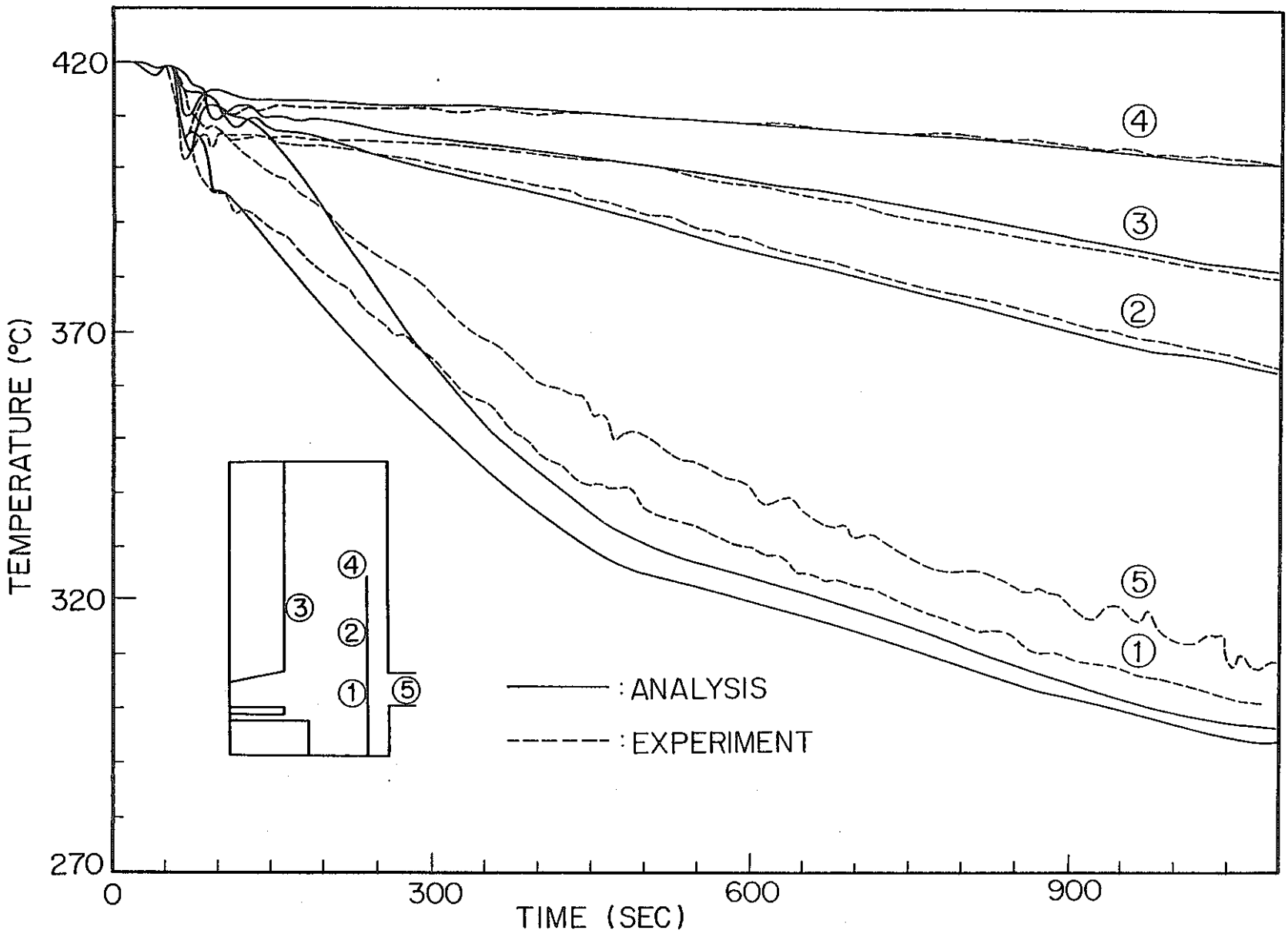

Fig.-B7-5a TIME VARIATION OF TEMPERATURE (TEST No.19)

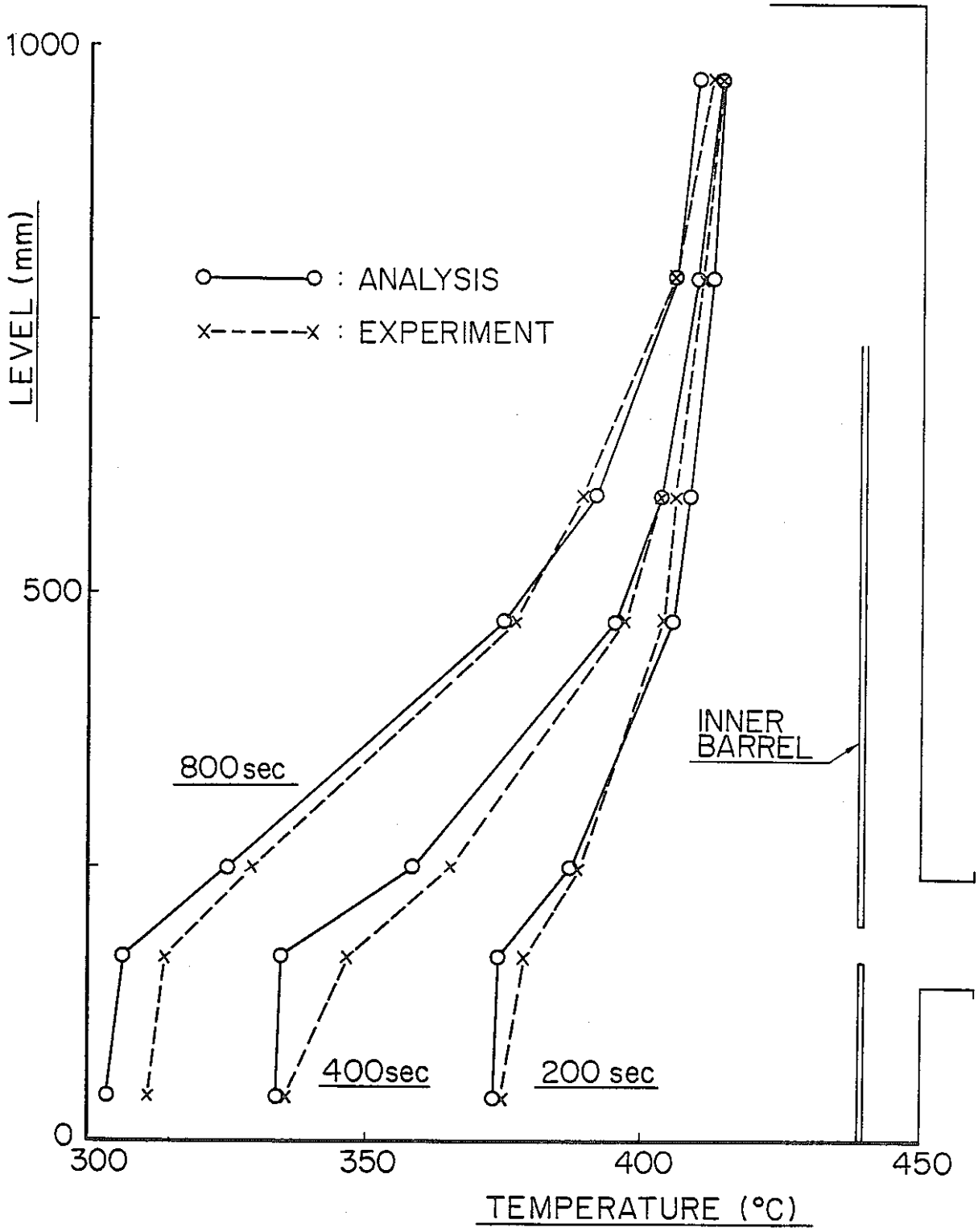

Fig-B7-6a AXIAL TEMPERATURE DISTRIBUTION
(TEST No.19)

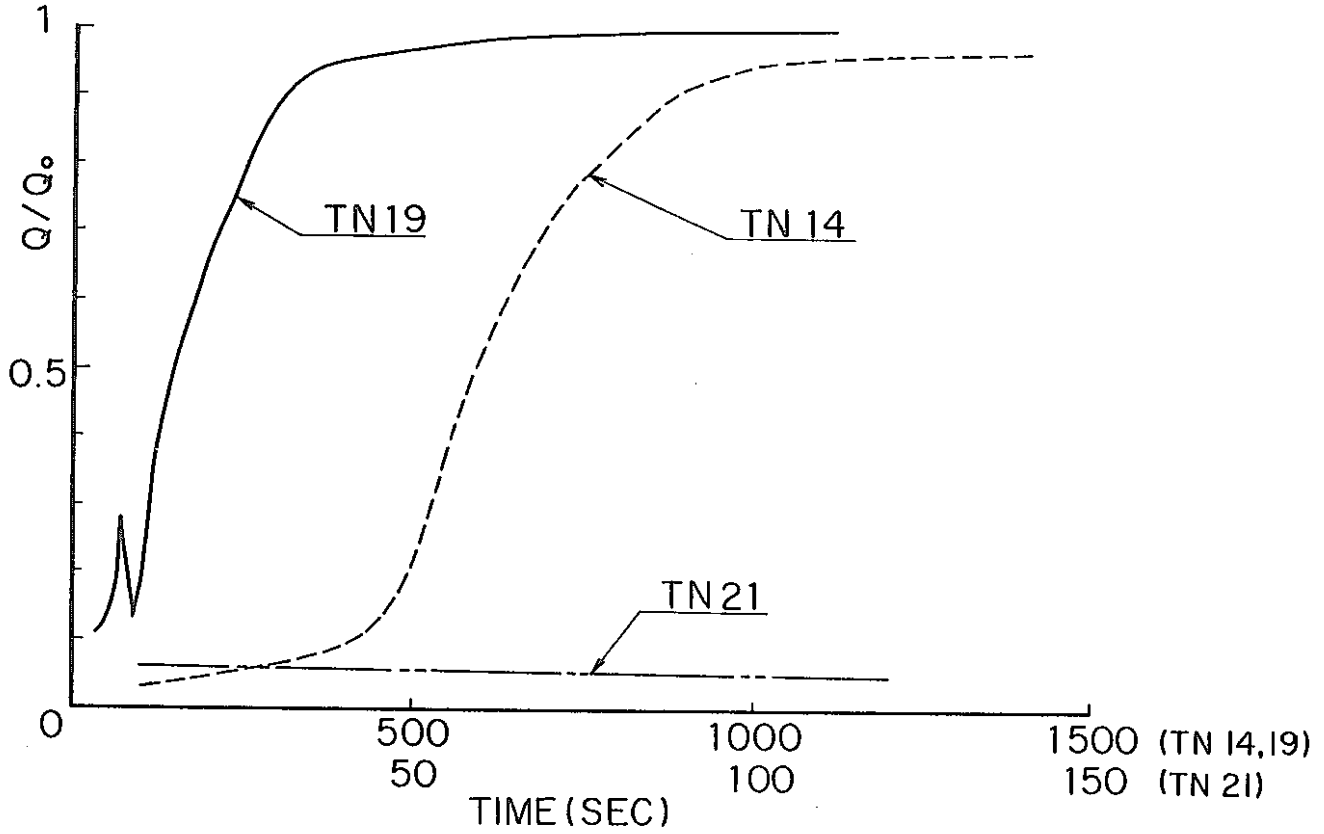

Fig-B7-7a PER-CENT FLOW THROUGH THE INNER BARREL FLOW HOLES

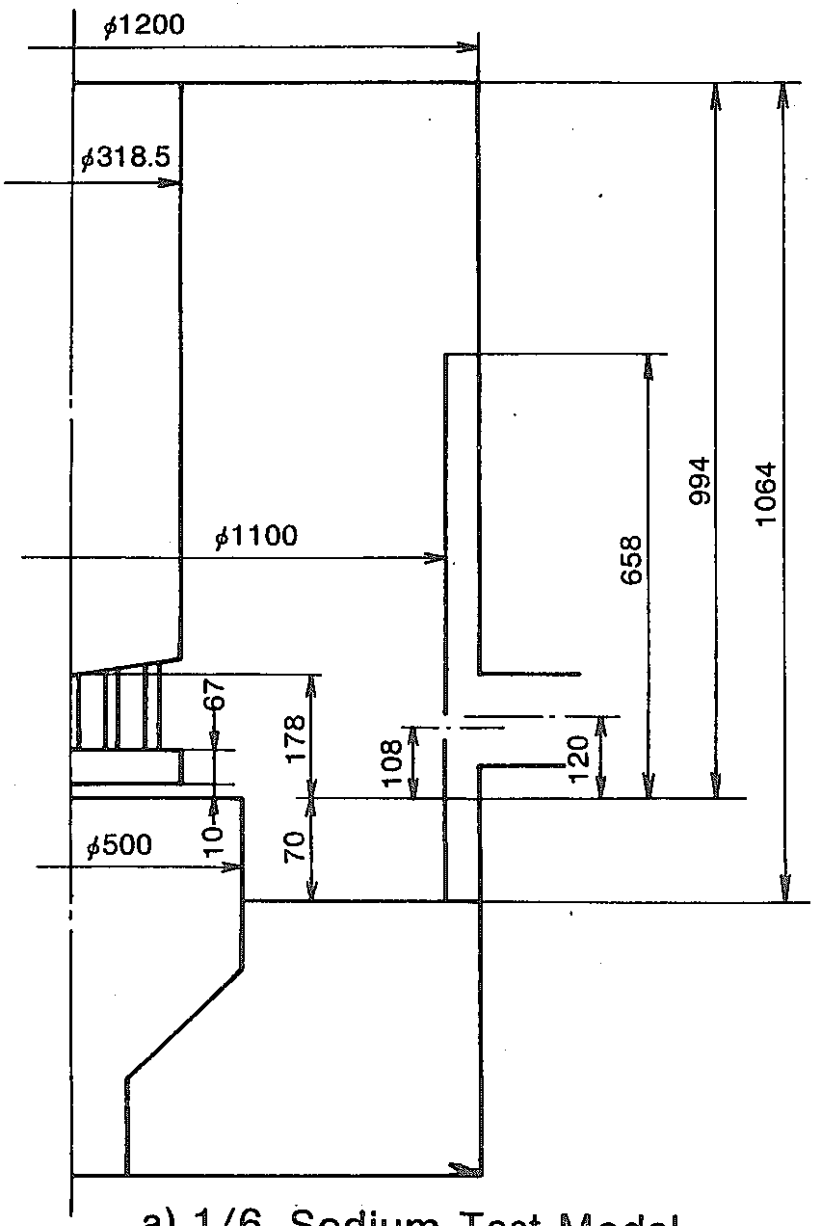

a) 1/6, Sodium Test Model

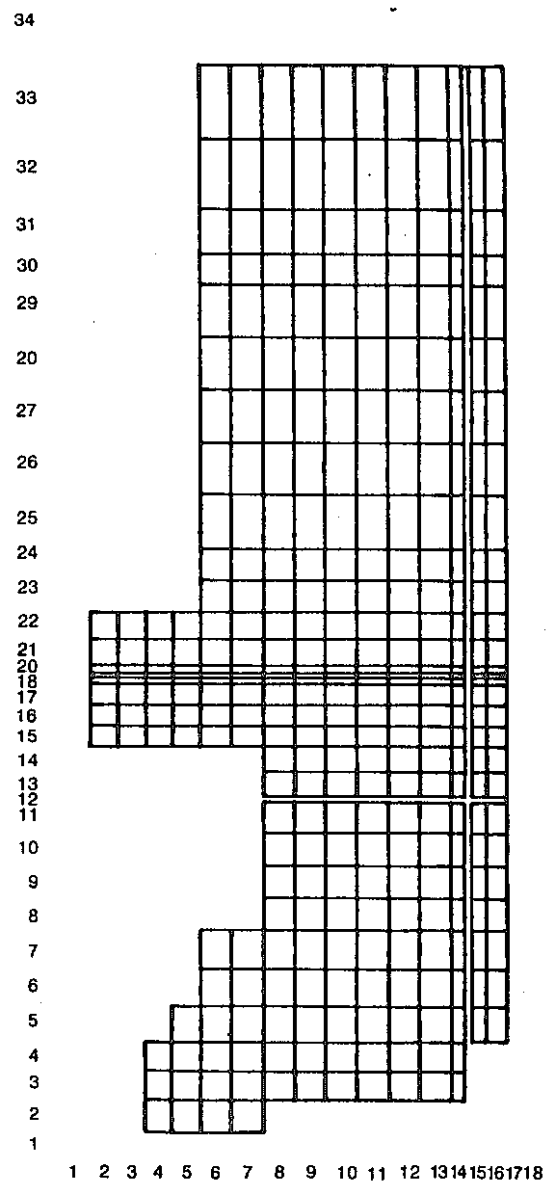

(b) Mesh Arrangement

Fig. B7-1b 1/6, Sodium Test Model and Mesh Arrangement for Analysis.

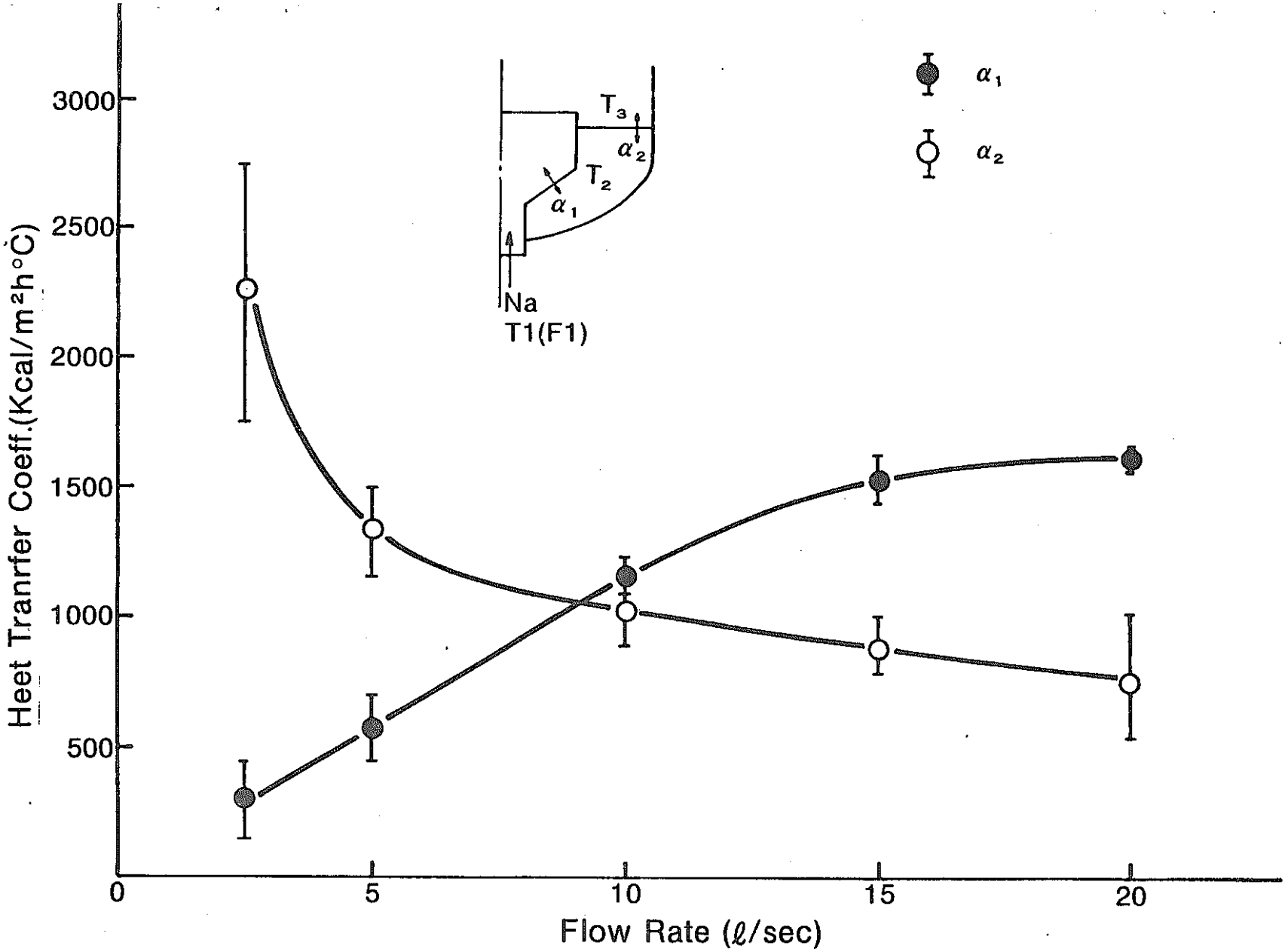

Fig. B7-2b Heat Transfer Coefficients (α_1, α_2) Calculation

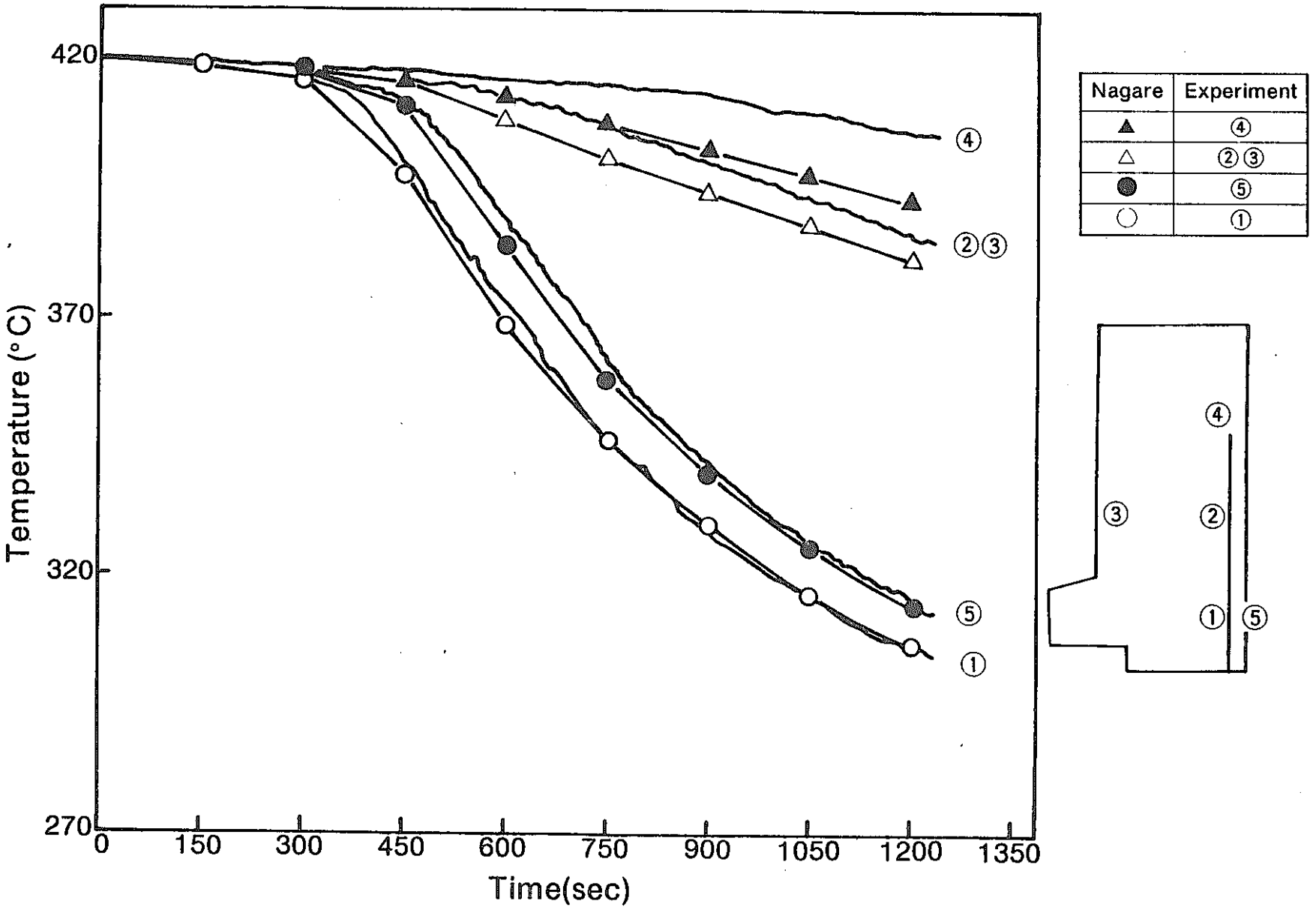

Fig. B7-3b Comparison of Temperature Change-in-Time (Test No.14)

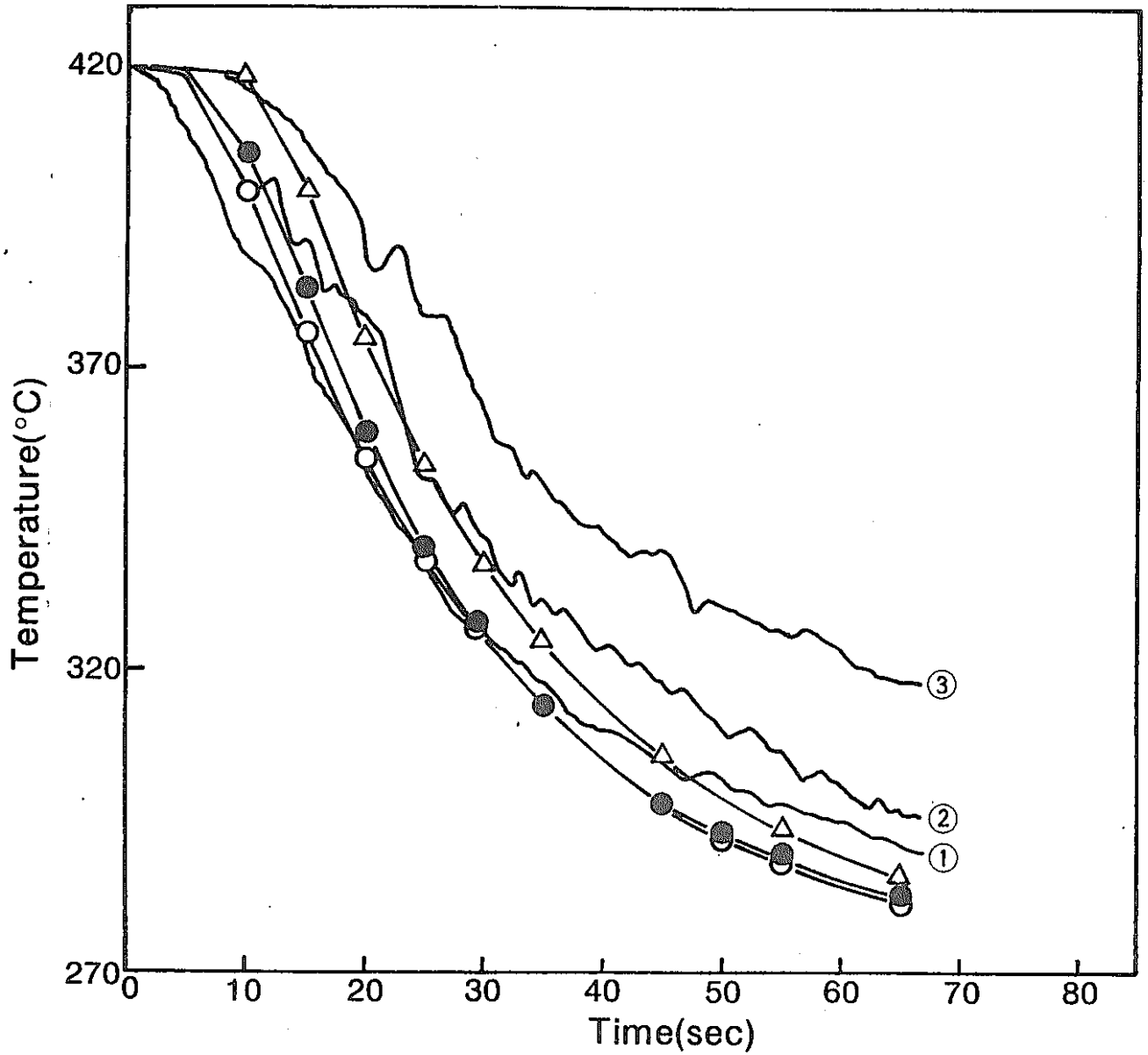

Nagare	Experiment
△	③
●	②
○	①

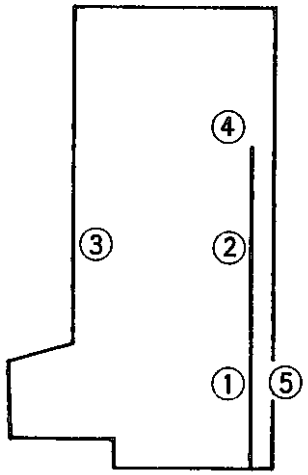

Fig. B7-4b Comparison of Temperature Change-in-Time (Test No.21)

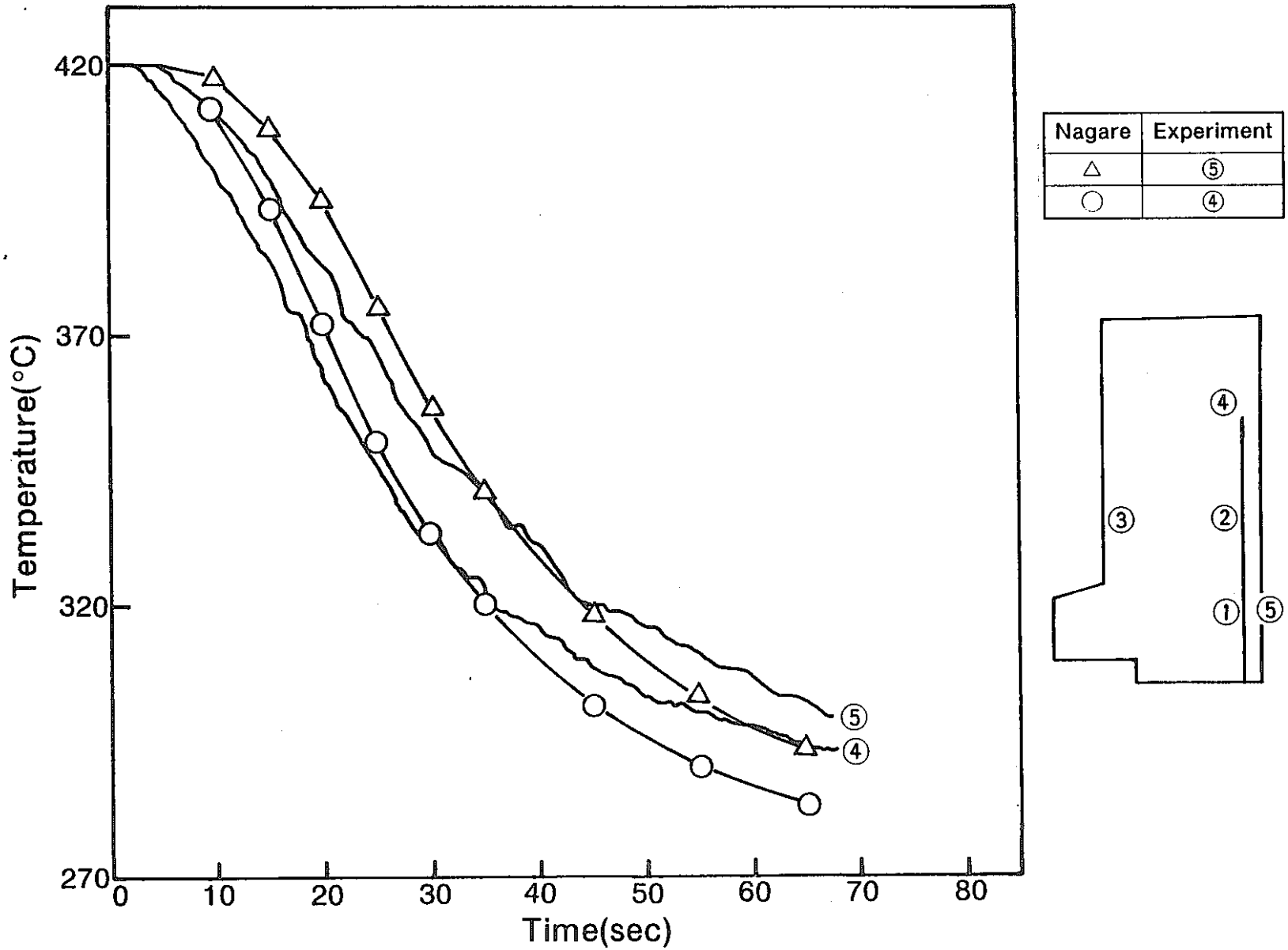

Fig. B7-5b Comparison of Temperature Change-in-Time (Test No.21)

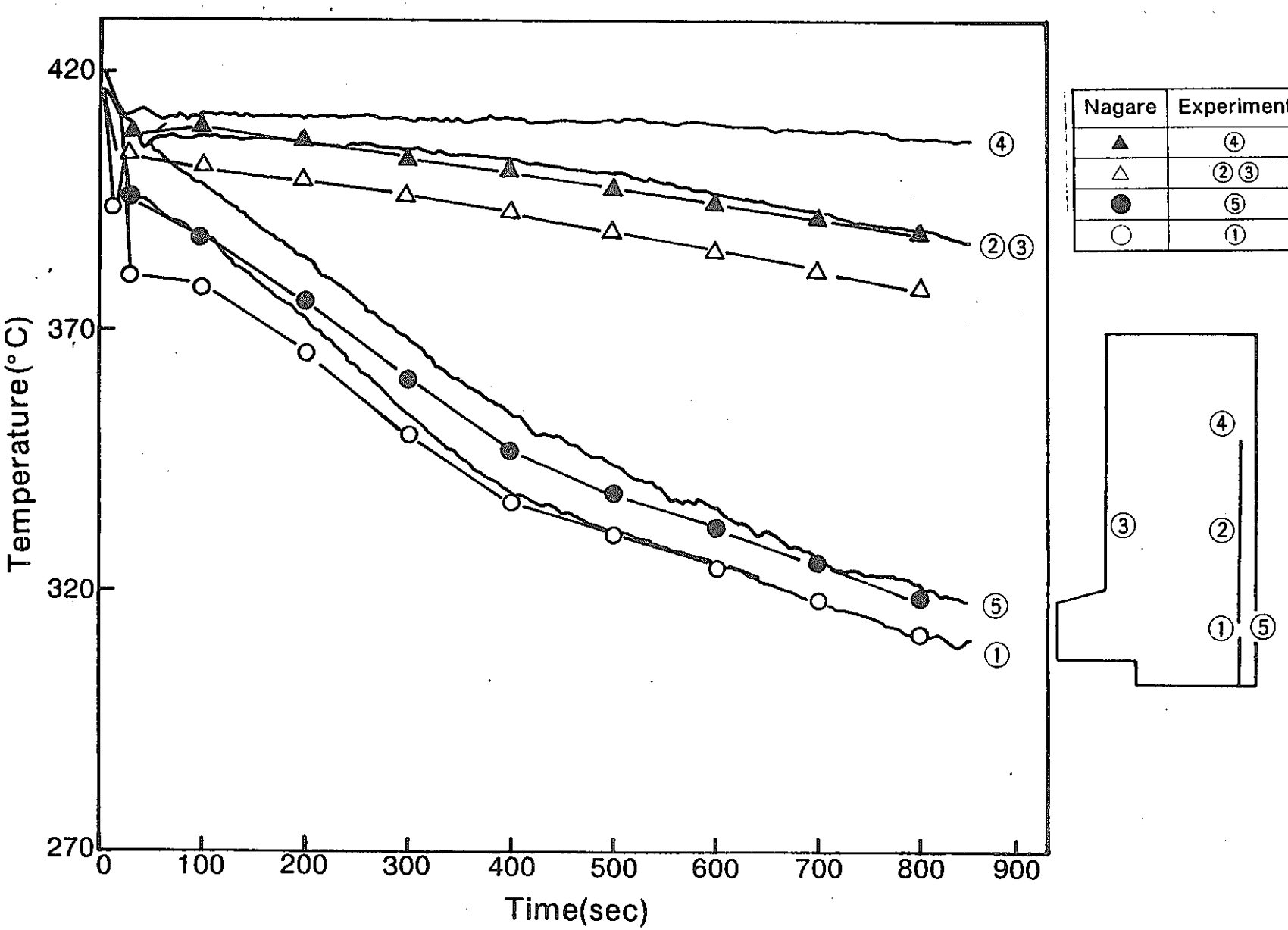

Fig. B7-6b Comparison of Temperature Change-in-Time (Test No.19)

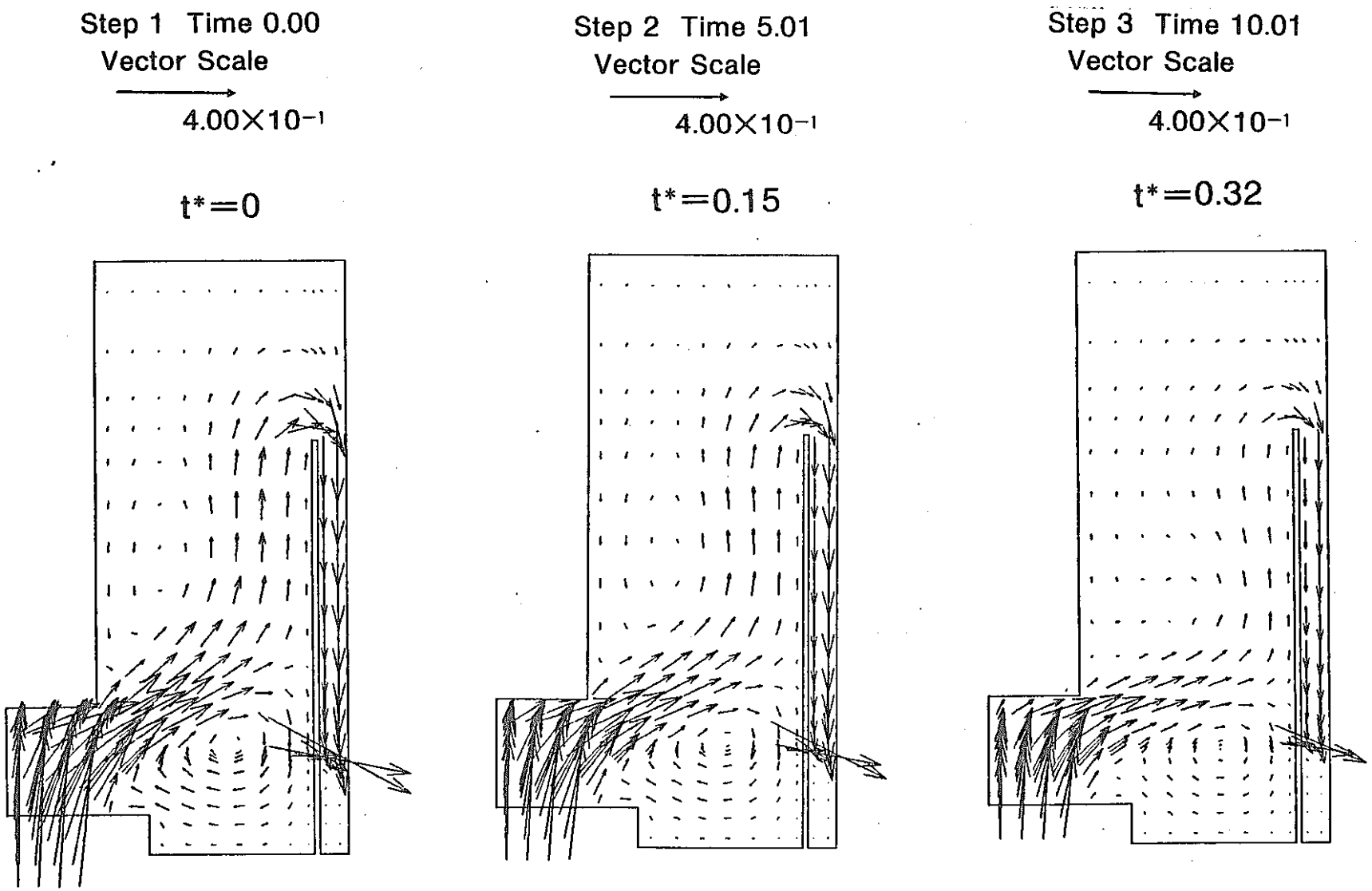

Fig. B7-7b Iso-thermal Lines in the Upper Plenum(Test No.19)

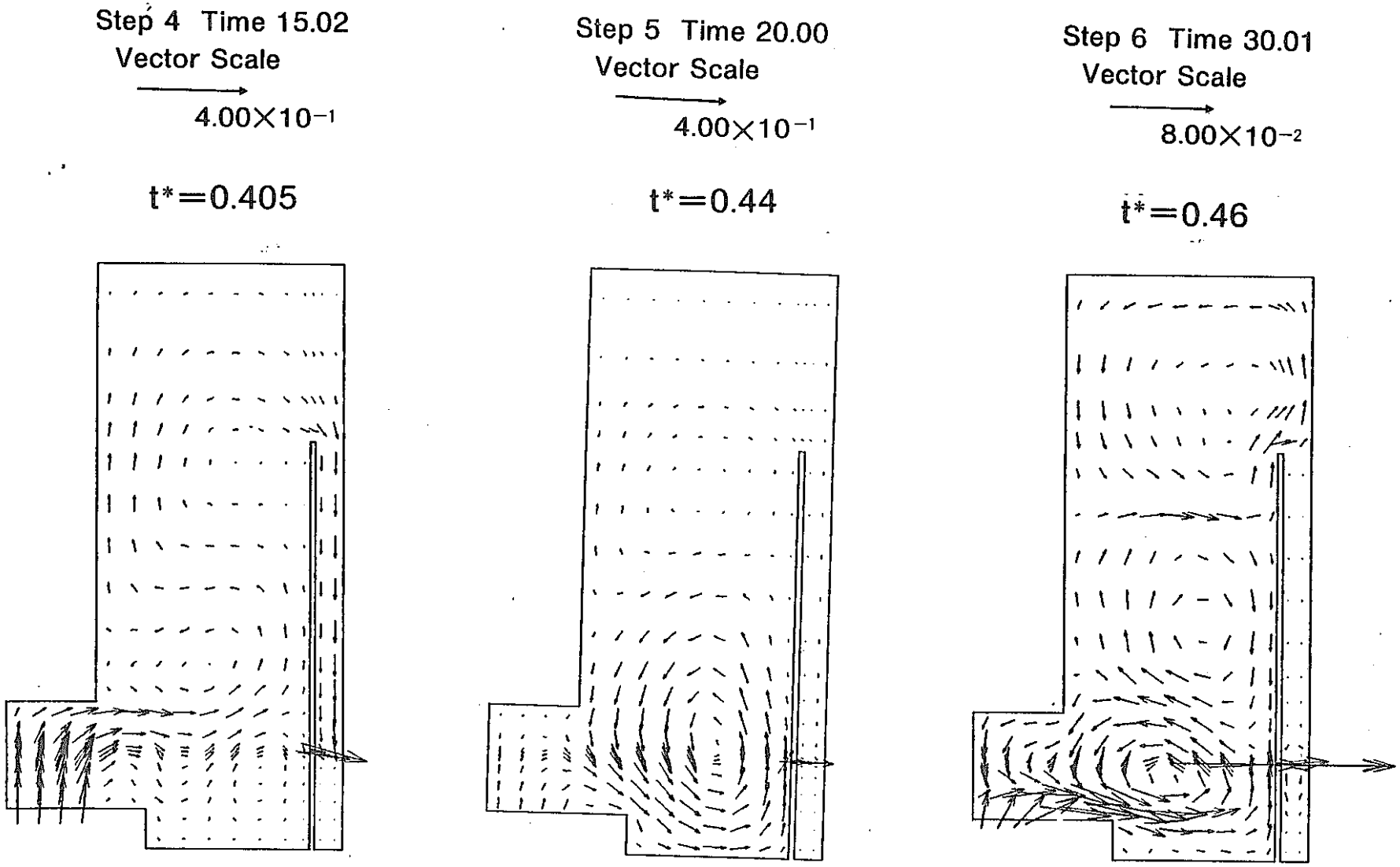

Fig. B7-8b Iso-thermal Lines in the Upper Plenum(Test No.19)

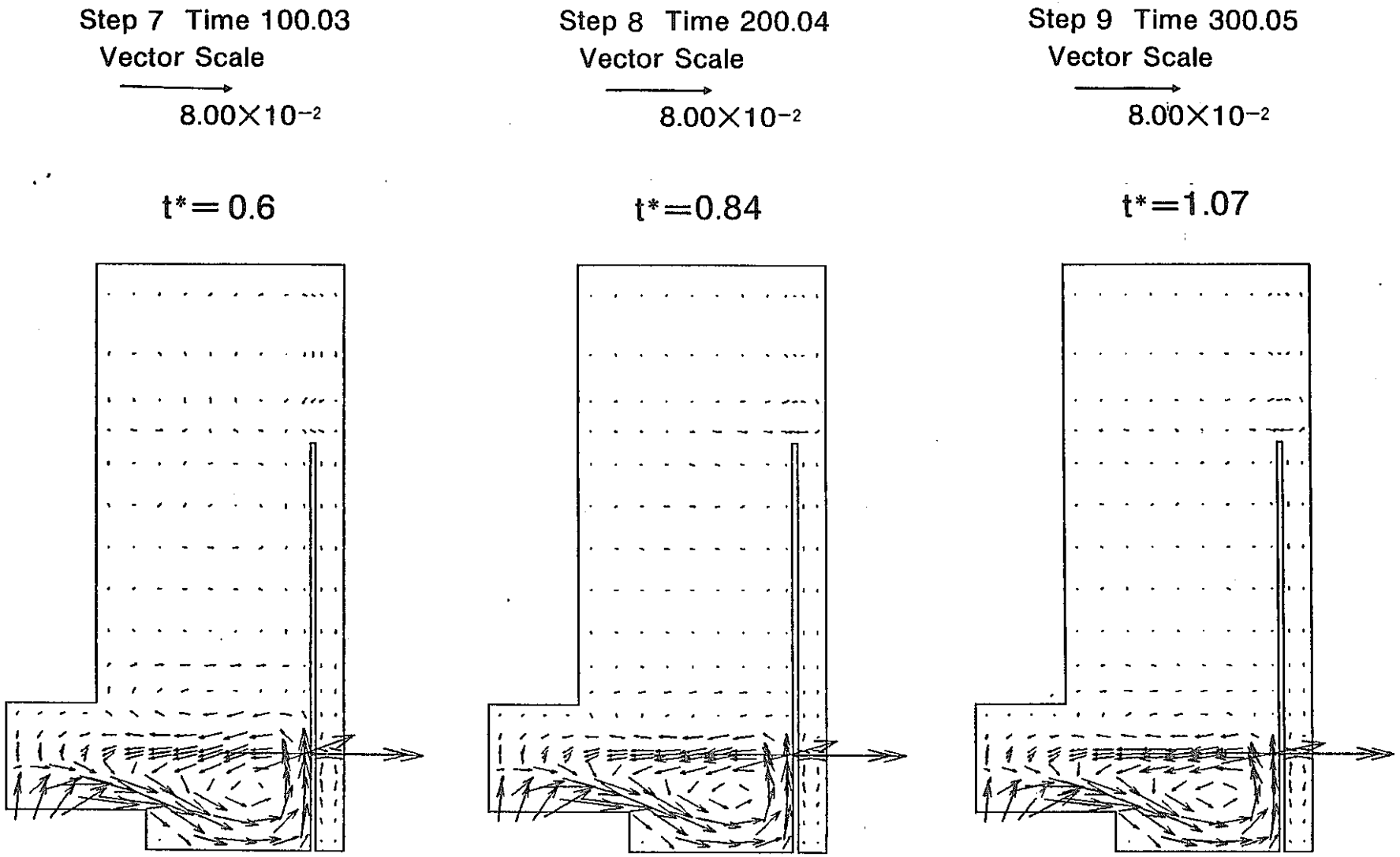

Fig. B7-9b Iso-thermal Lines in the Upper Plenum(Test No.19)

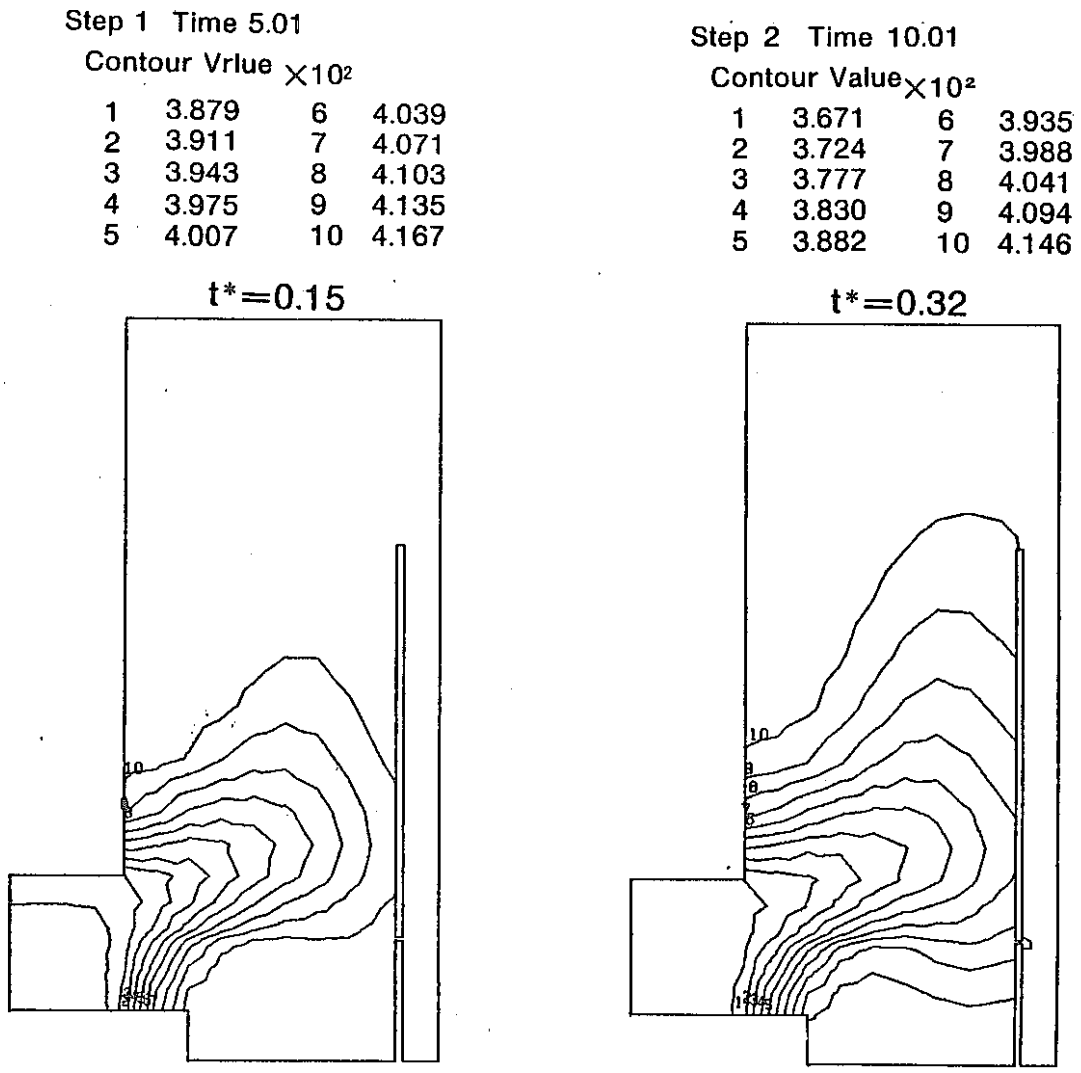

Fig. B7-10b Iso-thermal Lines in the Upper Plenum (Test No.19)

Step 3 Time 15.02

Contour Value $\times 10^2$

1	3.605	6	3.902
2	3.665	7	3.962
3	3.724	8	4.021
4	3.783	9	4.080
5	3.843	10	4.140

Step 4 Time 20.00

Contour Value $\times 10^2$

1	3.584	6	3.892
2	3.646	7	3.953
3	3.707	8	4.015
4	3.769	9	4.076
5	3.830	10	4.138

Step 5 Time 30.01

Contour Value $\times 10^2$

1	3.584	6	3.892
2	3.646	7	3.953
3	3.707	8	4.015
4	3.769	9	4.076
5	3.830	10	4.138

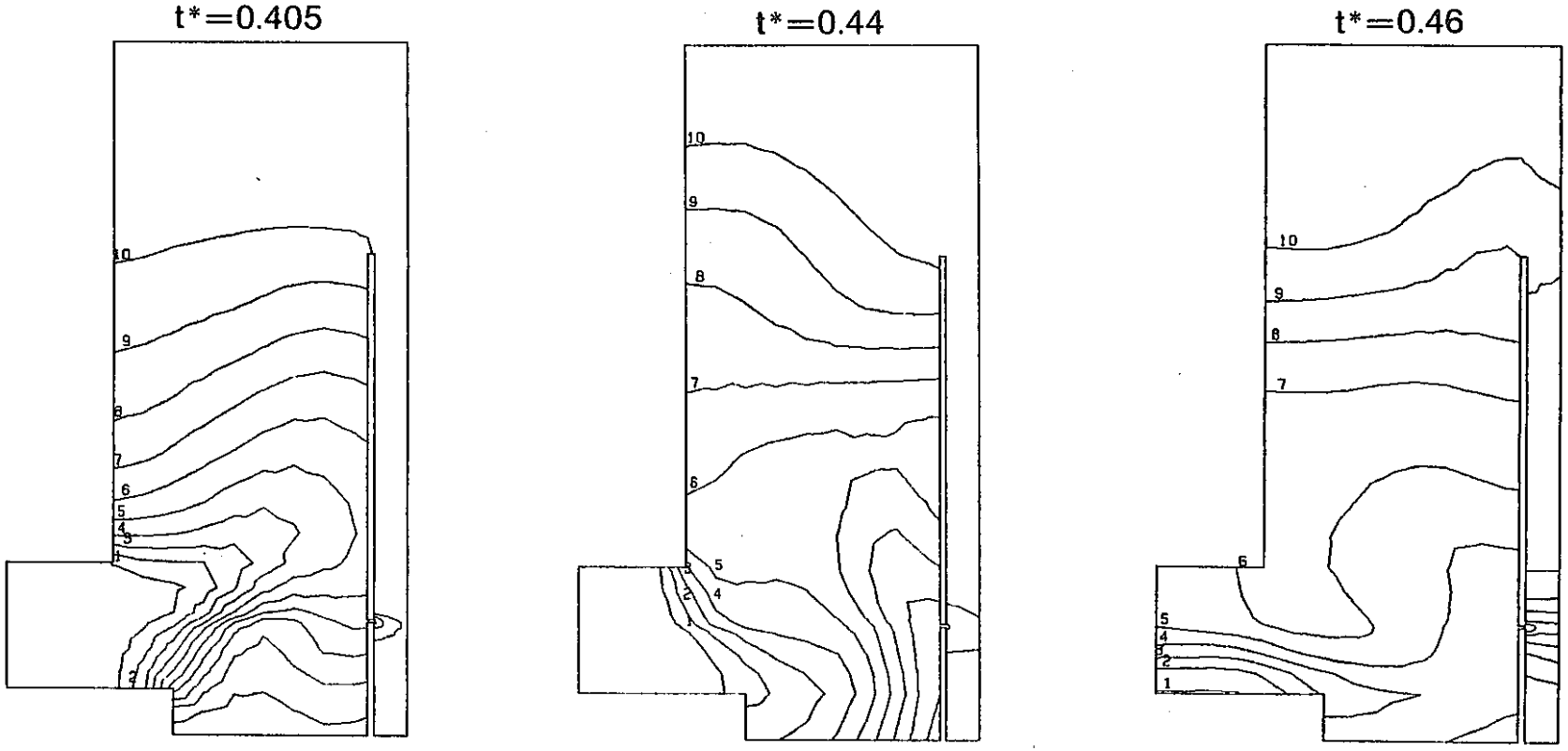

Fig. B7-11b Iso-thermal Lines in the Upper Plenum(Test No.19)

Step 6 Time 100.03

Contour Value $\times 10^2$

1	3.572	6	3.886
2	3.635	7	3.948
3	3.698	8	4.011
4	3.760	9	4.074
5	3.823	10	4.137

Step 7 Time 200.04

Contour Value $\times 10^2$

1	3.440	6	3.819
2	3.516	7	3.895
3	3.592	8	3.971
4	3.667	9	4.047
5	3.743	10	4.123

Step 8 Time 300.05

Contour Value $\times 10^2$

1	3.236	6	3.668
2	3.322	7	3.754
3	3.409	8	3.841
4	3.495	9	3.927
5	3.581	10	4.014

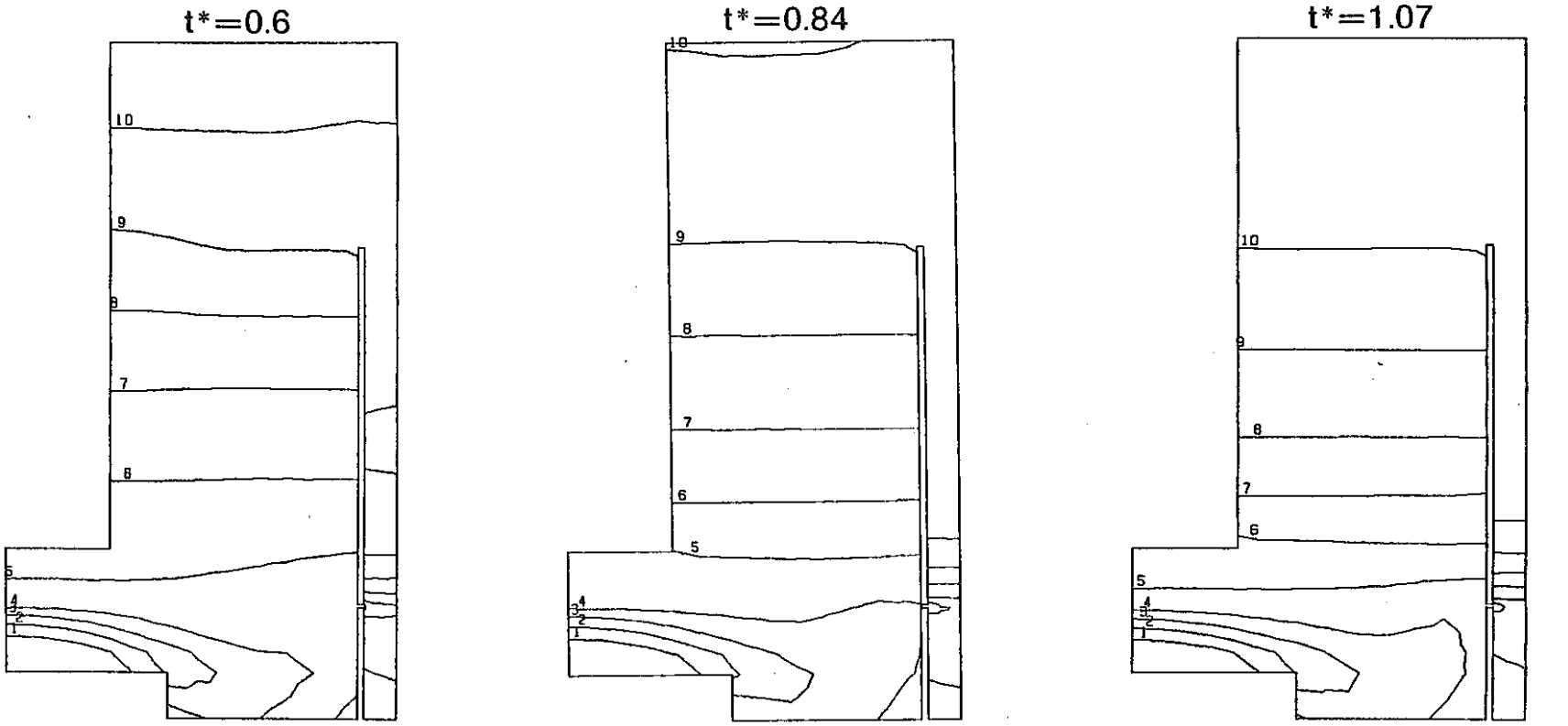

Fig. B7-12b Iso-thermal Lines in the Upper Plenum (Test No.19)

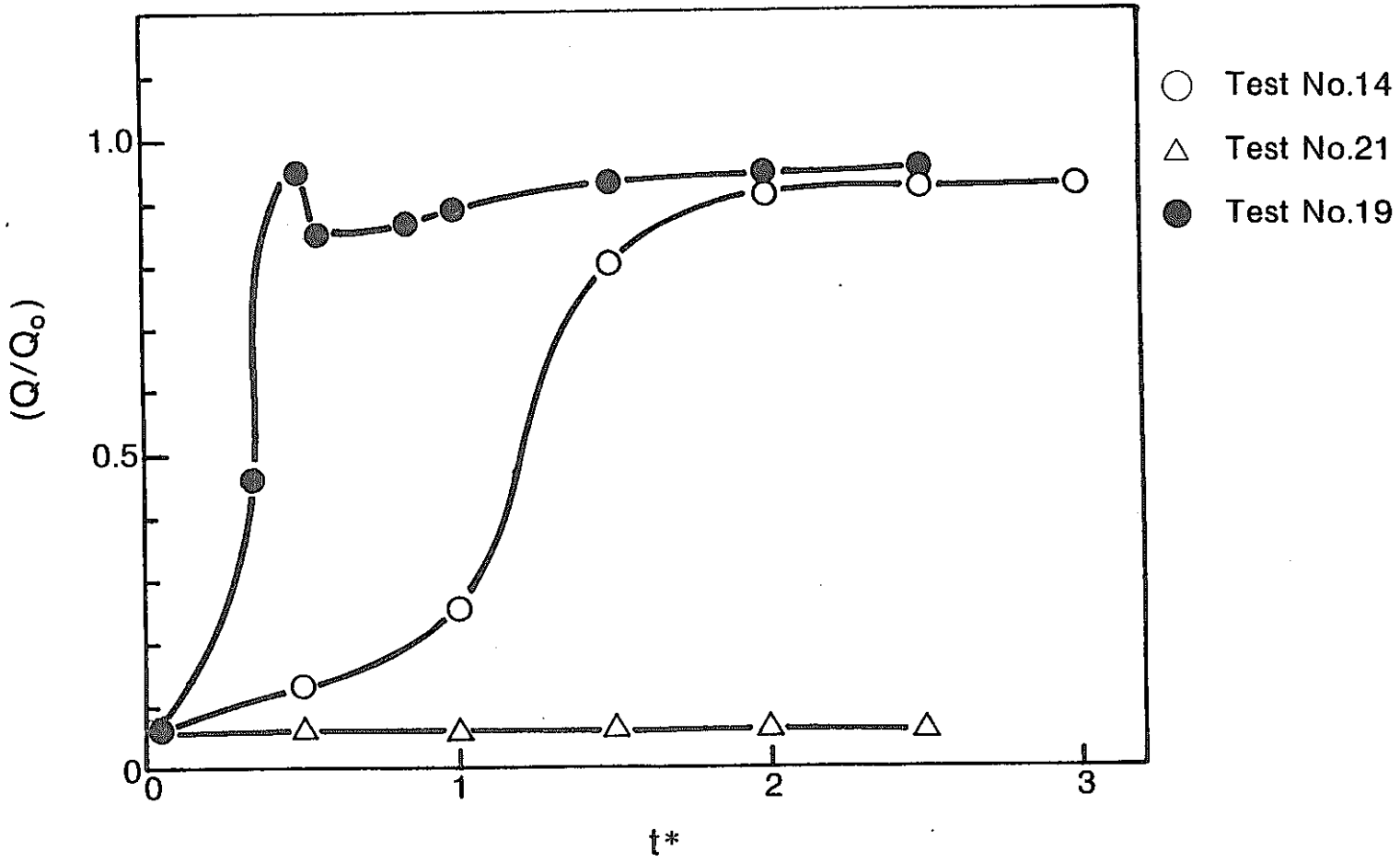

Fig. B7-13b Change-in-Time of Flow through Inner Barrel Flow Holes

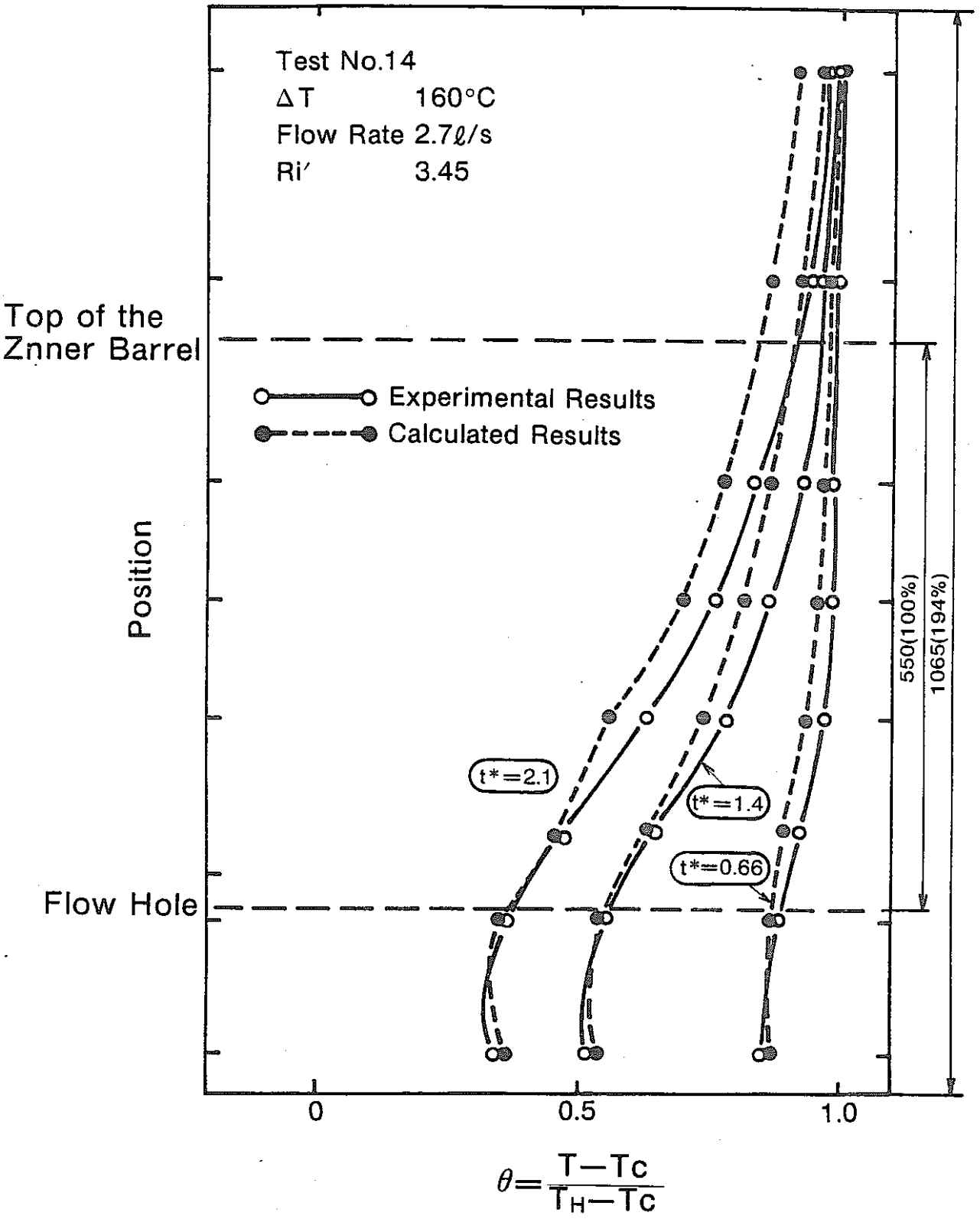

Fig. B7-14b Axial Temperature Distribution (Test No.14)

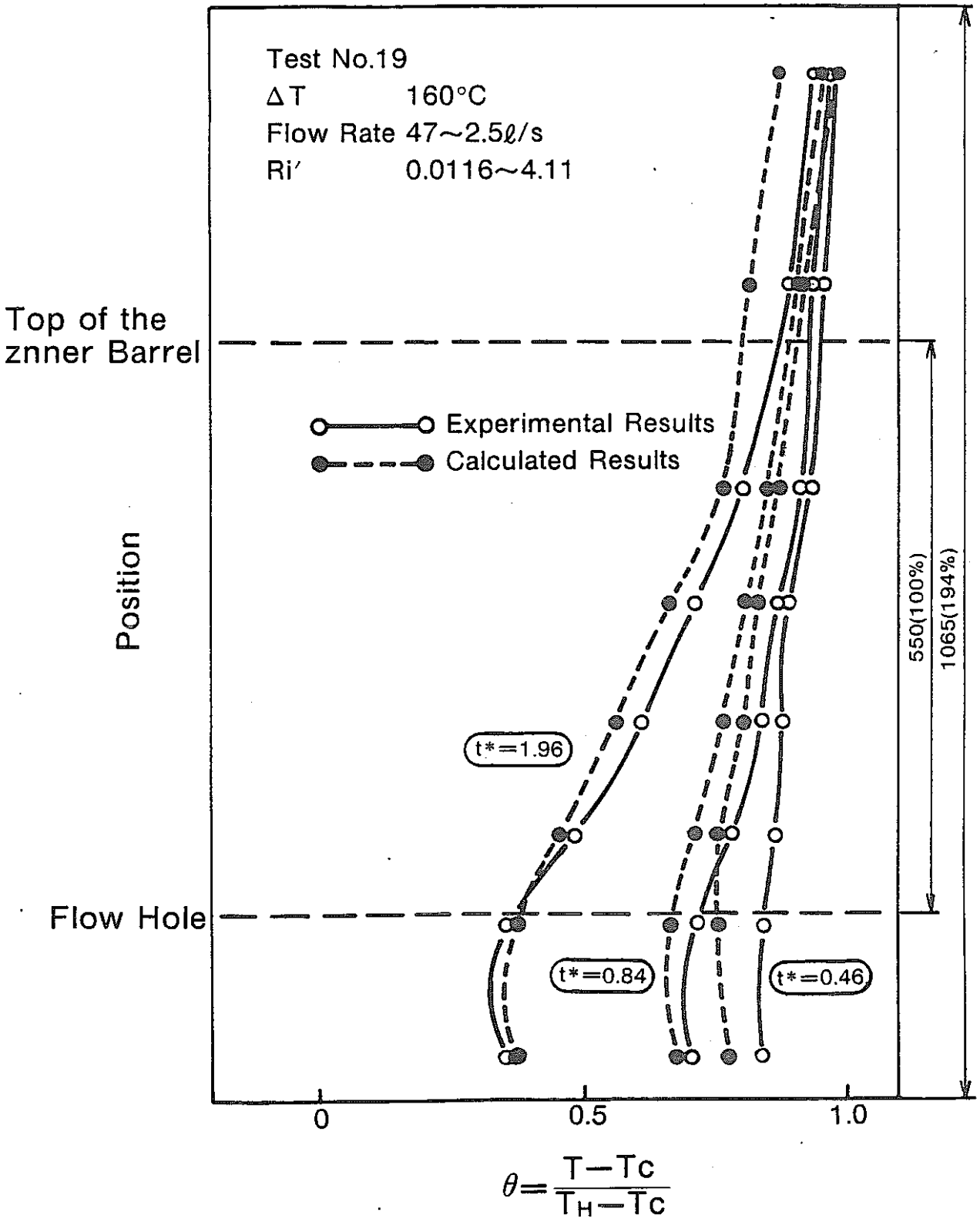

Fig. B7-15b Axial Temperature Distribution (Test No.19)

t* =0.46
Ti=30sec

t*=0.84
Ti=200sec

t*=1.96
Ti=700sec

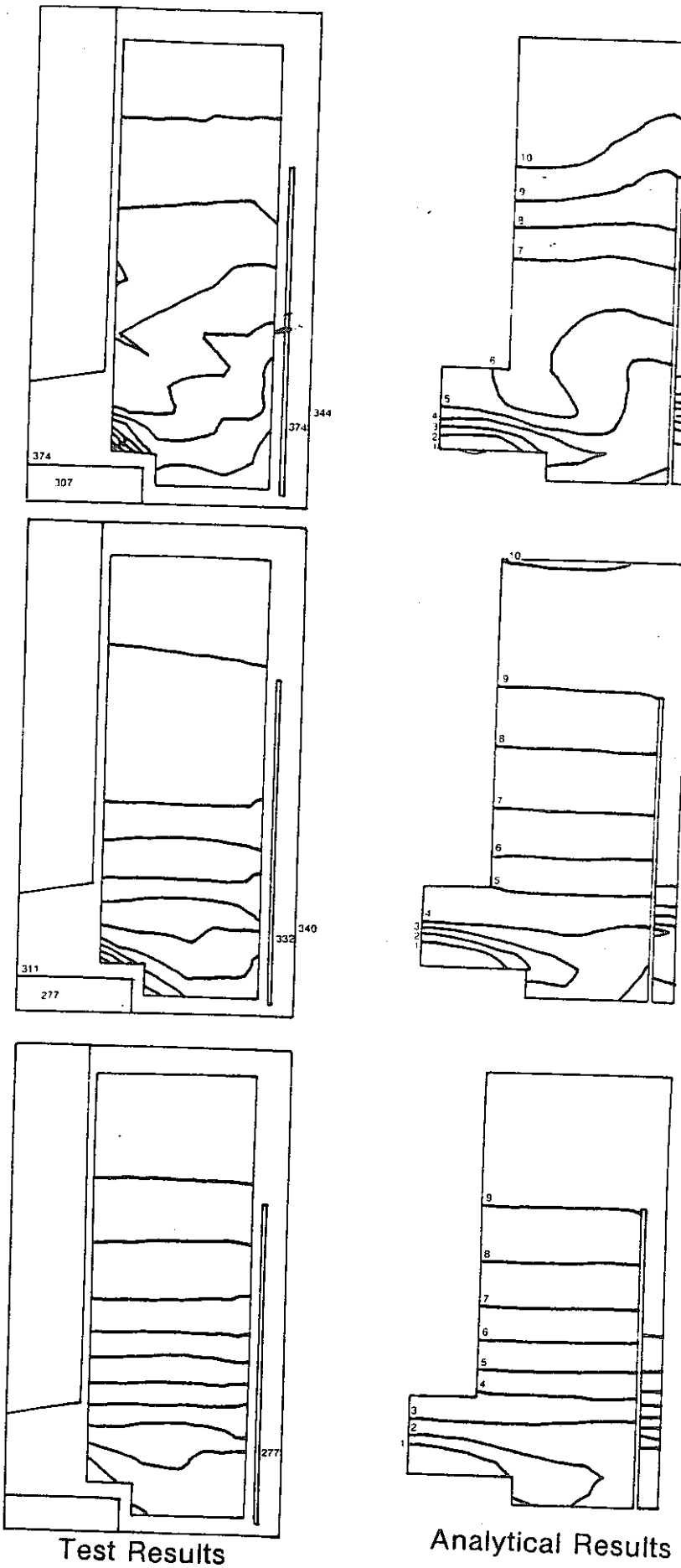

Test Results

Analytical Results

Fig. B7-16b Comparison of Iso-thermal Lines (Test No.19)

Outlet Plenum Stratification Modeling

for

Plant Thermal Transient Analysis Code

Outlet Plenum Stratification Modeling for Plant Thermal Transient Analysis Code

Yutaka Sagayama*

Mikio Tanji*

Abstract

In Monju, a stratification phenomenon occurs in the core outlet plenum during the flow coast-down after the reactor scram. And, it induces a degradation of the fluid mixing condition in the outlet plenum. The degradation tends to a high rate of the temperature change at the reactor vessel outlet nozzle, so that the plenum modeling for thermal transient analysis needs to simulate carefully a change of the fluid mixing structure, caused by a stratification phenomenon. But, the use of three or two dimensional analysis for flow dynamics is very expensive.

From this point of view, a one-dimensional plenum modeling with the changeable mixing structure, which depends on the sodium flow rate and temperature change, has been developed for predicting thermal conditions in the outlet plenum at a steady-state or during a scram transient.

---

* Advanced Reactors Engineering Department, Mitsubishi Atomic Power Industries, Inc.

Requirements to useful computer model
of core outlet plenum under stratification

(1) Simplified modeling for the flow pattern change in the core outlet plenum thermal transients.

(2) Keep of the validity of the model under the wide range, from the steady-state condition to the serious transient condition.

(3) Adequate conservative results using a simplified model.

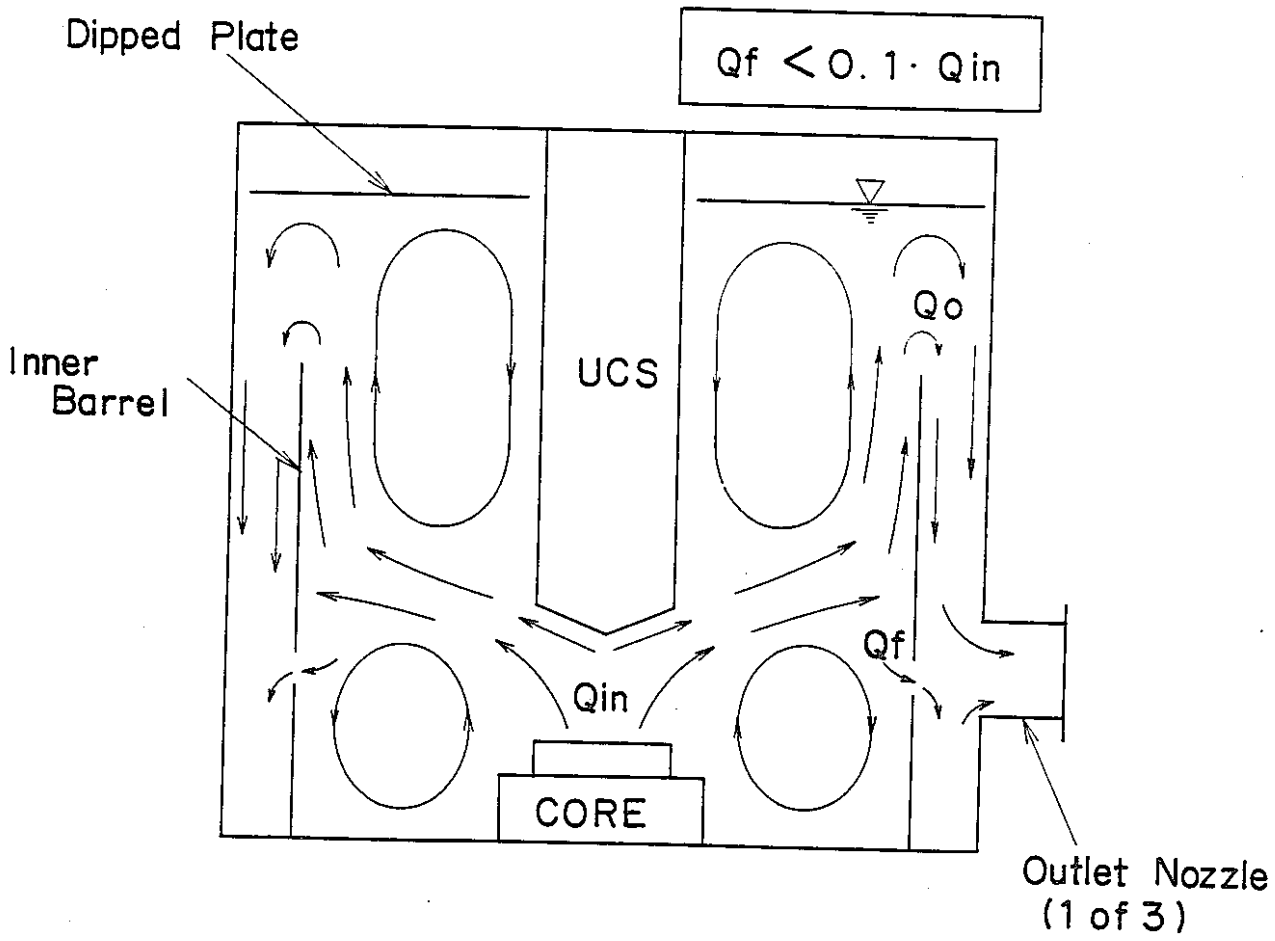

Fig-B8-1 FLOW PATTERN AT STEADY STATE
(STAGE 1)

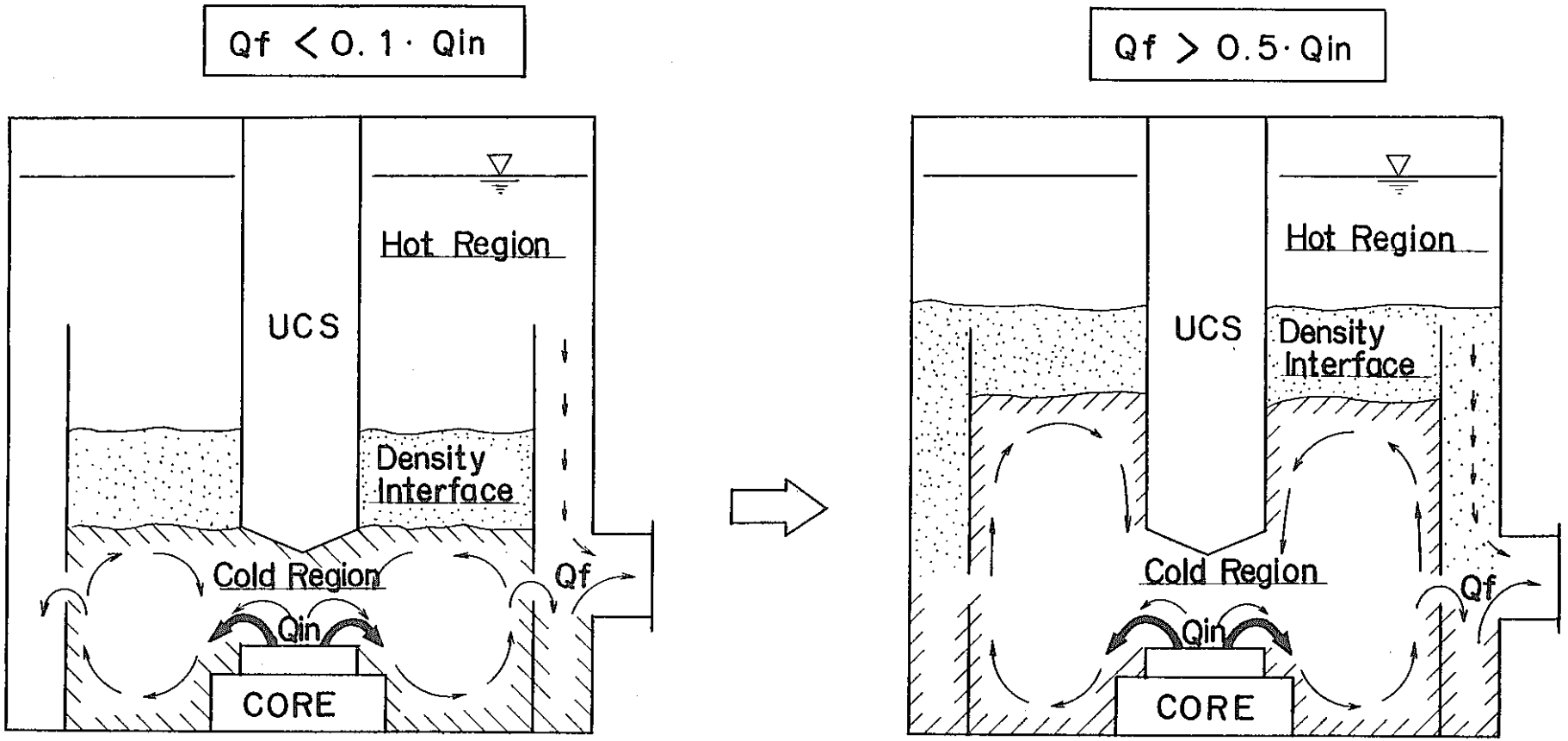

Fig-B8-2 FLOW PATTERN UNDER STRATIFICATION
(STAGE 2)

Characteristics of Flow Pattern

Stage 1

The steady-state or the biginning of the transient with good mixing due to well circulation of sodium in the plenum.

Stage 2

(1) Establishment of a hot-cold interface due to the poor mixing condition.

(2) The circulating regions disappear in the plenum.

(3) Increase of the flow through inner barrel flow holes.

(4) Hot stagnant region remains in the upper-part of plenum volume.

Model Description

(1) Flow pattern changes adapted to the variation of buoyant force.

(2) The two major passes are modeled, one is over the inner barrel to the outlet nozzle and, the other is through the inner barrel flow holes.

(3) Outlet plenum is divided into the several regions which are in complete mixing model.

A ~ F : Complete mixing region

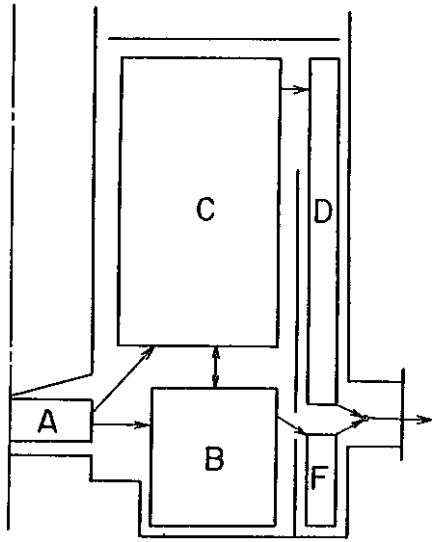

Model 1 (Stage 1)

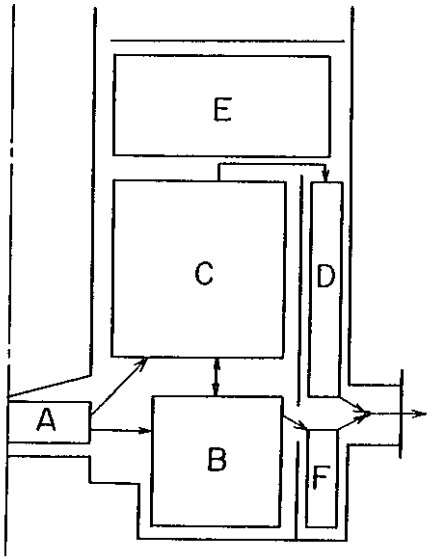

Model 2 (Stage 2)

Fig-B8-3. SCHEMATIC DIAGRAM FOR FLUID MIXING MODEL IN THE OUTLET PLENUM

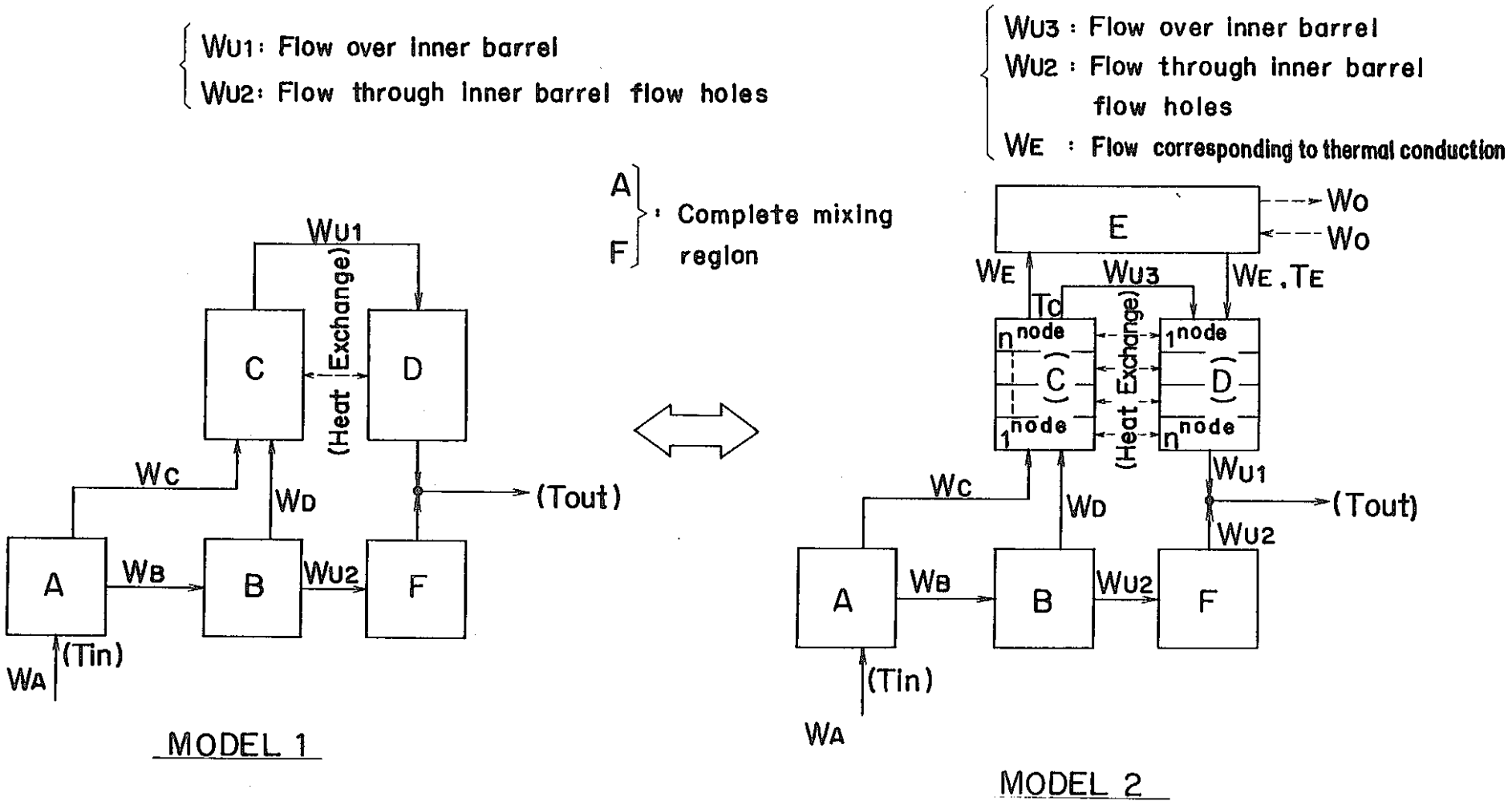

Fig-B8-4 FLOW CORRELATION IN PLENUM MODEL

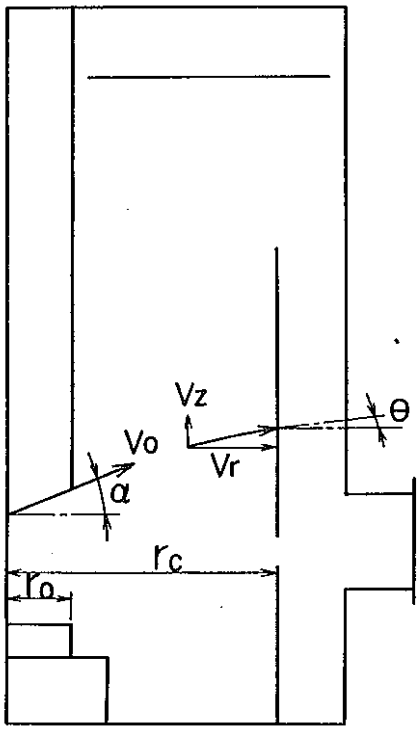

Impinging Angle

$$\tan\Theta = \frac{Vz}{Vr} = \tan\alpha - \frac{g \cdot t \cdot \frac{\Delta\rho}{\rho}}{\frac{ro}{rc} \cdot Vo \cdot \cos\alpha}$$

Flow Distribution

$$Wc = \frac{WA}{2} \cdot (1 + \sin\Theta)$$

$$WB = \frac{WA}{2} \cdot (1 - \sin\Theta)$$

if $Wc = 0$ ⟶ Stratification occur

(Apply model 2)

Fig-B8-5. FLOW ANALYTICAL MODEL BETWEEN B AND C REGION

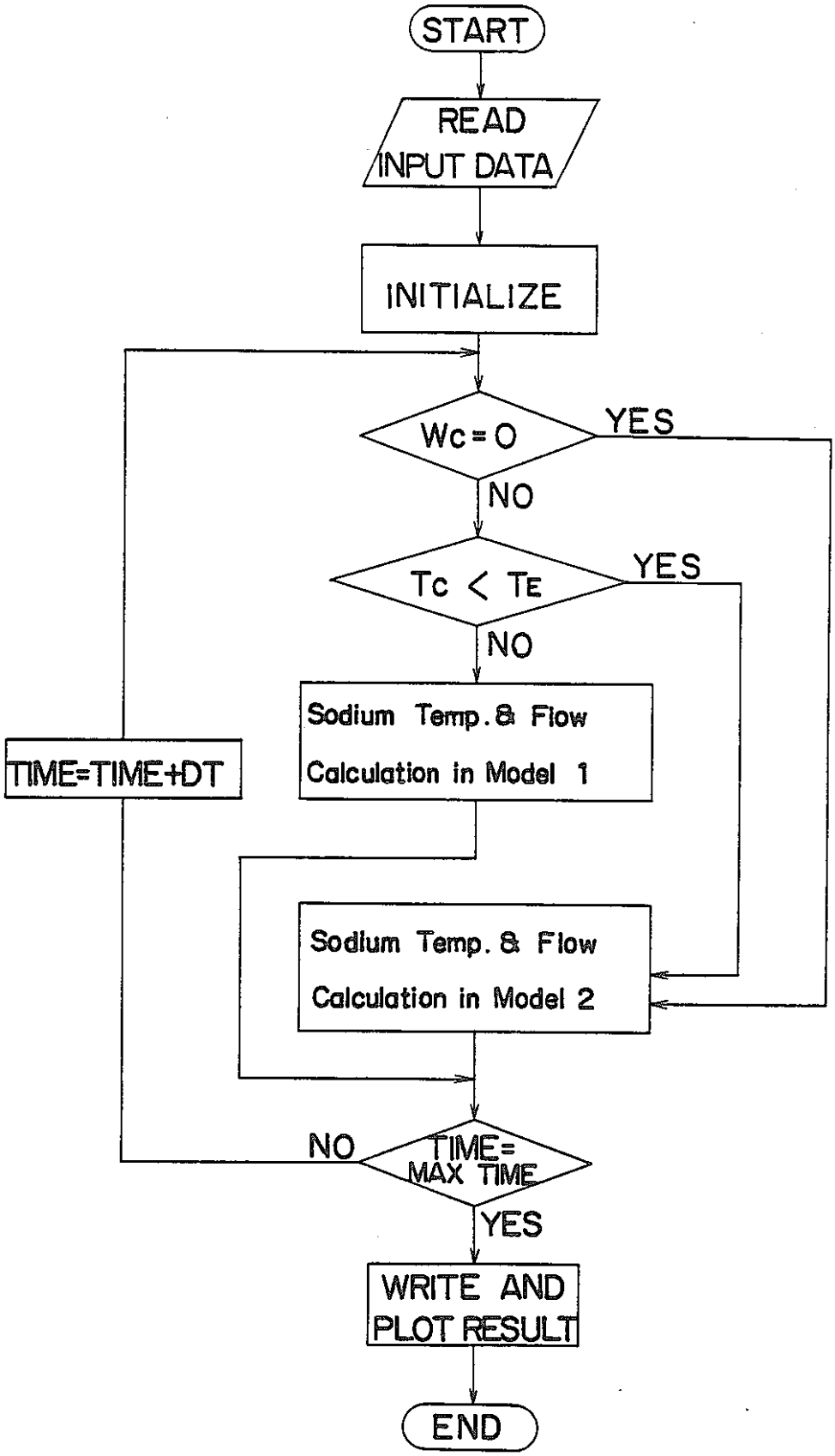

Fig-B8-6 FLOW CHART FOR COMPUTING PROGRAM

Model Verification with 1/6 scale stratification test results

The model is verified with experimental results and analytical results show good agreement with the experimental results.

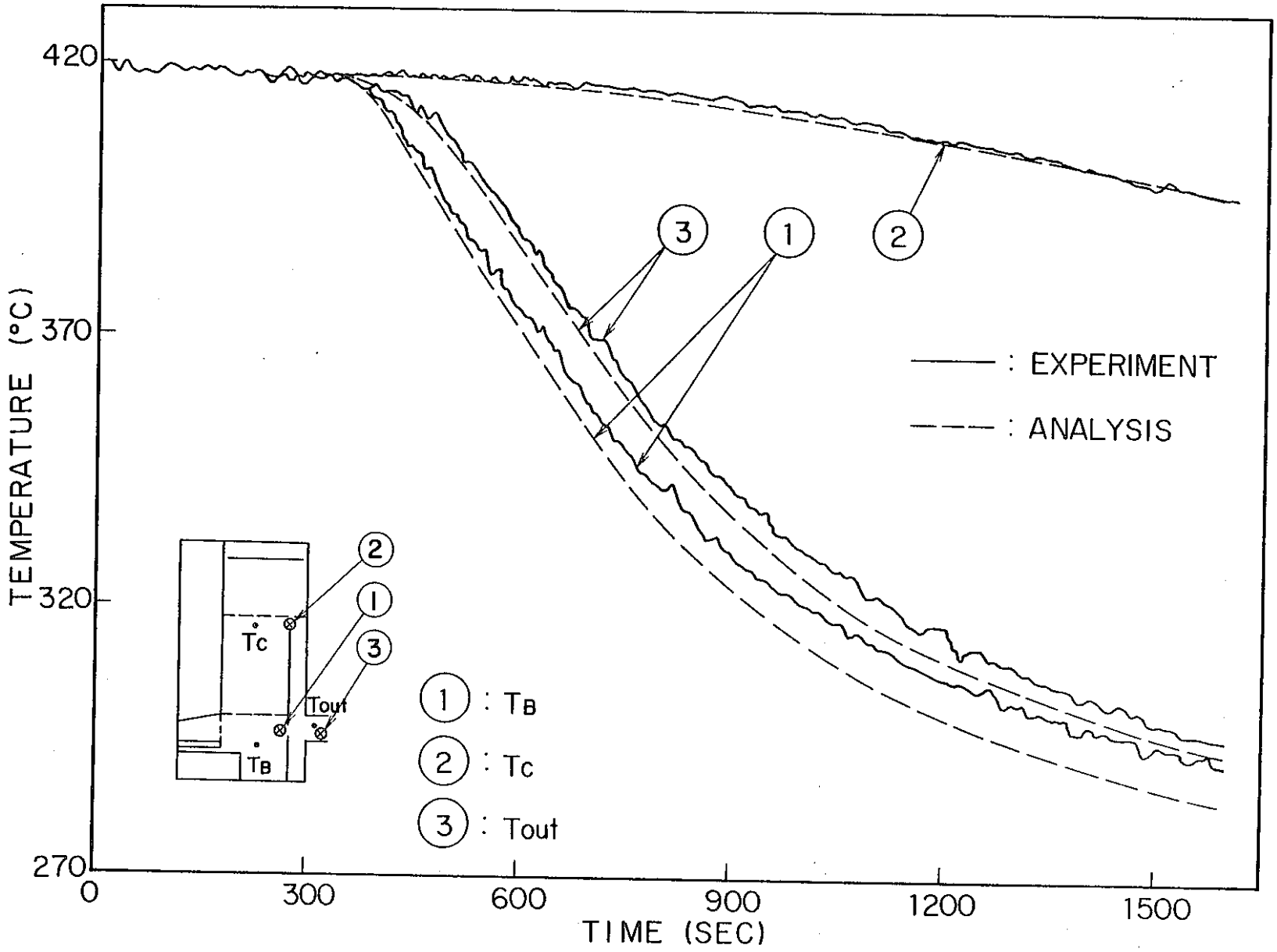

Fig-B8-7 VERIFICATION 1-1 (TEST No.14)

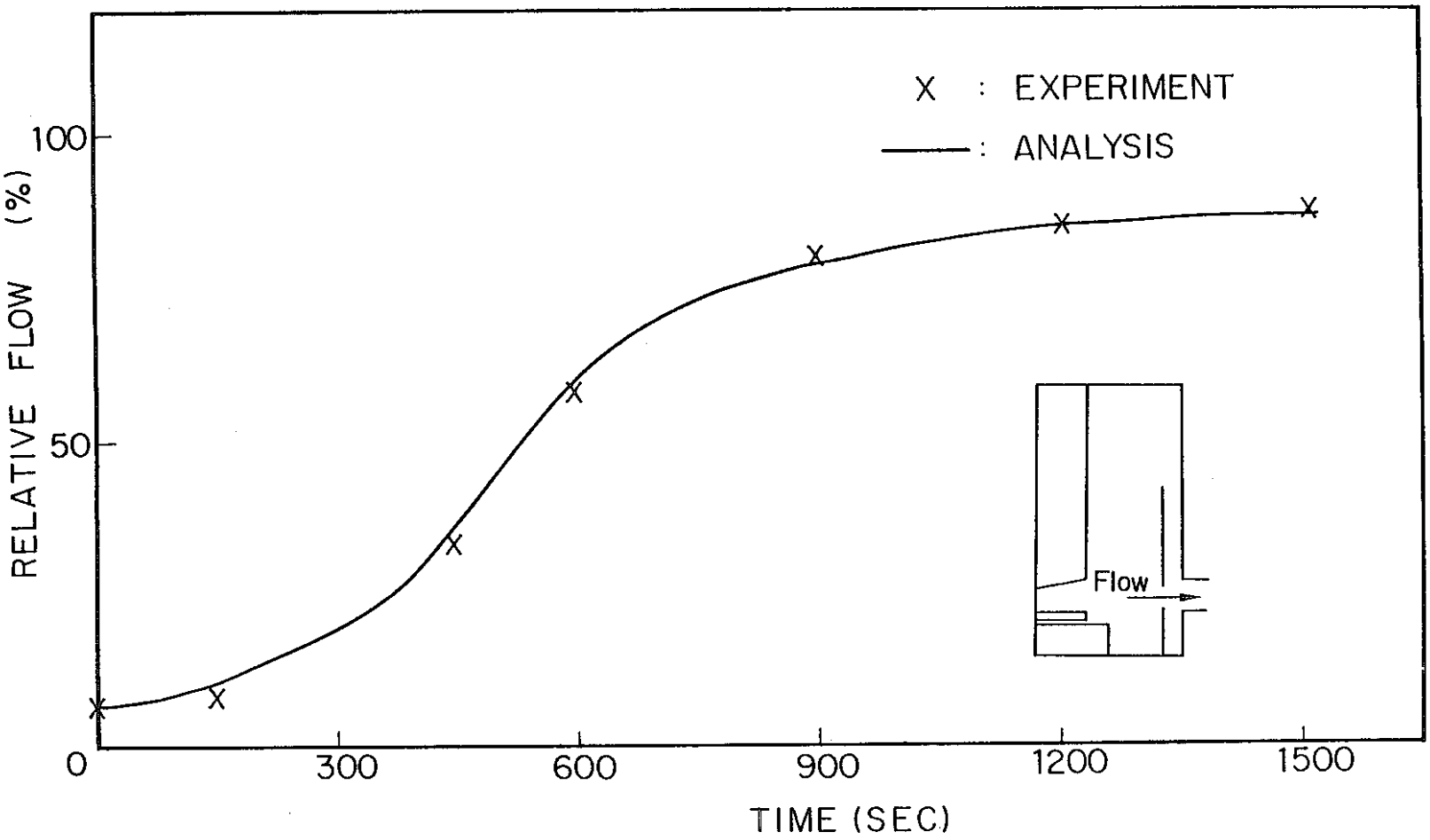

Fig-B8-8 VERIFICATION 1-2 (TEST No.14)

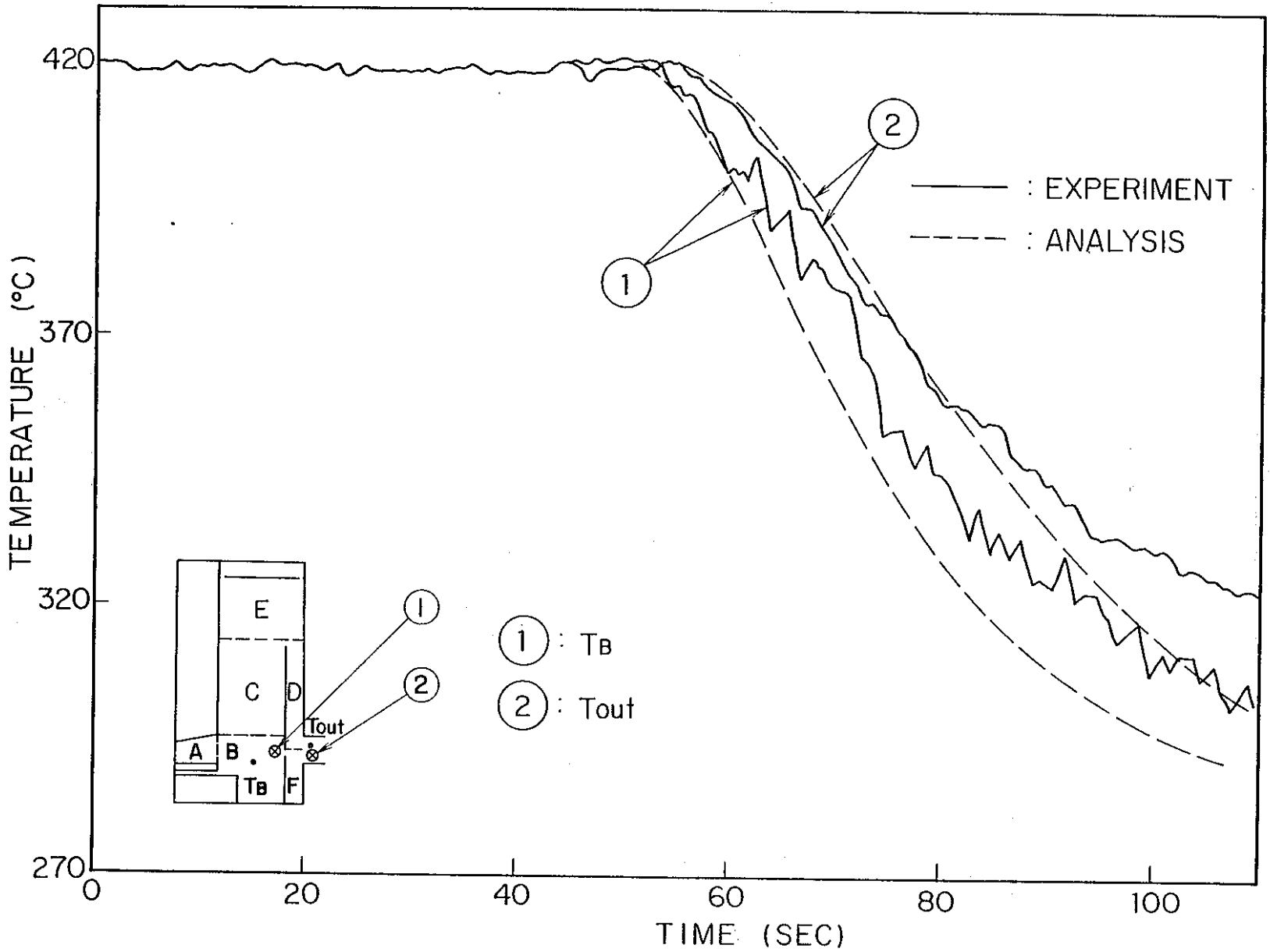

Fig - B8-9 VERIFICATION 2 (TEST No.21)

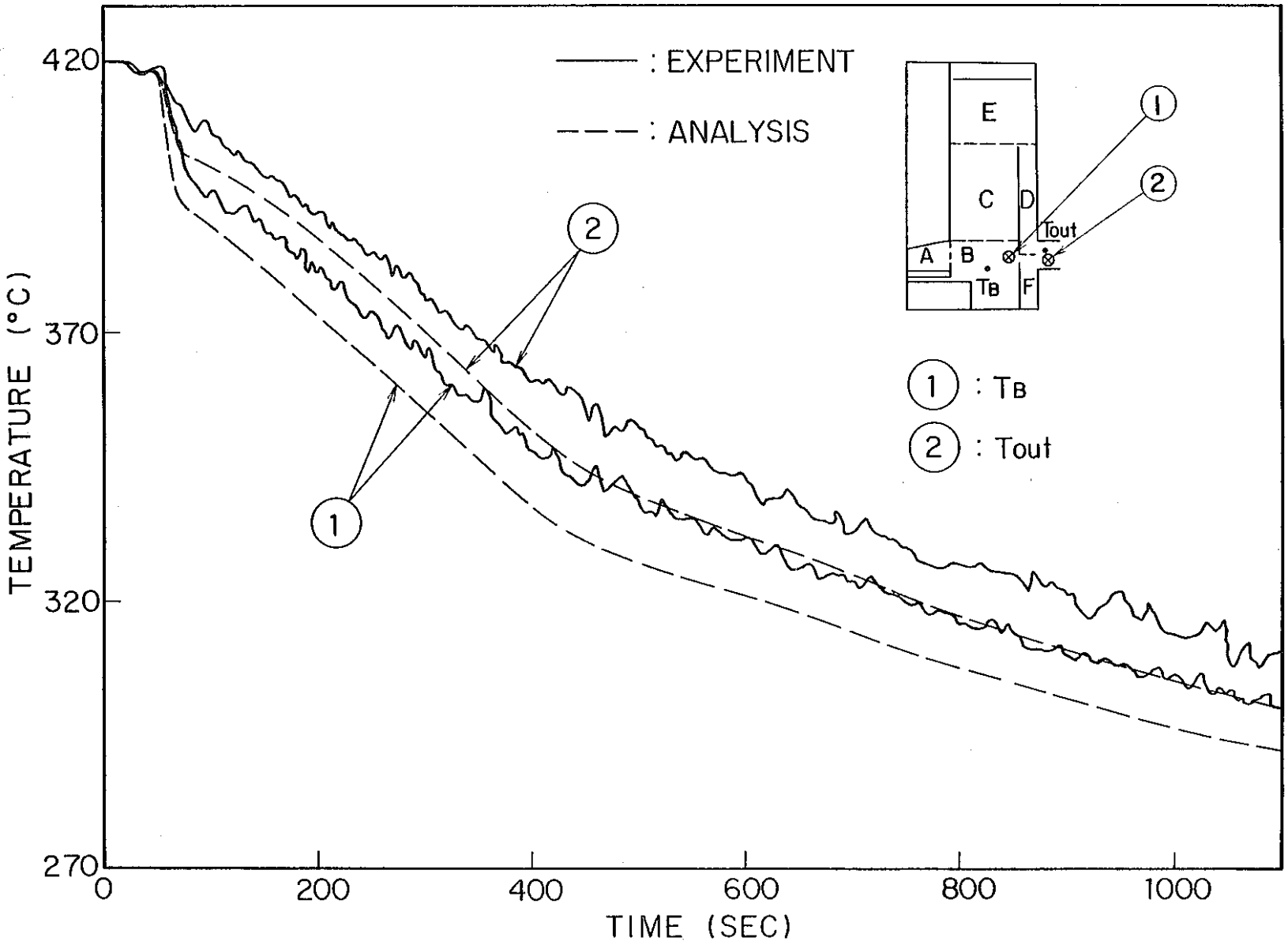

Fig-B8-10 VERIFICATION 3 (TEST No.19)